

**DEVELOPMENT OF ARYL ISONITRILES AS ANTIMICROBIAL  
AGENTS, AND  
TOTAL SYNTHESIS OF 17-NOR-EXCELSINIDINE**

by

**Kwaku Kyei-Baffour**

**A Dissertation**

*Submitted to the Faculty of Purdue University*

*In Partial Fulfillment of the Requirements for the degree of*

**Doctor of Philosophy**



Department of Chemistry

West Lafayette, Indiana

May 2019

**THE PURDUE UNIVERSITY GRADUATE SCHOOL  
STATEMENT OF COMMITTEE APPROVAL**

Dr. Mingji Dai, Chair

Department of Chemistry

Dr. Christopher Uyeda

Department of Chemistry

Dr. Hilikka Kenttamaa

Department of Chemistry

Dr. Mohamed Seleem

Department of Comparative Pathobiology

**Approved by:**

Dr. Christine Hrycyna

Head of the Graduate Program

*To my beloved family*

## ACKNOWLEDGMENTS

My special gratitude and sincerest appreciation to my advisor, Professor Mingji Dai, for his guidance, instruction and continuous encouragement throughout the course of this work.

For the invaluable support, discussions, advice, and encouragement, I will like to thank my committee members, Professor Chris Uyeda, Professor Hilikka Kenttamaa, and Professor Mohamed Seleem. Not only were you tremendously helpful and supportive as thesis committee members, you also took the time to step outside of your roles as instructors and become closer mentors. Thank you.

My gratitude also goes to the past and present members of the Dai lab. Special thanks to Brandon and Saayak for their friendship and helpful discussions. And to Dexter Davis for his great and continued friendship and mentorship over these years.

I have had the opportunity to meet and work with great scientist at Purdue without whom most of my graduate work would not have materialized. My sincere appreciation to members of the Seleem lab, most especially, Haroon Mohammad and Waleed Younis for the great collaboration and their continued friendship.

I am also grateful to my fellow graduate students, faculty, and staff members of the Purdue chemistry department for the knowledge they imparted in me, and also for the friendly and pleasant association throughout my stay at Purdue University. Special thanks to Neetu Dayal, Monessa Nambiar, Caroline Karanja, and Sudipta Pal.

Special thanks to Victoria Boulos for always being there to inspire and motivate me, for always putting a smile on my face, for offering ears to my infrequent whining and for all the positive distractions you gave me. I couldn't have imagined how this journey would have turned out without you.

Lastly, and certainly not least I would like to thank my late grandmother and my beloved family. Without you, I wouldn't be where I am. Words cannot express how blessed I am to be able to call myself a son and a brother to you all. Thank you so much for always being there to love, support and encourage me.

“The LORD is my light and my salvation—whom shall I fear? The LORD is the stronghold of my life—of whom shall I be afraid?” -Psalm 27:

“Give thanks to the LORD, for he is good; his love endures forever.” -Psalm 107:1

## TABLE OF CONTENTS

LIST OF TABLES.....	8
LIST OF FIGURES .....	10
LIST OF SCHEMES .....	11
LIST OF ABBREVIATIONS.....	12
ABSTRACT.....	14
CHAPTER 1. DISCOVERY, OPTIMIZATION, AND BIOLOGICAL EVALUATION OF ARYL ISONITRILES AS ANTIBACTERIAL AGENTS .....	16
1.1 Introduction .....	16
1.2 Results .....	19
1.2.1 Synthesis of new aryl isonitrile analogues .....	19
1.2.2 Initial screening and structure-activity relationship of new aryl isonitrile analogues against MRSA NRS123 (USA400).....	21
1.2.3 Evaluation of most potent analogues against additional strains of <i>S. aureus</i> .....	23
1.2.4 The aryl isonitrile compounds are bacteriostatic agents against MRSA.....	25
1.2.5 Investigation of the antibacterial spectrum of activity of the aryl isonitrile compounds .....	26
1.2.6 Effect of the outer membrane and efflux pump on antibacterial activity against Gram-negative bacterial pathogens.....	27
1.2.7 In silico pharmacokinetic evaluation of compound <b>1.3</b> .....	29
1.2.8 The active aryl isonitrile compounds are safe to mammalian keratinocytes.....	31
1.2.9 The aryl isonitrile compounds effectively reduce the burden of MRSA in a murine skin infection model .....	32
1.2.10 Compound <b>1.4</b> exhibits good permeability and is stable to hepatic metabolism ....	33
1.2.11 Compound <b>1.4</b> successfully reduced the burden of MRSA in a neutropenic thigh infection mouse model .....	34
1.3 Discussion.....	35
1.4 Conclusion.....	40
1.5 Experimental Section.....	40

1.5.1	General Chemistry.....	40
1.5.2	Biological Methods .....	52
1.6	References .....	57
CHAPTER 2. INVESTIGATION OF ARYL ISONITRILES AS POTENT, BROAD-SPECTRUM ANTIFUNGAL AGENTS.....		62
2.1	Introduction .....	62
2.2	Results and Discussion: First series of aryl isonitriles .....	65
2.2.1	Aryl isonitrile compounds exhibit fungistatic behavior against <i>C. albicans</i> .....	68
2.2.2	Aryl isonitrile compounds exhibit broad-spectrum antifungal activity .....	69
2.2.3	Aryl isonitriles are not toxic to mammalian cells at high concentration.....	71
2.3	Results and Discussion: Second series of aryl isonitriles.....	73
2.3.1	Aryl isonitrile compounds exhibit broad-spectrum antifungal activity .....	76
2.3.2	Aryl isonitriles are not toxic to mammalian cells at high concentrations .....	78
2.4	Conclusion.....	79
2.5	Experimental Section.....	80
2.5.1	Biological Materials and Methods .....	80
2.5.2	General chemistry and synthesis of compounds .....	81
2.6	References .....	82
CHAPTER 3. INVESTIGATION OF ARYL ISONITRILES AS ANTIMALARIAL AGENTS ...		84
3.1	Introduction .....	84
3.2	Results and Discussion.....	85
3.2.1	Structure-activity relationship of aryl isonitriles against chloroquine-resistant <i>Plasmodium falciparum</i> .....	85
3.3	Conclusion.....	92
3.4	References .....	92
CHAPTER 4. TOTAL SYNTHESIS OF (±)-17-NOR-EXCELSINIDINE .....		94
4.1	Introduction .....	94
4.2	Previous synthetic approach towards (-)-17-nor-Excelsinidine. ....	95
4.3	Synthetic strategy towards (±)17-nor-Excelsinidine .....	98
4.4	Results and Discussion.....	100
4.5	Conclusion.....	104

4.6	Experimental Section.....	105
4.7	References .....	110
SPECTRAL DATA I: DEVELOPMENT OF ARYL ISONITRILES AS ANTIMICROBIAL AGENTS.....		
		112
SPECTRAL DATA II: TOTAL SYNTHESIS OF (±)-17-NOR-EXCELSINIDINE .....		
		132
VITA.....		
		137
PUBLICATIONS.....		
		138

## LIST OF TABLES

Table 1.1. Minimum inhibitory concentration (MIC, in $\mu\text{M}$ ) of second-generation aryl isonitrile analogues and control antibiotics against methicillin-resistant <i>Staphylococcus aureus</i> (MRSA) NRS123 (USA400). .....	23
Table 1.2. Minimum inhibitory concentration (MIC, in $\mu\text{M}$ ) and MBC of the four most potent aryl isonitrile compounds and control antibiotics against methicillin-sensitive (MSSA), methicillin-resistant (MRSA), linezolid-resistant (LRSA), and vancomycin-resistant <i>S. aureus</i> . .....	24
Table 1.3. Minimum inhibitory concentration (MIC, in $\mu\text{M}$ ) of the three most potent aryl isonitrile compounds and control antibiotics against clinically-relevant Gram-positive and Gram-negative bacterial pathogens. ....	27
Table 1.4. Minimum inhibitory concentration (MIC, in $\mu\text{M}$ ) of <b>1.3</b> and control antibiotics against Gram-negative bacterial pathogens in the presence of a subinhibitory concentration of colistin (COL). ....	29
Table 1.5. <i>In silico</i> pharmacokinetic analysis for <b>1.3</b> and linezolid (simulated at 600 mg). .....	30
Table 1.6. Caco-2 bidirectional permeability analysis for compounds <b>1.4</b> . ....	33
Table 1.7. Metabolic stability evaluation for compound <b>1.4</b> in human liver microsomes. ....	34
Table 2.1. The minimum inhibitory concentration (MIC in $\mu\text{M}$ ) and minimum fungicidal concentration (MFC in $\mu\text{M}$ ) of synthesized compounds and fluconazole screened against <i>C. albicans</i> NR-29448. ....	67
Table 2.2. The minimum inhibitory concentration (MIC in $\mu\text{M}$ ) of isonitriles and fluconazole screened against clinical isolates of <i>Candida albicans</i> and non- <i>albicans Candida</i> species. ....	70
Table 2.3. The minimum inhibitory concentration (MIC in $\mu\text{M}$ ) of synthesized compounds and fluconazole screened against clinical isolates of <i>Cryptococcus</i> and <i>Aspergillus</i> . ....	71
Table 2.4. Minimum inhibitory concentration (MIC) and minimum fungicidal concentration (MFC) of aryl isonitrile analogues against <i>Candida albicans</i> . ....	76
Table 2.5. Minimum inhibitory concentration (MIC) and minimum fungicidal concentration (MFC) of aryl isonitrile analogues against <i>Candida albicans</i> and species of <i>Cryptococcus</i> . ....	77
Table 2.6. Minimum inhibitory concentration (MIC) and minimum fungicidal concentration (MFC) of aryl isonitrile analogues against additional species of <i>Candida</i> . ....	78
Table 3.1. Antimalarial activity of evaluated <i>ortho</i> -aryl isonitriles. ....	86

Table 3.2. Antimalarial activity of pyridine, quinoline, and furan stilbene aryl isonitriles.....	88
Table 3.3. Antimalarial activity of stilbene aryl isonitriles with small molecule groups. ....	89
Table 3.4. Antimalarial activity of bis-isonitriles. ....	90
Table 3.5. Antimalarial activity of aryl isonitriles with alkane bridge. ....	91
Table 4.1. Optimization of carbonylation reaction: ligand screening.....	101
Table 4.2. Optimization of carbonylation reaction: solvent and additive screening. ....	102
Table 4.3. Optimization of carbonylation reaction: base and additive screening. ....	103

## LIST OF FIGURES

Figure 1.1. First generation SAR. ....	17
Figure 1.2. Design strategy for the second-generation aryl isonitrile compounds. ....	18
Figure 1.3. Structural evolution leading to current lead aryl isonitrile. ....	18
Figure 1.4. Time-kill analysis of aryl isonitrile compounds <b>1.3</b> , <b>1.4</b> , <b>1.9</b> , <b>1.20</b> and linezolid .....	26
Figure 1.5. Toxicity analysis of aryl isonitriles against human keratinocytes (HaCaT).....	31
Figure 1.6. Reduction of MRSA USA300 in infected lesions of mice.....	32
Figure 1.7. Reduction of MRSA in infected thigh of mice after treatment with <b>1.4</b> or linezolid.	35
Figure 2.1. First series of compounds studied. ....	64
Figure 2.2. Structure-activity relationship of aryl isonitriles.....	68
Figure 2.3. Time-kill analysis of aryl isonitrile compounds. ....	69
Figure 2.4. Toxicity analysis of compounds against human epithelial colorectal cells.....	72
Figure 2.5. Second-generation aryl isonitrile compounds presented in this study. ....	74
Figure 2.6. Structure-activity relationship leading to the second-generation lead of isonitriles. .	75
Figure 2.7. Toxicity analysis of aryl isonitriles against human colorectal cells (HRT-18). ....	79
Figure 3.1. Structure-activity relationship leading to current lead compounds.....	91
Figure 4.1. Structure of ( $\pm$ )-17-nor-Excelsinidine ( <b>4.1</b> ). ....	94
Figure 4.2. Jarret's proposed oxidative cyclization strategy to ( $-$ )-17-nor-Excelsinidine. ....	95
Figure 4.3. Retrosynthetic strategy towards ( $\pm$ )-17-nor-Execelsinidine ( <b>4.1</b> ).....	99

## LIST OF SCHEMES

Scheme 1.1. Synthesis of stilbene aryl isonitrile compounds.....	19
Scheme 1.2. Synthesis of stilbene bis-isonitriles.....	20
Scheme 1.3. Synthesis of isonitriles with an alkane bridge.....	21
Scheme 4.1. Jarret's synthesis of <b>4.2</b> .....	96
Scheme 4.2. Jarret's synthesis of (+)-16-deformylgeissoschizine (+)- <b>4.2</b> .....	97
Scheme 4.3. Jarret's completion of total synthesis of (-)-17-nor-Excelsinidine.....	98
Scheme 4.4. Synthesis of carbonylation precursor <b>4.17</b> .....	100
Scheme 4.5. Completion of total synthesis of ( $\pm$ )-17-nor-Excelsinidine ( <b>4.1</b> ).....	104

**LIST OF ABBREVIATIONS**

$[\alpha]_D$	specific optical rotation; deg mL/(g dm)
Ac	acetyl
Bn	benzyl
br	broad peak
Bu	butyl
Bz	benzoyl
Calcd.	calculated
$\delta$	chemical shift
DBU	1,8-Diazabicyclo[5.4.0]undec-7-ene
DCE	1,2-Dichloroethane
DCM	dichloromethane
DMF	N,N-dimethylformamide
dr	diastereomeric ratio
eq.	equivalent
Equiv.	equivalent
ESI	electrospray ionization
Et	ethyl
Et <sub>2</sub> O	diethyl ether
EtOAc	ethyl acetate
h	hour
HPLC	high performance liquid chromatography
HMDS	hexamethyldisilazane
IC <sub>50</sub>	inhibitory concentration, 50 percent
iPr	isopropyl
IR	infrared (spectroscopy)
KHMDS	potassium bis(trimethylsilyl)amide
LAH	lithium aluminum hydride
$\mu$	micro
M	molar

mCPBA	meta-chloroperoxybenzoic acid
M.S.	molecular sieves
MS	mass spectrometry
Me	methyl
MHz	megahertz
Min	minute
m/z	mass to charge ratio
NMR	nuclear magnetic resonance (spectroscopy)
p	para
Ph	phenyl
PMB	para-methoxybenzyl
q	quartet
rt	room temperature
rxn	reaction
sat.	saturated
TBAF	tetrabutylammonium fluoride
TBS	<i>tert</i> -butyldimethylsilyl
Tf <sub>2</sub> O	trifluoromethanesulfonic anhydride
TfOH	trifluoromethanesulfonic acid
THF	tetrahydrofuran
TLC	thin layer chromatography
TMS	trimethylsilyl
TsOH	<i>p</i> -toluenesulfonic acid

## ABSTRACT

Author: Kyei-Baffour, Kwaku. PhD

Institution: Purdue University

Degree Received: May 2019

Title: Development of Aryl Isonitriles as Antimicrobial Agents, and Total Synthesis of 17-nor-Excelsinidine

Committee Chair: Mingji Dai

Infectious diseases caused by bacteria, fungi, and plasmodium parasites are a huge global health problem which ultimately leads to millions of deaths annually. The emergence of strains that exhibit resistance to nearly every class of antimicrobial agents, and the inability to keep up with these resistance trends has brought to the fore the need for new therapeutic agents (antibacterial, antifungal, and antimalarial) with novel scaffolds and functionalities capable of targeting microbial resistance. A novel class of compounds featuring an aryl isonitrile moiety has been discovered that exhibits potent inhibitory activity against several clinically relevant strains of methicillin-resistant *Staphylococcus aureus* (MRSA). Synthesis, structure-activity relationship (SAR) studies, and biological investigations have led to lead molecules that exhibit anti-MRSA inhibitory activity as low as 1 – 2  $\mu\text{M}$ . The most potent compounds have also been shown to have low toxicity against mammalian cells and exhibit *in vivo* efficacy in MRSA skin and thigh infection mouse models.

The novel aryl isonitriles have also been evaluated for antifungal activity. This study examines the SAR of aryl isonitrile compounds and showed the isonitriles as compounds that exhibit broad spectrum antifungal activity against species of *Candida* and *Cryptococcus*. The most potent derivatives are capable of inhibiting growth of these pathogens at concentrations as low as 0.5  $\mu\text{M}$ . Notably, the most active compounds exhibit excellent safety profile and are non-toxic to mammalian cells up to 256  $\mu\text{M}$ .

Beyond the antibacterial and antifungal activities, structure-antimalarial relationship analysis of over 40 novel aryl isonitrile compounds has established the importance of the isonitrile functionality as an important moiety for antimalarial activity. Of the many isonitrile compounds exhibiting potent antimalarial activity, two have emerged as leads with activity comparable to that of Artemisinin. The SAR details presented in this study will prove essential for the

development new aryl isonitrile analogues to advance them to the next step in the antimalarial drug discovery process.

17-nor-Excelsinidine, a zwitterion monoterpene indole alkaloid isolated from *Alstonia scholaris* is a subject of synthetic scrutiny. This is primarily due to its intriguing chemical structure which includes a bridged bicyclic ammonium moiety, and its anti-adenovirus and anti-HSV activity. Herein we describe a six-step total synthesis of ( $\pm$ )-17-nor-Excelsinidine from tryptamine. Key to the success of this synthesis is the use of palladium-catalyzed carbonylative heck lactamization methodology which built the 6, 7-membered ring lactam in one step. The resulting pentacyclic product, beyond facilitating the easy access to ( $\pm$ )-17-nor-Excelsinidine, could also serve as a precursor to other related indole alkaloids.

# CHAPTER 1. DISCOVERY, OPTIMIZATION, AND BIOLOGICAL EVALUATION OF ARYL ISONITRILES AS ANTIBACTERIAL AGENTS

## 1.1 Introduction

Bacterial infections resistant to current antibiotics continue to pose a major global health problem that requires the constant identification and development of new antibacterial agents. Extensive research efforts and funding over the years have focused on identifying new agents to treat Gram-negative bacterial infections, particularly those caused by carbapenem-resistant Enterobacteriaceae (CRE); however, the reality remains that Gram-positive bacteria (particularly methicillin-resistant *S. aureus* (MRSA)) are more frequent sources of community-acquired and nosocomial infections, particularly in the United States of America.<sup>1-3</sup> In 2013, the US Center for Disease Control and Prevention noted that serious infections caused by MRSA (>80,000) alone outnumbered infections attributed to extended-spectrum  $\beta$ -lactamase producing Enterobacteriaceae (26,000), CRE (9,000), multidrug-resistant *Acinetobacter* (7,300), and multidrug-resistant *Pseudomonas aeruginosa* (6,700) combined.<sup>4</sup> In addition, there has been remarkably more fatalities attributed to MRSA infections (11,285 deaths) relative to infections caused by drug-resistant Gram-negative pathogens (3,240 deaths).<sup>4</sup> Given MRSA infections continue to be a problem in both healthcare and community settings, and resistant isolates to key antibiotics (vancomycin and linezolid) used to treat MRSA infections have emerged,<sup>3,5-8</sup> new antibacterial agents are urgently needed.

Although there are numerous antibacterial development programs ongoing to develop new therapeutics, most of these often focus on the optimization of already existing antibiotic scaffolds (i.e.  $\beta$ -lactams, quinolones, glycopeptides, oxazolidinones). This line of action has led to the regulatory approval of a variety of new antibacterial agents to treat MRSA infections. These include delafloxacin, dalbavancin, oritavancin, and tedizolid phosphate with improved potency relative to other antibiotics in the same drug class.<sup>9</sup>

Nonetheless, bacterial resistance to these newer agents is most probably unpreventable, particularly given the structural similarity to existing antibiotics, which will further hinder clinicians' ability to effectively treat drug-resistant bacterial infections. Identifying novel antibacterial agents with unique and unexploited scaffolds or mechanisms of action is vital to circumvent the growing challenge of treating drug-resistant bacterial infections.

In an ongoing effort to identify compounds with unique functionalities and scaffolds capable of targeting multidrug-resistant bacterial infections, we recently identified aryl isonitriles as a unique class of compounds with anti-MRSA activity.<sup>10</sup> Though extensive efforts in isolating naturally occurring isonitriles from marine sponges and cyanobacteria have led to isonitriles that exhibit antimicrobial activity, these compounds have been precluded from extensive medicinal chemistry and structure-activity-relationship (SAR) studies.<sup>11-14</sup> This is primarily because their complex structural motifs make them very difficult to access. Therefore, the isonitrile functionality and the aryl isonitrile scaffold remain one of the least extensively studied scaffolds. SAR studies on the first series of over 40 aryl isonitriles revealed the isonitrile functionality as the most essential structural component that contributed to the antibacterial activity of the compounds. The presence of a second non-isonitrile-bearing aromatic ring and an alkene bridge/linker were also shown to be important. However, substituents incorporated on this bridge did not result in improved antibacterial activity (Figure 1.1).

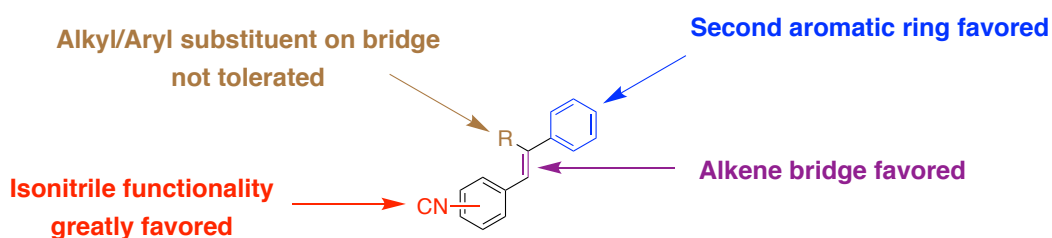


Figure 1.1. First generation SAR.

In light of this, the current work further explores the structural-anti-bacterial activity of a second-generation of aryl isonitriles, understand their spectrum of antibacterial activity, and evaluate the most promising analogue's activity in a mouse model of MRSA infection. These

studies take into account a novel group of stilbene bis-isonitriles and also explores new stilbene aryl isonitriles with medicinally-relevant structural molecules and heterocyclic moieties. Aryl isonitriles with a saturated linker have also been evaluated (Figure 1.2). From this effort, compound **1.3** and **1.4** emerged as new lead compounds with antibacterial activity *in vitro* and *in vivo* against MRSA (Figure 1.3).

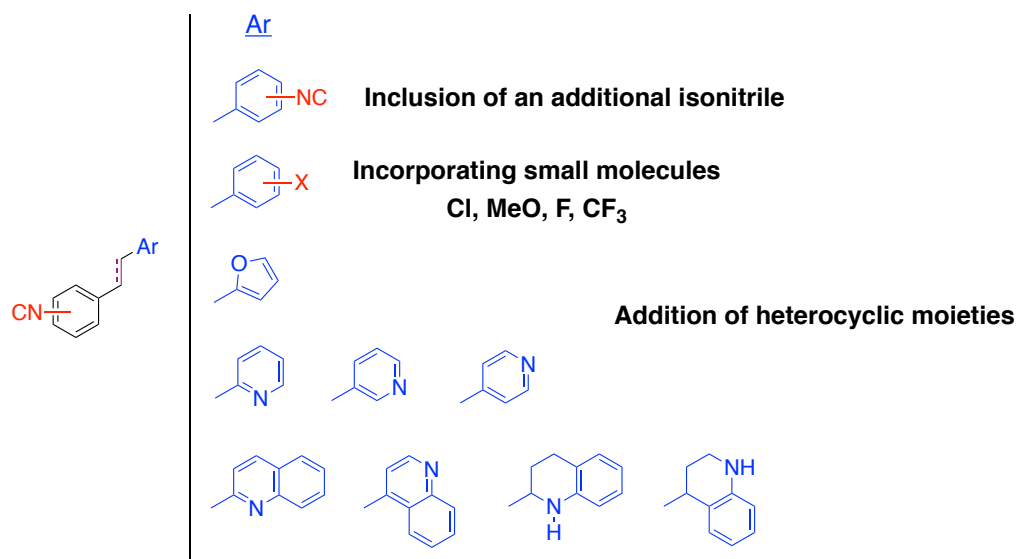


Figure 1.2. Design strategy for the second-generation aryl isonitrile compounds.

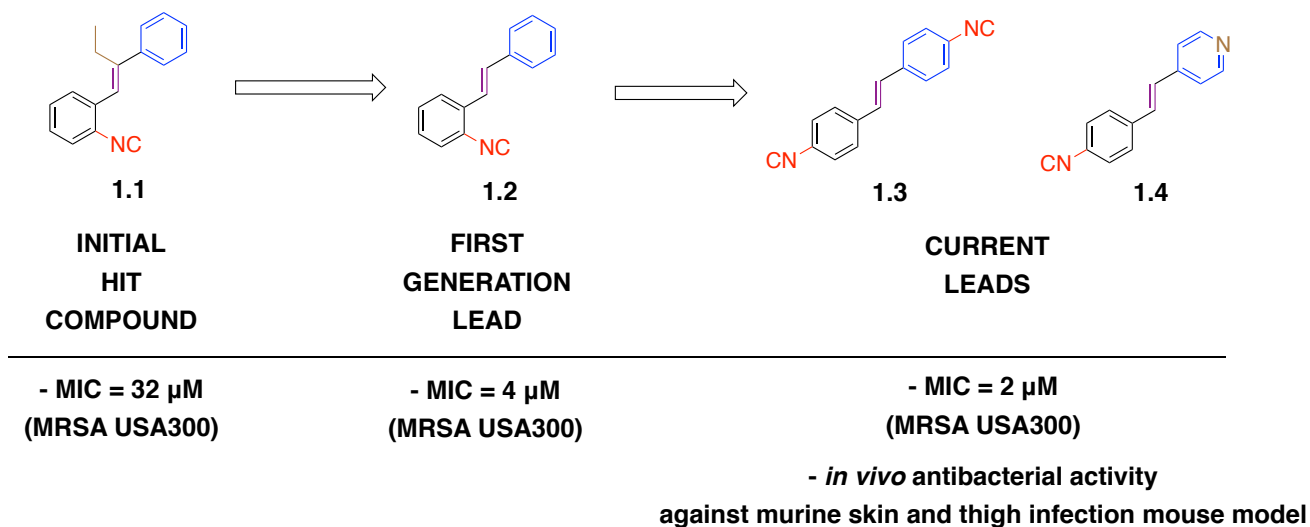
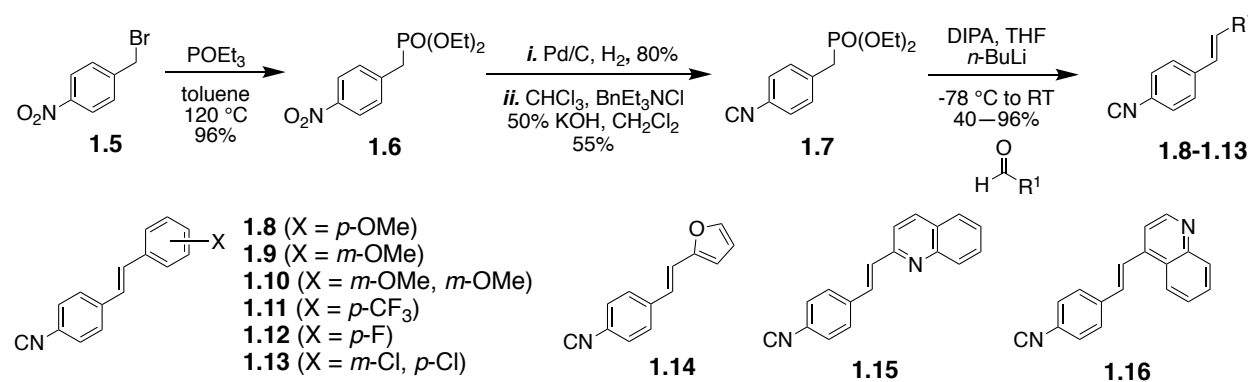


Figure 1.3. Structural evolution leading to current lead aryl isonitrile compound and minimum inhibitory concentration (MIC) values against methicillin-resistant *S. aureus* (MRSA).

## 1.2 Results

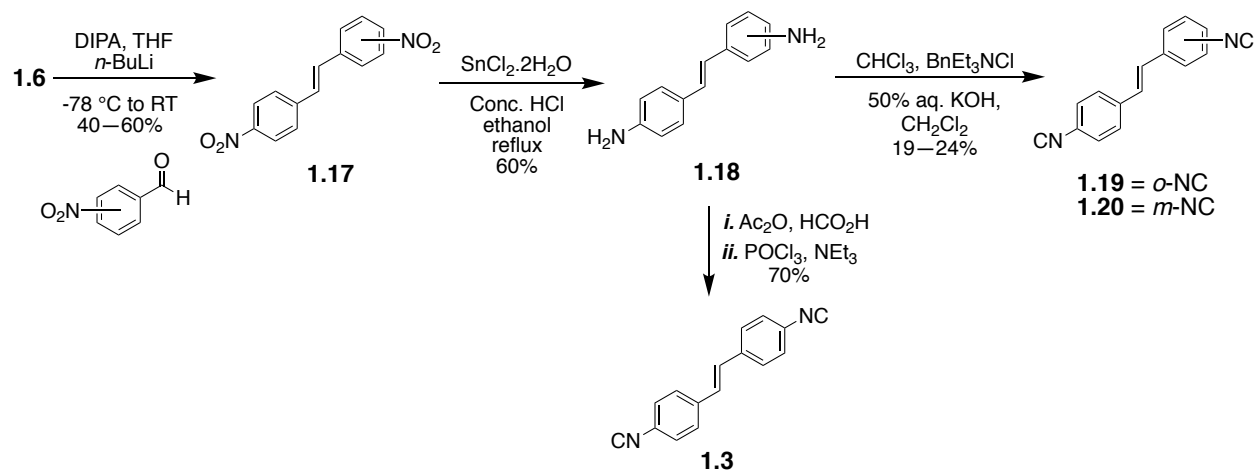
### 1.2.1 Synthesis of new aryl isonitrile analogues

Following the identification of **1.1** as the initial hit aryl isonitrile from the first-generation compounds and subsequent synthetic exploration leading to **1.2** as the lead molecule (Figure 1.3), our initial synthetic efforts were geared towards incorporating medicinally-relevant groups to the aryl isonitrile core. These groups include electron donating and electron withdrawing small molecules such as fluoro, chloro, trifluoromethyl, and methoxy groups.<sup>15-17</sup> To access these novel stilbene isonitriles, a Michaelis-Arbuzov reaction involving the commercially available nitrobenzyl bromide starting material (**1.5**) was used to form nitrobenzyl phosphonate (**1.6**).<sup>18</sup> Subsequent reduction of the nitro group, followed by Hofmann isonitrile conversion of the resulting amine, led to the formation of the isonitrile phosphonate (**1.7**).<sup>19</sup> Serving as the divergent point, the isonitrile phosphonate was then subjected to Horner-Wadsworth-Emmons (HWE)<sup>20</sup> reaction to produce isonitrile compounds **1.8-1.13**, from their respective aldehydes (Scheme 1.1). The above-mentioned synthetic process was also employed to synthesize aryl isonitriles to explore the importance of incorporating heterocyclic moieties as the second aromatic ring. These analogues included furan (**1.14**) and quinoline (**1.15** and **1.16**) groups.



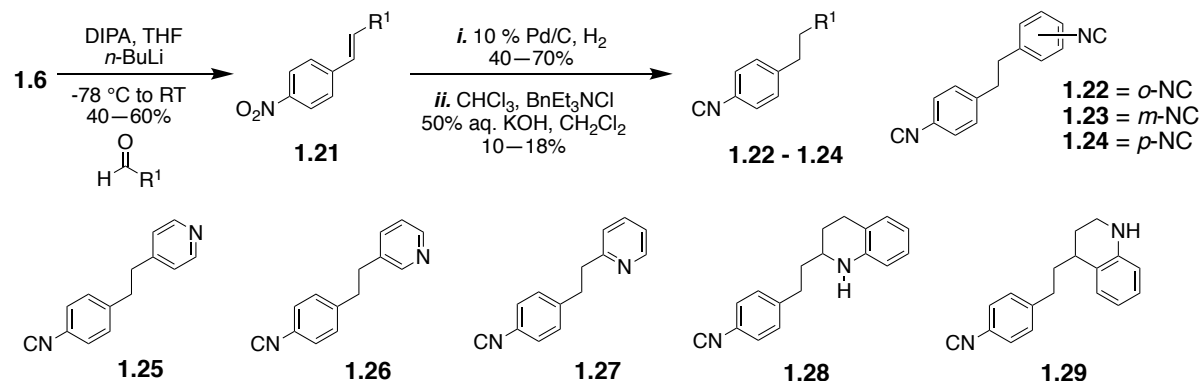
Scheme 1.1. Synthesis of stilbene aryl isonitrile compounds.

As part of SAR studies on the first-generation molecules, the isonitrile functionality was identified as the integral component of the stilbene aryl isonitriles (Figure 1.1). Bis-isonitriles **1.19**, **1.20**, and **1.3** were therefore synthesized to explore the influence of an additional isonitrile group on the antibacterial activity of the lead molecule **1.2**. Similarly, using **1.6** as the divergent point, the stilbene bis-isonitriles **1.19**, **1.20**, and **1.3** were synthesized (Scheme 1.2). HWE reaction involving **1.6** and the corresponding nitro substituted benzaldehydes was employed as the first step in the formation of dinitrostilbenes. The selective reduction of the nitro group followed by Hoffmann isonitrile synthesis led to compounds **1.19** and **1.20**. Bis-isonitrile **1.3** was prepared by a stepwise formylation and POCl<sub>3</sub>-promoted dehydration of the corresponding diamine.



Scheme 1.2. Synthesis of stilbene bis-isonitriles.

Finally, after the synthesis of the stilbene isonitriles and the bis-isonitriles, the question regarding the impact of an alkane bridge on the biological activity arose. This led to the synthesis of compounds **1.22-1.29** (Scheme 1.3). In the synthesis of aryl isonitriles with an alkane linker, HWE reaction involving **1.6** and various aldehydes was first employed to form the stilbene compounds. A sequence of reduction and Hofmann isonitrile synthesis afforded the corresponding aryl isonitriles in good yields.



Scheme 1.3. Synthesis of isonitriles with an alkane bridge.

### 1.2.2 Initial screening and structure-activity relationship of new aryl isonitrile analogues against MRSA NRS123 (USA400)

In order to investigate the antibacterial activity of the newly synthesized isonitrile analogues, the minimum inhibitory concentration (MIC) against MRSA NRS123 was determined using the broth microdilution assay (Table 1.1). The newly synthesized stilbene bis-isonitriles **1.19** (MIC = 16  $\mu\text{M}$ ), **1.20** (MIC = 4  $\mu\text{M}$ ), and **1.3** (MIC = 8  $\mu\text{M}$ ) all exhibited moderate to good anti-MRSA activity. The most potent analogues were compounds where the isonitrile moiety was located in the meta- (**1.20**) or para- position (**1.3**). The moderate to good activity exhibited by the stilbene bis-isonitriles further emphasized the importance of the isonitrile group for antibacterial activity against MRSA. An eight-fold reduction in activity was observed when the most potent stilbene bis-isonitrile **1.20** (MIC = 4  $\mu\text{M}$ ) was transformed to its saturated bis-isonitrile analogue **1.23** (MIC = 32  $\mu\text{M}$ ). The observance of a similar pattern for bis-isonitriles **1.19** (MIC = 16  $\mu\text{M}$ ) and **1.3** (MIC = 8  $\mu\text{M}$ ) with respect to the saturated bis-isonitrile analogues **1.22** and **1.24** (MIC > 64  $\mu\text{M}$ ) further emphasized the importance of the alkene linker.

Intrigued by the importance of the non-isonitrile-bearing aromatic ring resulting from the previous SAR studies, heterocyclic moieties with established therapeutic properties and widely known in medicinal chemistry to improve the physicochemical and pharmacokinetic properties of lead molecules were investigated.<sup>21, 22</sup> While none of these heterocyclic-containing aryl isonitriles positively improved the activity of the lead compound, the quinoline-containing compound **1.15**

(MIC = 8  $\mu$ M) was more potent than the quinoline analogue **1.16** (MIC > 64  $\mu$ M) and furan analogue **1.14** (MIC = 32  $\mu$ M). The anti-MRSA activity was however not comparable to that of the previously reported most active pyridine compound **1.4** (MIC = 8  $\mu$ M). All of the saturated pyridine derivatives exhibited weaker anti-MRSA activity compared to their corresponding stilbene isonitriles.

With the knowledge of the medicinal importance of F, -OCH<sub>3</sub>, Cl and CF<sub>3</sub> and their value in the enhancement of the pharmacokinetic and physiochemical activity of several therapeutic small molecule candidates, installing these species on the aryl isonitrile compounds was investigated.<sup>15-17</sup> Of the methoxy substituted derivatives, the meta-substituted methoxy **1.9** (MIC = 2  $\mu$ M) was the most potent analogue, but adding the second methoxy group (**1.10**) significantly reduced the compound's anti-MRSA activity (MIC = 64  $\mu$ M). Interestingly, none of the analogues with electron-withdrawing fluoro, chloro, and trifluoromethyl groups exhibited a major improvement in anti-MRSA activity. This reveals that having the right electronic environment around the second aromatic ring is essential.

Table 1.1. Minimum inhibitory concentration (MIC, in  $\mu\text{M}$ ) of second-generation aryl isonitrile analogues and control antibiotics against methicillin-resistant *Staphylococcus aureus* (MRSA) NRS123 (USA400).

Compound/Drug Name	MRSA NRS123 (USA 400)	
	MIC	
<b>1.3</b>	8	>64
<b>1.4</b>	8	>64
<b>1.8</b>	32	N.D.
<b>1.9</b>	2	N.D.
<b>1.10</b>	64	N.D.
<b>1.11</b>	32	N.D.
<b>1.12</b>	64	N.D.
<b>1.13</b>	>64	N.D.
<b>1.14</b>	32	N.D.
<b>1.15</b>	8	>64
<b>1.16</b>	>64	N.D.
<b>1.19</b>	16	N.D.
<b>1.20</b>	4	>64
<b>1.22</b>	>64	N.D.
<b>1.23</b>	32	N.D.
<b>1.24</b>	>64	N.D.
<b>1.25</b>	64	N.D.
<b>1.26</b>	>64	N.D.
<b>1.27</b>	>64	N.D.
<b>1.28</b>	16	N.D.
<b>1.29</b>	32	N.D.
<b>Linezolid</b>	1	16
<b>Vancomycin</b>	1	1

<sup>1</sup>N.D. = Not determined

### 1.2.3 Evaluation of most potent analogues against additional strains of *S. aureus*

The four most potent analogues from the initial screening (**1.9**, **1.15**, **1.20**, and **1.3**), together with **1.4** which had shown promising anti-MRSA activity (Table 1.1) were further evaluated against additional MRSA clinical isolates (Table 1.2). The *S. aureus* clinical isolates included strains resistant to linezolid (NRS119) and vancomycin (VRS10, VRS11a), two antibiotics frequently prescribed to treat MRSA infections. When evaluated against MRSA NRS384 (USA300), all five aryl isonitrile compounds inhibited growth at concentrations ranging from 1 – 4  $\mu\text{M}$ . Methoxy analog **1.9** (MIC = 1  $\mu\text{M}$ ) and bis-isonitrile **1.3** (MIC = 2  $\mu\text{M}$ ) were more

potent than first generation lead **1.2** (MIC = 4  $\mu$ M) against MRSA NRS384. However, quinoline isonitrile **1.15** (MIC = 4  $\mu$ M), bis-isonitrile **1.20** (MIC = 4  $\mu$ M), and pyridine isonitrile **1.4** (MIC = 4  $\mu$ M) exhibited similar potency to **1.2**. Against MRSA NRS119, **1.9** and **1.3** were the most potent analogues (MIC = 1  $\mu$ M), followed by **1.4** (MIC = 2  $\mu$ M), **1.15** (MIC = 4  $\mu$ M), and **1.20** (MIC = 4  $\mu$ M). Once again, the second-generation analogues **1.3** and **1.9** proved more potent than the first-generation lead **1.2** (MIC = 4  $\mu$ M). All five compounds were more potent than linezolid (MIC = 32  $\mu$ M) against MRSA NRS119. The MIC results obtained against MRSA NRS384 (USA300) and MRSA NRS119 (linezolid-resistant *S. aureus*) demonstrate that incorporating a second isonitrile functionality (as in compound **1.3**) improved the antibacterial activity of the first-generation lead molecule **1.2**.

Against two *S. aureus* strains (VRS10 and VRS11a) resistant to vancomycin (MIC > 64  $\mu$ M), compounds **1.3**, **1.4**, and **1.9** retained their antibacterial activity (MIC ranged from 2 – 8  $\mu$ M). Interestingly, **1.15** (MIC = 32  $\mu$ M) exhibited very poor antibacterial activity against VRS10. Thus, this compound was eliminated from further biological evaluation.

Table 1.2. Minimum inhibitory concentration (MIC, in  $\mu$ M) and MBC of the four most potent aryl isonitrile compounds and control antibiotics against methicillin-sensitive (MSSA), methicillin-resistant (MRSA), linezolid-resistant (LRSA), and vancomycin-resistant *S. aureus*.

Compound Name	MRSA NRS119 (LRSA)		MRSA NRS384 (USA300)		MRSA NRS385 (USA500)	VRS10 (VRSA)		VRS11a (VRSA)
	MIC	MBC	MIC	MBC	MIC	MIC	MBC	MIC
<b>1.3</b>	1	>64	2	>64	8	8	>64	8
<b>1.4</b>	2	>64	4	>64	N.D.	8	>64	8
<b>1.9</b>	1	>64	1	>64	4	2	>64	4
<b>1.15</b>	4	>64	4	>64	N.D.	32	>64	N.D.
<b>1.20</b>	2	4	4	>64	16	8	>64	16
<b>Linezolid</b>	32	64	2	16	4	2	32	2
<b>Vancomycin</b>	1	1	1	1	1	>64	>64	>64

<sup>1</sup>N.D. = Not determined

#### 1.2.4 *The aryl isonitrile compounds are bacteriostatic agents against MRSA*

Previously, the first-generation aryl isonitrile compounds were found to exhibit bacteriostatic activity against MRSA *in vitro*.<sup>10</sup> To determine if the second-generation aryl isonitriles exhibit a similar behavior, the minimum bactericidal concentration (MBC) against MRSA and VRSA was determined for the four most potent analogues (**1.3**, **1.4**, **1.9**, and **1.20**). The MBC was found to exceed 64  $\mu\text{M}$  for all four compounds against MRSA NRS123 (Table 1.1), MRSA NRS119, MRSA NRS384, and VRSA VRS10 (Table 1.2). The MBC values were more than three-fold higher than the MIC values for each compound, indicating these compounds are bacteriostatic. A similar result was observed for linezolid, an antibiotic previously shown to exhibit bacteriostatic activity against MRSA *in vitro*.<sup>10-12</sup> In order to confirm the aryl isonitrile compounds were in fact bacteriostatic agents against MRSA *in vitro*, a time-kill assay was conducted against MRSA NRS123 (USA400). A three-log decrease in MRSA CFU within 24 hours would be indicative of bactericidal activity. As depicted in Figure 1.4, no decrease in MRSA CFU was observed in the presence of  $4 \times \text{MIC}$  of compounds **1.3**, **1.4**, and **1.20** over the course of 24 hours, confirming the compounds possess bacteriostatic activity against MRSA *in vitro*. Interestingly, strong bacterial growth was observed in the presence of compound **1.9** after four hours ( $> 2\text{-log}_{10}$  increase). We observed the same result when the time-kill assay was repeated with **1.9**. This suggests a higher concentration/dose of **1.9** may be needed to achieve the same effect observed with the other three aryl isonitrile compounds. Linezolid (at  $4 \times \text{MIC}$ ) was able to decrease MRSA CFU by  $1.89\text{-log}_{10}$  over 24 hours, confirming its bacteriostatic activity *in vitro*.

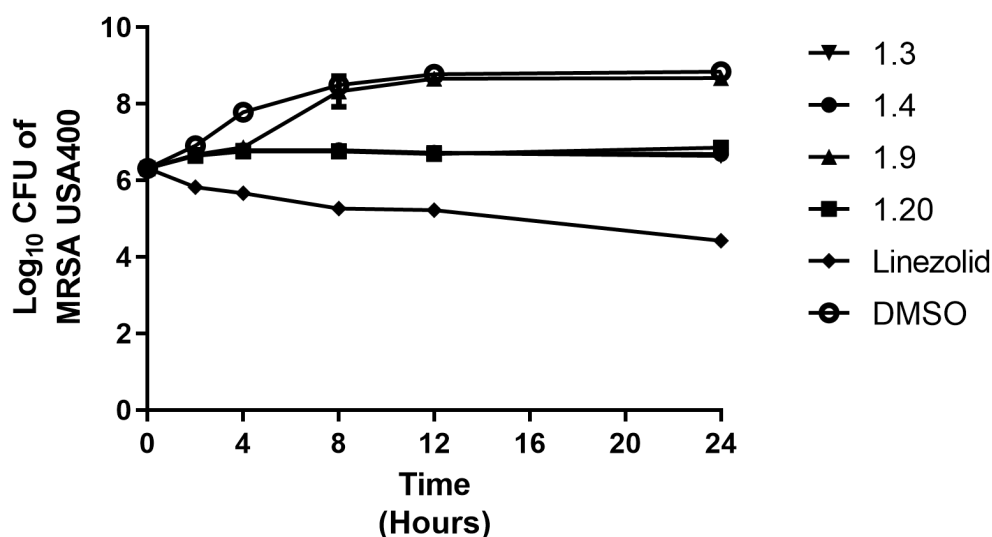


Figure 1.4. Time-kill analysis of aryl isonitrile compounds **1.3**, **1.4**, **1.9**, **1.20** and linezolid (all at  $4 \times \text{MIC}$ ) against methicillin-resistant *Staphylococcus aureus* (MRSA NRS123) over a 24-hour incubation period at  $37^\circ\text{C}$ . DMSO served as a negative.

### 1.2.5 Investigation of the antibacterial spectrum of activity of the aryl isonitrile compounds

To examine their spectrum of antibacterial activity, compounds **1.3**, **1.4**, **1.9**, and **1.20** were examined against clinical isolates from the ESKAPE pathogens (*Enterococcus faecium* (E), *Klebsiella pneumoniae* (K), *Acinetobacter baumannii* (A), *Pseudomonas aeruginosa* (P), and *Enterobacter* species (E) (Table 1.3). Collectively, these six pathogens are a significant source of hospital-acquired bacterial infections and exhibit resistance to most clinically available antibiotics.<sup>23, 24</sup> All four compounds were significantly less potent or inactive ( $\text{MIC} \geq 64 \mu\text{M}$ ) against vancomycin-resistant *E. faecium* (VRE), *K. pneumoniae*, *A. baumannii*, *P. aeruginosa*, and *E. cloacae*, similar to the antibiotics erythromycin, linezolid, and vancomycin. The compounds were also evaluated against two additional clinically-relevant Gram-positive bacterial pathogens, *Staphylococcus epidermidis* and *Streptococcus pneumoniae*. Three compounds exhibited potent activity against methicillin-resistant *S. epidermidis* ( $\text{MIC} = 1 \mu\text{M}$ ). Against, penicillin-resistant *S. pneumoniae*, **1.9** was the most potent compound ( $\text{MIC} = 4 \mu\text{M}$ ) followed by **1.3** ( $\text{MIC} = 8 \mu\text{M}$ ). Compound **1.20** was the least potent analogue against *S. pneumoniae* ( $\text{MIC} = 16 \mu\text{M}$ ).

Table 1.3. Minimum inhibitory concentration (MIC, in  $\mu\text{M}$ ) of the three most potent aryl isonitrile compounds and control antibiotics against clinically-relevant Gram-positive and Gram-negative bacterial pathogens..

Test Agent	Bacterial Strain						
	<i>S. epidermidis</i> NRS101	<i>S. pneumoniae</i> ATCC 700677	<i>E. faecium</i> ATCC700 221	<i>A. baumannii</i> BAA-1605	<i>E. cloacae</i> BAA-1134	<i>K. pneumoniae</i> ATCC BAA-1705	<i>Pseudomonas aeruginosa</i> ATCC 15442
<b>1.3</b>	1	8	>64	>64	>64	>64	>64
<b>1.4</b>	N.D.	N.D.	>64	>64	>64	>64	>64
<b>1.9</b>	1	4	>64	>64	>64	>64	>64
<b>1.20</b>	1	16	>64	>64	>64	>64	>64
<b>Erythromycin</b>	N.D. <sup>1</sup>	N.D.	N.D.	16	>64	>64	>64
<b>Linezolid</b>	2	2	0.50	>64	>64	>64	>64
<b>Vancomycin</b>	4	1	>64	32	>64	>64	>64

<sup>1</sup>N.D. = Not determined

#### 1.2.6 Effect of the outer membrane and efflux pump on antibacterial activity against Gram-negative bacterial pathogens

We hypothesized that the lack of antibacterial activity against Gram-negative bacteria observed for the aryl isonitrile compounds was due either to the presence of the outer membrane (OM) or due to expulsion via efflux pumps, two common resistance mechanisms utilized by Gram-negative bacterial pathogens.<sup>25</sup> The OM has been known to prevent numerous antibiotics (including erythromycin) from gaining entry into the bacterial cell at sufficient concentrations to bind to/inhibit the molecular target. To examine if the OM was impeding the antibacterial activity of the aryl isonitrile compounds, compound **1.3** and control antibiotics were incubated with the same Gram-negative bacterial species presented in Table 1.3 in the presence of a subinhibitory concentration of the membrane-permeabilizing agent colistin. As presented in Table 1.4, a noticeable improvement in the antibacterial activity of compound **1.3** was observed against *A. baumannii* (MIC = 16  $\mu\text{M}$ ) and *E. cloacae* (MIC = 4  $\mu\text{M}$ ) indicating the OM was having a deleterious effect on the antibacterial activity of this compound. Interestingly, no improvement in antibacterial activity for **1.3**, in the presence of colistin, was observed against *K. pneumoniae* and *P. aeruginosa*, (similar to linezolid) suggesting the presence of the outer membrane was not solely

responsible for the lack of activity observed in these particular pathogens. The antibacterial activity of the antibiotic erythromycin, in the presence of colistin, improved against *A. baumannii* (MIC = 4  $\mu$ M), *E. cloacae* (MIC = 1  $\mu$ M), *K. pneumoniae* (MIC = 16  $\mu$ M), and *P. aeruginosa* (MIC = 4  $\mu$ M). Erythromycin is thought to be capable of diffusing across the OM but at a very slow rate.<sup>26</sup> Thus permeabilizing the OM is expected to enhance penetration of the antibiotic into bacterial cells.

We next examined if the presence of efflux pumps may be responsible for the lack of antibacterial activity observed for the aryl isonitrile compounds against Gram-negative bacteria (Table 1.4). These pathogens express different efflux pumps that confer resistance to numerous antibiotics including the AdeIJK efflux pump in *A. baumannii*, AcrAB-TolC efflux pump (present in *E. coli*, *E. cloacae*, and *K. pneumoniae*) and its homologue MexAB-OprM (expressed by *P. aeruginosa*).<sup>26, 27</sup> We evaluated the antibacterial activity of **1.3** against an *Escherichia coli* strain (JW25113) deficient in the AcrAB-TolC efflux pump responsible for excluding many xenobiotics from accumulating inside *E. coli* cells.<sup>25</sup> No discernible improvement in antibacterial activity of **1.3** was observed against the mutant *E. coli* strain relative to the wild-type strain (BW25113). In contrast, there was noticeable improvement in the antibacterial activity of erythromycin (MIC = 2  $\mu$ M) and linezolid (MIC = 16  $\mu$ M), two substrates of the AcrAB-TolC efflux pump.<sup>26, 28</sup> This suggests that the presence of efflux pumps alone on the surface of the OM on Gram-negative bacteria may not be responsible for conferring resistance to the aryl isonitrile compounds. We next investigated if the combination of the outer membrane and efflux pumps may impede the antibacterial activity of the aryl isonitrile compounds. The compound and control antibiotics were incubated with a subinhibitory concentration of colistin against *E. coli* BW25113 and *E. coli* JW25113. No improvement in the antibacterial activity of **1.3** (MIC > 64  $\mu$ M) was observed in the presence of colistin against *E. coli* JW25113. Similarly, no improvement in the MIC of linezolid was observed against *E. coli* JW25113 in the absence and presence of colistin, indicating the lack of antibacterial activity of linezolid observed against *E. coli* is due primarily to efflux. The MIC of erythromycin against *E. coli* JW25113, in contrast, improved one-fold in the presence of colistin indicating both the OM and efflux pumps interfere with the effect of this antibiotic against Gram-negative bacteria, in agreement with previous reports.<sup>26, 29</sup> Due to the lack of antibacterial activity observed against VRE and Gram-negative bacterial pathogens, we moved to evaluate the aryl isonitrile compounds antibacterial activity *in vivo* against MRSA

Table 1.4. Minimum inhibitory concentration (MIC, in  $\mu\text{M}$ ) of **1.3** and control antibiotics against Gram-negative bacterial pathogens in the presence of a subinhibitory concentration of colistin (COL).

Test Agent	Bacterial Strain							
	<i>A. baumannii</i> BAA-1605	<i>E. cloacae</i> BAA-1134	<i>K. pneumoniae</i> ATCC BAA-1705	<i>P. aeruginosa</i> ATCC 15442	<i>E. coli</i> BW25113		<i>E. coli</i> JW25113 ( $\Delta\text{tolC}$ )	
					(- COL) <sup>1</sup>	(+COL)	(- COL)	(+COL)
<b>1.3</b>	16	4	>64	>64	>64	>64	>64	>64
Erythromycin	4	1	16	4	64	1	2	0.50
Linezolid	>64	16	>64	>64	>64	>64	16	16

<sup>1</sup> No colistin added to the media

### 1.2.7 *In silico* pharmacokinetic evaluation of compound **1.3**

MRSA is a source of infection for both superficial skin lesions and complicated systemic infections. To determine a suitable animal model of MRSA infection to evaluate the aryl isonitrile compounds, the pharmacokinetic profile of compound **1.3** and linezolid were simulated utilizing a dose of 600 mg (as is commonly administered for linezolid in adult human patients). As shown in Table 1.5, the results indicate that compound **1.3** would not be suitable for oral administration for the treatment of systemic MRSA infections as it is not expected to attain a concentration in plasma/blood sufficient to inhibit bacterial growth. The maximum plasma concentration ( $C_{\text{max}}$ ) predicted for compound **1.3** is 0.17  $\mu\text{g/mL}$  (0.73  $\mu\text{M}$ ), whereas the MIC against MRSA ranges from 1 to 8  $\mu\text{M}$ . Intravenous administration of compound **1.3** is predicted to result in a slow rate of clearance (12.58 mL/min-kg) correlating with a long half-life (22.90 hours) which could alleviate the need for multiple daily dosing. The high values obtained for the volume of distribution at steady-state for **1.3** (24.94 L/kg compared to 1.11 L/kg for linezolid) indicate this compound is expected to distribute extensively into tissues. This may be due to the high degree of lipophilicity ( $\text{cLogP} = 3.88$ ) present with the compound. These pharmacokinetic simulations suggest that though intravenous administration of **1.3** may be possible for treatment of systemic MRSA infections, the extensive distribution of the compound into tissues would necessitate a higher dose

be administered/continuous infusion of compound (to ensure the concentration remained above the MIC to inhibit MRSA growth). The values obtained for linezolid via the *in silico* pharmacokinetic simulation overall were in close proximity to experimental values obtained by Stalker, *et al.* from healthy human subjects administered a single 625 mg dose of linezolid either orally or intravenously.<sup>30</sup> However, the simulation underestimated the  $C_{\max}$  for linezolid and overestimated the half-life and volume of distribution compared to the experimental values. Based upon the *in silico* pharmacokinetic simulation, **1.3** appears most suitable for evaluation topically to treat localized/uncomplicated MRSA skin infections.

Table 1.5. *In silico* pharmacokinetic analysis for **1.3** and linezolid (simulated at 600 mg).

	Oral			Intravenous		Linezolid (Experimental)
	<b>1.3</b> (Simulated)	Linezolid (Simulated)	Linezolid (Experimental) <sup>1</sup>	<b>1.3</b> (Simulated)	Linezolid (Simulated)	
$C_{\max}$ <sup>2</sup> ( $\mu\text{g/mL}$ )	0.17	5.33	12.7	-	-	13.4
$t_{\max}$ <sup>3</sup> (hours)	3	2.75	1.33	-	-	0.5
Fraction absorbed ( $FA_{\text{last}}$ )	0.80	0.92	1.03	-	-	-
CL <sup>4</sup> (mL/min-kg)	-	-	-	12.58	1.09	1.74 <sup>9</sup>
$t_{1/2}$ <sup>5</sup> (hours)	-	-	-	22.90	12.31	4.40
MRT <sup>6</sup> (hours)	-	-	-	12.82	17.04	-
$V_d$ <sup>7</sup> (L/kg)	-	-	-	24.94	1.11	0.58 <sup>10</sup>
$V_{ss}$ <sup>8</sup> (L/kg)	-	-	-	9.68	1.12	-

<sup>1</sup>(adapted from Stalker DJ *et al.* *J Antimicrob Chemother* **2003**, 51: 1239–46 (Table 2, 625 mg dose))

<sup>2</sup> $C_{\max}$  = maximum concentration of drug in plasma/blood; <sup>3</sup> $t_{\max}$  = time required to reach  $C_{\max}$

<sup>4</sup>CL = rate of clearance; <sup>5</sup> $t_{1/2}$  = half-life; <sup>6</sup>MRT = mean residence time

<sup>7</sup> $V_d$  = volume of distribution; <sup>8</sup> $V_{ss}$  = volume of distribution at steady-state

<sup>7</sup>Clearance for linezolid (experimental) obtained by dividing the mean clearance value by the mean weight of patients

<sup>8</sup>Volume of distribution for linezolid (experimental) obtained by dividing the mean  $V_d$  by the mean weight of patients.

### 1.2.8 The active aryl isonitrile compounds are safe to mammalian keratinocytes

*S. aureus* is a leading source of skin and soft tissue infections, both uncomplicated and invasive, globally.<sup>31-34</sup> As such, based upon the *in silico* pharmacokinetic data, we decided to investigate the antibacterial activity of the second-generation aryl isonitriles as topical antibacterial agents in a MRSA murine skin infection mouse model. Before exposing mice to the compounds, we evaluated the safety profile of **1.3**, **1.4**, **1.9**, and **1.20** against keratinocytes (HaCaT). All four compounds were safe up to the maximum tested concentration of 128  $\mu\text{M}$  (more than 90% of HaCaT cells remained viable after 24 hours of exposure to the compounds) (Figure 1.5).

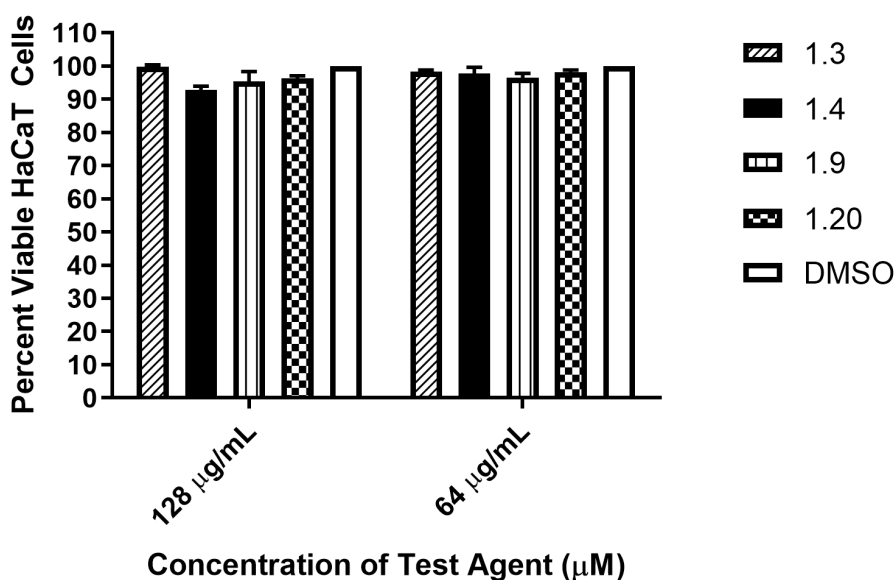


Figure 1.5. Toxicity analysis of aryl isonitrile compounds against human keratinocytes (HaCaT).

Percent viable mammalian cells (measured as average absorbance ratio (test agent relative to DMSO)) for cytotoxicity analysis of compounds **1.3**, **1.4**, **1.9**, and **1.20** (tested in triplicate) at 64 and 128  $\mu\text{M}$  against HaCaT cells over a 24 hour period using the MTS 3-(4,5-dimethylthiazol-2-yl)-5-(3-carboxymethoxyphenyl)-2-(4-sulfophenyl)-2H-tetrazolium assay. Dimethyl sulfoxide (DMSO) was used as a negative control to determine a baseline measurement for the cytotoxic impact of each compound. The absorbance values represent an average of a minimum of three samples analyzed for each compound. Error bars represent standard deviation values. A one-way ANOVA, with post-hoc Dunnet's multiple comparisons test, determined statistical difference between the values obtained for each compound and DMSO ( $P < 0.05$ ).

### 1.2.9 The aryl isonitrile compounds effectively reduce the burden of MRSA in a murine skin infection model

After confirming the aryl isonitrile compounds are safe to keratinocytes, the antibacterial activity of the compounds was investigated in a mouse model of MRSA skin infection. Compounds **1.3** and **1.4** were selected for this experiment. **1.9** was excluded from evaluation as the compound was ineffective in reducing the burden of MRSA *in vitro* in the time-kill assay. Given **1.3** and **1.20** are structurally similar, the most potent compound *in vitro* against MRSA USA300 was selected for evaluation. MRSA USA300 was used to infect mice as this particular strain is the most frequently isolated MRSA strain from skin and soft tissue infections in the United States.<sup>21</sup> After the formation of an abscess at the site of infection, mice were treated twice daily for five days. As the skin wounds were uncomplicated and localized, treatment was administered topically directly onto the surface of the abscesses. Mice were euthanized 12 hours after the last dose was administered and the abscesses were harvested to enumerate MRSA CFU. As presented in Figure 1.6, both compounds **1.4** (74.10% reduction) and **1.3** (79.02% reduction) were as effective as the control antibiotic fusidic acid (77.78% reduction) in reducing the burden of MRSA in the wounds of infected mice after five days of treatment. No excess inflammation (redness or swelling around the wound site) or toxicity was observed in wounds after exposure to the compounds or fusidic acid.

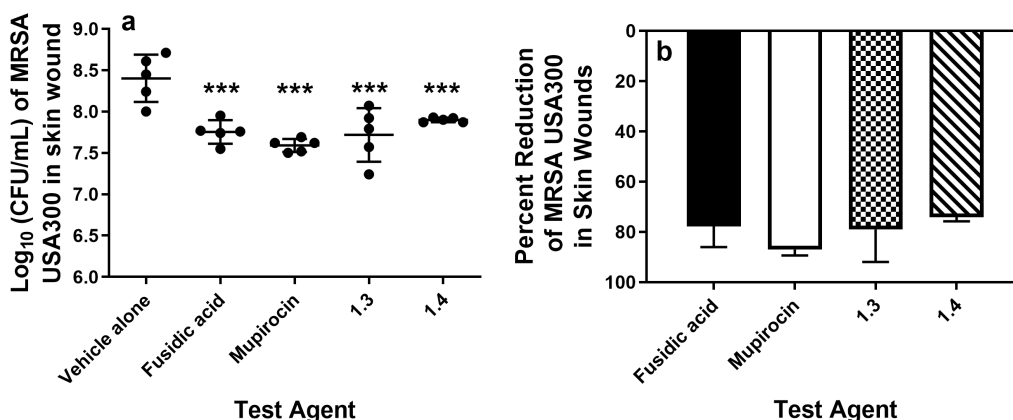


Figure 1.6. Reduction of MRSA USA300 in infected lesions of mice.

Average percent reduction of MRSA CFU/mL in murine skin lesions after treatment with **1.3**, **1.4**, or fusidic acid. A one-way ANOVA with post-hoc Dunnet's multiple comparisons found no statistical difference between mice treated with fusidic acid and mice treated with compound **1.3** or **1.4**.

### 1.2.10 Compound **1.4** exhibits good permeability and is stable to hepatic metabolism

The successful performance of **1.4** in reducing the burden of MRSA in a localized murine skin infection model led us to investigate the effectiveness of this compound in treating a systemic MRSA infection. Due to an inability to effectively formulate **1.3** in a suitable vehicle to administer orally/intravenously in mice, we removed this compound from the MRSA systemic mice study. Prior to investigating the efficacy of **1.4** in a systemic MRSA mouse model, we evaluated the compound's ability to permeate across the gastrointestinal (GI) tract and its stability to hepatic metabolism. To simulate **1.4**'s ability to cross the GI tract, the compound was evaluated in a Caco-2 bidirectional permeability assay (Table 1.6). The compound rapidly permeated across the Caco-2 monolayer from the apical to basolateral compartment (mean apparent permeability rate of  $36.20 \times 10^{-6}$  cm/sec) similar to the high permeability control drug propranolol (mean apparent permeability rate of  $46.50 \times 10^{-6}$  cm/sec). The low efflux ratio (0.33) observed for **1.4** indicates the compound most likely is not a substrate for P-glycoprotein, a major source of efflux of compounds/drugs from the GI tract.

Table 1.6. Caco-2 bidirectional permeability analysis for compounds **1.4**.

Test Article	Mean A→B $P_{app}$ ( $10^{-6}$ cm/sec)	Mean B→A $P_{app}$ ( $10^{-6}$ cm/sec)	Efflux ratio <sup>1</sup>	Notes
Colchicine	0.20	4.90	24.50	P-gp substrate
Ranitidine	0.40	2.00	5.00	Poor-permeability control
Labetolol	17.40	41.40	2.38	Moderate-permeability control
Propranolol	46.50	59.30	1.28	High-permeability control
<b>1.4</b>	36.20	12.00	0.33	High permeability

<sup>1</sup>Efflux ratio =  $P_{app}$  (B → A)/ $P_{app}$  (A → B)

Next, we assessed the stability of **1.4** to hepatic metabolism by incubating the compound with pooled human liver microsomes (Table 1.7). The compound was slowly cleared by hepatic microsomes (mean intrinsic rate of clearance <115.50  $\mu$ L/min-mg) resulting in an excellent half-life of over 11 hours. This exceeded the result obtained for two of the positive control drugs,

propranolol (>2 hours) and imipramine (>2 hours). The long half-life observed for **1.4** suggests that once daily dosing may be a viable option for treatment of MRSA infections.

Table 1.7. Metabolic stability evaluation for compound **1.4** in human liver microsomes.

Test Article	Mean CL <sub>int</sub> (μL/min-mg)	Mean t <sub>1/2</sub> (minutes)	Notes
Terfenadine	752.20	9.25	High clearance control
Verapamil	352.20	20	High clearance control
Propranolol	<115.50	131.50	Low clearance control
Imipramine	<115.50	129.90	Low clearance control
<b>1.4</b>	<115.50	660.50	Stable to hepatic metabolism

#### 1.2.11 *Compound 1.4 successfully reduced the burden of MRSA in a neutropenic thigh infection mouse model*

Compound **1.4** was next evaluated in the MRSA neutropenic thigh infection mouse model. Mice were infected with MRSA USA300 and subsequently treated twice (2 and 12 hours post-infection) with 20 mg/kg of either **1.4** or linezolid. One day post-infection, mice were humanely euthanized, and the infected thighs were harvested to enumerate MRSA CFU. As presented in Figure 1.7, **1.4** produced a statistically significant reduction in MRSA USA300 (75.44% reduction) when compared to mice receiving the vehicle alone. This was similar to the positive control antibiotic, linezolid (91.66% reduction), at the same test concentration (20 mg/kg).

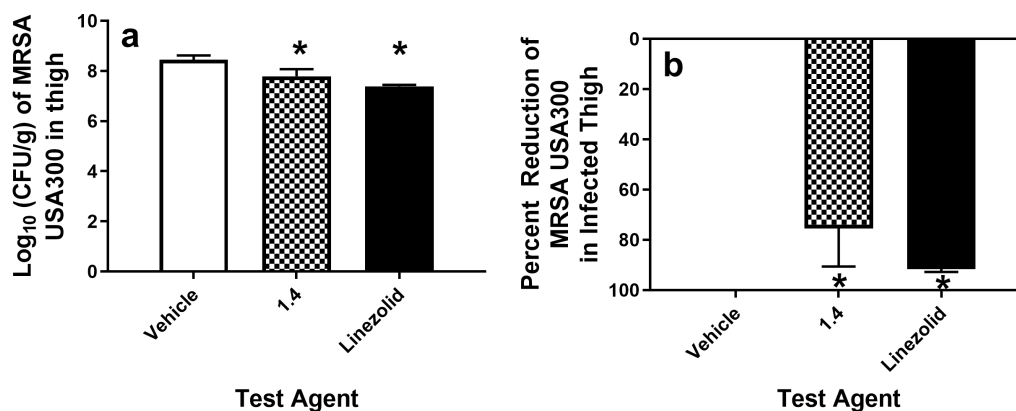


Figure 1.7. Reduction of MRSA USA300 in infected thigh of mice after treatment with **1.4** or linezolid. Average percent reduction of MRSA CFU/g tissue in murine right thighs. A one-way ANOVA with post-hoc Dunnet's multiple comparisons found statistical significance for mice treated either with **1.4** or linezolid (\*,  $P < 0.05$ ) compared to mice receiving the vehicle (10% DMSO, 10% Tween 80, 80% PBS) alone.

### 1.3 Discussion

Antimicrobial agents have played a crucial role in stemming the problem of bacterial infection over the decades. Nonetheless, bacteria have shown to be capable of acquiring resistance to multiple antibiotics. As such, there is a continuous need to discover and develop novel antibacterial agents capable of treating drug-resistant bacterial infections. MRSA remains a significant cause of superficial and invasive antibiotic-resistant infections worldwide. Though several antibacterial agents effective against MRSA are currently in clinical trials, the remarkable ability of this organism to develop resistance to different antibiotics necessitates new antibacterial agents, particularly from unexploited scaffolds, be discovered and developed.

Our research lab, in an effort to discover novel entities for drug discovery, previously synthesized and evaluated over 40 aryl isonitrile compounds for antimicrobial activity against MRSA.<sup>10</sup> The first-generation compounds inhibited MRSA growth at concentrations ranging from 2 – 64  $\mu\text{M}$ <sup>10</sup> but none of the compounds possessed a suitable physicochemical profile to evaluate their effectiveness in an animal model of MRSA infection. The present study aimed to expand the library of aryl isonitrile compounds to better understand these limitations and further characterize the compounds' structure-antibacterial activity relationship. To this end, 20 second-generation aryl isonitrile compounds consisting of stilbene bis-isonitriles, stilbene aryl isonitriles with

medicinally-relevant molecules and heterocyclic moieties, and those with a saturated linker were synthesized and evaluated for antibacterial activity.

The newly synthesized analogues were initially evaluated against a clinical isolate of MRSA USA400. From the initial screening, inclusion of an additional isonitrile moiety, the stilbene core, and the non-isonitrile-bearing aromatic ring all proved essential for anti-MRSA activity. Four compounds (**1.3**, **1.4**, **1.9**, and **1.20**) inhibited growth of MRSA at a concentration ranging from 2 – 8  $\mu$ M, similar to the lead compound (**1.2**) from the first-generation aryl isonitriles. Bis-isonitrile **1.3** was more potent than the first-generation lead **1.2** against MRSA NRS384 (USA300) and MRSA NRS119 (LRSA) which further confirmed the importance of the isonitrile functionality.

Importantly, four compounds retained potent antibacterial activity against MRSA isolates exhibiting resistance to vancomycin and linezolid, antibiotics frequently used as agents of last resort for treatment of MRSA infections.<sup>35,36</sup> Though not prevalent clinically, the identification of *S. aureus* strains exhibiting resistance to vancomycin and linezolid, two key therapeutic options for treatment of MRSA infections, is a noteworthy problem. The lack of cross-resistance observed between the aryl isonitrile compounds and vancomycin and linezolid is important therapeutically as it provides a potential alternative source of treatment against linezolid-resistant and vancomycin-resistant *S. aureus* infections.

Previously, the first-generation aryl isonitrile analogues were only evaluated against clinical isolates of *S. aureus*. We were curious to investigate the spectrum of antibacterial activity of the second-generation aryl isonitrile compounds. Thus, four of the most potent analogues against MRSA (**1.3**, **1.4**, **1.9**, and **1.20**) were evaluated against a panel of clinically-relevant pathogens, including members of the ESKAPE group, *S. epidermidis*, and *S. pneumoniae*. The compounds exhibited potent antibacterial activity against the Gram-positive pathogens *S. epidermidis* and *S. pneumoniae*. Interestingly, the compounds were inactive against vancomycin-resistant *E. faecium*. The lack of antibacterial activity against VRE (a Gram-positive pathogen similar to MRSA) is not entirely surprising given certain antibiotics that are active against *S. aureus* (such as ampicillin and vancomycin) are inactive against vancomycin-resistant *E. faecium*.<sup>37</sup> The aryl isonitrile compounds also showed no antibacterial activity against five Gram-negative bacterial pathogens tested (*A. baumannii*, *K. pneumoniae*, *E. cloacae*, *E. coli*, and *P. aeruginosa*). The lack of antibacterial activity against Gram-negative pathogens is not surprising

given most small molecules are unable to permeate the complex outer membrane (OM) present in Gram-negative bacteria. Those that are capable of diffusing across the OM may be susceptible to expulsion (decreasing the intracellular concentration of compound/drug) by a number of different efflux pumps expressed by Gram-negative bacteria, including the AcrAB-TolC pump present in *E. coli*.<sup>25</sup> Thus we evaluated the antibacterial activity of the aryl isonitrile compounds after permeabilizing the OM (using a subinhibitory concentration of colistin) and against an *E. coli* strain deficient in the AcrAB-TolC efflux pump. Interestingly, there was improvement in the MIC for compound **1.3** observed in the presence of colistin against *A. baumannii* and *E. cloacae* but not against *E. coli*, *K. pneumoniae*, and *P. aeruginosa*. Against a mutant *E. coli* strain deficient in AcrAB-TolC, no improvement in the MIC of **1.3** was observed indicating that this compound may not be a substrate for efflux. This suggests that though the outer membrane may contribute to the lack of antibacterial activity for the aryl isonitrile compounds observed against specific Gram-negative bacterial pathogens, additional resistance mechanism(s) may play a role as well. Alternatively, the compounds may have a weaker affinity for the molecular target in Gram-negative bacteria as opposed to against MRSA, *S. epidermidis*, and *S. pneumoniae*. Though the molecular target of the aryl isonitrile compounds is currently unknown, this question is being intensely investigated using both genetic and phenotypic approaches. Identification of the molecular target may provide key insight into the difference in potency observed for the aryl isonitrile compounds against *S. aureus* relative to other bacterial pathogens.

The aryl isonitrile compounds possessed good *in vitro* activity against drug-resistant *S. aureus* isolates and were safe to mammalian cells (non-toxic to human keratinocytes at 128  $\mu$ M, more than 30-fold higher than the concentration where they inhibited MRSA growth *in vitro*). However, an *in silico* pharmacokinetic evaluation of **1.3** revealed this compound may not be effective in treatment of systemic MRSA infections (as the maximum predicted concentration of the compound in plasma was lower than the MIC of the compound against MRSA).

Furthermore, when investigated in a multi-step resistance selection experiment, no MRSA mutants exhibiting resistance to **1.4** were isolated, even after 14 passages. This suggests that repeated exposure/dosing to this compound is unlikely to induce resistant MRSA mutants to emerge rapidly. These important features led us to investigate if the aryl isonitrile compounds could retain their antibacterial activity *in vivo* in a relevant animal model of MRSA infection.

Based upon the *in vitro* antibacterial activity assay results and *in silico* pharmacokinetic simulation, we proceeded to evaluate the effectiveness of **1.3** together with **1.4** as a topical antibacterial to treat MRSA skin infection. MRSA remains a major source of skin and soft tissue infections (SSTIs) throughout the world.<sup>31-34,38,39</sup> Treatment of SSTIs can be challenging given the emergence of resistance to several antibiotics frequently used in the clinic. One example is the antibiotic fusidic acid, which is prescribed for use topically in Europe for the treatment of SSTIs. Extensive use of fusidic acid has resulted in the emergence of resistant isolates<sup>40</sup> that necessitates new therapeutic agents to treat uncomplicated, localized *S. aureus* SSTIs. In the United States of America, MRSA USA300 is the predominant strain linked to community-acquired SSTIs.<sup>41</sup> As such, we moved to evaluate the efficacy of compound **1.3** and **1.4** administered topically in a MRSA USA300 skin wound mouse model. Both compounds significantly reduced the burden of MRSA USA300 in infected abscesses by over 70% (after only five days of treatment) in a manner similar to fusidic acid, an agent used topically in Europe to treat MRSA skin infections.<sup>42</sup>

The promising result obtained from the MRSA skin wound mouse model piqued our interest to evaluate the aryl isonitrile compounds in a systemic MRSA infection mouse model. Unfortunately, the lead compound (**1.2**) identified from the first-generation aryl isonitrile compounds exhibited a limited physicochemical profile that precluded its evaluation in a suitable animal model of MRSA systemic infection. This finding is not unexpected as many early-stage lead compounds tend to exhibit a poor physicochemical profile and necessitate further optimization.<sup>43</sup> It has been observed that compounds with a  $\log P$  ranging from 1 – 4 tend to exhibit optimal physicochemical properties, particularly for drugs administered systemically.<sup>43</sup> We suspected that the stilbene backbone in **1.2** ( $\log P = 4.22$ ) resulted in a highly lipophilic molecule susceptible to hepatic metabolism. Due to the fact that their binding site is lipophilic, enzymes responsible for metabolism tend to bind more tightly to lipophilic compounds. Substitution of a benzene ring with a pyridine group is one strategy that has been employed by medicinal chemists to improve the stability of a molecule to hepatic metabolism by decreasing the molecule's lipophilicity.<sup>44</sup> Using this approach, the benzene ring (lacking the isonitrile moiety) in **1.2** was substituted with a pyridine (compound **1.4**,  $\log P = 3.16$ ). This molecule was subsequently evaluated for stability to hepatic metabolism by incubating the compound with human liver microsomes.

As anticipated, a noticeable improvement in metabolic stability for **1.4** was observed. Compound **1.2** was previously found to exhibit a half-life of less than one hour.<sup>10</sup> Compound **1.4**, in contrast, exhibited a significantly improved half-life of over 11 hours, which may permit once daily dosing (ideal for patient compliance). It is important to note that the benzene to pyridine substitution can result in a loss of biological activity, given lipophilic groups play an important role in binding to the molecular target.<sup>44</sup> However, no loss in the antibacterial activity *in vitro* for **1.4** (relative to compound **1.2**) was observed against MRSA. In addition to the improvement in metabolic stability observed for compound **1.4**, there was a significant improvement in the molecule's ability to permeate across the GI tract. Previously, compound **1.2** was unable to cross the GI tract as simulated by the Caco-2 bidirectional permeability assay (mean apparent permeability rate of  $0.0 \times 10^{-6}$  cm/sec).<sup>9</sup> Remarkably, **1.4** exhibited a pronounced improvement in the ability to permeate across the Caco-2 bilayer (mean apparent permeability rate from the apical to basolateral compartment of  $36.20 \times 10^{-6}$  cm/sec), suggesting oral dosing of this molecule may be possible.

Buoyed by the positive improvement in the physicochemical profile and lack of resistance emergence against MRSA observed with **1.4**, we moved to evaluate this compound in a MRSA neutropenic thigh infection mouse model. This model evaluates the efficacy of an antibacterial agent in the absence of the host's innate immune response and exhibits excellent translatability to the efficacy of a drug/compound in humans. After only two doses of **1.4** (at 20 mg/kg), a significant reduction (75.44% reduction) in MRSA CFU was observed in the infected thighs of mice, relative to mice receiving the vehicle alone. This was lower than the result observed for the control antibiotic, linezolid (91.66% reduction), at the same test concentration.

We hypothesized that the difference in effectiveness *in vivo* between **1.4** and linezolid in the murine thigh infection model may be due to binding to serum proteins (decreasing the free fraction of compound available in circulation). This would necessitate increasing the size or frequency of doses administered to account for the reduced free fraction of compound in circulation. The MIC of **1.4** and the control antibiotic linezolid was determined against MRSA USA300 via the broth microdilution assay, in the presence and absence of a physiological concentration (4%) of human serum albumin (the major protein component present in serum) (Supplementary Table 2).<sup>45</sup> The MIC of **1.4** against MRSA USA300 did increase seven-fold from 1  $\mu\text{g/mL}$  to 8  $\mu\text{g/mL}$ , in the presence of serum albumin. Though this increase may partially

interfere with **1.4**'s antibacterial activity if administered systemically, using a higher concentration of the compound could potentially resolve this issue. No increase in the MIC of linezolid was observed in the presence of serum albumin, in agreement with a previous report.<sup>45</sup>

## 1.4 Conclusion

In conclusion, the present study identified four new aryl isonitrile compounds bearing potent antibacterial activity against MRSA *in vitro*. The analogues were inactive against important Gram-negative bacterial pathogens, and their activity appeared to be negatively impacted by the presence of the outer membrane. The newly synthesized analogues were safe to keratinocytes at concentrations up to 128  $\mu$ M. **1.3** and **1.4** significantly reduced the burden of MRSA in infected wounds in a mouse model of MRSA skin infection. However, *in silico* pharmacokinetic simulation revealed compound **1.3** would not effectively permeate across the GI tract and may extensively distribute into tissues thus precluding its evaluation in a systemic animal model of MRSA infection. Beyond its potency against MRSA, safety to mammalian cells, lack of MRSA resistance formation, and enhanced physicochemical profile, **1.4** significantly reduced the burden of MRSA in both a murine skin infection model and neutropenic thigh infection model. However, **1.4** appears to bind to serum albumin which slightly reduced its effectiveness (when compared to linezolid) when administered systemically. Addressing these limitations and deducing the molecular target of new leads **1.3** and **1.4** are necessary questions to resolve to further develop aryl isonitrile compounds as a novel class of antibacterial agents to treat drug-resistant *S. aureus* infections.

## 1.5 Experimental Section

### 1.5.1 General Chemistry

All chemical reactions were performed using standard syringe techniques under argon unless otherwise stated. Starting materials and reagents were used as received from commercial suppliers. Acetonitrile (CH<sub>3</sub>CN), methanol (MeOH), and toluene were purified by passing the previously degassed solvents through activated alumina columns. Dichloromethane (CH<sub>2</sub>Cl<sub>2</sub>) and tetrahydrofuran (THF) were distilled prior to use.

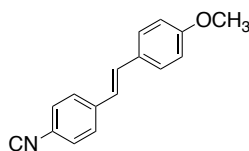
All compounds were purified using flash chromatography with silica gel (230-400 mesh). Thin layer chromatography (TLC) was performed using glass-backed silica plates (Silicycle).

NMR spectra were recorded on a Bruker ARX-400 spectrometer or AV-500 spectrometer at room temperature. Chemical shifts  $\delta$  (in ppm) are given in reference to the solvent signal [ $^1\text{H}$  NMR:  $\text{CDCl}_3$  (7.26);  $^{13}\text{C}$  NMR:  $\text{CDCl}_3$  (77.2)].  $^1\text{H}$  NMR data are reported as follows: chemical shifts ( $\delta$  ppm), multiplicity (s = singlet, d = doublet, t = triplet, q = quartet, quin = quintuplet, m = multiplet, br = broad), coupling constant (Hz), and integration.  $^{13}\text{C}$  NMR data are reported in terms of chemical shift and multiplicity. IR data were recorded on a Thermo Nicolet Nexus 470 FTIR. High-resolution mass measurements for compound characterization were determined using a FinniganMAT XL95 double focusing mass spectrometer system.

All compounds for biological testing were confirmed to be of >95% purity based on HPLC.

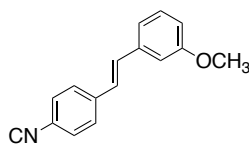
*General procedure for the synthesis of stilbene aryl isonitriles 1.8-1.16 from 1.7.*

A solution of *n*-BuLi (2.5 M in hexane, 0.2 ml, 0.46 mmol, 1.15 equiv) was added dropwise to a stirring solution of diisopropyl amine (53 mg, 0.52 mmol, 1.3 equiv) in THF (1.5 ml) at  $-78\text{ }^\circ\text{C}$ . After stirring for 5 mins at  $-78\text{ }^\circ\text{C}$ , a solution of diethyl (4-isocyanobenzyl)phosphonate **5** (100 mg, 0.40 mmol, 1 equiv) in THF (1 ml) was added dropwise, after which the solution was allowed to sit and stir for 30-60 mins. Still at  $-78\text{ }^\circ\text{C}$ , the respective aldehyde (0.36 mmol, 0.9 equiv) dissolved in THF (1 ml) was added dropwise and allowed to sit and stir for an additional 30-40 mins. The resulting mixture was then warmed to room temperature and stirred for 2 h. Water, saturated aqueous ammonium chloride and  $\text{Et}_2\text{O}$  were added. The aqueous layer was then extracted with  $\text{Et}_2\text{O}$  (3x) followed by the washing of the combined organic fractions with brine. The organic layer was then dried over anhydrous sodium sulfate and concentrated *in vacuo*. The crude residue was purified by flash column chromatography to obtain the required stilbene aryl isonitrile.

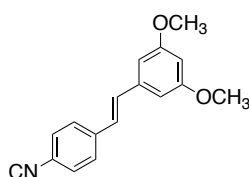


**1.8**

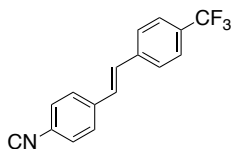
**(E)-1-isocyano-4-(4-methoxystyryl)benzene (1.8).** Analogue **1.8** was synthesized from intermediate **1.7** and 4-methoxybenzaldehyde according to the general procedure (70% yield).  $^1\text{H}$  NMR (500 MHz,  $\text{CDCl}_3$ )  $\delta$  7.47 (dd,  $J = 11.6, 8.6$  Hz, 4H), 7.34 (d,  $J = 8.5$  Hz, 2H), 7.08 (d,  $J = 16.3$  Hz, 1H), 6.96 – 6.88 (m, 3H), 3.84 (s, 3H);  $^{13}\text{C}$  NMR (125 MHz,  $\text{CDCl}_3$ )  $\delta$  164.27, 159.85, 138.96, 130.66, 129.34, 128.06 (2C), 126.90 (2C), 126.71 (2C), 124.85, 124.64, 114.27 (2C), 55.37; IR (neat,  $\text{cm}^{-1}$ ):  $\nu = 3054, 3021, 2963, 2935, 2840, 2122, 1603, 1596, 1573, 1512, 1458, 1424, 1307, 1297, 1267, 1253, 1175, 1031, 972, 835$ . HRMS (ESI):  $m/z = 236.1070$  calculated for  $\text{C}_{16}\text{H}_{14}\text{NO}$   $[\text{M}+\text{H}]^+$ , found 236.1072

**1.9**

**(E)-1-(4-isocyanostyryl)-3-methoxybenzene (1.9).** Analogue **1.9** was synthesized from intermediate **1.7** and 3-methoxybenzaldehyde according to the general procedure (53% yield).  $^1\text{H}$  NMR (500 MHz,  $\text{CDCl}_3$ )  $\delta$  7.51 (d,  $J = 8.5$  Hz, 2H), 7.36 (d,  $J = 8.5$  Hz, 2H), 7.30 (t,  $J = 7.9$  Hz, 1H), 7.13 – 7.02 (m, 4H), 6.86 (ddd,  $J = 8.3, 2.5, 0.9$  Hz, 1H), 3.85 (s, 1H);  $^{13}\text{C}$  NMR (125 MHz,  $\text{CDCl}_3$ )  $\delta$  164.56, 159.97, 138.50, 137.99, 131.02, 129.81, 127.26 (2C), 127.09 (2C), 126.75, 125.30, 119.47, 113.95, 112.06, 55.31. IR (neat,  $\text{cm}^{-1}$ ):  $\nu = 3088, 3060, 3019, 2964, 2943, 2840, 2125, 2089, 1600, 1576, 1568, 1506, 1432, 1274, 1257, 1173, 1050, 973, 862, 781$ . HRMS (ESI):  $m/z = 236.1070$  calculated for  $\text{C}_{16}\text{H}_{14}\text{NO}$   $[\text{M}+\text{H}]^+$ , found 236.1071.

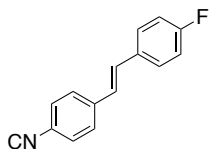
**1.10**

**(E)-1-(4-isocyanostyryl)-3,5-dimethoxybenzene (1.10)**. Analogue **1.10** was synthesized from intermediate **1.7** and 3,5-dimethoxybenzaldehyde according to the general procedure (79% yield).  $^1\text{H}$  NMR (500 MHz,  $\text{CDCl}_3$ )  $\delta$  7.51 (d,  $J = 8.5$  Hz, 2H), 7.36 (d,  $J = 8.5$  Hz, 2H), 7.05 (d,  $J = 2.6$  Hz, 2H), 6.66 (d,  $J = 2.2$  Hz, 2H), 6.43 (t,  $J = 2.2$  Hz, 1H), 3.84 (s, 6H);  $^{13}\text{C}$  NMR (125 MHz,  $\text{CDCl}_3$ )  $\delta$  164.58, 161.07 (2C), 138.53, 138.41, 131.11 (2C), 127.29 (2C), 126.75 (2C), 125.35, 104.86 (2C), 100.55, 55.42 (2C); IR (neat,  $\text{cm}^{-1}$ ):  $\nu = 3093, 3064, 3051, 3001, 2940, 2842, 2121, 1608, 1582, 1458, 1429, 1339, 1320, 1311, 1207, 1167, 1151, 1070, 1059, 959, 946$ . HRMS (ESI):  $m/z = 266.1176$  calculated for  $\text{C}_{16}\text{H}_{16}\text{NO}_2$   $[\text{M}+\text{H}]^+$ , found 266.1174.



**1.11**

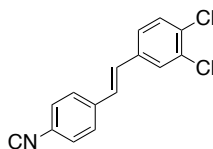
**(E)-1-isocyano-4-(4-(trifluoromethyl)styryl)benzene (1.11)**. Analogue **1.11** was synthesized from intermediate **1.7** and 4-trifluoromethylbenzaldehyde according to the general procedure (50% yield).  $^1\text{H}$  NMR (500 MHz,  $\text{CDCl}_3$ )  $\delta$  7.65 – 7.58 (m, 4H), 7.54 (d,  $J = 8.4$  Hz, 2H), 7.39 (d,  $J = 8.5$  Hz, 2H), 7.15 (s, 2H);  $^{13}\text{C}$  NMR (125 MHz,  $\text{CDCl}_3$ )  $\delta$  165.00, 139.99, 137.85, 130.07, 129.81, 129.49, 129.24, 127.54, 127.34, 126.86, 126.82, 125.79, 125.76, 125.18, 123.02; IR (neat,  $\text{cm}^{-1}$ ):  $\nu = 3052, 2926, 2854, 2127, 1614, 1504, 1421, 1322, 1265, 1222, 1162, 1124, 1107, 1066, 1016, 961$ . HRMS (ESI):  $m/z = 274.0838$  calculated for  $\text{C}_{16}\text{H}_{11}\text{F}_3\text{N}$   $[\text{M}+\text{H}]^+$ , found 273.8538.



**1.12**

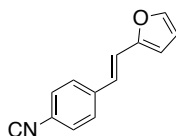
**(E)-1-fluoro-4-(4-isocyanostyryl)benzene (1.12)**. Analogue **1.12** was synthesized from intermediate **1.7** and 4-fluorobenzaldehyde according to the general procedure (47% yield).  $^1\text{H}$

NMR (500 MHz, CDCl<sub>3</sub>)  $\delta$  7.52 – 7.45 (m, 4H), 7.36 (d,  $J$  = 8.2 Hz, 2H), 7.12 – 7.04 (m, 3H), 6.98 (d,  $J$  = 16.3 Hz, 1H); <sup>13</sup>C NMR (125 MHz, CDCl<sub>3</sub>)  $\delta$  164.58, 163.71, 161.74, 138.43, 132.75, 129.88, 128.35, 128.29, 127.16, 126.78 (2C), 126.58, 115.92, 115.75; IR (neat, cm<sup>-1</sup>):  $\nu$  = 3408, 3032, 2925, 2854, 2121, 2043, 1595, 1509, 1233, 1159, 968, 838. HRMS (ESI):  $m/z$  = 224.0870 calculated for C<sub>15</sub>H<sub>11</sub>FN [M+H]<sup>+</sup>, found 224.0866.



**1.13**

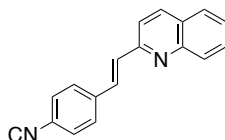
**(E)-1,2-dichloro-4-(4-isocyanostyryl)benzene (1.13).** Analogue **1.13** was synthesized from intermediate **1.7** and 1,2-dichlorobenzaldehyde according to the general procedure (80% yield). <sup>1</sup>H NMR (500 MHz, CDCl<sub>3</sub>)  $\delta$  7.59 (d,  $J$  = 2.1 Hz, 1H), 7.50 (d,  $J$  = 8.5 Hz, 2H), 7.44 (d,  $J$  = 8.3 Hz, 1H), 7.37 (d,  $J$  = 8.5 Hz, 2H), 7.33 (dd,  $J$  = 8.3, 2.1 Hz, 1H), 7.10 – 6.96 (m, 2H); <sup>13</sup>C NMR (125 MHz, CDCl<sub>3</sub>)  $\delta$  164.98, 137.78, 136.68, 133.03, 131.96, 130.73 (2C), 128.63, 128.52, 128.31, 127.44 (2C), 126.87 (2C), 125.86; IR (neat, cm<sup>-1</sup>):  $\nu$  = 3408, 3038, 2924, 2853, 2123, 1505, 1475, 1131, 961, 857, 823. HRMS (ESI):  $m/z$  = 274.0185 calculated for C<sub>16</sub>H<sub>10</sub>Cl<sub>2</sub>N [M+H]<sup>+</sup>, found 274.0188.



**1.14**

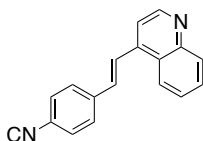
**(E)-2-(4-isocyanostyryl)furan (1.4).** Analogue **1.4** was synthesized from intermediate **1.7** and furan 2-carbaldehyde according to the general procedure (97% yield). <sup>1</sup>H NMR (500 MHz, CDCl<sub>3</sub>)  $\delta$  7.48 – 7.40 (m, 3H), 7.34 (d,  $J$  = 8.4 Hz, 2H), 7.02 – 6.85 (m, 2H), 6.47 – 6.37 (m, 2H); <sup>13</sup>C NMR (125 MHz, CDCl<sub>3</sub>)  $\delta$  164.52, 152.58, 142.83, 138.32, 126.98 (2C), 126.75 (2C), 125.23,

125.05, 118.59, 111.89, 110.07; IR (neat,  $\text{cm}^{-1}$ ):  $\nu = 3337, 3146, 2970, 2931, 2883, 2125, 1635, 1507, 1476, 1378, 1305, 1146, 1128, 1108, 969, 952, 926, 828, 738$ . HRMS (ESI):  $m/z = 196.0757$  calculated for  $\text{C}_{13}\text{H}_{10}\text{NO}$   $[\text{M}+\text{H}]^+$ , found 196.0759.



**1.15**

**(E)-2-(4-isocyanostyryl)quinolone (1.5).** Analogue **1.5** was synthesized from intermediate **1.7** and quinoline-2-carbaldehyde according to the general procedure (36% yield).  $^1\text{H}$  NMR (500 MHz,  $\text{CDCl}_3$ )  $\delta$  8.15 (d,  $J = 8.5$  Hz, 1H), 8.08 (d,  $J = 8.5$  Hz, 1H), 7.80 (dd,  $J = 8.1, 1.4$  Hz, 1H), 7.73 (ddd,  $J = 8.5, 6.8, 1.4$  Hz, 1H), 7.67 (d,  $J = 16.3$  Hz, 1H), 7.64 (d,  $J = 8.5$  Hz, 3H), 7.52 (ddd,  $J = 8.0, 6.9, 1.1$  Hz, 1H), 7.43 – 7.38 (m, 3H);  $^{13}\text{C}$  NMR (125 MHz,  $\text{CDCl}_3$ )  $\delta$  165.00, 155.10, 148.29, 137.80, 136.60, 132.27, 131.20, 129.98, 129.33, 128.00, 127.93, 127.57, 127.55, 126.87, 126.81, 126.58, 126.51, 119.49; IR (neat,  $\text{cm}^{-1}$ ):  $\nu = 3048, 3035, 2924, 2854, 2120, 1614, 1593, 1556, 1507, 1432, 1418, 1317, 1300, 1206, 1111, 969, 953$ . HRMS (ESI):  $m/z = 257.1073$  calculated for  $\text{C}_{18}\text{H}_{13}\text{N}_2$   $[\text{M}+\text{H}]^+$ , found 257.1076.



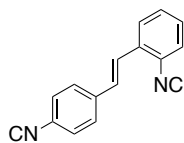
**1.16**

**(E)-4-(4-isocyanostyryl)quinolone (1.6).** Analogue **1.6** was synthesized from intermediate **1.7** and quinoline-4-carbaldehyde according to the general procedure (96% yield).  $^1\text{H}$  NMR (500 MHz,  $\text{CDCl}_3$ )  $\delta$  8.93 (d,  $J = 4.6$  Hz, 1H), 8.17 (dd,  $J = 14.9, 8.4$  Hz, 2H), 7.84 (d,  $J = 16.1$  Hz, 1H), 7.75 (t,  $J = 7.1$  Hz, 1H), 7.65 – 7.55 (m, 4H), 7.43 (d,  $J = 8.4$  Hz, 2H), 7.27 (d,  $J = 16.1$  Hz, 1H);  $^{13}\text{C}$  NMR (125 MHz,  $\text{CDCl}_3$ )  $\delta$  165.34, 150.24, 148.74, 142.13, 137.70, 133.12, 130.30, 129.53,

127.93 (3C), 126.97 (2C), 126.82, 126.26, 125.42, 123.28, 117.29; IR (neat,  $\text{cm}^{-1}$ ):  $\nu = 3059, 3031, 2922, 2853, 2121, 1630, 1600, 1578, 1572, 1563, 1507, 1463, 1423, 1389, 1301, 1253, 976, 964, 863$ . HRMS (ESI):  $m/z = 257.1073$  calculated for  $\text{C}_{18}\text{H}_{13}\text{N}_2$   $[\text{M}+\text{H}]^+$ , found 257.1069.

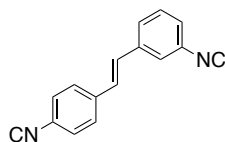
*General procedure for the synthesis of stilbene aryl bisisonitriles 1.19-1.20 from 1.18.*

$\text{CHCl}_3$  (0.50 mL, 6.21 mmol, 15 equiv) was added to a stirring solution of requisite diamine (120 mg, 0.57 mmol, 1 equiv) in  $\text{CH}_2\text{Cl}_2$  (0.8 mL). Triethylbenzylammonium chloride (11.40 mg, 0.012 mmol, 0.12 equiv) was added to the mixture followed by 50 % aqueous KOH (0.8 mL). The resulting mixture was stirred vigorously at room temperature. Solvent began to reflux, and the mixture was allowed to stir until the reaction was confirmed complete via TLC. Water, saturated aqueous ammonium chloride and  $\text{Et}_2\text{O}$  were added. The organic layer was separated, and the aqueous layer extracted with large amounts of  $\text{Et}_2\text{O}$  (4x). The combined organic layer was dried over anhydrous  $\text{Na}_2\text{SO}_4$  and concentrated *in vacuo*. The crude residue was purified by column chromatography to obtain the desired isonitrile.



**1.19**

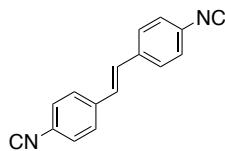
**(E)-1-isocyano-2-(4-isocyanostyryl)benzene (1.19).** Analogue **1.19** was synthesized from intermediate **1.18** according to the general procedure (19% yield).  $^1\text{H}$  NMR (500 MHz,  $\text{CDCl}_3$ )  $\delta$  7.74 (d,  $J = 7.7$  Hz, 1H), 7.59 (d,  $J = 8.4$  Hz, 2H), 7.47 – 7.38 (m, 5H), 7.32 (t,  $J = 7.7$  Hz, 1H), 7.15 (d,  $J = 16.3$  Hz, 1H);  $^{13}\text{C}$  NMR (125 MHz,  $\text{CDCl}_3$ )  $\delta$  167.53, 165.14, 137.62, 132.95, 130.71, 129.57, 128.76 (2C), 127.81 (2C), 127.45 (2C), 126.90 (2C), 125.64, 124.59; IR (neat,  $\text{cm}^{-1}$ ):  $\nu = 3063, 3039, 2924, 2853, 2119, 1648, 1596, 1505, 1480, 1449, 1417, 1379, 1293, 1263, 1225, 1198, 1090, 963$ . HRMS (ESI):  $m/z = 231.0917$  calculated for  $\text{C}_{16}\text{H}_{11}\text{N}_2$   $[\text{M}+\text{H}]^+$ , found 230.0839.

**1.20**

**(E)-1-isocyano-3-(4-isocyanostyryl)benzene (1.20).** Analogue **1.20** was synthesized from intermediate **1.18** according to the general procedure (24% yield).  $^1\text{H}$  NMR (500 MHz,  $\text{CDCl}_3$ )  $\delta$  7.53 – 7.50 (m, 4H), 7.42 – 7.37 (m, 3H), 7.30 (d,  $J = 7.9$  Hz, 1H), 7.12 – 7.04 (m, 2H);  $^{13}\text{C}$  NMR (125 MHz,  $\text{CDCl}_3$ )  $\delta$  165.05, 164.50, 138.25, 137.66, 129.88, 129.12, 128.78 (2C), 127.60 (2C), 127.53 (2C), 126.89 (2C), 125.76, 124.23; IR (neat,  $\text{cm}^{-1}$ ):  $\nu = 3033, 2925, 2122, 1599, 1580, 1505, 1443, 1228, 1167, 1107, 962, 863, 820, 787, 679$ . HRMS (ESI):  $m/z = 231.0917$  calculated for  $\text{C}_{16}\text{H}_{11}\text{N}_2$   $[\text{M}+\text{H}]^+$ , found 231.0918.

*General procedure for the synthesis of stilbene aryl bis-isonitriles 1.3 from 1.18.*

A mixture of diamine (200 mg, 0.95 mmol, 1 equiv), formic acid (0.14 mL, 3.8 mmol, 4 equiv) and toluene (2 mL) was refluxed for eight hours. After allowing to cool to room temperature, the mixture was evaporated to complete dryness. Toluene (2 mL) was added and evaporated to dryness to give diformamide. Triethylamine (0.95 ml, 6.84 mmol, 7.2 equiv) and dichloromethane (4 mL) was added to a flask containing crude diformamide. The resulting mixture was cooled to 0 °C and  $\text{POCl}_3$  (0.26 mL, 2.28 mmol, 2.4 equiv) was added dropwise over 30 minutes. The mixture was stirred for one hour at 0 °C and for an additional two hours at room temperature. The resultant mixture was cooled to 0 °C and a solution of 0.5 g  $\text{Na}_2\text{CO}_3$  in 2 mL of water was added dropwise for over 20 minutes. The mixture was then stirred for one hour. The organic layer was separated, and the aqueous layer extracted with dichloromethane (3x). The combined organics were washed with brine, dried over sodium sulfate, concentrated *in vacuo* and recrystallized to yield **1.3**.

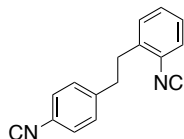


1.3

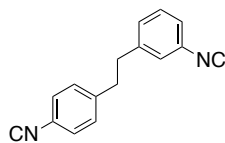
**(E)-1,2-bis(4-isocyanophenyl)ethane (1.3).** Analogue **1.3** was synthesized from intermediate **1.18** according to the general procedure (70% yield).  $^1\text{H}$  NMR (500 MHz,  $\text{CDCl}_3$ )  $\delta$  7.54 (dd,  $J = 8.6$ , 2.0 Hz, 4H), 7.42 – 7.35 (m, 2H), 7.09 (s, 2H);  $^{13}\text{C}$  NMR (125 MHz, C)  $\delta$  165.04 (2C), 137.76 (2C), 129.13 (4C), 127.51 (4C), 127.51 (2 C), 126.8 (2C); IR (neat,  $\text{cm}^{-1}$ ):  $\nu = 3036, 2604, 2499, 2157, 2124, 2022, 2013, 1997, 1971, 1696, 1603, 1507, 1422, 1305, 962, 942, 862, 834$ . HRMS (ESI):  $m/z = 231.0917$  calculated for  $\text{C}_{16}\text{H}_{11}\text{N}_2$   $[\text{M}+\text{H}]^+$ , found 231.0920.

*General procedure for the synthesis of saturated isonitriles 1.22-1.29 from intermediate 1.17 (Scheme 1.3).*

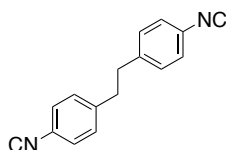
$\text{CHCl}_3$  (0.12 mL, 1.51 mmol) was added to a stirring solution of 4-(2-(pyridin-2-yl)ethyl)aniline (120 mg, 0.61 mmol) in  $\text{CH}_2\text{Cl}_2$  (1.2 mL). Triethylbenzylammonium chloride (2.73 mg, 0.012 mmol) was added to the mixture followed by 50 % aqueous KOH (1.2 mL). The resulting mixture was stirred vigorously at room temperature. Solvent began to reflux, and the mixture was allowed to stir until the reaction was confirmed complete via TLC. Water, saturated aqueous ammonium chloride and  $\text{Et}_2\text{O}$  were added. The organic layer was separated, and the aqueous layer extracted with large amounts of  $\text{Et}_2\text{O}$  (4x). The combined organic layer was dried over anhydrous  $\text{Na}_2\text{SO}_4$  and concentrated *in vacuo*. The crude residue was purified by column chromatography to obtain the desired isonitrile.

**1.22**

***1-isocyano-2-(4-isocyanophenethyl)benzene (1.22)***. Analogue **1.22** was synthesized from corresponding dinitro intermediate **1.17** (10 yield).  $^1\text{H}$  NMR (500 MHz,  $\text{CDCl}_3$ )  $\delta$  7.38 – 7.36 (m, 1H), 7.33 – 7.28 (m, 3H), 7.17 (dd,  $J = 17.6, 7.8$  Hz, 4H), 3.04 (dd,  $J = 9.6, 6.4$  Hz, 2H), 2.96 (dd,  $J = 9.0, 6.0$  Hz, 2H);  $^{13}\text{C}$  NMR (125 MHz,  $\text{CDCl}_3$ )  $\delta$  166.31, 163.56, 142.40 (2C), 137.36, 129.95, 129.58 (2C), 129.51 (2C), 127.43, 127.02, 126.49 (2C), 35.65, 34.24; IR (neat,  $\text{cm}^{-1}$ ):  $\nu = 2956, 2921, 2851, 2121, 1739, 1659, 1633, 1520, 1487, 1463, 1347, 1250, 1092, 1053, 1026, 967$ . HRMS (ESI):  $m/z = 233.1073$  calculated for  $\text{C}_{16}\text{H}_{13}\text{N}_2$   $[\text{M}+\text{H}]^+$ , found 233.1074.

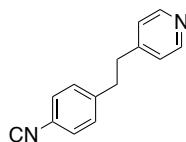
**1.23**

***1-isocyano-3-(4-isocyanophenethyl)benzene (1.23)***. Analogue **1.23** was synthesized from corresponding dinitro intermediate **1.17** (15% yield).  $^1\text{H}$  NMR (500 MHz,  $\text{CDCl}_3$ )  $\delta$  7.30 (dt,  $J = 7.8, 3.6$  Hz, 3H), 7.24 – 7.20 (m, 1H), 7.15 – 7.11 (m, 4H), 2.94 – 2.91 (m, 4H);  $^{13}\text{C}$  NMR (125 MHz,  $\text{CDCl}_3$ )  $\delta$  163.91, 163.79, 142.61, 142.41, 129.60, 129.47 (2C), 129.45 (2C), 126.72, 126.47, 126.30, 124.81, 124.30, 37.00, 36.87; IR (neat,  $\text{cm}^{-1}$ ):  $\nu = 2954, 2923, 2852, 2177, 2162, 2144, 2124, 2041, 2025, 1601, 1554, 1520, 1505, 1485, 1464, 1379, 1346, 1247, 1102, 1053, 1042$ . HRMS (ESI):  $m/z = 233.1073$  calculated for  $\text{C}_{16}\text{H}_{13}\text{N}_2$   $[\text{M}+\text{H}]^+$ , found 233.1077.



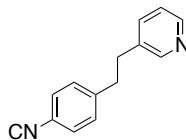
1.24

**1,2-bis(4-isocyanophenyl)ethane (1.24).** Analogue **1.24** was synthesized from corresponding dinitro intermediate **1.17** (18% yield).  $^1\text{H}$  NMR (500 MHz,  $\text{CDCl}_3$ )  $\delta$  7.28 (d,  $J = 8.3$  Hz, 4H), 7.11 (d,  $J = 8.2$  Hz, 4H), 2.93 (s, 4H);  $^{13}\text{C}$  NMR (125 MHz,  $\text{CDCl}_3$ )  $\delta$  163.78 (2C), 142.46 (2C), 129.46 (4C), 126.45 (4C), 124.77 (2C), 37.07 (2C); IR (neat,  $\text{cm}^{-1}$ ):  $\nu = 3062, 3047, 2948, 2925, 2854, 2160, 2130, 2038, 1990, 1733, 1534, 1505, 1457, 1295, 1294, 1167, 1092, 1022$ . HRMS (ESI):  $m/z = 233.1073$  calculated for  $\text{C}_{16}\text{H}_{13}\text{N}_2$   $[\text{M}+\text{H}]^+$ , found 233.1077.



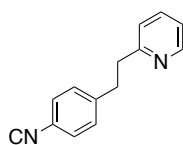
1.25

**4-(4-isocyanophenethyl)pyridine (24).** Analogue **24** was synthesized from corresponding intermediate **1.21** (45% yield).  $^1\text{H}$  NMR (500 MHz,  $\text{CDCl}_3$ )  $\delta$  8.49 – 8.47 (m, 2H), 7.28 (d,  $J = 1.9$  Hz, 2H), 7.15 – 7.13 (m, 2H), 7.05 – 7.03 (m, 2H), 2.95 – 2.90 (m, 4H);  $^{13}\text{C}$  NMR (125 MHz,  $\text{CDCl}_3$ )  $\delta$  163.81, 149.86 (2C), 149.59 (2C), 142.31, 129.44 (2C), 126.47 (2C), 123.86 (2C), 36.59, 36.18; IR (neat,  $\text{cm}^{-1}$ ):  $\nu = 3060, 2951, 2936, 2899, 2854, 2128, 1690, 1607, 1558, 1507, 1431, 1414, 992, 868$ . HRMS (ESI):  $m/z = 209.1073$  calculated for  $\text{C}_{14}\text{H}_{13}\text{N}_2$   $[\text{M}+\text{H}]^+$ , found 209.1075.



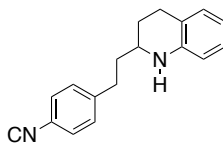
1.26

**3-(4-isocyanophenethyl)pyridine (1.26).** Analogue **1.26** was synthesized from corresponding intermediate **1.21** (36% yield).  $^1\text{H}$  NMR (500 MHz,  $\text{CDCl}_3$ )  $\delta$  8.46 (dd,  $J = 4.8, 1.6$  Hz, 1H), 8.39 (d,  $J = 2.3$  Hz, 1H), 7.39 (dt,  $J = 7.8, 2.0$  Hz, 1H), 7.28 (d,  $J = 8.4$  Hz, 2H), 7.19 (dd,  $J = 7.8, 4.8$  Hz, 1H), 7.15 – 7.13 (m, 2H), 2.97 – 2.88 (m, 5H);  $^{13}\text{C}$  NMR (125 MHz,  $\text{CDCl}_3$ )  $\delta$  163.73, 149.96, 147.82, 142.45, 135.95, 135.90 (2C), 129.50 (2C), 126.46, 123.32 (2C), 37.07, 34.50; IR (neat,  $\text{cm}^{-1}$ ):  $\nu = 3030, 2995, 2926, 2859, 2123, 1592, 1575, 1506, 1478, 1443, 1423, 1192, 1099, 1027$ . HRMS (ESI):  $m/z = 209.1073$  calculated for  $\text{C}_{14}\text{H}_{13}\text{N}_2$   $[\text{M}+\text{H}]^+$ , found 209.1075.



1.27

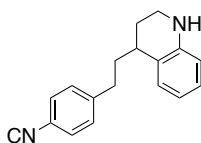
**2-(4-isocyanophenethyl)pyridine (1.27).** Analogue **1.27** was synthesized from corresponding intermediate **1.21** (43% yield).  $^1\text{H}$  NMR (500 MHz,  $\text{CDCl}_3$ )  $\delta$  8.56 (ddd,  $J = 4.9, 1.9, 1.0$  Hz, 1H), 7.56 (td,  $J = 7.6, 1.9$  Hz, 1H), 7.27 (d,  $J = 4.5$  Hz, 2H), 7.20 – 7.16 (m, 2H), 7.12 (ddd,  $J = 7.5, 4.9, 1.1$  Hz, 1H), 7.03 (dd,  $J = 7.8, 1.0$  Hz, 1H), 3.07 – 3.09 (m, 4H);  $^{13}\text{C}$  NMR (125 MHz,  $\text{CDCl}_3$ )  $\delta$  163.41, 160.36, 149.47, 143.33, 136.40, 129.46, 126.34 (2C), 124.54 (2C), 123.03, 121.41, 39.67, 35.49; IR (neat,  $\text{cm}^{-1}$ ):  $\nu = 3062, 3009, 2925, 2855, 2124, 1591, 1569, 1506, 1474, 1435, 1197, 1147, 1089, 1051, 1020, 993, 869$ . HRMS (ESI):  $m/z = 209.1073$  calculated for  $\text{C}_{14}\text{H}_{13}\text{N}_2$   $[\text{M}+\text{H}]^+$ , found 209.1072.



1.28

**2-(4-isocyanophenethyl)-1,2,3,4-tetrahydroquinoline (1.28).** Analogue **1.28** was synthesized from corresponding intermediate **1.21** (8% yield).  $^1\text{H}$  NMR (500 MHz,  $\text{CDCl}_3$ )  $\delta$  7.31 (d,  $J = 8.4$

Hz, 2H), 7.23 (d,  $J = 8.2$  Hz, 2H), 6.97 (t,  $J = 8.2$  Hz, 2H), 6.63 (dd,  $J = 7.4, 1.2$  Hz, 1H), 6.48 (d,  $J = 7.8$  Hz, 1H), 3.75 (s, 1H), 3.34 – 3.28 (m, 1H), 2.78 (ddd,  $J = 21.3, 10.9, 6.7$  Hz, 4H), 2.03 – 1.96 (m, 1H), 1.82 (ddd,  $J = 13.7, 7.9, 6.0$  Hz, 2H), 1.73 – 1.64 (m, 1H);  $^{13}\text{C}$  NMR (125 MHz,  $\text{CDCl}_3$ )  $\delta$  163.55, 144.30, 143.69, 129.31 (2C), 126.84 (2C), 126.48 (2C), 121.23, 117.29, 114.21 (2C), 50.98, 37.97, 31.81, 27.82, 26.10; IR (neat,  $\text{cm}^{-1}$ ):  $\nu = 3386, 3016, 2923, 2853, 2122, 1622, 1605, 1597, 1579, 1494, 1455, 1417, 1355, 1310, 1276, 1254, 1202, 1155, 1117, 1019, 965$ . HRMS (ESI):  $m/z = 263.1546$  calculated for  $\text{C}_{18}\text{H}_{19}\text{N}_2$   $[\text{M}+\text{H}]^+$ , found 263.1543.



**1.29**

**4-(4-isocyanophenethyl)-1,2,3,4-tetrahydroquinoline (1.29).** Analogue **1.29** was synthesized from corresponding intermediate **1.21** (5.3% yield).  $^1\text{H}$  NMR (500 MHz,  $\text{CDCl}_3$ )  $\delta$  7.30 (d,  $J = 8.2$  Hz, 2H), 7.22 (d,  $J = 8.4$  Hz, 2H), 6.98 (t,  $J = 7.5$  Hz, 2H), 6.61 (t,  $J = 7.0$  Hz, 1H), 6.49 (d,  $J = 7.8$  Hz, 1H), 3.88 (s, 1H), 3.38 – 3.27 (m, 2H), 2.83 – 2.66 (m, 3H), 2.03-1.94 (m, 2H), 1.89 – 1.79 (m, 2H);  $^{13}\text{C}$  NMR (125 MHz,  $\text{CDCl}_3$ )  $\delta$  163.35, 144.31, 144.22, 129.33 (2C), 129.01, 127.09, 126.37 (2C), 124.45, 124.37, 116.71, 114.25, 38.36, 37.89, 35.17, 33.04, 26.22; IR (neat,  $\text{cm}^{-1}$ ):  $\nu = 3405, 3049, 3018, 2923, 2854, 2122, 1605, 1582, 1501, 1473, 1443, 1359, 1313, 1270, 1193, 1155, 1121, 1107, 1048, 1019$ . HRMS (ESI):  $m/z = 263.1543$  calculated for  $\text{C}_{18}\text{H}_{19}\text{N}_2$   $[\text{M}+\text{H}]^+$ , found 263.1540.

## 1.5.2 Biological Methods

### *Bacterial strains and reagents*

Relevant information pertaining to all bacterial isolates used in this study are presented in Supplementary Table 1. Clinical isolates of *S. aureus* and *S. epidermidis* were obtained through the Network of Antimicrobial Resistance in *Staphylococcus aureus* (NARSA) program. Isolates of *S. pneumoniae*, *E. faecium*, *A. baumannii*, *K. pneumoniae*, *E. cloacae*, and *P. aeruginosa* were obtained from the American Type Culture Collection (ATCC). *E. coli* strains BW25113 and

JW25113 were obtained from The Coli Genetic Stock Center (CGSC), Yale University. Antibiotics were purchased commercially and dissolved in DMSO (for linezolid), ethanol (for erythromycin), or sterile deionized water (for colistin and vancomycin). Stock 10 mM solutions were prepared for all antibiotics. Brain heart infusion broth (BHI), Tryptic soy broth (TSB), Tryptic soy agar (TSA), phosphate-buffered saline (PBS), Dulbecco's modified Eagle's medium (DMEM), fetal bovine serum (FBS), and 96-well plates were all purchased from commercial vendors.

#### *Evaluation of antibacterial activity of compounds and control antibiotics*

The minimum inhibitory concentration of the aryl isonitrile analogues and control antibiotics was determined using the broth microdilution assay following the Clinical and Laboratory Standards Institute guidelines, with the following modifications.<sup>43</sup> Bacteria were cultured either in TSB or BHI (for *E. faecium*) and exposed to either compounds or control antibiotics, in triplicate, in 96-well plates. For permeabilization of the outer membrane, Gram-negative bacterial pathogens were exposed to a subinhibitory concentration of colistin equivalent to either  $\frac{1}{4} \times \text{MIC}$  (for *A. baumannii*, *E. cloacae*, *E. coli*, and *P. aeruginosa*) or  $\frac{1}{2} \times \text{MIC}$  (for *K. pneumoniae*). Plates were incubated aerobically at 37 °C for 18 – 24 hours before the MIC values were recorded. *S. pneumoniae* was incubated with compounds at 37 °C + 5% CO<sub>2</sub>. The MICs reported represent the lowest concentration of each compound/drug necessary to inhibit visual bacterial growth.

#### *In silico pharmacokinetic evaluation of 1.3*

Compound **1.3**'s pharmacokinetic profile was examined *in silico*, using chemPK version 2.0 (Cyprotex, Inc.) simulating a dose of 600 mg administered both orally and intravenously.

### *Toxicity assessment of aryl isonitrile analogues against human keratinocytes*

Compounds **1.3**, **1.4**, **1.9**, and **1.20** were assayed (at concentrations of 16, 32, 64, and 128  $\mu\text{M}$ ) against a human keratinocyte (HaCaT) cell line (AddexBio, San Diego, CA, USA) to determine the potential toxic effect to mammalian skin cells *in vitro*, as previously described.<sup>44-48</sup> In brief, cells were cultured in DMEM supplemented with 10% FBS at 37 °C with CO<sub>2</sub> (5%). Control cells received DMSO alone at a concentration equal to that in drug-treated cell samples. The cells were incubated with the compounds (in triplicate) in a 96-well plate at 37 °C with CO<sub>2</sub> (5%) for 24 hours. The assay reagent MTS 3-(4,5-dimethylthiazol-2-yl)-5-(3-carboxymethoxyphenyl)-2-(4-sulfophenyl)-2*H*-tetrazolium) (Promega, Madison, WI, USA) was subsequently added and the plate was incubated for four hours. Absorbance readings (at OD<sub>490</sub>) were taken using a kinetic microplate reader (Molecular Devices, Sunnyvale, CA, USA). The quantity of viable cells after treatment with each compound was expressed as a percentage of the viability of DMSO-treated control cells (average of triplicate wells  $\pm$  standard deviation). The toxicity data was analyzed via a one-way ANOVA, with post-hoc Dunnet's multiple comparisons test ( $P < 0.05$ ), utilizing GraphPad Prism 6.0 (GraphPad Software, La Jolla, CA).

### *Evaluation of 1.3 and 1.4 in a murine model of MRSA skin infection*

The mice study was conducted under the guidelines of the Purdue University Animal Care and Use Committee (PACUC) and carried out in strict accordance with the recommendations in the Guide for the Care and Use of Laboratory Animals of the National Institutes of Health. The method used for this study was similar to one described in previous reports, with slight modifications.<sup>44,49-53</sup> Four groups ( $n = 5$ ) of eight-week old female Balb/c mice (obtained from Envigo, Indianapolis, IN, USA) were used in this study. To initiate the formation of an abscess/open wound, all mice received an intradermal injection (40  $\mu\text{L}$ ) containing  $1.32 \times 10^9$  CFU/mL MRSA USA300. Following formation of the abscess, topical treatment was initiated subsequently with each group of mice receiving a 2% suspension (formulated in petroleum jelly) of the following agents, fusidic acid, **1.3**, or **1.4**. One group of mice was treated with the vehicle alone (negative control). Each group of mice receiving a particular treatment regimen was housed separately in a ventilated cage with appropriate bedding, food, and water. Mice were checked at least four times daily during infection and treatment to ensure no adverse reactions were observed. Mice were treated twice daily for five days, before they were humanely euthanized via CO<sub>2</sub>

asphyxiation 12 hours after the last dose was administered. Wounds were aseptically extracted and subsequently homogenized in PBS (2 mL). The homogenized tissue was then serially diluted in PBS before plating onto mannitol salt agar plates. Plates were incubated for at least 16 hours at 37 °C before viable CFU were counted and MRSA reduction in the skin wound (relative to the negative control) post-treatment was determined for each group.

#### *Caco-2 bidirectional permeability evaluation of 1.4*

The Caco-2 bidirectional permeability assay was conducted similar to previously published studies.<sup>10</sup> Caco-2 cells were grown in tissue culture flasks, trypsinized, suspended in medium, and were seeded ( $1 \times 10^5$  cells/cm<sup>2</sup>) onto wells of a Millipore 96-well Caco-2 plate. The cells were allowed to grow and differentiate for three weeks, feeding at two-day intervals. The test compounds were prepared at 10 µM in HBSS-MES (pH 6.50) or HBSS-HEPES (pH 7.40) with a final DMSO concentration of 1%. The working solution was then centrifuged, and the supernatant added to the donor side. For Apical to Basolateral (A→B) permeability, the test article was added to the Apical (A) side and amount of permeation on the Basolateral (B) side was determined; for Basolateral to Apical (B→A) permeability, the test article was added to the B side and the amount of permeation on the A side was determined. To test tight junctions and monolayer integrity, the A-side buffer contained 100 µM Lucifer yellow dye in Transport Buffer (1.98 g/L glucose in 10 mM HEPES, 1 × Hank's Balanced Salt Solution) with pH 6.50 while the B-side buffer was Transport Buffer with pH 7.40. Caco-2 cells were incubated with these buffers for 60 minutes (A→B) or 40 minutes (B→A), and the receiver side buffer was removed for analysis by LC/MS/MS. Fluorescein was used as the cell monolayer integrity marker. Fluorescein permeability assessment (A→B direction at pH 7.40 on both sides) was performed after the permeability assay for the test compound. The cell monolayer that had a fluorescein permeability of less than  $1.50 \times 10^{-6}$  cm/s for Caco-2 was considered intact, and the permeability result of the test compound from intact cell monolayer is reported. The apparent permeability coefficient ( $P_{app}$ ) of the test compound was calculated as follows:  $P_{app}(\text{cm/s}) = [(V_R * C_{R,\text{end}}) / \Delta t] * [(1 / (A * (C_{D,\text{mid}} - C_{R,\text{mid}})))]$  where  $V_R$  is the volume of the receiver chamber.  $C_{R,\text{end}}$  is the concentration of the test compound in the receiver chamber at the end time point,  $\Delta t$  is the incubation time and  $A$  is the surface area of the cell monolayer.  $C_{D,\text{mid}}$  is the calculated mid-point concentration of the test compound in the donor side, which is the mean value of the donor concentration at time zero and

the donor concentration at the end time point.  $C_{R,mid}$  is the mid-point concentration of the test compound in the receiver side, which is one half of the receiver concentration at the end time point. Concentrations of the test compound were expressed as peak areas of the test compound.

#### *Metabolic stability analysis of 1.4*

To investigate the stability of compound **1.4** to hepatic metabolism, the compound was evaluated with pooled human liver microsomes, as described in a previous report.<sup>55</sup> The test agents were incubated in duplicate with pooled human liver microsomes at 37 °C. The test compounds were pre-incubated with pooled human liver microsomes in phosphate buffer (pH 7.40) for five minutes in a 37 °C shaking water bath. The reaction was initiated by adding NADPH-generating system and incubated for 0, 15, 30, 45, and 60 minutes. The reaction was stopped by transferring the incubation mixture to acetonitrile/methanol. Samples were then mixed and centrifuged. Supernatants were used for HPLC-MS/MS analysis. Data was calculated as % parent remaining by assuming zero minute time point peak area ratio (analyte/IS) as 100% and dividing remaining time point peak area ratios by the zero minute time point peak area ratio. Data was subjected to fit a first-order decay model to calculate slope and thereby half-life. Intrinsic clearance was calculated from the half-life and the human liver microsomal protein concentrations using the following equations:

$$CL_{int} = \ln(2) / (t_{1/2} [\text{microsomal protein}])$$

$$t_{1/2} = 0.693 / -k$$

$$CL_{int} = \text{intrinsic clearance}; t_{1/2} = \text{half-life}; k = \text{slope}$$

#### *Investigation of 1.4 in a neutropenic murine MRSA thigh infection model*

Female BALB/c mice (obtained from The Jackson Laboratory, Bar Harbor, ME, USA), 6-8 weeks old, weighing 19 to 20 grams, were used in this study. The mice study was conducted similar to a previously published report.<sup>47</sup> All mice were rendered neutropenic via two intraperitoneal (i.p.) injections of 150 and 100 mg/kg of body weight cyclophosphamide four days and one day pre-infection, respectively. To initiate infection, the right thigh of mice was injected with an aliquot (100  $\mu$ L) of MRSA USA300 ( $5.35 \times 10^7$  CFU/mL). Groups of mice (n = 5) were treated two- and 12-hours post-infection, with a dose of 20 mg/kg i.p. injection of compound **1.4** (using a vehicle consisting of 10% DMSO, 10% Tween 80, and 80% PBS) or 20 mg/kg linezolid

(prepared in 10% DMSO, 90% PBS). Mice receiving a single i.p. injection of the vehicle (10% DMSO, 10% Tween 80, and 80% PBS) two hours post-infection served as the negative control group. Three mice were humanely euthanized via CO<sub>2</sub> asphyxiation three hours post-infection to enumerate the bacterial load in infected thighs ( $1.29 \times 10^6$  CFU). The remaining groups of mice were humanely euthanized via CO<sub>2</sub> asphyxiation 24 hours post-infection. The right thigh muscle was harvested aseptically, weighed, and homogenized in PBS. To determine the bacterial load in the infected thighs post-treatment, the homogenate was serially diluted in PBS and aliquots of each dilution were plated on mannitol salt agar plates. The plates were incubated for at least 18 hours at 37 °C before MRSA colonies were enumerated and compared to the negative control (vehicle alone) group.

## 1.6 References

1. Blaskovich, M. A. T.; Hansford, K. A.; Butler, M. S.; Jia, Z.; Mark, A. E.; Cooper, M. A. Developments in Glycopeptide Antibiotics. *ACS Infect Dis* **2018**, *4*, 715-735.
2. Sievert, D. M.; Ricks, P.; Edwards, J. R.; Schneider, A.; Patel, J.; Srinivasan, A.; Kallen, A.; Limbago, B.; Fridkin, S.; National Healthcare Safety Network, T.; Participating, N. F. Antimicrobial-resistant pathogens associated with healthcare-associated infections: summary of data reported to the National Healthcare Safety Network at the Centers for Disease Control and Prevention, 2009-2010. *Infect Control Hosp Epidemiol* **2013**, *34*, 1-14.
3. Mohammad, H.; Thangamani, S.; Seleem, M. N. Antimicrobial peptides and peptidomimetics - potent therapeutic allies for staphylococcal infections. *Curr Pharm Des* **2015**, *21*, 2073-88.
4. Centers for Disease Control and Prevention (CDC). *Antibiotic Resistance Threats in the United States*, **2013**, 2013, 1-114.
5. De Dios Caballero, J.; Pastor, M. D.; Vindel, A.; Maiz, L.; Yague, G.; Salvador, C.; Cobo, M.; Morosini, M. I.; del Campo, R.; Canton, R.; Group, G. S. Emergence of cfr-Mediated Linezolid Resistance in a Methicillin-Resistant Staphylococcus aureus Epidemic Clone Isolated from Patients with Cystic Fibrosis. *Antimicrob Agents Chemother* **2015**, *60*, 1878-82.
6. Gu, B.; Kelesidis, T.; Tsiodras, S.; Hindler, J.; Humphries, R. M. The emerging problem of linezolid-resistant Staphylococcus. *J Antimicrob Chemother* **2013**, *68*, 4-11.
7. Smith, T. L.; Pearson, M. L.; Wilcox, K. R.; Cruz, C.; Lancaster, M. V.; Robinson-Dunn, B.; Tenover, F. C.; Zervos, M. J.; Band, J. D.; White, E.; Jarvis, W. R. Emergence of

- vancomycin resistance in *Staphylococcus aureus*. Glycopeptide-Intermediate *Staphylococcus aureus* Working Group. *N Engl J Med* **1999**, *340*, 493-501.
8. Srinivasan, A.; Dick, J. D.; Perl, T. M. Vancomycin resistance in staphylococci. *Clin Microbiol Rev* **2002**, *15*, 430-8.
  9. Khan, A.; Wilson, B.; Gould, I. M. Current and future treatment options for community-associated MRSA infection. *Expert Opin Pharmacother* **2018**, *19*, 457-470.
  10. Davis, D. C.; Mohammad, H.; Kyei-Baffour, K.; Younis, W.; Creemer, C. N.; Seleem, M. N.; Dai, M. J. Discovery and characterization of aryl isonitriles as a new class of compounds versus methicillin- and vancomycin-resistant *Staphylococcus aureus*. *European Journal of Medicinal Chemistry* **2015**, *101*, 384-390.
  11. Brown, D. G.; Lister, T.; May-Dracka, T. L. New natural products as new leads for antibacterial drug discovery. *Bioorg Med Chem Lett* **2014**, *24*, 413-8.
  12. Mo, S.; Kronic, A.; Chlipala, G.; Orjala, J. Antimicrobial ambiguine isonitriles from the cyanobacterium *Fischerella ambigua*. *J Nat Prod* **2009**, *72*, 894-9.
  13. Schwarz, O., Brun, R., Bats, J. W., Schmalz, H. Synthesis and biological evaluation of new antimalarial isonitriles related to marine diterpenoids. *Tetrahedron Letters* **2002**, 1009–1013.
  14. Wright, A. D.; Wang, H.; Gurrath, M.; Konig, G. M.; Kocak, G.; Neumann, G.; Loria, P.; Foley, M.; Tilley, L. Inhibition of heme detoxification processes underlies the antimalarial activity of terpene isonitrile compounds from marine sponges. *J Med Chem* **2001**, *44*, 873-85.
  15. Kirk, K. L. Fluorine in medicinal chemistry: Recent therapeutic applications of fluorinated small molecules. *Journal of Fluorine Chemistry* **2006**, *127*, 1013-1029.
  16. Wilcken, R.; Zimmermann, M. O.; Lange, A.; Joerger, A. C.; Boeckler, F. M. Principles and Applications of Halogen Bonding in Medicinal Chemistry and Chemical Biology. *Journal of Medicinal Chemistry* **2013**, *56*, 1363-1388.
  17. Yale, H. L. The Trifluoromethyl Group in Medical Chemistry. *Journal of Medicinal and Pharmaceutical Chemistry* **1959**, *1*, 121-133.
  18. Arbusow, B. A. Michaelis-Arbusow- und Perkow-Reaktionen. In *Pure and Applied Chemistry*, 1964, *9*, 307.
  19. Weber, W. P.; Gokel, G. W. An improved procedure for the Hofmann carbylamine synthesis of isonitriles. *Tetrahedron Letters* **1972**, *13*, 1637-1640.
  20. Zhang, B.; Studer, A. 2-Trifluoromethylated Indoles via Radical Trifluoromethylation of Isonitriles. *Organic Letters* **2014**, *16*, 1216-1219.

21. Banerjee, R.; Hks, K.; Banerjee, M. *Medicinal significance of furan derivatives: A Review*. **2018**.
22. Kaur, K.; Jain, M.; Reddy, R. P.; Jain, R. Quinolines and structurally related heterocycles as antimalarials. *European Journal of Medicinal Chemistry* **2010**, *45*, 3245-3264.
23. Pendleton, J. N.; Gorman, S. P.; Gilmore, B. F. Clinical relevance of the ESKAPE pathogens. *Expert Rev Anti Infect Ther* **2013**, *11*, 297-308.
24. Santajit, S.; Indrawattana, N. Mechanisms of Antimicrobial Resistance in ESKAPE Pathogens. *Biomed Res Int* **2016**, 2475067.
25. Munita, J. M.; Arias, C. A. Mechanisms of Antibiotic Resistance. *Microbiol Spectr* **2016**, *4*.
26. Zgurskaya, H. I.; Lopez, C. A.; Gnanakaran, S. Permeability Barrier of Gram-Negative Cell Envelopes and Approaches To Bypass It. *ACS Infect Dis* **2015**, *1*, 512-522.
27. Padilla, E.; Llobet, E.; Domenech-Sanchez, A.; Martinez-Martinez, L.; Bengoechea, J. A.; Alberti, S. Klebsiella pneumoniae AcrAB efflux pump contributes to antimicrobial resistance and virulence. *Antimicrob Agents Chemother* **2010**, *54*, 177-83.
28. Schumacher, A.; Trittler, R.; Bohnert, J. A.; Kummerer, K.; Pages, J. M.; Kern, W. V. Intracellular accumulation of linezolid in Escherichia coli, Citrobacter freundii and Enterobacter aerogenes: role of enhanced efflux pump activity and inactivation. *J Antimicrob Chemother* **2007**, *59*, 1261-4.
29. Krishnamoorthy, G.; Wolloscheck, D.; Weeks, J. W.; Croft, C.; Rybenkov, V. V.; Zgurskaya, H. I. Breaking the Permeability Barrier of Escherichia coli by Controlled Hyperporination of the Outer Membrane. *Antimicrob Agents Chemother* **2016**, *60*, 7372-7381.
30. Stalker, D. J.; Jungbluth, G. L.; Hopkins, N. K.; Batts, D. H. *Pharmacokinetics and tolerance of single- and multiple-dose oral or intravenous linezolid, an oxazolidinone antibiotic, in healthy volunteers*. *J Antimicrob Chemother* **2003**, *51*, 1239-46
31. European Centre for Disease Prevention and Control (ECDC). *Surveillance of antimicrobial resistance in Europe 2016. Annual Report of the European Antimicrobial Resistance Surveillance Network (EARS-Net)*. Stockholm, 2017, 1-88.
32. Edelsberg, J.; Weycker, D.; Barron, R.; Li, X.; Wu, H.; Oster, G.; Badre, S.; Langeberg, W. J.; Weber, D. J. Prevalence of antibiotic resistance in US hospitals. *Diagn Microbiol Infect Dis* **2014**, *78*, 255-62.
33. Moet, G. J.; Jones, R. N.; Biedenbach, D. J.; Stilwell, M. G.; Fritsche, T. R. Contemporary causes of skin and soft tissue infections in North America, Latin America, and Europe: report from the SENTRY Antimicrobial Surveillance Program (1998-2004). *Diagn Microbiol Infect Dis* **2007**, *57*, 7-13.

34. Russo, A.; Concia, E.; Cristini, F.; De Rosa, F. G.; Esposito, S.; Menichetti, F.; Petrosillo, N.; Tumbarello, M.; Venditti, M.; Viale, P.; Viscoli, C.; Bassetti, M. Current and future trends in antibiotic therapy of acute bacterial skin and skin-structure infections. *Clin Microbiol Infect* **2016**, *22*, S27-36.
35. Gardete, S.; Tomasz, A. Mechanisms of vancomycin resistance in *Staphylococcus aureus*. *J Clin Invest* **2014**, *124*, 2836-40.
36. Rodvold, K. A.; McConeghy, K. W. Methicillin-resistant *Staphylococcus aureus* therapy: past, present, and future. *Clin Infect Dis* **2014**, *58*, 20-27.
37. Kristich, C. J.; Rice, L. B.; Arias, C. A. Enterococcal Infection-Treatment and Antibiotic Resistance. In *Enterococci: From Commensals to Leading Causes of Drug Resistant Infection*, Boston, **2014**.
38. Grundmann, H.; Schouls, L. M.; Aanensen, D. M.; Pluister, G. N.; Tami, A.; Chlebowicz, M.; Glasner, C.; Sabat, A. J.; Weist, K.; Heuer, O.; Friedrich, A. W.; Markers, E. S. G. o. M. E.; European Staphylococcal Reference Laboratory Working, G. The dynamic changes of dominant clones of *Staphylococcus aureus* causing bloodstream infections in the European region: results of a second structured survey. *Euro Surveill* **2014**, *19*.
39. Tian, L.; Sun, Z.; Zhang, Z. Antimicrobial resistance of pathogens causing nosocomial bloodstream infection in Hubei Province, China, from 2014 to 2016: a multicenter retrospective study. *BMC Public Health* **2018**, *18*, 1121.
40. Castanheira, M.; Watters, A. A.; Mendes, R. E.; Farrell, D. J.; Jones, R. N. Occurrence and molecular characterization of fusidic acid resistance mechanisms among *Staphylococcus* spp. from European countries (2008). *J Antimicrob Chemother* **2010**, *65*, 1353-8.
41. Johnson, J. K.; Khoie, T.; Shurland, S.; Kreisel, K.; Stine, O. C.; Roghmann, M. C. Skin and soft tissue infections caused by methicillin-resistant *Staphylococcus aureus* USA300 clone. *Emerg Infect Dis* **2007**, *13*, 1195-200.
42. Vingsbo Lundberg, C.; Frimodt-Moller, N. Efficacy of topical and systemic antibiotic treatment of methicillin-resistant *Staphylococcus aureus* in a murine superficial skin wound infection model. *Int J Antimicrob Agents* **2013**, *42*, 272-5.
43. Clinical and Laboratory Standards Institute (CLSI). Methods for Dilution Antimicrobial Susceptibility Tests for Bacteria That Grow Aerobically—Ninth Edition: Approved Standard M07-A9. In Wayne, PA, **2012**.
44. Mohammad, H.; Cushman, M.; Seleem, M. N. Antibacterial Evaluation of Synthetic Thiazole Compounds In Vitro and In Vivo in a Methicillin-Resistant *Staphylococcus aureus* (MRSA) Skin Infection Mouse Model. *PLoS One* **2015**, *10*, e0142321.
45. Kotb, A.; Abutaleb, N. S.; Seleem, M. A.; Hagrass, M.; Mohammad, H.; Bayoumi, A.; Ghiaty, A.; Seleem, M. N.; Mayhoub, A. S. Phenylthiazoles with tert-Butyl side chain: Metabolically stable with anti-biofilm activity. *Eur J Med Chem* **2018**, *151*, 110-120.

46. Hagra, M.; Abutaleb, N. S.; Ali, A. O.; Abdel-Aleem, J. A.; Elsebaei, M. M.; Seleem, M. N.; Mayhoub, A. S. Naphthylthiazoles: Targeting Multidrug-Resistant and Intracellular Staphylococcus aureus with Biofilm Disruption Activity. *ACS Infect Dis* **2018**, *148*, 195-209
47. Elsebaei, M. M.; Mohammad, H.; Abouf, M.; Abutaleb, N. S.; Hegazy, Y. A.; Ghiaty, A.; Chen, L.; Zhang, J.; Malwal, S. R.; Oldfield, E.; Seleem, M. N.; Mayhoub, A. S. Alkynyl-containing phenylthiazoles: Systemically active antibacterial agents effective against methicillin-resistant Staphylococcus aureus (MRSA). *Eur J Med Chem* **2018**, *148*, 195-209.
48. ElAwamy, M.; Mohammad, H.; Hussien, A.; Abutaleb, N. S.; Hagra, M.; Serya, R. A. T.; Taher, A. T.; Abouzeid, K. A.; Seleem, M. N.; Mayhoub, A. S. Alkoxyphenylthiazoles with broad-spectrum activity against multidrug-resistant gram-positive bacterial pathogens. *Eur J Med Chem* **2018**, *152*, 318-328.
49. Thangamani, S.; Mohammad, H.; Abushahba, M. F.; Sobreira, T. J.; Seleem, M. N. Repurposing auranofin for the treatment of cutaneous staphylococcal infections. *Int J Antimicrob Agents* **2016**, *47*, 195-201.
50. Thangamani, S.; Younis, W.; Seleem, M. N. Repurposing celecoxib as a topical antimicrobial agent. *Front Microbiol* **2015**, *6*, 750.
51. Thangamani, S.; Younis, W.; Seleem, M. N. Repurposing ebselen for treatment of multidrug-resistant staphylococcal infections. *Sci Rep* **2015**, *5*, 11596.
52. Thangamani, S.; Mohammad, H.; Abushahba, M. F.; Hamed, M. I.; Sobreira, T. J.; Hedrick, V. E.; Paul, L. N.; Seleem, M. N. Exploring simvastatin, an antihyperlipidemic drug, as a potential topical antibacterial agent. *Sci Rep* **2015**, *5*, 16407.
53. Mohamed, M. F.; Seleem, M. N. Efficacy of short novel antimicrobial and anti-inflammatory peptides in a mouse model of methicillin-resistant Staphylococcus aureus (MRSA) skin infection. *Drug Des Devel Ther* **2014**, *8*, 1979-1983.
54. Mohammad, H.; Mayhoub, A. S.; Ghafour, A.; Soofi, M.; Alajlouni, R. A.; Cushman, M.; Seleem, M. N. Discovery and characterization of potent thiazoles versus methicillin- and vancomycin-resistant Staphylococcus aureus. *J Med Chem* **2014**, *57*, 1609-15.

## CHAPTER 2. INVESTIGATION OF ARYL ISONITRILES AS POTENT, BROAD-SPECTRUM ANTIFUNGAL AGENTS

### 2.1 Introduction

*Candida*, *Cryptococcus*, and *Aspergillus* represent invasive fungal infections which afflict over 1.5 million humans globally each year. Despite having a staggering mortality rate which often exceeds 50%,<sup>1</sup> the effect of fungal infections on human health is still widely underestimated. *Candida* is the most common etiological agent of superficial and invasive fungal infections worldwide; notably, *Candida albicans* is the fourth-leading cause of hospital-acquired bloodstream infections, and is particularly problematic in immunocompromised patients.<sup>2</sup> There are 17 different species of *Candida*, however, the global increase in the prevalence of invasive *Candida* infections has in part been due to the emergence of non-*albicans* *Candida* species including *Candida glabrata*, *Candida tropicalis*, *Candida parapsilosis*, and *Candida krusei*.<sup>3,4</sup> In addition to *Candida*, another pathogenic yeast, *Cryptococcus* (including *C. neoformans* and *C. gatti*) is responsible for over one million invasive fungal infections each year, resulting in an astounding 625,000 deaths.<sup>5</sup> Patients suffering from HIV are more susceptible to severe cryptococcal infections that manifest primarily as pneumonia or meningoencephalitis.<sup>6</sup> The third fungal pathogen of concern involves species of *Aspergillus* (namely *A. fumigatus*) which are responsible for over 300,000 fungal infections each year.<sup>7</sup> Invasive disease (particularly pulmonary infections) caused by *Aspergillus* primarily occur in patients with underlying conditions such as AIDS, cancer, cystic fibrosis, asthma, or individuals undergoing solid organ transplants. The severity of such infections can be seen by the low rate of survival (59%) reported for solid organ transplant recipients afflicted with invasive aspergillosis.<sup>8</sup>

The difficulty in treating invasive fungal infections has been exacerbated by the limited number of approved antifungal drugs. Currently, only three structurally-distinct classes of antifungal drugs are primarily used for treatment of invasive fungal infections – azoles (such as fluconazole), polyenes (such as amphotericin B), and echinocandins (such as caspofungin).<sup>9</sup>

Azole antifungals, including fluconazole, are considered the drugs of choice due to their high oral bioavailability and reduced toxicity to host tissues. However, the clinical utility of fluconazole and other antifungal drugs has become increasingly limited due to the emergence of clinical isolates exhibiting resistance to these agents.<sup>10,11</sup> This necessitates the development of new therapeutic agents. However, only one new antifungal drug class has been successfully developed in the past 30 years.<sup>12</sup> The development of new antifungal agents is very challenging given fungi and mammals are both eukaryotes; thus many proteins that are potential targets for antifungal therapy are also found in human cells, opening the door for potential toxicity concerns.<sup>12,13</sup>

Ideally, a novel therapeutic agent for invasive fungal infections should possess broad-spectrum antifungal activity with limited toxicity to host (human) tissues. In the search for new antimicrobial drug scaffolds, our research group recently discovered synthetic aryl isonitrile compounds that exhibit notable antibacterial activity against drug-resistant *Staphylococcus aureus*.<sup>14</sup> It has been shown that natural product compounds containing the isonitrile functional group can possess dual antibacterial and antifungal activity, particularly against *C. albicans*.<sup>15,16</sup> Per this observation, this present study investigates the structure-activity relationship of the first and second series of synthetic aryl isonitrile compounds (Figure 2.1) as antifungal agents, examines their spectrum of activity against pertinent species of *Candida*, *Cryptococcus*, and *Aspergillus*, and evaluates the most promising compounds' toxicity against mammalian cells.

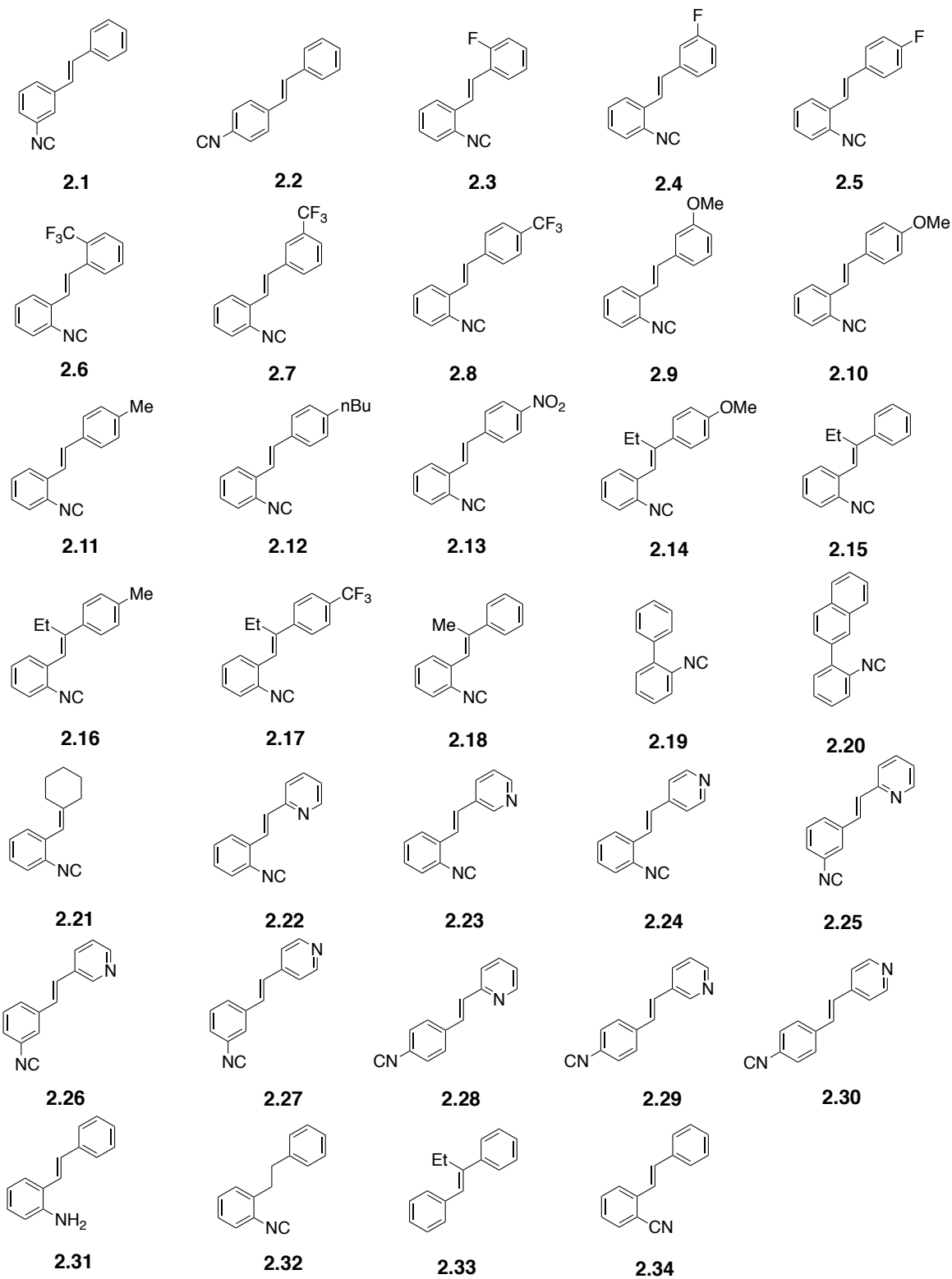


Figure 2.1. First series of compounds studied.

## 2.2 Results and Discussion: First series of aryl isonitriles

As noted by Beck-Sague, *Candida albicans* has been identified as the most common fungal pathogen isolated from healthcare-associated infections in humans.<sup>17</sup> Thus we initially evaluated our collection of compounds for antifungal activity against a clinical isolate of *C. albicans* (Table 2.1). Using the broth microdilution assay, the minimum inhibitory concentration (MIC) was determined. The initial screening provided key insight into the structure-antifungal activity relationship of the compounds. Most notably, the presence of the isonitrile group appears to be critical for the compounds to possess antifungal activity. Compounds lacking the isonitrile group (as in **2.33**) or where the isonitrile was substituted with alternative groups including an isosteric cyano group (**2.34**) or an amine (**2.31**) were inactive (MIC  $\geq$  64  $\mu$ M).

Most of the stilbene-backbone isonitriles showed promising antifungal activity against *C. albicans* (MIC = or < 8  $\mu$ M) with several exceptions (cf. **2.5**, **2.6**, **2.8**, **2.9**, **2.14**, **2.15**, **2.17**, MIC  $\geq$  16  $\mu$ M). The effect of different substituents on the aromatic ring without the isonitrile group varies. Both electron-donating (cf. OMe, Me, *n*Bu) and electron-withdrawing (F, CF<sub>3</sub>, NO<sub>2</sub>) groups can be tolerated to a certain extent based on their position. In general, adding alkyl substituents (Me or Et) on the *trans* double bond decreased the antifungal activity. For example, compound **2.10** (MIC = 1  $\mu$ M) is much more potent than compound **2.14** with an extra ethyl group on the double bond (MIC = 64  $\mu$ M); compound **2.11** (MIC = 2  $\mu$ M) and compound **2.8** (MIC = 32  $\mu$ M) are two-fold more potent than compound **2.16** (MIC = 4  $\mu$ M) and compound **2.17** (MIC > 64  $\mu$ M), respectively. The *para*-CF<sub>3</sub> positioning of compounds **2.8** and **2.17** has a dramatic effect on their antifungal activity, and both compounds **2.8** and **2.17** are significantly less potent (16-fold higher MIC) than their corresponding *para*-CH<sub>3</sub> substituted analogs. The possession of the stilbene backbone is not necessary for the aryl isonitriles' antifungal activity against *C. albicans*, though it does enhance potency in several cases. For example, replacing the second aromatic group with a cyclohexane (**2.21**) resulted in a compound with good antifungal activity against *C. albicans* (MIC = 4  $\mu$ M). The biaryl isonitriles **2.19** and **2.20** are potent antifungal compounds against *C. albicans* with 0.5  $\mu$ M and 2  $\mu$ M MIC values respectively, and the naphthyl group decreased the potency about 4-fold. Interestingly, in our previous studies,<sup>14</sup> both **2.19** and **2.20** only displayed weak or even no antimicrobial activity against methicillin-resistant *Staphylococcus aureus* (MRSA) strains. Compound **2.32**, with a saturated two-carbon linker between the two aryl groups showed potent anti *C. albicans* activity as well (MIC = 0.5  $\mu$ M). Again, compound **2.32** was not a good

candidate against several MRSA strains in our previous studies. These observations suggest that the antifungal and antibacterial mode of actions for these isonitrile compounds are very likely to be different.

Replacing the non-isonitrile-bearing aromatic ring with pyridine had beneficial effect on the antifungal activity against *C. albicans*. For example, the MIC values of isomeric compounds **2.22** to **2.30** range from 0.5  $\mu\text{M}$  to 4  $\mu\text{M}$ , with compound **2.25** emerging as the most potent analogue. The effect of the positions of the isonitrile group on the aromatic ring as well as the nitrogen atom of the pyridine ring ranges from two- to eight-fold, which are quite significant. When the isonitrile group is *ortho* to the double bond (**2.22**, **2.23**, **2.24**), the 2 and 3-pyridyl substituted compounds **2.22** and **2.23** (MIC = 1  $\mu\text{M}$ ) are four times more potent than the 4-pyridyl substituted compound **2.24** (MIC = 4  $\mu\text{M}$ ). When the isonitrile group is *meta* to the double bond (**2.25**, **2.26**, **2.27**), the 2-pyridyl substituted compound **2.25** (MIC = 0.5  $\mu\text{M}$ ) is four- or eight-fold more active than the 3 or 4-pyridyl substituted **2.26** (MIC = 2  $\mu\text{M}$ ) or **2.27** (MIC = 4  $\mu\text{M}$ ), respectively. When the isonitrile group is *para* to the double bond (**2.28**, **2.29**, **2.30**), the effect of the position of the pyridine nitrogen is quite small and 4-pyridyl substituted **2.30** (MIC = 1  $\mu\text{M}$ ) is two-fold more active than the 2 and 3-pyridyl substituted compounds.

In general, the structure-activity analysis of the first series of aryl isonitriles revealed three key findings: the presence of the aryl isonitrile functional group is essential for antifungal activity, the addition of a second aromatic functional group enhances the antifungal activity of the compounds, and the location of the isonitrile group on the aromatic ring also influences the biological activity of the compounds. Interestingly, analogues exhibiting the most potent antifungal activity (including **2.7**, **2.11**, **2.19**, **2.20**, and **2.32**) possessed only modest or weak antibacterial activity against drug-resistant *S. aureus*.<sup>14</sup> This information is critical to help guide the synthesis of future aryl isonitrile analogues to improve their specificity as antifungal agents.

Table 2.1. The minimum inhibitory concentration (MIC in  $\mu\text{M}$ ) and minimum fungicidal concentration (MFC in  $\mu\text{M}$ ) of synthesized compounds and fluconazole screened against *C. albicans* NR-29448.

Compound /Drug Name	<i>Candida albicans</i>	
	MIC	MFC
2.1	4	32
2.2	2	>64
2.3	2	>64
2.4	8	64
2.5	64	N.D. <sup>1</sup>
2.6	>64	>64
2.7	2	>64
2.8	32	N.D.
2.9	16	N.D.
2.10	1	>64
2.11	2	>64
2.12	8	64
2.13	8	64
2.14	>64	>64
2.15	16	N.D.
2.16	4	>64
2.17	>64	>64
2.18	8	>64
2.19	0.5	>64
2.20	2	16
2.21	4	>64
2.22	1	16
2.23	1	32
2.24	4	4
2.25	0.5	64
2.26	2	2
2.27	4	4
2.28	2	16
2.29	2	16
2.30	1	1
2.31	64	N.D.
2.32	0.5	64
2.33	>64	>64
2.34	>64	>64
<b>Fluconazole</b>	0.5	>64

<sup>1</sup>N.D. = Not determined

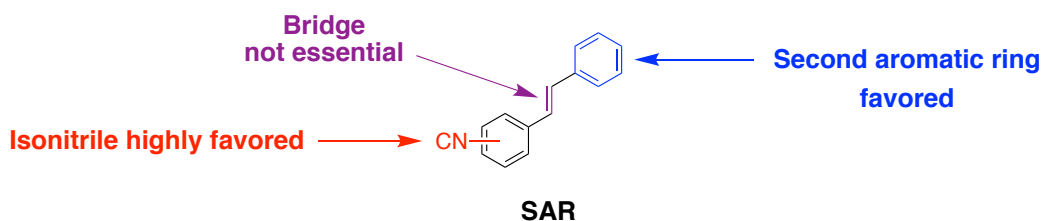


Figure 2.2. Structure-activity relationship of aryl isonitriles.

### 2.2.1 Aryl isonitrile compounds exhibit fungistatic behavior against *C. albicans*

After discovering the aryl isonitrile compounds are potent inhibitors of *C. albicans* growth, we were curious to evaluate whether the compounds simply inhibit fungal growth (are fungistatic) or are capable of killing the microorganism (are fungicidal). Previously, we determined the aryl isonitrile compounds are static against bacteria, thus we postulated the compounds would be fungistatic. To investigate this point, the minimum fungicidal concentration (MFC) required to reduce the number of colony-forming units (CFU) by 99.9%,<sup>18</sup> was determined for the active compounds against *C. albicans* NR-29351. The MFC values for the active compounds were found to be noticeably higher (more than 8-fold) when compared to their MIC results (Table 2.1), supporting the notion that the compounds are fungistatic. These results aligned with the results obtained with fluconazole, an antifungal drug known to exhibit fungistatic activity against *C. albicans*.<sup>18</sup>

In order to verify this observation, two of the most potent antifungal compounds were subjected to a traditional time-kill assay. Even at a high concentration ( $4 \times \text{MIC}$ ), the aryl isonitrile compounds exhibited fungistatic behavior against *C. albicans* (Figure 2.3). Neither **2.30** nor **2.32** produced a 3- $\log_{10}$  reduction in fungal CFU within 24 hours, which would be characteristic of fungicidal activity. The compounds' behavior matches that observed with fluconazole. Thus, preliminary inspection indicates the aryl isonitrile compounds are fungistatic agents (particularly against *C. albicans*).

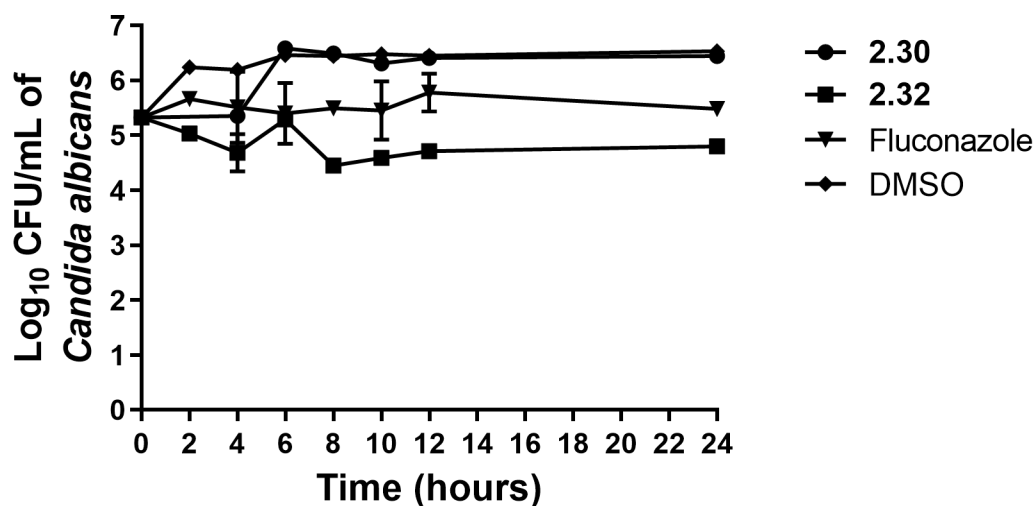


Figure 2.3. Time-kill analysis of aryl isonitrile compounds **2.30**, **2.32**, and fluconazole against *Candida albicans* NR-29351 over a 24-hour incubation period at 37°C. DMSO served as a negative control. The error bars represent standard deviation values obtained from triplicate samples used for each compound/antifungal drug studied.

### 2.2.2 Aryl isonitrile compounds exhibit broad-spectrum antifungal activity

Given the potent antifungal activity observed with several aryl isonitrile compounds against *C. albicans*, we next moved to assess their spectrum of activity against key pathogenic fungi. Interestingly, several current antifungal drugs suffer from their inability to inhibit growth of multiple species of fungi. For example, azole antifungals such as fluconazole are generally very effective at inhibiting growth of yeasts such *Candida albicans* and species of *Cryptococcus*; however, fluconazole is ineffective at inhibiting growth of molds such as *Aspergillus* species.<sup>12</sup> Even more discouraging, non-*albicans* *Candida* species including *Candida glabrata* and *Candida krusei* are intrinsically resistant or less susceptible to fluconazole.<sup>12</sup> In contrast, echinocandins are effective against *Candida* and *Aspergillus* but are ineffective as treatment options for infections caused by *Cryptococcus*.<sup>12</sup> Thus finding antifungal compounds capable of inhibiting growth of species of *Candida*, *Cryptococcus*, and *Aspergillus* is highly desirable.

Based upon their potent inhibitory effect against *C. albicans*, six aryl isonitrile compounds (**2.2**, **2.22**, **2.23**, **2.25**, **2.26**, and **2.32**) were screened against 21 additional clinical isolates including non-*albicans* *Candida* species such as *Candida glabrata*, *Candida tropicalis*, *Candida parapsilosis*, *Candida krusei* (Table 2.2) in addition to species of *Cryptococcus* and *Aspergillus*

(Table 3). Interestingly, all seven compounds were able to inhibit growth of all species of the yeasts *Candida* and *Cryptococcus*. In general, compound **2.32** proved the most potent compound as it inhibited growth of all clinical isolates, with the exception of *C. krusei*, with a MIC ranging from 0.5 to 1  $\mu\text{M}$  (Table 2.2). This proved to be more potent than fluconazole (MIC = 2  $\mu\text{M}$ ) against strains of *C. albicans* and *Cryptococcus gattii* that are sensitive to this drug. Against fluconazole-resistant strains of *Candida albicans*, compounds where the second aromatic substituent was replaced with a pyridine were generally more active than **2.32**. For example, compounds **2.22**, **2.23**, **2.25**, and **2.26** had MIC values that were lower than compound **2.32** against fluconazole-resistant *C. albicans*. However, against non-*albicans* *Candida* species, compounds containing the pyrimidine functional group, with the exception of **2.26**, had MIC values that were 2- to 32-fold higher than the analogue containing a second aromatic group (**2.32**).

Table 2.2. The minimum inhibitory concentration (MIC in  $\mu\text{M}$ ) of isonitriles and fluconazole screened against clinical isolates of *Candida albicans* and non-*albicans* *Candida* species.

Strain Name	Compound/Drug Name						Fluconazole
	<b>2.2</b>	<b>2.22</b>	<b>2.23</b>	<b>2.25</b>	<b>2.26</b>	<b>2.32</b>	
<i>Candida albicans</i> ATCC 29351	1	1	2	1	$\leq 0.5$	$\leq 0.5$	$\leq 0.5$
<i>Candida albicans</i> ATCC 27365	1	1	2	2	1	$\leq 0.5$	1
<i>Candida albicans</i> NR-29368	2	$\leq 0.5$	4	2	2	8	>64
<i>Candida albicans</i> NR-29446	1	$\leq 0.5$	1	2	2	8	>64
<i>Candida albicans</i> ATCC MYA 573	1	$\leq 0.5$	1	2	2	16	>64
<i>Candida albicans</i> ATCC 64124	2	$\leq 0.5$	2	2	2	64	>64
<i>Candida krusei</i> ATCC 14243	32	4	32	64	32	> 64	64
<i>Candida krusei</i> ATCC 34135	16	2	16	32	8	> 64	64
<i>Candida parapsilosis</i> ATCC 22019	2	4	8	4	1	$\leq 0.5$	1
<i>Candida glabrata</i> ATCC MYA-2950	8	16	8	8	$\leq 0.5$	$\leq 0.5$	>64
<i>Candida glabrata</i> ATCC 66032	8	16	8	4	1	1	>64
<i>Candida tropicalis</i> ATCC 1369	16	16	8	2	2	1	>64
<i>Candida tropicalis</i> ATCC 13803	4	4	8	4	1	$\leq 0.5$	>64

Though the six aryl isonitrile compounds exhibited potent antifungal activity against yeasts (*Candida* and *Cryptococcus*), they were less active against molds. Against *Aspergillus fumigatus*, the MIC values were equal to or higher than 16  $\mu\text{M}$  for all six compounds (Table 2.3). Compound **2.22** exhibited the most potent activity against both *A. niger* and *A. brasiliensis* with MIC values ranging from 4 to 8  $\mu\text{M}$ . This was a marked improvement over fluconazole, which proved ineffective at inhibiting growth of both *A. niger* and *A. brasiliensis* (MIC > 64  $\mu\text{M}$ ).

Table 2.3. The minimum inhibitory concentration (MIC in  $\mu\text{M}$ ) of synthesized compounds and fluconazole screened against clinical isolates of *Cryptococcus* and *Aspergillus*.

Strain Name	Compound/Drug Name						Fluconazole
	2.2	2.22	2.23	2.25	2.26	2.32	
<i>Cryptococcus gattii</i> NR-43208	$\leq 0.5$	$\leq 0.5$	$\leq 0.5$	$\leq 0.5$	$\leq 0.5$	$\leq 0.5$	8
<i>Cryptococcus gattii</i> NR-43209	$\leq 0.5$	$\leq 0.5$	1	$\leq 0.5$	$\leq 0.5$	$\leq 0.5$	8
<i>Cryptococcus neoformans</i> NR-41292	$\leq 0.5$	$\leq 0.5$	1	$\leq 0.5$	$\leq 0.5$	$\leq 0.5$	8
<i>Aspergillus brasiliensis</i> ATCC 16404	> 64	4	32	64	32	> 64	>64
<i>Aspergillus niger</i> ATCC 6275	> 64	8	16	> 64	32	> 64	>64
<i>Aspergillus niger</i> ATCC 16888	> 64	8	8	> 64	16	> 64	>64
<i>Aspergillus fumigatus</i> NR-35302	32	32	> 64	64	16	> 64	>64
<i>Aspergillus fumigatus</i> NR-35301	64	32	> 64	64	16	> 64	>64

### 2.2.3 Aryl isonitriles are not toxic to mammalian cells at high concentration

Toxicity is a fundamental parameter to evaluate in early-stage drug discovery to ensure compounds with promising biological activity do not also cause harmful effects to host (human) tissues. A significant challenge with several currently approved antifungal drugs is toxicity. Amphotericin B is a broad-spectrum, fungicidal agent effective against *Candida*, *Cryptococcus*, and *Aspergillus*. However, one of Amphotericin B's (and polyenes in general) most significant limitations is its significant toxicity to host tissues.<sup>12</sup> Though a lipid formulation of Amphotericin

B has been developed that exhibits less toxicity, the formulation is too expensive to be administered in resource-limited regions where invasive fungal infections are endemic.<sup>12</sup> Thus identifying antifungal agents with broad-spectrum activity and limited toxicity to host tissues is highly desirable.

Previously, we evaluated the toxicity of the aryl isonitrile compounds against murine macrophage cells and found the most potent analogues were not toxic up to a concentration of 64  $\mu\text{M}$ .<sup>14</sup> To further examine the toxicity profile of the aryl isonitrile compounds, the MTS assay was utilized to evaluate the compounds' toxicity against a human epithelial colorectal (HRT-18) cell line at very high concentrations (up to 256  $\mu\text{M}$ ). As presented in Figure 2.4, no compound was toxic to HRT-18 cells at a concentration of 128  $\mu\text{M}$ . Astonishingly, even at a concentration of 256  $\mu\text{M}$ , all compounds were non-toxic with the exception of **2.11** and **2.20**. This represents a nearly 512-fold difference between the MIC of the most potent compounds against fungi (such as **2.26** and **2.32**) and the highest concentration where no toxicity was observed to mammalian cells.

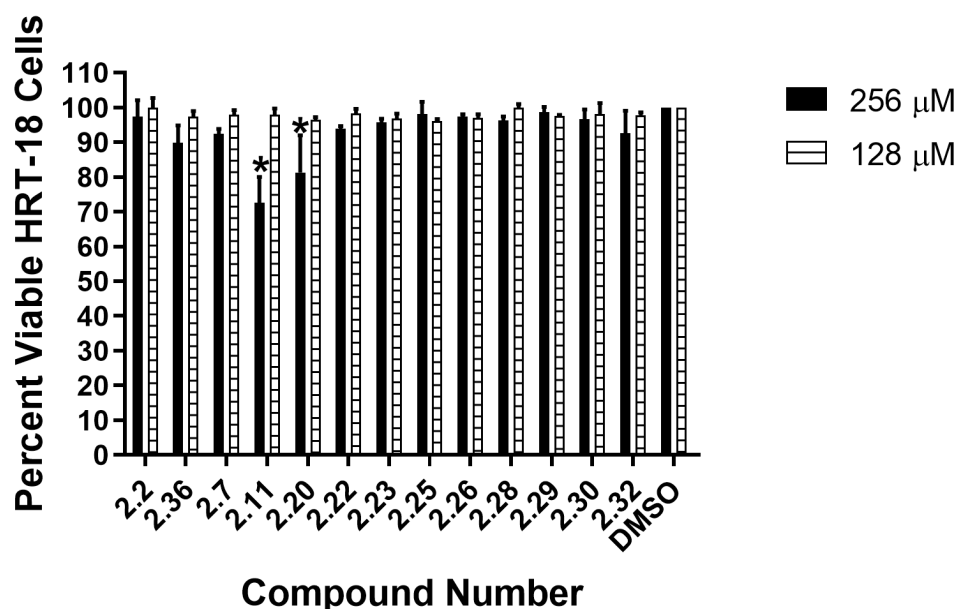


Figure 2.4. Toxicity analysis of aryl isonitrile compounds against human epithelial colorectal cells (HRT-18). Percent viable mammalian cells (measured as average absorbance ratio (test agent relative to DMSO)) for cytotoxicity analysis of compounds (tested in triplicate) at 128 and 256  $\mu\text{M}$  against HRT-18 cells using the MTS assay. Dimethyl sulfoxide (DMSO) served as a negative control to determine a baseline measurement for the cytotoxic impact of each compound. The absorbance values represent an average of a minimum of three samples analyzed for each compound. Error bars represent standard deviation values for the absorbance values. A two-way ANOVA, with post-hoc Dunnett's multiple comparisons test, determined no statistical difference between the values obtained for each compound and DMSO ( $P < 0.05$ ).

### 2.3 Results and Discussion: Second series of aryl isonitriles

To further understand the importance of the various functionalities on the aryl isonitrile for antifungal activity, a second series of aryl isonitriles were evaluated for antifungal activity (Figure 2.5). These compounds include those with an additional isonitrile functional group, those with furan, pyridine and isoquinoline heterocyclic moieties, those with other small molecule entities, and those with an alkane bridge. We started off by evaluating our collection of compounds for antifungal activity against a clinical isolate of *C. albicans* (Table 2.4). Using the broth microdilution assay, the MIC was determined. This initial screening provided insights into the structure-activity relationship of the second series of compounds.

The presence of an additional isonitrile group as shown in bis-isonitriles **2.35**, **2.36**, and **2.37** improved the activity of the stilbene isonitriles. Compared to the monosubstituted analogues, bis-isonitriles **2.35**, **2.36**, and **2.37** (MIC = 2, 2, and 1  $\mu\text{M}$  respectively) exhibited an overall better activity. This trend reinforces the antifungal relevance of the isonitrile group.

The importance of the alkene bridge was also evaluated. With the exception of **2.38**, all the bis-isonitriles with an alkane bridge exhibited good activity. **2.40** (MIC = 1  $\mu\text{M}$ ) with the isonitrile on the *para*-position of the second aromatic ring showed the best activity followed by *meta*-positioned isonitrile **2.39** (MIC = 2  $\mu\text{M}$ ) and then the *ortho*-substituted derivative **2.38** (MIC = 32  $\mu\text{M}$ ). This therefore highlights the inconsequentiality of the stilbene core; a trend that was also observed in the first series. A deeper analysis of both sets of bis-isonitriles revealed that the symmetrical *para*-isonitrile compounds, that is, **2.37** (MIC = 1  $\mu\text{M}$ ) and **2.40** (MIC = 1  $\mu\text{M}$ ) exhibited the best activity in both sets. This shows that beyond the importance of the isonitrile functionality, the *para*-positioning of both groups is particularly important for the best antifungal activity.

To understand the value of the second aromatic ring regarding antifungal activity, our curiosity led to the evaluation of furan, pyridine and isoquinoline heterocyclic moieties. None of these modifications showed activity comparable to the bis-isonitriles **2.37** (MIC = 1  $\mu\text{M}$ ) and **2.40** (MIC = 1  $\mu\text{M}$ ). However, isoquinoline **2.49** (MIC = 2  $\mu\text{M}$ ) had activity comparable to **2.35** (MIC = 2  $\mu\text{M}$ ), **2.36** (MIC = 2  $\mu\text{M}$ ), and **2.39** (MIC = 2  $\mu\text{M}$ ). Furan containing **2.47** (MIC = 8  $\mu\text{M}$ ), pyridine compounds **2.50** (MIC = 8  $\mu\text{M}$ ), **2.51** (MIC = 8  $\mu\text{M}$ ), and **2.52** (MIC = 4  $\mu\text{M}$ ), isoquinoline compound **2.48** (MIC = 4  $\mu\text{M}$ ), **2.53** (MIC = 4  $\mu\text{M}$ ), and **2.54** (MIC = 4  $\mu\text{M}$ ) exhibited good activity but were not comparable to the bis-isonitriles.

The importance of the second aromatic group, as revealed by these results, led to the evaluation of medicinally relevant small molecules such as methoxy, trifluoromethyl, fluoro, and chloro groups. All the compounds exhibited moderate to good activity, however meta-methoxy and para-methoxy derivatives **2.42** and **2.43** exhibited the best activity (MIC = 2  $\mu$ M). With the activity exhibited by these methoxy compounds we evaluated **2.44**, a compound with two methoxy groups. This modification however led to a reduced activity (MIC = 4  $\mu$ M).

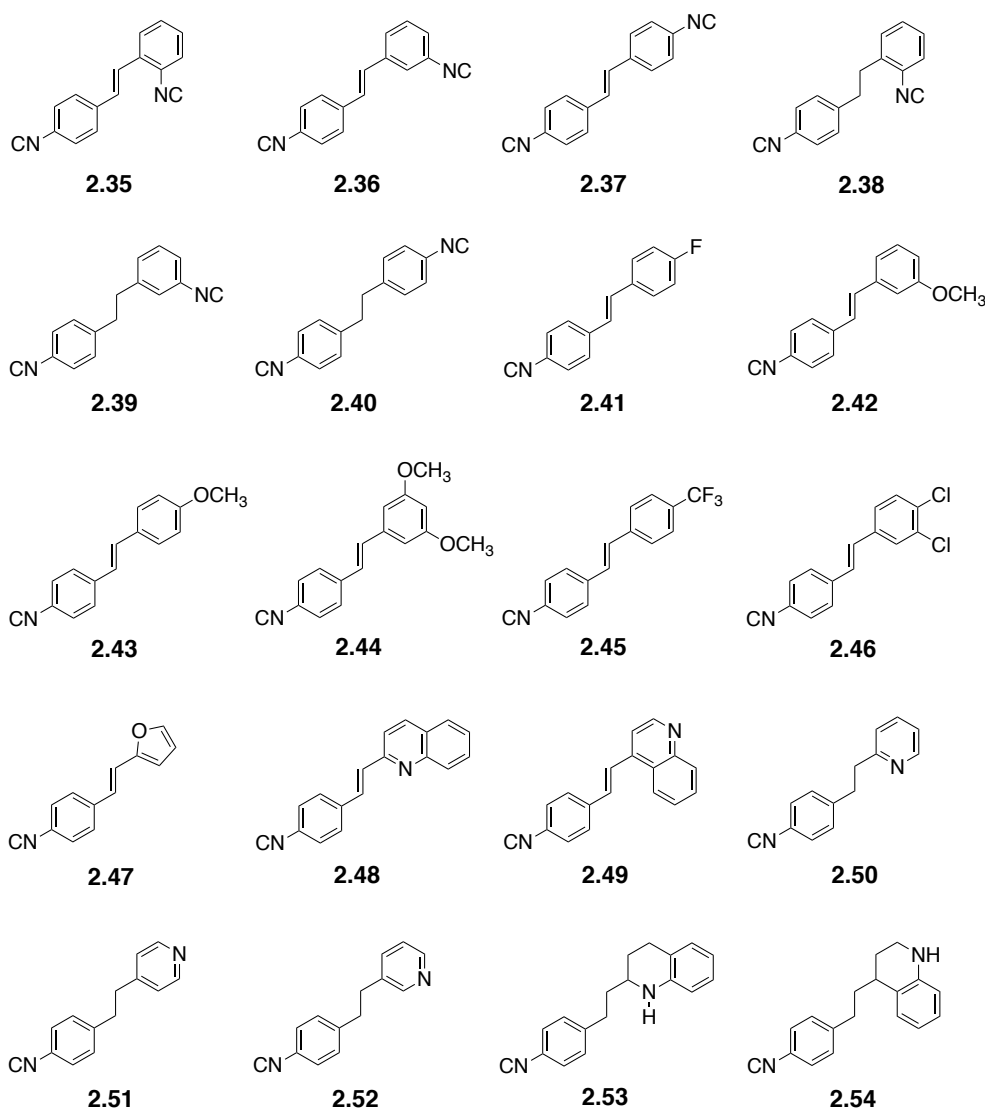


Figure 2.5. Second-generation aryl isonitrile compounds presented in this study.

Overall, the structure-activity relationship study revealed three key findings (Figure 2.6). The presence of the additional aryl isonitrile functional group proved essential for antifungal activity, the addition of a second aromatic functional group enhances the antifungal activity of the compounds, changing the aromatic ring to pyridine, isoquinoline, or furan has no effect on the antifungal activity, and the *para*-positioning of the isonitrile group on the aromatic ring also impacts the biological activity of the compounds.

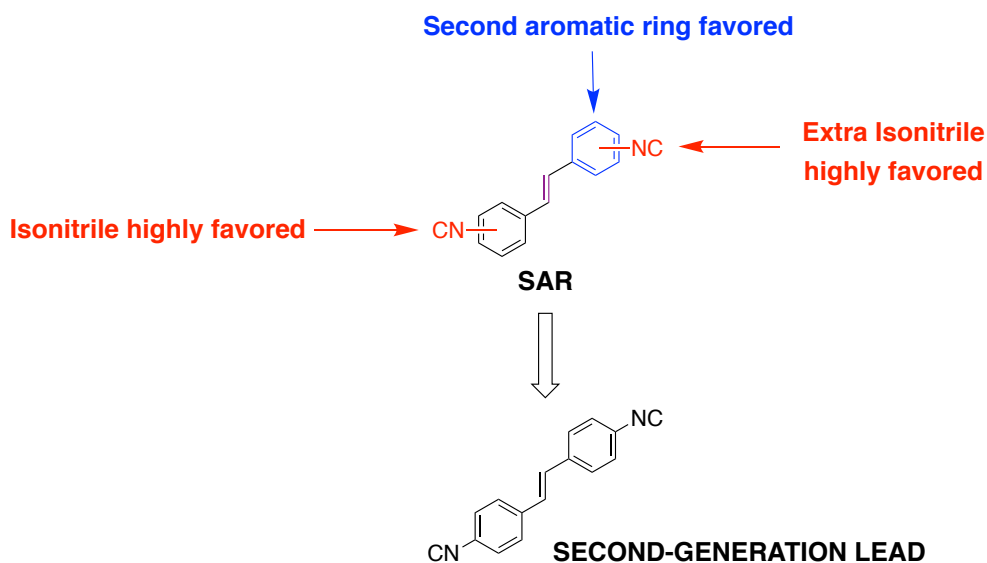


Figure 2.6. Structure-activity relationship leading to the second-generation lead of aryl isonitriles.

Table 2.4. Minimum inhibitory concentration (MIC) and minimum fungicidal concentration (MFC) of aryl isonitrile analogues against *Candida albicans*.

Compound Name	<i>Candida albicans</i> P60002 (catalog #: NR-29448)	
	MIC	MFC
<b>2.35</b>	2	8
<b>2.36</b>	2	32
<b>2.37</b>	1	4 or 8
<b>2.38</b>	32	>64
<b>2.39</b>	2	64
<b>2.40</b>	1	>64
<b>2.41</b>	8	>64
<b>2.42</b>	2	>64
<b>2.43</b>	2	>64
<b>2.44</b>	4	>64
<b>2.45</b>	4	>64
<b>2.46</b>	4	>64
<b>2.47</b>	8	64
<b>2.48</b>	4	64
<b>2.49</b>	2	>64
<b>2.50</b>	8	16
<b>2.51</b>	8	16
<b>2.52</b>	4	8
<b>2.53</b>	4	>64
<b>2.54</b>	4	64
<b>Amphotericin B</b>	1	1
<b>Fluconazole</b>	0.5	>64

### 2.3.1 *Aryl isonitrile compounds exhibit broad-spectrum antifungal activity*

Based on the potent antifungal inhibitory activity exhibited by several aryl isonitrile compounds against *C. albicans*, we assessed their spectrum of activity against key pathogenic fungi. Eight of the potent aryl isonitrile compounds (**2.35**, **2.36**, **2.37**, **2.39**, **2.40**, **2.42**, **2.43**, and **2.49**) were therefore screened against 10 additional clinical isolates. These include non-*albicans* *Candida* species such as *Candida glabrata*, *Candida tropicalis*, *Candida parapsilosis*, and species of *Cryptococcus* and *Candida albicans* (Table 2.5 and 2.6).

All eight compounds were able to greatly inhibit growth of all clinical isolates of *Candida albicans* (MIC = 0.5-1  $\mu$ M). This activity was higher than that of Amphotericin B (MIC = 2  $\mu$ M)

against the same strains. Against species of *Cryptococcus* all eight compounds exhibited a MIC of 0.5  $\mu\text{M}$  (Table 2.5). This proved to be more potent than fluconazole (MIC = 2  $\mu\text{M}$ ) against strains of *C. albicans* and *Cryptococcus gattii* that are sensitive to this drug. A closer look at fluconazole-resistant strains of *Candida albicans*, showed that, bis-isonitrile compounds (MIC = 0.5  $\mu\text{M}$ ) were more active than methoxy containing aryl isonitriles **2.42** and **2.43** (MIC = 1  $\mu\text{M}$ ).

Against non-*albicans Candida* species such as *parapsilosis* and *glabrata*, all of the compounds, with the exception of methoxy containing aryl isonitriles **2.42** and **2.43** (MIC = 8 and 4  $\mu\text{M}$  respectively for *C. glabrata* ATCC 66032), exhibited a MIC within the range of 0.5 to 2  $\mu\text{M}$ . Against *C. tropicalis*, compounds without bis-isonitriles, **2.49** (MIC = 8  $\mu\text{M}$ ), exhibited the least activity, with **2.42** and **2.43** (MIC >64  $\mu\text{M}$ ) showing no activity at all. All bis-isonitriles showed activity within the 0.5  $\mu\text{M}$  to 4  $\mu\text{M}$  range, thus justifying their importance. **2.37** and **2.40**, the most active compounds from the initial screening, showed the best activity (MIC = 0.5-2  $\mu\text{M}$ ) against all the clinical isolates studied.

Table 2.5. Minimum inhibitory concentration (MIC) and minimum fungicidal concentration (MFC) of aryl isonitrile analogues against *Candida albicans* and species of *Cryptococcus*.

Compound/ Drug Name	<i>Candida albicans</i> ATCC 29351		<i>Candida albicans</i> ATCC 27365		<i>Cryptococcus gattii</i> NR- 43208		<i>Cryptococcus gattii</i> NR- 43209		<i>Cryptococcus neoformans</i> NR-41292	
	MIC ( $\mu\text{g}/\text{mL}$ )	MFC ( $\mu\text{g}/\text{mL}$ )	MIC ( $\mu\text{g}/\text{mL}$ )	MFC ( $\mu\text{g}/\text{mL}$ )	MIC ( $\mu\text{g}/\text{mL}$ )	MFC ( $\mu\text{g}/\text{mL}$ )	MIC ( $\mu\text{g}/\text{mL}$ )	MFC ( $\mu\text{g}/\text{mL}$ )	MIC ( $\mu\text{g}/\text{mL}$ )	MFC ( $\mu\text{g}/\text{mL}$ )
<b>2.35</b>	0.5	16	0.5	64	0.5	0.5	0.5	0.5	0.5	0.5
<b>2.36</b>	0.5	8	0.5	32	0.5	0.5	0.5	0.5	0.5	2
<b>2.37</b>	0.5	2	0.5	2	0.5	1	0.5	0.5	0.5	0.5
<b>2.39</b>	0.5	16	0.5	>64	0.5	0.5	0.5	0.5	0.5	2
<b>2.40</b>	0.5	>64	0.5	4	0.5	1	0.5	0.5	0.5	1
<b>2.42</b>	0.5	4	1	>64	0.5	-	0.5	4	0.5	2
<b>2.43</b>	0.5	>64	1	>64	0.5	2	0.5	0.5	0.5	4
<b>2.49</b>	0.5	>64	0.5	>64	0.5	2	0.5	2	0.5	1
<b>Amphotericin B</b>	2	2	2	2	2	2	2	4	0.5	0.5
<b>Fluconazole</b>	0.5	8	1	8	8	32	8	32	8	16

Table 2.6. Minimum inhibitory concentration (MIC) and minimum fungicidal concentration (MFC) of aryl isonitrile analogues against additional species of *Candida*.

Compound/ Drug Name	<i>Candida parapsilosis</i>		<i>Candida glabrata</i> ATCC MYA-2950		<i>Candida glabrata</i> ATCC 66032		<i>Candida tropicalis</i> ATCC 1369		<i>Candida tropicalis</i> ATCC 13803	
	MIC ( $\mu\text{g}/\text{mL}$ )	MFC ( $\mu\text{g}/\text{mL}$ )	MIC ( $\mu\text{g}/\text{mL}$ )	MFC ( $\mu\text{g}/\text{mL}$ )	MIC ( $\mu\text{g}/\text{mL}$ )	MFC ( $\mu\text{g}/\text{mL}$ )	MIC ( $\mu\text{g}/\text{mL}$ )	MFC ( $\mu\text{g}/\text{mL}$ )	MIC ( $\mu\text{g}/\text{mL}$ )	MFC ( $\mu\text{g}/\text{mL}$ )
<b>2.35</b>	0.5	2	0.5	>64	0.5	>64	4	8	2	2
<b>2.36</b>	0.5	2	0.5	16	0.5	>64	2	4	1	8
<b>2.37</b>	0.5	2	0.5	2	1	>64	2	8	0.5	1
<b>2.39</b>	0.5	>64	0.5	64	0.5	32	2	32	0.5	2
<b>2.40</b>	0.5	0.5	0.5	>64	1	>64	2	>64	0.5	>64
<b>2.42</b>	1	>64	2	>64	4	>64	>64	>64	1	>64
<b>2.43</b>	1	>64	2	>64	8	>64	>64	>64	4	>64
<b>2.49</b>	2	>64	1	>64	1	>64	8	>64	1	>64
<b>Fluconazole</b>	1	>64	>64	>64	>64	>64	>64	>64	>64	>64

### 2.3.2 Aryl isonitriles are not toxic to mammalian cells at high concentrations

The first-generation compounds, as shown previously, are not toxic to human epithelial colorectal (HRT-18) cell line at concentrations as high as 256  $\mu\text{M}$ . To understand the effect of the extra isonitrile group on toxicity, we examined the toxicity profile of the second-generation aryl isonitrile compounds. The MTS assay was utilized to evaluate the compounds' toxicity against a human epithelial colorectal (HRT-18) cell line at very high concentrations (up to 256  $\mu\text{M}$ ). As presented in Figure 2.7, no compound was toxic to HRT-18 cells at a concentration of 128  $\mu\text{M}$ . Astonishingly, even at a concentration of 256  $\mu\text{M}$ , all compounds were non-toxic. This also represents a nearly 512-fold difference between the MIC of the most potent compounds (such as **2.37** and **2.40**) against fungi, and the highest concentration where no toxicity was observed to mammalian cells. This result supports our previous findings that the aryl isonitrile compounds have an excellent safety profile against mammalian cells which therefore warrants further evaluation. The lack of toxicity observed against mammalian cells suggests the aryl isonitrile compounds may exert their antifungal effect via a unique mechanism. Though the antifungal mechanism of action of the aryl isonitrile compounds is currently unknown, it is being intensely investigated.

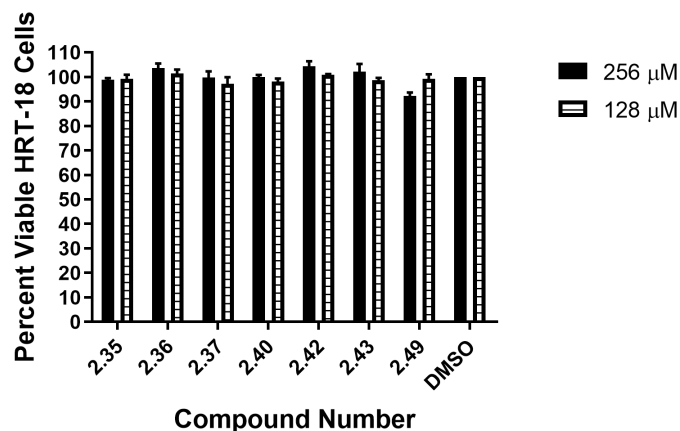


Figure 2.7. Toxicity analysis of aryl isonitriles against human colorectal cells (HRT-18). Percent viable mammalian cells (measured as average absorbance ratio (test agent relative to DMSO)) for cytotoxicity analysis of aryl isonitrile compounds (tested in triplicate) at 128 and 256  $\mu$ M against HRT-18 cells using the MTS 3-(4,5-dimethylthiazol-2-yl)-5-(3-carboxymethoxyphenyl)-2-(4-sulfophenyl)-2H-tetrazolium assay. Dimethyl sulfoxide (DMSO) was used as a negative control to determine a baseline measurement for the cytotoxic impact of each compound. The absorbance values represent an average of a minimum of three samples analyzed for each compound. Error bars represent standard deviation values for the absorbance values. A two-way ANOVA, with post hoc Dunnet's multiple comparisons test, was utilized to determine statistical difference between the values obtained for each compound and DMSO ( $P < 0.05$ ) (denoted as asterisks).

## 2.4 Conclusion

Given the dearth of antifungal drug classes and the emergence of resistance to key antifungal drugs (such as fluconazole), there is a need for new chemical scaffolds and compounds exhibiting potent, broad-spectrum antifungal activity and low toxicity to host (mammalian) tissues. This study examines the promise of aryl isonitrile compounds as a new scaffold for the development of antifungal agents. Structure-activity relationship studies of a first and second series of aryl isonitriles reveal the presence of the isonitrile group at the para position and the inclusion of a second aromatic functional group is critical for the compounds to possess antifungal activity. Compounds bearing the aryl isonitrile functional group exhibited broad-spectrum activity inhibiting growth of notable species of *Candida* and *Cryptococcus* at a concentration as low as 0.5  $\mu$ M. The compounds appear to be fungistatic against *C. albicans*. The most active compounds exhibit an excellent safety profile as they are non-toxic to mammalian cells, even at concentrations up to 256  $\mu$ M. The SAR information presented in this study will prove critical for the medicinal

chemistry community to develop new aryl isonitrile analogues to advance them to the next step in the antifungal drug discovery process.

## 2.5 Experimental Section

### 2.5.1 Biological Materials and Methods

#### *Fungal strains and reagents used in this study*

Clinical isolates of *Candida*, *Cryptococcus*, and *Aspergillus* were obtained from the American Type Cell Culture (ATCC, Manassas, VA, USA) and BEI Resources (Manassas, VA, USA). HRT-18 cells were purchased from the American Type Culture Collection. Fluconazole was purchased commercially and dissolved in dimethyl sulfoxide (DMSO) to prepare a stock solution (10 mM). Yeast extract peptone dextrose (YPD), RPMI-1640 for MIC determination, 3-(N-Morpholino)propanesulfonic acid, 4-Morpholinepropanesulfonic acid (MOPS), phosphate-buffered saline (PBS), RPMI-1640 medium for cell culture assay, fetal horse serum, and 96-well plates were all purchased from commercial vendors.

#### *Determination of minimum inhibitory concentration (MIC) and minimum fungicidal concentration (MFC)*

The broth dilution assay, following the guidelines of the Clinical and Laboratory Standards Institute for yeasts (M27-A3)<sup>19</sup> and molds (M38-A2)<sup>20</sup>, was utilized to determine the MIC of compounds and fluconazole against species of *Candida*, *Cryptococcus*, and *Aspergillus* using 96-well plates. Plates containing fungi and test agents were incubated at 37 °C for at least 44 hours for *Candida* spp. and *Aspergillus* spp. or 68 hours for *Cryptococcus* spp. before the MIC was determined by visual inspection. For determination of the minimum fungicidal concentration (MFC) against *C. albicans* NR-29448, aliquots (5 µL) were transferred from wells with no growth onto yeast extract peptone dextrose (YPD) agar plates. Plates were incubated at 37 °C for 18 hours before MFC (> 99.9% decrease in colony-forming units) was recorded.

#### *Time-kill assay against C. albicans*

*C. albicans* NR-29351 cells (OD<sub>600</sub> = 0.524) were diluted to  $2.08 \times 10^5$  colony-forming units (CFU/mL) and exposed to concentrations equivalent to  $4 \times \text{MIC}$  (in triplicate) of compounds **30**,

**32**, and fluconazole in YPD medium. Aliquots (100  $\mu$ L) were collected from each treatment after 0, 2, 4, 6, 8, 10, 12, and 24 hours of incubation at 37 °C and subsequently serially diluted in PBS. Fungi were then spotted onto YPD agar plates and incubated at 37 °C for at least 20 hours before viable CFU/mL was determined.

#### *Cytotoxicity analysis of aryl isonitrile compounds*

Compounds were assayed (at concentrations of 32, 64, 128, and 256  $\mu$ M) against a human colorectal (HRT-18) cell line to determine the potential toxic effect to mammalian cells *in vitro*. Briefly, cells were cultured in RPMI-1640 medium supplemented with 10% fetal horse serum at 37 °C with CO<sub>2</sub> (5%). Control cells received DMSO alone at a concentration equal to that in drug-treated cell samples. The cells were incubated with the compounds (in triplicate) in a 96-well plate at 37 °C with CO<sub>2</sub> (5%) for two hours. The assay reagent MTS 3-(4,5-dimethylthiazol-2-yl)-5-(3-carboxymethoxyphenyl)-2-(4-sulfophenyl)-2*H*-tetrazolium) (Promega, Madison, WI, USA) was subsequently added and the plate was incubated for four hours. Absorbance readings (at OD<sub>490</sub>) were taken using a kinetic microplate reader (Molecular Devices, Sunnyvale, CA, USA). The quantity of viable cells after treatment with each compound was expressed as a percentage of the viability of DMSO-treated control cells (average of triplicate wells  $\pm$  standard deviation). The toxicity data was analyzed via a two-way ANOVA, with post hoc Dunnet's multiple comparisons test ( $P < 0.05$ ), utilizing GraphPad Prism 6.0 (GraphPad Software, La Jolla, CA).

#### 2.5.2 General chemistry and synthesis of compounds

Synthetic schemes, and spectral data of the first-generation compounds, in addition to all intermediates, have been previously reported.<sup>15</sup> The synthetic schemes, and spectral data of second-generation compounds are shown in Chapter 1 of this thesis.

## 2.6 References

1. Brown, G. D. *et al.* Hidden Killers: Human Fungal Infections. *Sci Transl Med* . **2012**, *4*.
2. Wisplinghoff, H. *et al.* Nosocomial bloodstream infections in US hospitals: analysis of 24,179 cases from a prospective nationwide surveillance study. *Clin Infect Dis*. **2004**, *39*, 309-317.
3. Pfaller, M. A. Antifungal drug resistance: mechanisms, epidemiology, and consequences for treatment. *The American Journal of Medicine*. **2012**, *125*, S3-13.
4. Sardi, J. C.; Scorzoni, L.; Bernardi, T.; Fusco-Almeida, A. M.; Mendes Giannini, M. J. *Candida* species: current epidemiology, pathogenicity, biofilm formation, natural antifungal products and new therapeutic options. *Journal of Medical Microbiology*. **2013**, *62*, 10-24.
5. Silva, S. *et al.* *Candida glabrata*, *Candida parapsilosis* and *Candida tropicalis*: biology, epidemiology, pathogenicity and antifungal resistance. *FEMS Microbiology Reviews*. **2012**, *36*, 288-305.
6. Park, B. J. *et al.* Estimation of the current global burden of cryptococcal meningitis among persons living with HIV/AIDS. *Aids*. **2009**, *23*, 525-530.
7. Butts, A. *et al.* Estrogen Receptor Antagonists Are Anti-Cryptococcal Agents That Directly Bind EF Hand Proteins and Synergize with Fluconazole In Vivo. *MBio*. **2014**, *5*, e00765-13.
8. The Fungal Infection Trust. How common are fungal diseases? Fungal Research Trust 20th Anniversary meeting. London June 18th 2011, updated September 2016.
9. Pappas, P. G. *et al.* Invasive Fungal Infections among Organ Transplant Recipients: Results of the Transplant-Associated Infection Surveillance Network (TRANSNET). *Clin Infect Dis*. **2010**, *50*, 1101-1111.
10. Koselny, K. *et al.* The Celecoxib Derivative AR-12 Has Broad-Spectrum Antifungal Activity *In Vitro* and Improves the Activity of Fluconazole in a Murine Model of Cryptococcosis. *Antimicrobial Agents and Chemotherapy*. **2016**, *60*, 7115-7127.
11. Kanafani, Z. A.; Perfect, J. R. Antimicrobial resistance: resistance to antifungal agents: mechanisms and clinical impact. *Clin Infect Dis*. **2008**, *46*, 120-128.
12. Ben-Ami, R. *et al.* Fitness and virulence costs of *Candida albicans* FKS1 hot spot mutations associated with echinocandin resistance. *J Infect Dis*. **2011**, *204*, 626-635.
13. Roemer, T.; Krysan, D. J. Antifungal drug development: challenges, unmet clinical needs, and new approaches. *Cold Spring Harbor perspectives in medicine*. **2014**, *4*, a019703

- 14 Denning, D. W.; Bromley, M. J. How to bolster the antifungal pipeline. *Science*. **2015** *347*, 1414-1416.
- 15 Davis, D. C. *et al.* Discovery and characterization of aryl isonitriles as a new class of compounds versus methicillin- and vancomycin-resistant *Staphylococcus aureus*. *European Journal of Medicinal Chemistry* **2015**, *101*, 384-390.
- 16 Raveh, A.; Carmeli, S. Antimicrobial ambiguines from the cyanobacterium *Fischerella* sp. collected in Israel. *Journal of Natural Products* **2007**, *70*, 196-201.
- 17 Mo, S. Y.; Krunic, A.; Chlipala, G.; Orjala, J. Antimicrobial Ambiguine Isonitriles from the Cyanobacterium *Fischerella ambigua*. *Journal of Natural Products* **2009**, *72*, 894-899.
- 18 Beck-Sague, C.; Jarvis, W. R. Secular trends in the epidemiology of nosocomial fungal infections in the United States, 1980-1990. National Nosocomial Infections Surveillance System. *J Infect Dis* **1993**, *167*, 1247-1251.
- 19 Graybill, J. R., Burgess, D. S. & Hardin, T. C. Key issues concerning fungistatic versus fungicidal drugs. *Eur J Clin Microbiol.* **1997**, *16*, 42-50.
- 20 Clinical and Laboratory Standards Institute. M27-A3, Reference Method for Broth Dilution Antifungal Susceptibility Testing of Yeasts; Approved Standard - Third Edition (Wayne, PA, 2008).
- 21 Clinical and Laboratory Standards Institute. M38-A2; Reference Method for Broth Dilution Antifungal Susceptibility Testing of Filamentous Fungi; Approved Standard (Wayne, PA, 2008).

## CHAPTER 3. INVESTIGATION OF ARYL ISONITRILES AS ANTIMALARIAL AGENTS

### 3.1 Introduction

Malaria, an infectious life-threatening disease, has over the decades remained amongst the most important and very widespread diseases in the world. In 2015, the World Health Organization (WHO) estimated 214 million cases of malaria worldwide and about 3.2 billion people (almost half the world's population) remain at risk of malaria.<sup>1</sup> With Africa and South-east Asia accounting for about 98% of global malaria cases, the mortality and susceptibility to malaria illness is particularly high among infants under five.<sup>1-3</sup> Malaria also represents a huge threat to travelers and military personnel deployed in malaria endemic countries.<sup>4</sup>

Of the different apicomplexan *Plasmodium* parasites causing malaria, *Plasmodium falciparum* is the deadliest, although *Plasmodium vivax*, *Plasmodium malariae*, and *Plasmodium ovale* still result in fatal illnesses. The occurring resistance of the parasites to the existing antimalarial drugs like the quinolones (chloroquine, amodiaquine and mefloquine), artemisinin-based combination therapies (ACTs), and the antifolate combination drugs (sulfadoxine and pyrimethamine) in malaria key areas, is making the fight against malaria increasingly complex.<sup>1-4</sup> Although there are continued attempts to develop a vaccine for malaria, drugs continue to be the mainstay when it comes to malaria treatment.<sup>5</sup> Coupled with the lack of continuous discovery of novel entities which target the plasmodium parasite, there is an urgent need for the identification of new antimalarial drug options.

The search for novel antimicrobial agents led our research group to identify aryl isonitriles as antibacterial and antifungal agents.<sup>6,7</sup> Over the last three decades, there has been reported cases of antimalarial isonitriles.<sup>8-11</sup> These diterpenes and sesquiterpenoids containing rare isonitrile functionalities have been predominantly isolated from marine sponges belonging to the Axinellidae family. Even though these compounds have been shown to possess potent antimalarial activity against both chloroquine-sensitive and chloroquine-resistant *Plasmodium falciparum* strains, their molecular complexity, which limits structural diversification, has precluded them from extensive antiplasmodial evaluation.

Inspired by the antimalarial isonitriles isolated from natural products and having discovered aryl isonitriles as a unique and unexplored chemotype in antimicrobial drug discovery, evaluating these novel entities as antimalarials was a must. Herein we evaluate a series of over 40 aryl isonitrile compounds for antimalarial activity against chloroquine-resistant Dd2 strain of malaria.

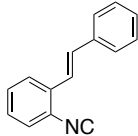
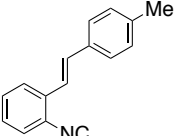
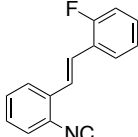
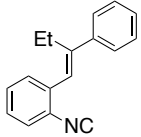
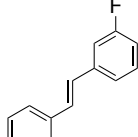
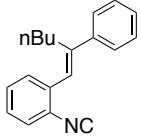
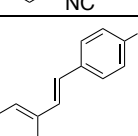
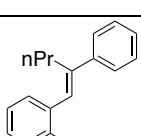
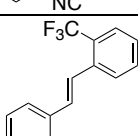
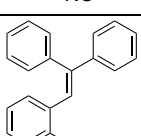
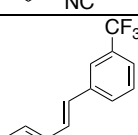
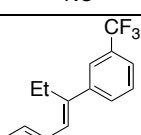
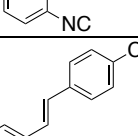
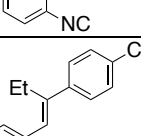
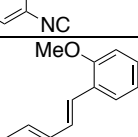
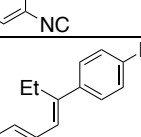
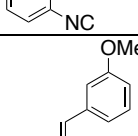
## 3.2 Results and Discussion

### 3.2.1 *Structure-activity relationship of aryl isonitriles against chloroquine-resistant Plasmodium falciparum*

Chloroquine resistant *Plasmodium falciparum*, as stated previously, has been implicated in over 70% of malarial infections; thus, we evaluated our aryl isonitriles for antiplasmodial activity against clinical isolates of *Plasmodium falciparum*. We began by screening the initially synthesized *ortho*-substituted stilbene aryl isonitrile derivatives (Table 3.1). Of the initial nine evaluated compounds, which consists of those with medicinally relevant small molecules such as trifluoromethyl, fluoro, and methoxy groups, **3.6** ( $IC_{50} = 0.265 \mu\text{M}$ ) with trifluoromethyl group showed the most potency. This was followed by fluoro derivative **3.4** ( $IC_{50} = 0.562 \mu\text{M}$ ), and methoxy derivative **3.10** ( $IC_{50} = 3.070 \mu\text{M}$ ). These small molecule modifications proved to be impactful considering **3.1** ( $IC_{50} = 11.53 \mu\text{M}$ ), which has no small molecule modification, exhibited decreased activity, comparatively.

Structural modifications on the alkene bridge of the *ortho*-substituted stilbene aryl isonitriles were then evaluated. **3.13** ( $IC_{50} = 3.064 \mu\text{M}$ ), with a propyl group on the bridge exhibited the most activity followed by the phenyl **3.14** ( $IC_{50} = 3.632 \mu\text{M}$ ), butyl **3.12** ( $IC_{50} = 5.247 \mu\text{M}$ ), and ethyl **3.11** ( $IC_{50} = 10.55 \mu\text{M}$ ) derivatives. None of the compounds with this modification were as active as the most active trifluoromethyl and fluoro analogues, thus modification is less favored. Incorporating ethyl-alkene bridge substitutions as in **3.15** ( $IC_{50} = 5.412 \mu\text{M}$ ), **3.16** ( $IC_{50} = 7.690 \mu\text{M}$ ), and **3.17** ( $IC_{50} = 9.84 \mu\text{M}$ ), for the most active fluoro and trifluoromethyl aryl isonitriles led to significant activity loss, further highlighting the low tolerability for alkene bridge modifications.

Table 3.1. Antimalarial activity of evaluated *ortho*-aryl isonitriles

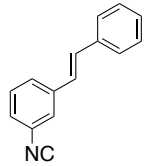
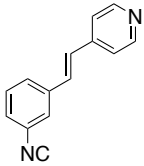
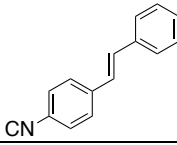
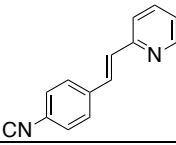
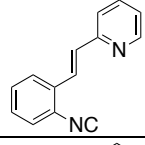
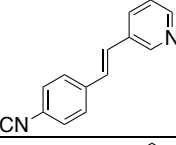
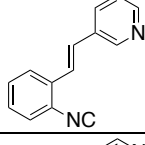
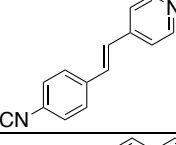
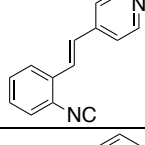
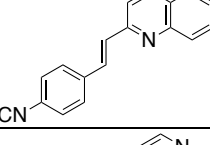
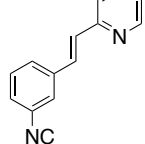
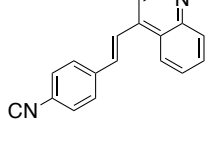
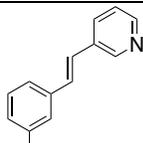
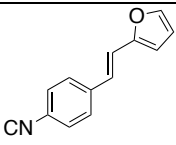
Isonitrile compound	Structure	Activity, IC <sub>50</sub> (μM)	Isonitrile compound	Structure	Activity IC <sub>50</sub> (μM)
3.1		11.53	3.10		3.070
3.2		3.682	3.11		10.55
3.3		12.440	3.12		5.247
3.4		0.562	3.13		3.064
3.5		4.305	3.14		3.632
3.6		0.265	3.15		5.412
3.7		5.803	3.16		7.690
3.8		21.630	3.17		9.84
3.9		6.447			

*Meta*- and *para*-substituted stilbene isonitriles were then evaluated (Table 3.2). The improved activity as shown in the *para*-derivative **3.19** ( $IC_{50} = 2.765 \mu M$ ) and the *meta*-derivative **3.18** ( $IC_{50} = 5.318 \mu M$ ) compared to the *ortho*-aryl isonitrile **3.1** ( $IC_{50} = 11.53 \mu M$ ) led to the consideration of their corresponding pyridine analogues (Table 3.2).

Replacing the second aromatic ring with that of pyridine led to improved activity only in some cases. For instance, the *ortho*-substituted **3.20**, **3.21**, and **3.22** ( $IC_{50} = 7.525$ ,  $12.98$ , and  $3.708$ , respectively) stilbene isonitriles, showed no improved activity when compared to the *para*-stilbene isonitrile **3.19** ( $IC_{50} = 2.765 \mu M$ ), the initial most active fluoro **3.4** ( $IC_{50} = 0.562 \mu M$ ) and trifluoromethyl **3.6** ( $IC_{50} = 0.265 \mu M$ ) derivatives. Although no *meta*-substituted pyridine containing aryl isonitrile was as effective as **3.4** and **3.6**, **3.24** ( $IC_{50} = 0.689 \mu M$ ) containing a 4-pyridyl group exhibited better activity than **3.19**. Interestingly, **3.28**, a *para*-substituted aryl isonitrile containing a 4-pyridyl group exhibited tremendous improvement in antiplasmodial activity when compared to all of the most potent compounds. In fact, **3.28** ( $IC_{50} = 0.08711 \mu M$ ) exhibited a tremendous improvement on compound **3.6**.

The activity exhibited by **3.28** led to assessment of aryl isonitriles with quinoline and furan heterocyclic moieties (Table 3.2). Of these heterocyclic containing isonitriles, furan containing compound **3.31** ( $IC_{50} = 2.658 \mu M$ ) exhibited the most activity followed by quinoline isonitriles **3.29** ( $IC_{50} = 5.247 \mu M$ ), and **3.30** ( $IC_{50} = 6.982 \mu M$ ), respectively. However, none of these were as active as **3.28**.

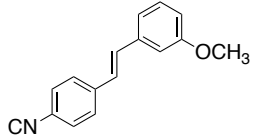
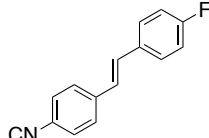
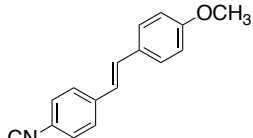
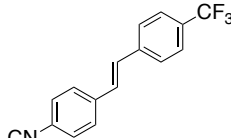
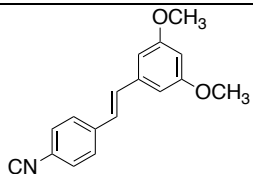
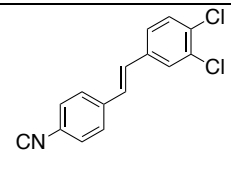
Table 3.2. Antimalarial activity of pyridine, quinoline, and furan stilbene aryl isonitriles.

Isonitrile compound	Structure	Activity IC <sub>50</sub> (μM)	Isonitrile compound	Structure	Activity IC <sub>50</sub> (μM)
3.18		5.318	3.25		-
3.19		2.765	3.26		10.330
3.20		7.525	3.27		5.177
3.21		12.98	3.28		0.08711
3.22		3.703	3.29		5.247
3.23		9.731	3.30		6.982
3.24		0.689	3.31		2.658

The noticeable increase in activity of the *ortho*-substituted derivatives upon the incorporation of the trifluoromethyl, fluoro, and methoxy groups, and the tremendous activity of the *para*-substituted pyridyl derivative **3.28**, led to the evaluation of the *para*-isonitrile analogues containing these fragments (Table 3.3). That of chloro was also evaluated to determine its effect. Methoxy derivatives **3.32** (IC<sub>50</sub> = 1.014 μM), **3.34** (IC<sub>50</sub> = 1.615 μM), **3.33** (IC<sub>50</sub> = 2.273 μM), chloro derivative **3.37** (IC<sub>50</sub> = 3.210 μM), fluoro derivative **3.35** (IC<sub>50</sub> = 4.694 μM), and trifluoro methyl derivative **3.36** (IC<sub>50</sub> = 2.174 μM) all exhibited good activity. However, none of these

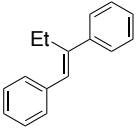
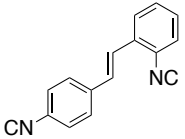
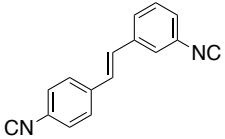
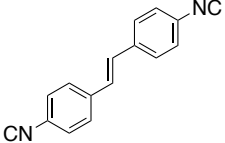
structural modifications led to a better antiplasmodial activity than the most active pyridine compound **3.28** ( $IC_{50} = 0.08711 \mu M$ ).

Table 3.3. Antimalarial activity of stilbene aryl isonitriles with small molecule groups.

Isonitrile compound	Structure	Activity $IC_{50}$ ( $\mu M$ )	Isonitrile compound	Structure	Activity $IC_{50}$ ( $\mu M$ )
<b>3.32</b>		1.014	<b>3.35</b>		4.694
<b>3.33</b>		2.273	<b>3.36</b>		2.174
<b>3.34</b>		1.615	<b>3.37</b>		3.210

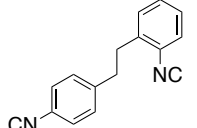
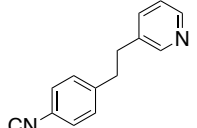
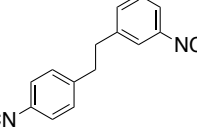
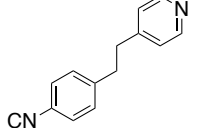
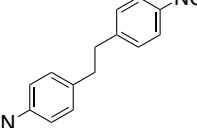
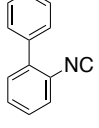
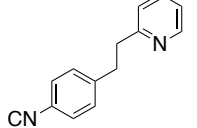
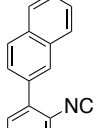
Emboldened by the activity aryl isonitriles and importance of the isonitrile functionality, we evaluated the effect of including an extra isonitrile functionality (Table 3.4). Compound **3.38**, lacking the isonitrile functionality, showed no antimalarial activity ( $IC_{50} > 100$ ). This is indicative of the importance of the isonitrile functional group for antimalarial activity. Incorporating an additional isonitrile group as in **3.39**, **3.40**, and **3.41** resulted in a stronger antimalarial efficacy compared to the monosubstituted isonitriles **3.1**, **3.18**, and **3.19** ( $IC_{50} = 11.53 \mu M$ ,  $5.318 \mu M$ ,  $2.765 \mu M$ ), respectively. With the most symmetrical *para*-analogue **3.41** exhibiting the most activity followed by the *ortho*-substituted analogue, and the *meta*-analogue. These results further prove the importance of the isonitrile functional group for antimalarial activity.

Table 3.4. Antimalarial activity of bis-isonitriles.

Isonitrile compound	Structure	Activity IC <sub>50</sub> (μM)
3.38		>100
3.39		0.0682
3.40		0.266
3.41		0.0273

To understand the activity of the stilbene isonitriles further, we evaluated bis-isonitriles without the alkene bridge (Table 3.5). Compared to their corresponding stilbene analogues, all the bis-isonitriles with the alkane bridge (**3.42** (IC<sub>50</sub> = 0.437 μM), **3.43** (IC<sub>50</sub> = 2.753 μM), **3.44** (IC<sub>50</sub> = 0.215 μM)) exhibited lower activity. Similar to the trend in the stilbene bis-isonitriles, the para analogue exhibited the best activity followed by the ortho and then the meta. Pyridine compounds with alkane bridge (**3.45** (IC<sub>50</sub> = -), **3.46** (IC<sub>50</sub> = 10.100 μM), **3.47** (IC<sub>50</sub> = 0.557 μM)) also exhibited significantly lower activity compared to their stilbene analogues. Compounds **3.48** (IC<sub>50</sub> = 10.82 μM) and **3.49** (IC<sub>50</sub> = 6.212 μM) without a bridge, had significantly reduced activity relative to the stilbene analogues. This result coupled with that of the alkane bridge showed the alkene bridge is highly favorable.

Table 3.5. Antimalarial activity of aryl isonitriles with alkane bridge.

Isonitrile compound	Structure	Activity IC <sub>50</sub> (μM)	Isonitrile compound	Structure	Activity IC <sub>50</sub> (μM)
3.42		0.437	3.46		10.100
3.43		2.753	3.47		0.557
3.44		0.215	3.48		10.82
3.45		-	3.49		6.212

Overall, the structure-antimalarial analysis revealed some key findings. The presence of the isonitrile group, the *para*-position of the isonitrile, and the alkene bridge appeared to be critical for antimalarial activity. This information is important to help guide the development of aryl isonitrile analogues as antimalarial agents.

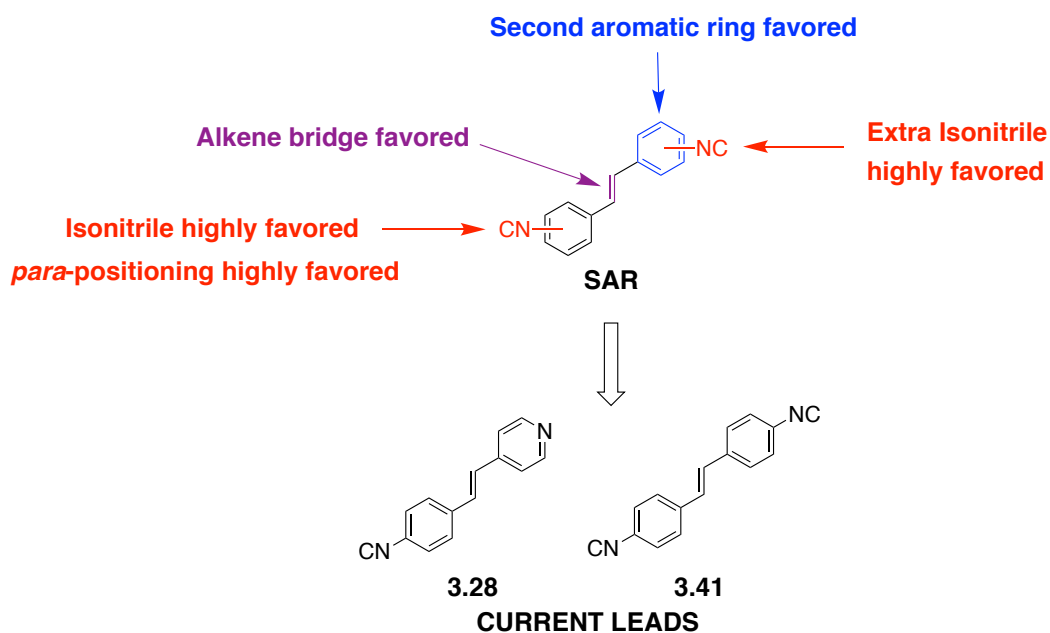


Figure 3.1. Structure-activity relationship leading to current lead compounds.

### 3.3 Conclusion

Structure-antimalarial relationship analysis of over 40 aryl isonitrile compounds have established the isonitrile functionality as an important moiety for antimalarial activity. Of the many isonitrile compounds exhibiting potent antimalarial activity, **3.28** and **3.41** have emerged as leads. These compounds exhibited activity comparable to that of Artemisinin. The SAR details presented in this study will prove essential for the development of new aryl isonitrile analogues to advance them to the next step in the antimalarial drug discovery process.

### 3.4 References

1. WHO, World Malaria Report: Geneva, Switzerland. **2015**.
2. Snow, R. W.; Guerra, C. A.; Noor, A. M.; Myint, H. Y.; Hay, S. I. The global distribution of clinical episodes of Plasmodium falciparum malaria. *Nature*. **2005**, *434*, 214-217.
3. Bathurst, I.; Hentschel, C. Medicines for Malaria Venture: Sustaining antimalarial drug development. *Trends Parasitology*. **2006**, *22*, 301-307.
4. Castelli, F.; Odolini, S.; Austino, B.; Foca, E.; Russo, R.; Malaria Prophylaxis: A comprehensive review. *Pharmaceuticals*. **2010**, *3*, 3212-3239.
5. Bawa, S.; Kumar, S.; Drabu, S.; Kumar, R. Structural modifications of quinolone-based antimalarial agents: Recent developments. *J. Pharm. Bioallied Sci.* **2010**, *2*, 64-71.
6. Davis, D. C.; Mohammad, H.; Kyei-Baffour, K.; Younis, W.; Creemer, C. N.; Seleem, M. N.; Dai, M. J. Discovery and characterization of aryl isonitriles as a new class of compounds versus methicillin- and vancomycin-resistant Staphylococcus aureus. *European Journal of Medicinal Chemistry* **2015**, *101*, 384-390.
7. Mohammad, H.; Kyei-Baffour, K.; Younis, W.; Davis, D. C.; Eldesouky, H.; Seleem, M. N.; Dai, M. J. Investigation of aryl isonitrile compounds with potent, broad-spectrum antifungal activity *Bioorganic & Medicinal Chemistry* **2017**, *25*, 2926-2931.
8. Fattorusso, E.; Tagliatela-Scafati, O. Marine Antimalarials. *Mar. Drugs*. **2009**, *7*, 130-152.
9. Angerhofer, C. K.; Pezzuto, J. M.; Wright, A. D.; Sticher, O. Antimalarial activity of sesquiterpenes from the marine sponge Acanthella klethra. *J. Nat. Prod.* **1992**, *55*, 1787-1787.

10. Koenig, G. M.; Wright, A. D.; Angerhofer, C. K. Novel Potent Antimalarial diterpene isocyanates, isothiocyanates, and isonitriles from the tropical marine sponge *Cymbastela hooperi*. *J. Org. Chem.* **1996**, *61*, 3259–3267.
11. Wright, A. D.; Lang-Unnasch, N. Diterpene formamides from the tropical marine sponge *Cymbastela hooperi* and their antimalarial activity in vitro. *J. Nat. Prod.* **2009**, *72*, 492-495.

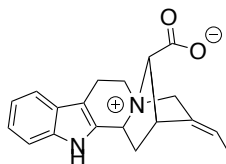
## CHAPTER 4. TOTAL SYNTHESIS OF ( $\pm$ )-17-NOR-EXCELSINIDINE

### 4.1 Introduction

Natural products have served as starting points for the discovery of drugs, drug leads, and compounds that enable the understanding of biological systems and disease states over decades. Indole alkaloids are particularly of extreme prominence because of their biological activities and for being a valuable source of novel drug entities.<sup>1,2</sup>

*Apocynaceae*, an abundant family of plants in the tropical regions of Africa and Asia, are widely known as a rich source of unique and unusual indole alkaloids. These alkaloids predominantly containing a monoterpene indole skeleton have been the subject of wide synthetic scrutiny and attention in the organic chemistry, biogenetic, biochemical, and biological fields. This is so primarily because, beyond their biological activity, these entities showcase unprecedented structural diversity and features.<sup>3</sup>

Recently, Zhang and coworkers reported the isolation of (-)-17-nor-Excelsinidine from the twigs and leaves of *Alstonia scholaris*.<sup>4</sup> This *Apocynaceae*, aside from being rich in indole alkaloids, has been previously shown *via* phytochemical examination to contain various indole alkaloids with diverse biological activity including cytotoxic, antiviral, and antiplasmodial activities.<sup>5,6</sup> Preliminary biological studies on (-)-17-nor-Excelsinidine revealed that this novel alkaloid possessed anti-HSV and anti-adenoviral activities. The structure was confirmed *via* NMR and x-ray crystallography to contain an unusual 1-azoniatricyclo [4.3.3.0] undecane moiety. The intriguing structural features, impressive biological activities, and the rising interest in exploring ways to assemble this family of monoterpene indole alkaloids makes 17-nor-Excelsinidine a notable target for synthetic exploration. Herein, we describe our recent efforts culminating in the total synthesis of ( $\pm$ )-17-nor-Excelsinidine (**4.1**).



( $\pm$ )-17-nor-Excelsinidine (**4.1**)

Figure 4.1. Structure of ( $\pm$ )-17-nor-Excelsinidine (**4.1**).

## 4.2 Previous synthetic approach towards (-)-17-nor-Excelsinidine.

In 2018, inspired by postulated biosynthesis of akuamilins, Jarrett and coworkers reported the first total synthesis of (-)-17-nor-Excelsinidine (**4.1b**).<sup>7</sup> The elegant synthesis features a bioinspired oxidative cyclization approach from the geissoschizine framework.

Geissoschizine, a corynantheoid alkaloid, has been shown over the years to be a pivotal intermediate and a common biosynthetic origin for several monoterpene indole alkaloids.<sup>7-9</sup> With this knowledge, Jarrett and coworkers envisioned that accessing the geissoschizine framework as in **4.2**, will enable the N4-C16 oxidative cyclization leading to (-)-17-nor-Excelsinidine.

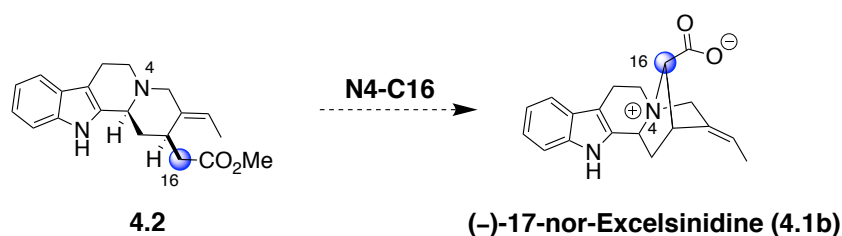
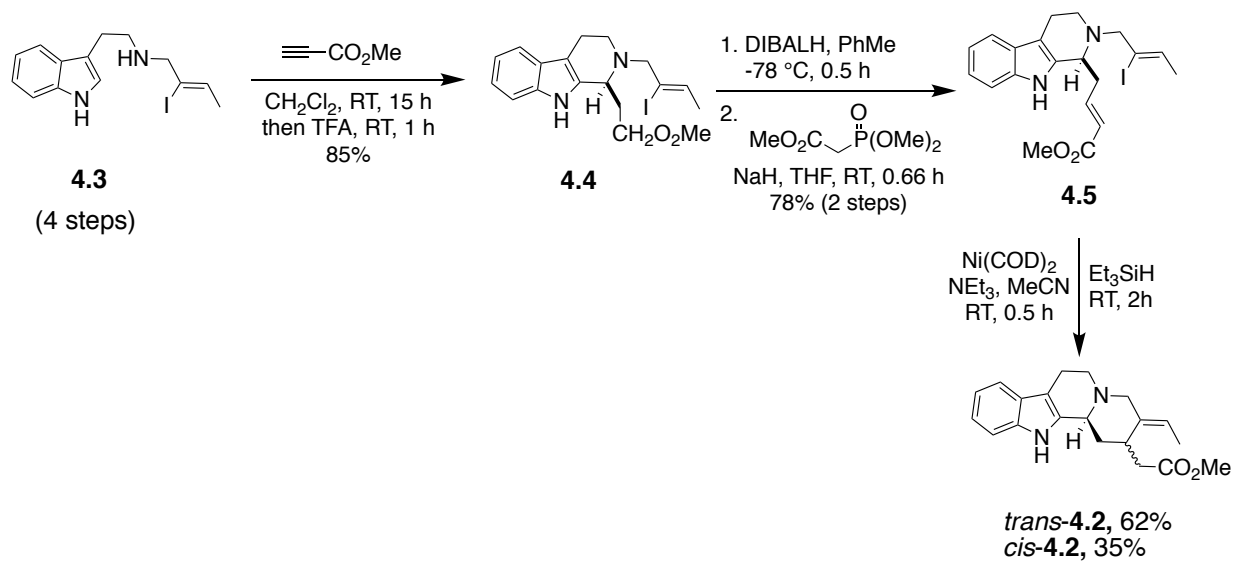
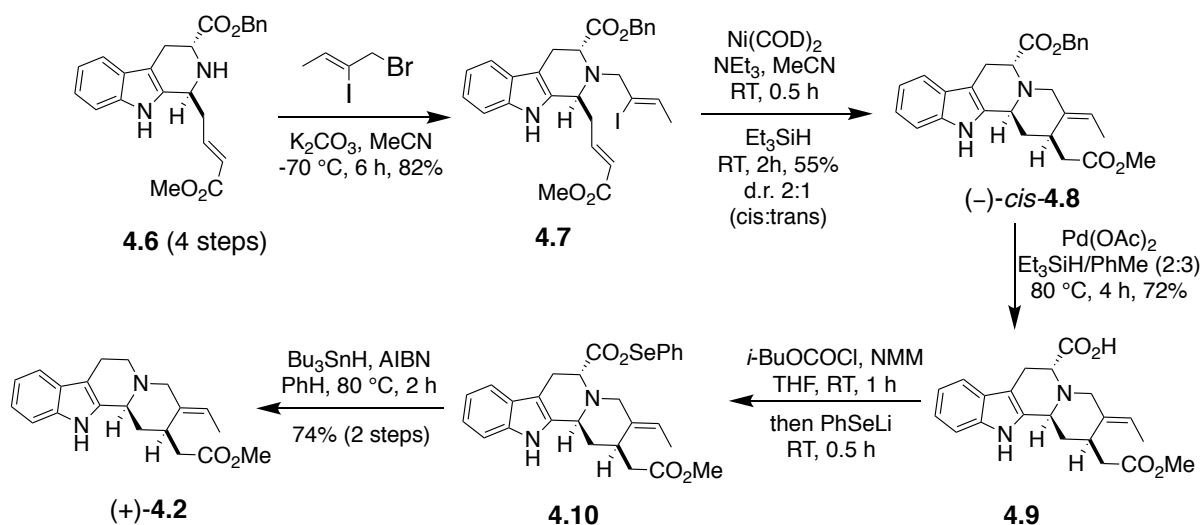


Figure 4.2. Jarrett's proposed oxidative cyclization strategy to (-)-17-nor-Excelsinidine.

Jarrett's synthesis initially commenced with a Pictet-Spengler-like reaction to obtain **4.4** from tryptamine derivative **4.3**. DIBAL-H reduction of **4.4** and subsequent olefination led to alkenyl iodide **4.5**. Nickel-mediated 1,4-intramolecular addition was then employed as a strategy to obtain the required cis-**4.2**. However, the intramolecular addition process led to the undesired trans-isomer as the major diastereomer. Jarrett and co-workers decided having a benzyloxycarbonyl substituent on C5 will stereoselectively control the addition – a strategy demonstrated by Cook et. al.<sup>10</sup>

Scheme 2.1. Jarret's synthesis of **4.2**

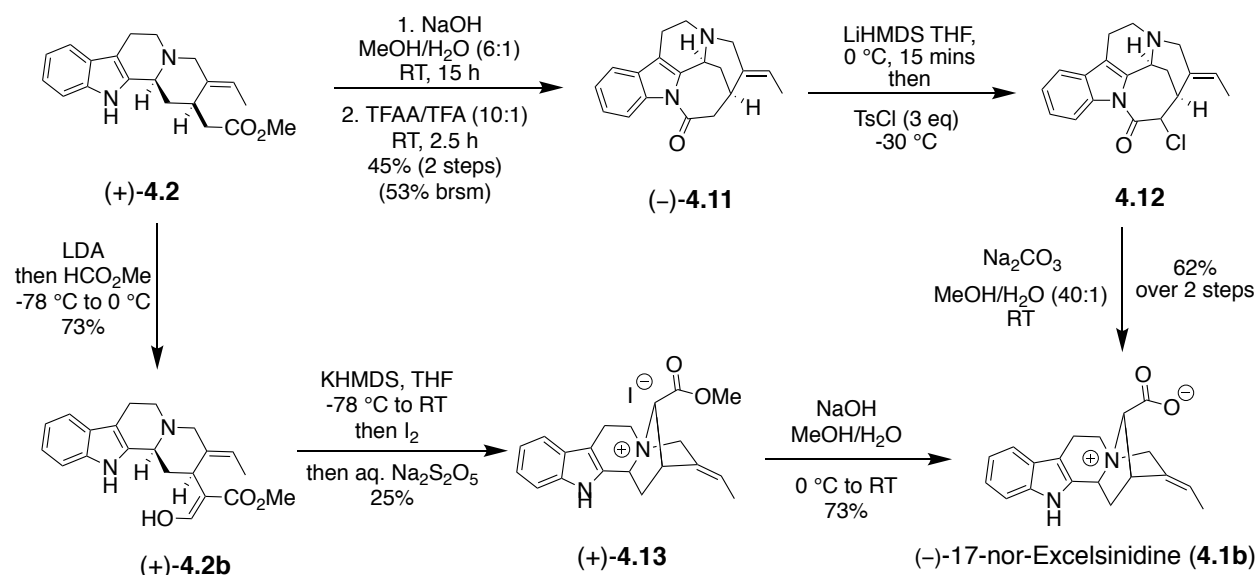
Starting with enantiopure D-tryptophan, a 4-step reaction sequence yielded tetrahydro- $\beta$ -carboline **4.6**. Nucleophilic N14 substitution on **4.6** with allyl bromide installed the desired iodoprene moiety to form **4.7**. Ni(COD)<sub>2</sub> mediated radical cyclization of **4.7** then led to the desired cis-**4.8** with 2:1 diastereoselectivity. After 4 steps involving debenzoylation to carboxylic acid **4.9**, formation of phenylselenoester **4.10**, and decarboxylation, the desired cis-deformylgeissoschizine **4.2** compound was formed.



Scheme 4.2. Jarret's synthesis of (+)-16-deformylgeissoschizine (+)-4.2

After the failure of the proposed N4-C16 oxidative cyclization on (+)-4.2, Vincent envisaged that accessing a more globular structure would facilitate the required oxidative cyclization. After successfully obtaining the desired structure (-)-4.11 from (+)-4.2, diastereoselective  $\alpha$ -chlorination followed by nucleophilic addition by N-14, and lactam cleavage, led to the desired (-)-17-nor-Excelsinidine in a total of 7% yield over 12 steps.

In an alternate strategy, Jarret and coworkers performed a formylation on (+)-4.2 to access (+)-geissoschizine, (+)-4.2b. KHMDS and iodine inspired ring closure to methyl ester (+)-4.13, followed by saponification led to the desired (-)-17-nor-Excelsinidine in a total of 2% yield over 11 steps.



Scheme 4.3. Jarret's completion of total synthesis of (-)-17-nor-Excelsinidine.

#### 4.3 Synthetic strategy towards ( $\pm$ )17-nor-Excelsinidine

Palladium-catalyzed carbonylation reactions have found wide utility in organic synthesis. Since the seminal work on palladium-catalyzed carbonylation of aryl and vinyl halides by Heck in 1974,<sup>11</sup> several efforts have been made in this area towards the synthesis of pharmacologically active compounds, and the total synthesis of complex natural products.

Quite recently, our lab has been interested in the utility of carbon monoxide as a one-carbon linchpin to facilitate the total synthesis of complex biologically active natural products.<sup>12-16</sup> In this regard, and after careful examination of **4.18**, we envisioned building the 6-membered and 7-membered lactam rings contiguously from alkenyl iodide **4.17** using an unprecedented palladium-catalyzed carbonylative Heck lactamization reaction as the key step. The success of this strategy means, we would have accomplished in a single step a reaction that previously took 5-7 from the alkenyl iodide. We believe the rigid nature of **4.18** together with the proximity of all reactive centers will not only facilitate the final steps of our total synthesis, but also aid in the synthesis of other indole natural products in this family by serving as a key pivotal intermediate, hence the need for a more efficient and expedient way to build this scaffold.

To achieve the synthesis of alkenyl iodide **4.17**, we envisioned using nucleophilic N4-substitution involving **4.15** and allyl bromide **4.16**. Pictet-Spengler-type reaction, followed by

Grignard reaction, will then allow the synthesis of **4.15** from commercially available tryptamine. Allyl bromide **4.16** can be readily obtained from crotonaldehyde. With access to **4.18**, we will employ Jarret's oxidative cyclization strategy to accomplish the synthesis of ( $\pm$ )-17-nor-Excelsinidine.<sup>7</sup>

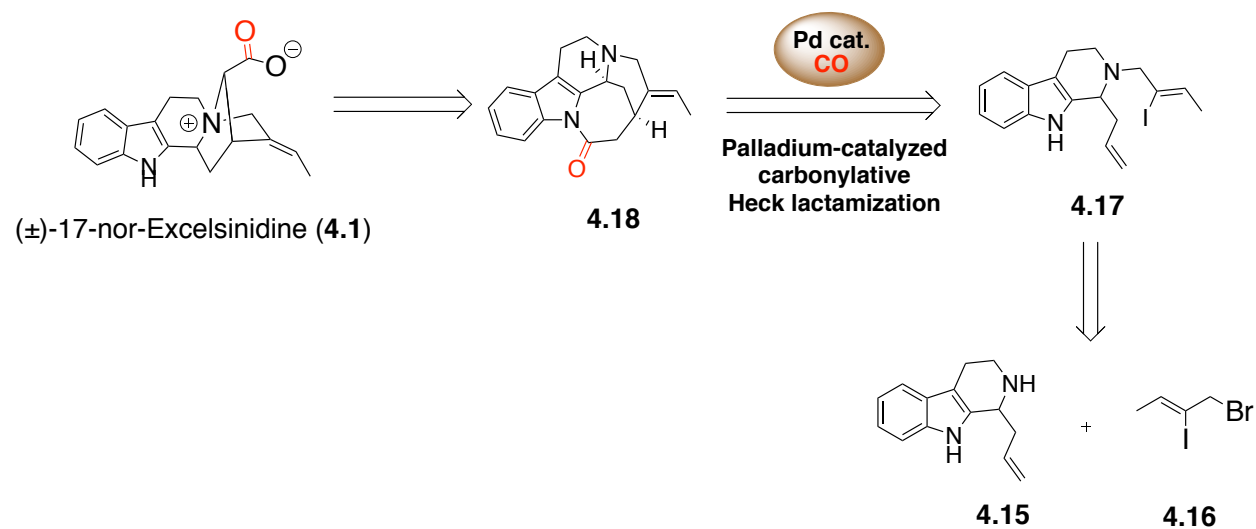
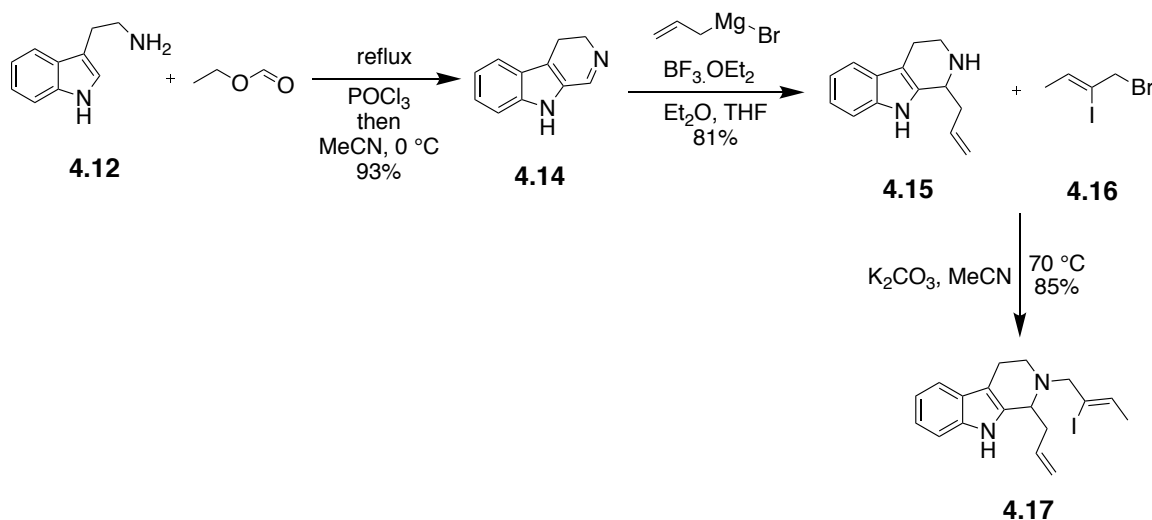


Figure 4.3. Retrosynthetic strategy towards ( $\pm$ )-17-nor-Excelsinidine (**4.1**).

## 4.4 Results and Discussion

Following the initial identification of **4.17** as an ideal carbonylation precursor for the synthesis of pentacyclic seven-membered lactam **4.18**, our initial synthetic efforts were geared towards this vinyl iodoprene compound. To access **4.17**, we first had to synthesize **4.15**. Using commercially available tryptamine and ethyl formate as starting materials, a Pictet-Spengler-like reaction was employed to synthesize carboline **4.14** in 93% yield. Subsequent precomplexation with  $\text{BF}_3 \cdot \text{OEt}_2$ , followed by the addition of allylmagnesium bromide yielded **4.15** in 81% yield. N4-nucleophilic reaction between **4.15** and allyl bromide **4.16** led to the installation of the iodoprene moiety of **4.17** in 85% yield.

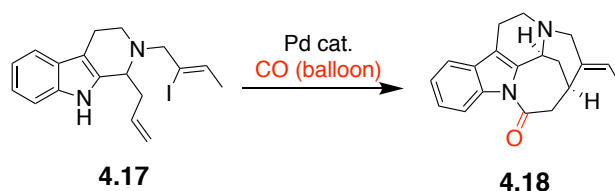


Scheme 4.4. Scheme 4.4. Synthesis of carbonylation precursor **4.17**.

With **4.17** in hand, we started to explore the key palladium-catalyzed carbonylation step. We started off by trying reaction conditions previously developed in our lab in a palladium-catalyzed macrolactonization process.<sup>13</sup> To our delight, this process involving 10%  $\text{Pd}(\text{OAc})_2$ , 20%  $\text{PPh}_3$ , 1.0 equiv.  $\text{Et}_4\text{NCl}$ , molecular sieves, and toluene as solvent yielded the 6-membered and 7-membered lactam rings in 13% yield in a single step (Table 1, entry 1). Buoyed by the success of this reaction condition, we decided to explore the effect ligand, solvent, temperature and other additives will have on chemical reactivity. With the initial success of  $\text{PPh}_3$ , we decided to explore other monodentate phosphine ligands of varying bulkiness. To our dismay, the use of

$P(o\text{-tol})_3$ ,  $P(2\text{-furyl})_3$  and  $P(1\text{-nap})_3$  proved futile in raising the yield of the carbonylation reaction (Table 1, entry 2-4). Since the initial reports by Buchwald and co-workers,<sup>17</sup> very bulky and electron-rich mono[dialkyl(biaryl)]phosphine]s have been shown to have the appropriate electronic and steric characteristics that favor key steps in the catalytic cycle of palladium-catalyzed carbonylation reactions.<sup>18</sup> In view of this, we decided to explore XPhos and JohnPhos as alternative ligands. Even though XPhos led to 2.7% carbonylation product (entry 5), JohnPhos produced no product (entry 6). Additionally, bidentate ligands DPPF and DPPE failed to help improve the yield (entry 7 and 8).

Table 4.1. Optimization of carbonylation reaction: ligand screening.

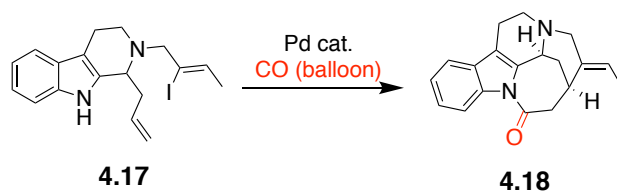


Entry	Pd Catalyst <sup>a</sup>	Ligand <sup>b</sup>	Additive <sup>c</sup>	Solvent <sup>d</sup>	Temp (°C)	Time (h)	Yield
<b>1</b>	Pd(OAc) <sub>2</sub>	PPh <sub>3</sub>	Et <sub>4</sub> NCl/ MS	Toluene	90 °C	48 h	13%
<b>2</b>	Pd(OAc) <sub>2</sub>	P(2-furyl) <sub>3</sub>	Et <sub>4</sub> NCl/ MS	Toluene	90 °C	48 h	Trace
<b>3</b>	Pd(OAc) <sub>2</sub>	P( <i>o</i> -tol) <sub>3</sub>	Et <sub>4</sub> NCl/ MS	Toluene	90 °C	48 h	Trace
<b>4</b>	Pd(OAc) <sub>2</sub>	P(1-nap) <sub>3</sub>	Et <sub>4</sub> NCl/ MS	Toluene	90 °C	48 h	Trace
<b>5</b>	Pd(OAc) <sub>2</sub>	XPhos	Et <sub>4</sub> NCl/ MS	Toluene	90 °C	48 h	2.7%
<b>6</b>	Pd(OAc) <sub>2</sub>	JohnPhos	Et <sub>4</sub> NCl/ MS	Toluene	90 °C	48 h	NR
<b>7</b>	Pd(OAc) <sub>2</sub>	DPPE	Et <sub>4</sub> NCl/ MS	Toluene	90 °C	48 h	Trace
<b>8</b>	Pd(OAc) <sub>2</sub>	DPPF	Et <sub>4</sub> NCl/ MS	Toluene	90 °C	48 h	5.4%

a = 0.1 equiv. b = 0.2 equiv. c = 1.0 equiv. d = 0.0096 M, NR = no reaction.

In light of the superior performance exhibited by  $\text{PPh}_3$ , we moved our attention to solvent screening (Table 2). Gratifyingly, of the solvents screened (DMF, THF, dioxane DCE, and MeCN), THF was found to help increase the yield from 13% to 23% (entry 13). Our attention then drifted to the exploration of additives other than  $\text{Et}_4\text{NCl}$ . With the initial results exhibited by  $\text{Et}_4\text{NCl}$  coupled with the knowledge of tetraalkylammonium salts being successful in enhancing intramolecular Heck-type reactions,<sup>19-21</sup>  $\text{Et}_4\text{NBr}$ ,  $\text{Et}_4\text{NI}$ , and  $\text{BnEt}_3\text{NCl}$  were screened (entry 14, 15, 16). Unfortunately, none of these phase transfer conditions yielded any tremendous effect.

Table 4.2. Optimization of carbonylation reaction: solvent and additive screening.



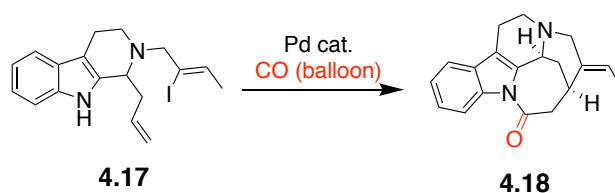
Entry	Pd Catalyst <sup>a</sup>	Ligand <sup>b</sup>	Additive <sup>c</sup>	Solvent <sup>d</sup>	Temp (°C)	Time (h)	Yield
9	$\text{Pd}(\text{OAc})_2$	$\text{PPh}_3$	$\text{Et}_4\text{NCl}/\text{MS}$	dioxane	95	48	5.4%
10	$\text{Pd}(\text{OAc})_2$	$\text{PPh}_3$	$\text{Et}_4\text{NCl}/\text{MS}$	DMF	140	48	Trace
11	$\text{Pd}(\text{OAc})_2$	$\text{PPh}_3$	$\text{Et}_4\text{NCl}/\text{MS}$	DCE	75	48	Trace
12	$\text{Pd}(\text{OAc})_2$	$\text{PPh}_3$	$\text{Et}_4\text{NCl}/\text{MS}$	MeCN	75	48	3.5%
13	$\text{Pd}(\text{OAc})_2$	$\text{PPh}_3$	$\text{Et}_4\text{NCl}/\text{MS}$	THF	65	48	23%
14	$\text{Pd}(\text{OAc})_2$	$\text{PPh}_3$	$\text{Et}_4\text{NI}/\text{MS}$	THF	65	48	NR
15	$\text{Pd}(\text{OAc})_2$	$\text{PPh}_3$	$\text{Et}_4\text{NBr}/\text{MS}$	THF	65	48	Trace
16	$\text{Pd}(\text{OAc})_2$	$\text{PPh}_3$	$\text{BnEt}_3\text{NCl}/\text{MS}$	THF	65	48	2.5%

a = 0.1 equiv. b = 0.2 equiv. c = 1.0 equiv. d = 0.0096 M, NR = no reaction.

After Cs<sub>2</sub>CO<sub>3</sub> had led to 12% isolated yield (Table 4.3, entry 17), other inorganic bases were explored. Neither Na<sub>2</sub>CO<sub>3</sub> nor K<sub>2</sub>CO<sub>3</sub> gave better yields (entry 18 and 19).

Intrigued by the results so far, we were curious as to the effect solid-liquid phase transfer conditions (tetraalkylammonium salts-base) will have on chemical reactivity (Table 4.3). To our utmost delight, the combination of Et<sub>4</sub>NCl-Cs<sub>2</sub>CO<sub>3</sub>, led to the isolation of the desired seven-membered lactam in 32% yield (entry 22).

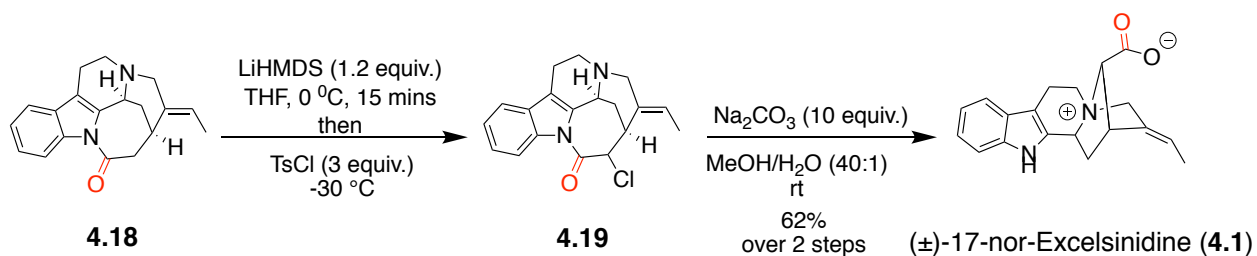
Table 4.3. Optimization of carbonylation reaction: base and additive screening.



Entry	Pd Catalyst	Ligand <sup>b</sup>	Additive <sup>c</sup>	Solvent <sup>d</sup>	Temp (°C)	Time (h)	Yield
17	Pd(OAc) <sub>2</sub>	PPh <sub>3</sub>	Cs <sub>2</sub> CO <sub>3</sub> / MS	THF	65	48	12%
18	Pd(OAc) <sub>2</sub>	PPh <sub>3</sub>	Na <sub>2</sub> CO <sub>3</sub> / MS	THF	65	48	NR
19	Pd(OAc) <sub>2</sub>	PPh <sub>3</sub>	K <sub>2</sub> CO <sub>3</sub> / MS	THF	65	48	3.2%
20	Pd(OAc) <sub>2</sub>	PPh <sub>3</sub>	Et <sub>4</sub> NCl-Cs <sub>2</sub> CO <sub>3</sub> , MS	THF	65	48 h	32%
21	Pd(OAc) <sub>2</sub>	PPh <sub>3</sub>	Et <sub>4</sub> NCl-K <sub>2</sub> CO <sub>3</sub> , MS	THF	65	48 h	Trace
22	Pd(OAc) <sub>2</sub>	PPh <sub>3</sub>	Et <sub>4</sub> NCl-Na <sub>2</sub> CO <sub>3</sub> , MS	THF	65	48 h	13%
23	Pd(OAc) <sub>2</sub>	PPh <sub>3</sub>	Et <sub>4</sub> NI-Cs <sub>2</sub> CO <sub>3</sub> , MS	THF	65	48 h	NR
24	Pd(OAc) <sub>2</sub>	PPh <sub>3</sub>	BnEt <sub>3</sub> NCl-Cs <sub>2</sub> CO <sub>3</sub> , MS	THF	65	48 h	22%

a = 0.1 equiv. b = 0.2 equiv. c = 1.0equiv.-1.0 equiv. d = 0.0096 M, NR = no reaction.

Having successfully assembled the pentacyclic core, we focused our efforts on completing the total synthesis of the natural product. Employing the oxidative cyclization strategy by Jarret et. al., we performed the  $\alpha$ -chlorination reaction using TsCl to afford **4.19**. Subsequent nucleophilic substitution of the  $\alpha$ -chloro by N-4, followed by cleavage of the lactam, afforded ( $\pm$ )-17-nor-Excelsinidine (**4.1**) (Scheme 4.5).



Scheme 4.5. Completion of total synthesis of ( $\pm$ )-17-nor-Excelsinidine (**4.1**).

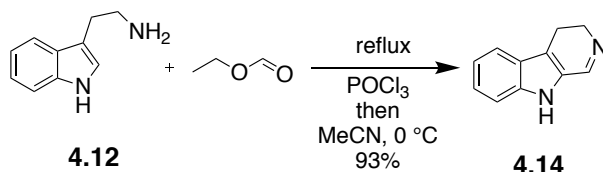
#### 4.5 Conclusion

In summary, we have successfully completed the total synthesis of ( $\pm$ )-17-nor-Excelsinidine, a zwitterionic monoterpene indole alkaloid that displays an unusual 1-azaniatricyclo [4.3.3.0] undecane moiety. The 6-step synthesis features the use of an unprecedented palladium-catalyzed carbonylative Heck lactamization procedure as the key step to assemble 6, 7-membered lactam in one step. This rigid pentacyclic product, which served as key precursor for the 6-step synthesis of ( $\pm$ )-17-nor-Excelsinidine in 13% overall yield, can also serve as a key synthetic intermediate useful for the synthesis of related indole alkaloids.

## 4.6 Experimental Section

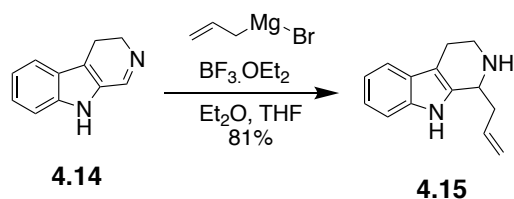
All reactions were performed using standard syringe techniques under argon unless stated otherwise. Starting materials and reagents were used as obtained from suppliers. Tetrahydrofuran (THF) was distilled over sodium benzophenone under argon prior to use. Acetonitrile (CH<sub>3</sub>CN), dichloromethane (CH<sub>2</sub>Cl<sub>2</sub>), methanol (MeOH), and toluene were purified by passing the previously degassed solvents through activated alumina columns. Thin layer chromatography (TLC) was performed using glass-backed silica plates (Silicycle). All compounds were purified using flash chromatography with silica gel (230-400 mesh).

NMR spectra were recorded on a Bruker ARX-400 spectrometer or AV-500 spectrometer at room temperature. Chemical shifts  $\delta$  (in ppm) are given in reference to the solvent signal [<sup>1</sup>H NMR: CDCl<sub>3</sub> (7.26); <sup>13</sup>C NMR: CDCl<sub>3</sub> (77.2)]. <sup>1</sup>H NMR data are reported as follows: chemical shifts ( $\delta$  ppm), multiplicity (s = singlet, d = doublet, t = triplet, q = quartet, quin = quintuplet, m = multiplet, br = broad), coupling constant (Hz), and integration. <sup>13</sup>C NMR data are reported in terms of chemical shift and multiplicity. IR data were recorded on a Thermo Nicolet Nexus 470 FTIR. High-resolution mass measurements for compound characterization were determined using an Agilent 6550 Q-TOF LC/MS.

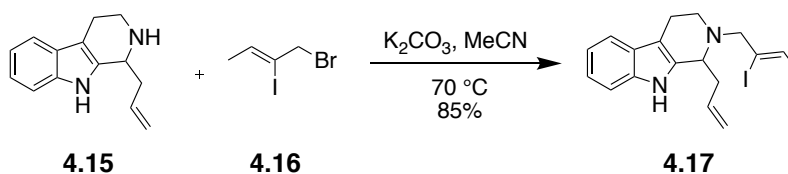


**4,9-dihydro-3H-β-carboline (4.14)** (Adapted from Snyder et. al.)<sup>22</sup>. An oven dried round-bottom flask containing tryptamine **4.12** (7.99 g, 49.9 mmol, 1.0 equiv) and ethyl formate (50 mL) was refluxed for 12 h. The reaction was allowed to cool to room temperature and the solvent removed *in vacuo*. The resulting residue was dissolved in MeCN (50 mL) and cooled to 0 °C after which POCl<sub>3</sub> (7.44 mL, 79.8 mmol, 1.6 equiv) in MeCN (10 mL) was added dropwise at 0 °C over 1 hr. The reaction was then stirred at 0 °C for an additional 4 h. The resultant mixture was poured into an erlenmeyer flask containing 200 mL of 1 M HCl and washed with Et<sub>2</sub>O (3x) in a separatory

funnel. The aqueous phase was then neutralized with saturated NaOH at 0 °C until pH 10 was reached. The resultant aqueous layer was then re-extracted with CH<sub>2</sub>Cl<sub>2</sub> (3 × 200 mL). The combined organic layers were dried over Na<sub>2</sub>SO<sub>4</sub>, filtered, and concentrated under reduced pressure to give **4.14** (8.03 g, 93% yield) as an orange solid. **4.14** was used in the next step without any further purification. All spectroscopic data matched that previously reported in literature.<sup>23</sup>

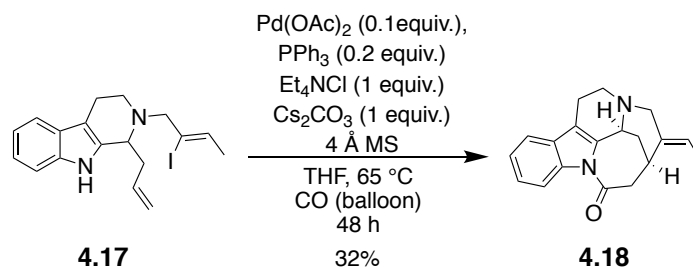


**1-Allyl-2,3,4,9-tetrahydro-1H-β-carboline (4.15)** (Adapted from Martin et. al.)<sup>24</sup>. 4,9-dihydro-3H-β-carboline **4.14** (2.0 g, 11.7 mmol, 1.0 equiv) in freshly distilled THF (59 mL) was cooled to -30 °C. To the solution at -30 °C was added BF<sub>3</sub>·OEt<sub>2</sub> (1.41 mL, 11.4 mmol, 0.97 equiv). The solution was stirred for 10 min, after which a 1.0 M solution of allylmagnesium bromide in ether (1.0 M, 35.3 mL, 25.6 mmol, 3.0 equiv) was added *via* addition funnel over 45 min. The resultant mixture was allowed to stir at -30 °C for an additional 6 h, after which saturated aqueous NaHCO<sub>3</sub> (10 mL) was added. The resulting mixture was poured into a separatory funnel containing saturated aqueous NaHCO<sub>3</sub> (50 mL) and water (50 mL), and the mixture was extracted with EtOAc (3 × 50 mL). The combined organic layers were dried over Na<sub>2</sub>SO<sub>4</sub> and concentrated under reduced pressure. The residue was purified by flash column chromatography, eluting with Et<sub>3</sub>N/MeOH/CH<sub>2</sub>Cl<sub>2</sub> (1: 3:97), to give 2.01 g (81% yield) as a yellow solid. All spectroscopic data matched that previously reported in the literature.<sup>25</sup>



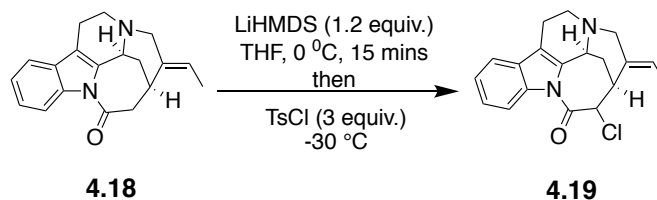
**Alkenyl iodide (4.17).** To a solution of (1.8 g, 8.5 mmol, 1.0 equiv) in anhydrous MeCN (19 mL) at room temperature was added *Z*-1-bromo-2-iodo-2-butene **4.16** (4.4 g, 16.96 mmol, 2 equiv). Subsequently,  $\text{K}_2\text{CO}_3$  (2.3 g, 16.96 mmol, 2 equiv) was added to the solution. The resulting solution was allowed to stir at 70 °C for 6 hours. After TLC confirmed completion, the solution was allowed to cool to room temperature and diluted with ethyl acetate. The resulting solution was quenched with water and extracted with ethyl acetate (3x) The combined organic layers were dried with  $\text{MgSO}_4$ , filtered and concentrated under reduced pressure. Purification of the crude product by flash chromatography was performed with EtOAc/hexanes (1:10) to afford the desired product **4.17** (2.84g, 85%) as a brown oil.

$^1\text{H}$  NMR (500 MHz, Chloroform-*d*)  $\delta$  7.75 (s, 1H), 7.50 (d,  $J = 7.8$  Hz, 1H), 7.31 (d,  $J = 8.0$  Hz, 1H), 7.16 (ddd,  $J = 8.2, 7.1, 1.3$  Hz, 1H), 7.10 (ddd,  $J = 8.1, 7.1, 1.1$  Hz, 1H), 6.13 – 6.03 (m, 1H), 5.88 (q,  $J = 6.4$  Hz, 1H), 5.19 – 5.13 (m, 2H), 3.74 (t,  $J = 6.9$  Hz, 1H), 3.48 – 3.39 (m, 2H), 3.29 – 3.21 (m, 1H), 2.99 – 2.93 (m, 1H), 2.86 – 2.78 (m, 1H), 2.72 – 2.59 (m, 2H), 2.57 – 2.48 (m, 1H), 1.82 (d,  $J = 6.4$  Hz, 2H).  $^{13}\text{C}$  NMR (126 MHz,  $\text{CDCl}_3$ )  $\delta$  136.44, 135.68, 135.04, 131.93, 127.09, 121.58, 119.36, 118.12, 117.31, 110.74, 110.08, 108.13, 64.98, 56.43, 44.48, 39.41, 21.79, 18.27. HRMS (ESI):  $m/z = 393.0822$  calculated for  $\text{C}_{18}\text{H}_{22}\text{N}_2\text{I}$   $[\text{M}+\text{H}]^+$ , found 393.0823



In a flame dried round bottom flask containing 4 Å MS, was added  $\text{Pd(OAc)}_2$  (3.43 mg, 0.01530 mmol, 0.1 equiv),  $\text{PPh}_3$  (8.02 mg, 0.0306 mmol, 0.2 equiv),  $\text{Et}_4\text{NCl}$  (25.3 mg, 0.1530 mmol, 1 equiv), and  $\text{Cs}_2\text{CO}_3$  (50 mg, 0.1530 mmol, 1 equiv). **4.17** (60 mg, 0.1530 mmol, 1 equiv) in THF (16 mL) was subsequently added. The resulting mixture was then purged multiple times with carbon monoxide. The reaction was then allowed to stir at 65 °C for 48 h whereupon the mixture was allowed to cool to room temperature. The mixture was passed through a pad of celite and the resulting solution was concentrated under reduced pressure. Preparative thin layer chromatography with  $\text{CH}_2\text{Cl}_2/\text{MeOH}$  (96:4) afforded the desired product in 32% (14 mg) yield.

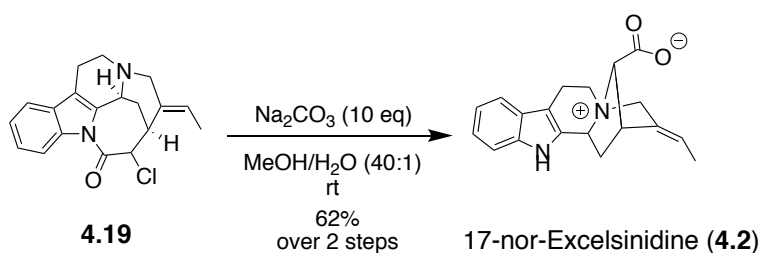
$^1\text{H}$  NMR (500 MHz, Chloroform-*d*)  $\delta$  7.97 – 7.94 (m, 1H), 7.44 – 7.40 (m, 1H), 7.32 – 7.26 (m, 2H), 5.39 (q,  $J = 6.7$  Hz, 1H), 4.34 (s, 1H), 3.60 – 3.46 (m, 2H), 3.38 – 3.31 (m, 1H), 3.17 – 2.96 (m, 4H), 2.71 (ddt,  $J = 17.0, 8.2, 2.0$  Hz, 1H), 2.50 (dt,  $J = 14.3, 2.8$  Hz, 1H), 2.35 (dd,  $J = 15.1, 4.2$  Hz, 1H), 2.17 (dt,  $J = 14.3, 4.4$  Hz, 1H), 1.60 (dd,  $J = 6.8, 2.1$  Hz, 3H).  $^{13}\text{C}$  NMR (126 MHz,  $\text{CDCl}_3$ )  $\delta$  174.34, 137.38, 135.91, 134.46, 129.56, 124.72, 123.47, 121.43, 118.35, 117.81, 114.59, 53.44, 51.23, 49.59, 45.46, 30.53, 29.72, 25.73, 18.13, 12.61.



Compound **4.19** was synthesized according to a procedure by Jarret.<sup>7</sup>

To a flame dried vial equipped with a stir bar was added **4.19** (13 mg, 0.0445 mmol, 1 equiv) in freshly distilled THF (0.9 mL). The solution was cooled to 0 °C whereupon LiHMDS (53.4  $\mu\text{L}$ , 1

M in THF, 0.0534 mmol, 1.2 equiv) was added dropwise. After 15 mins of stirring at 0 °C, the mixture was cooled to -30 °C. TsCl (25 mg, 0.1335 mmol, 3 equiv) in THF (0.3 mL) was subsequently added dropwise. The resulting mixture was stirred for an additional 1 h at 25 °C whereupon it was quenched with distilled H<sub>2</sub>O at -30 °C. The mixture was warmed to room temperature after which it was extracted with EtOAc (3 x 5 mL). The combined organic layers were washed with brine, dried over Na<sub>2</sub>SO<sub>4</sub>, filtered, and concentrated under reduced pressure. The resulting crude residue was subjected to preparative thin layer chromatography using CH<sub>2</sub>Cl<sub>2</sub>/MeOH (97:3) to afford **4.19** (9.4 mg).



Compound **4.2** was synthesized according to a procedure by Jarret.<sup>7</sup>

To compound 9.4 mg of **4.19** in a flame dried vial was added MeOH/H<sub>2</sub>O (40:1) (2.5 mL). Na<sub>2</sub>CO<sub>3</sub> (30.5 mg, 0.2876 mmol) was then added in one charge. The mixture was stirred for 1 h after which it was concentrated under reduced pressure. The crude residue was the subjected to preparative thin layer chromatography using CH<sub>2</sub>Cl<sub>2</sub>/MeOH (98:2) to afford **4.2** (8.5 mg) as a white solid in 62% yield over 2 steps.

<sup>1</sup>H NMR (500 MHz, Methanol-*d*<sub>4</sub>) δ 7.49 (d, *J* = 7.9 Hz, 1H), 7.35 (d, *J* = 8.2 Hz, 1H), 7.15 (td, 7.5, 1.0 Hz, 1H), 7.06 (td, *J* = 7.6, 1.0 Hz, 1H), 5.56 – 5.50 (m, 1H), 5.16 (t, *J* = 6.9 Hz, 1H), 4.83 – 4.77 (m, 2H), 4.18 – 4.13 (m, 1H), 4.13 (s, 1H), 3.82 (s, 1H), 3.73 (td, *J* = 12.2, 4.7 Hz, 1H), 3.17 – 2.99 (m, 2H), 2.39 – 2.35 (m, 2H), 1.76 (d, *J* = 6.9 Hz, 3H); <sup>13</sup>C NMR (125 MHz, Methanol-*d*<sub>4</sub>) δ 168.00, 137.50, 132.82, 129.62, 125.49, 122.21, 119.37, 117.96, 111.05, 104.11, 71.46, 69.15, 65.28, 50.90, 42.13, 33.97, 17.51, 12.98.

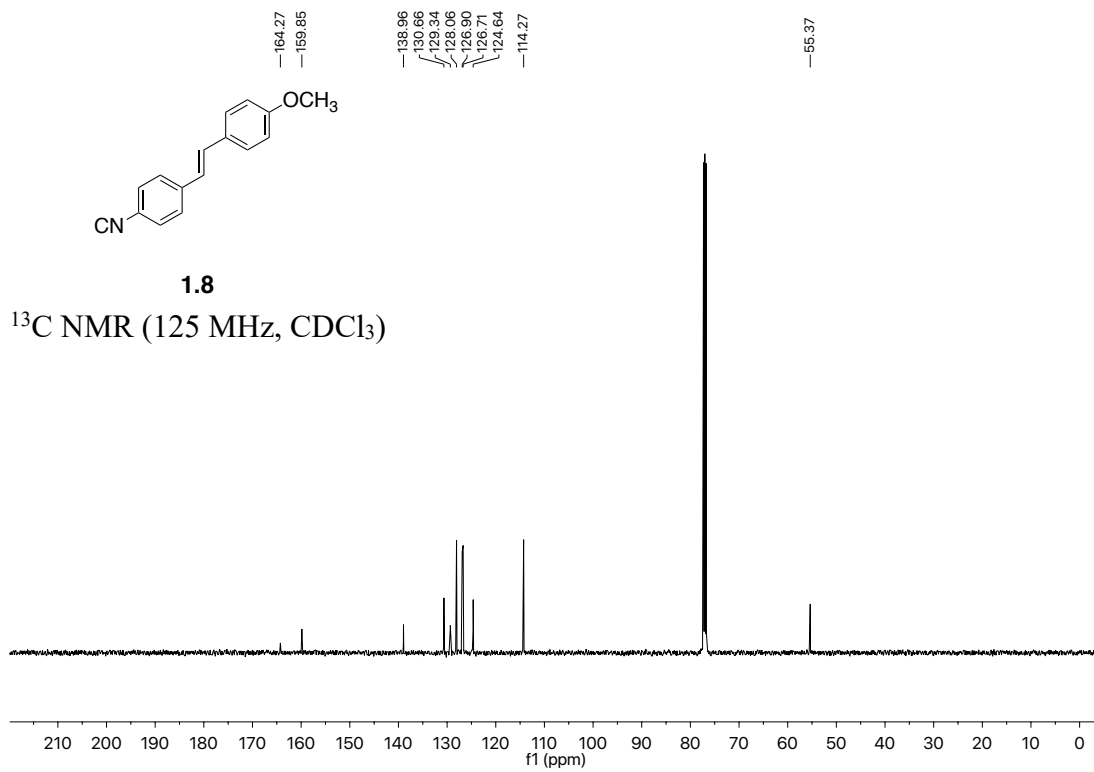
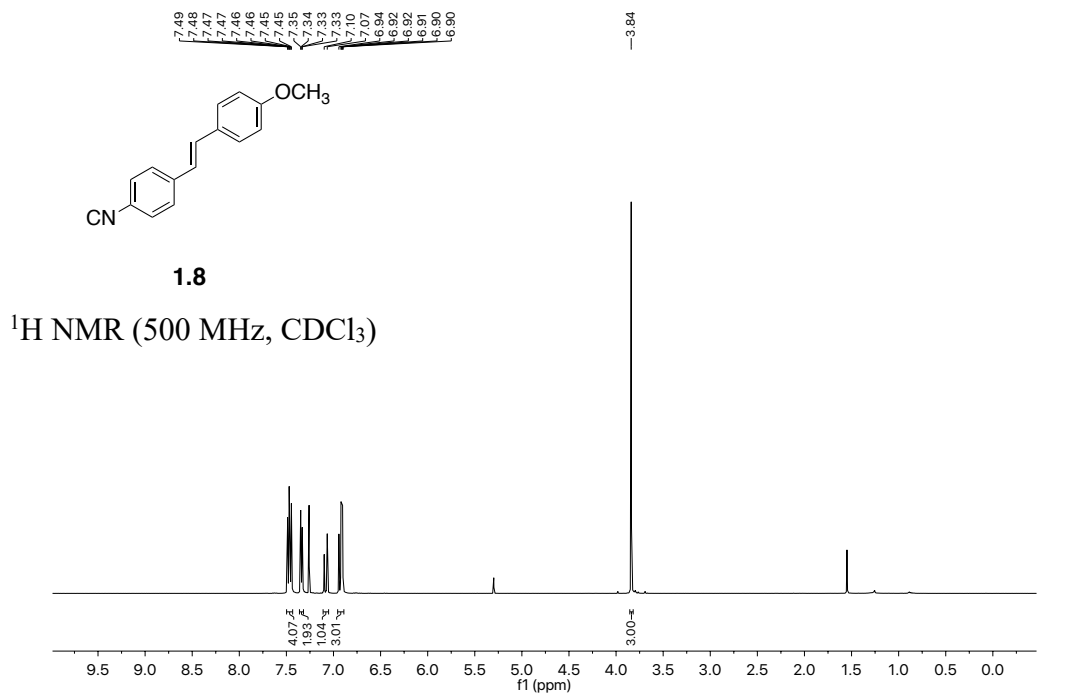
HRMS (ESI): *m/z* = 309.1597 calculated for C<sub>19</sub>H<sub>21</sub>N<sub>2</sub>O<sub>2</sub> [M+H]<sup>+</sup>, found 309.1597.

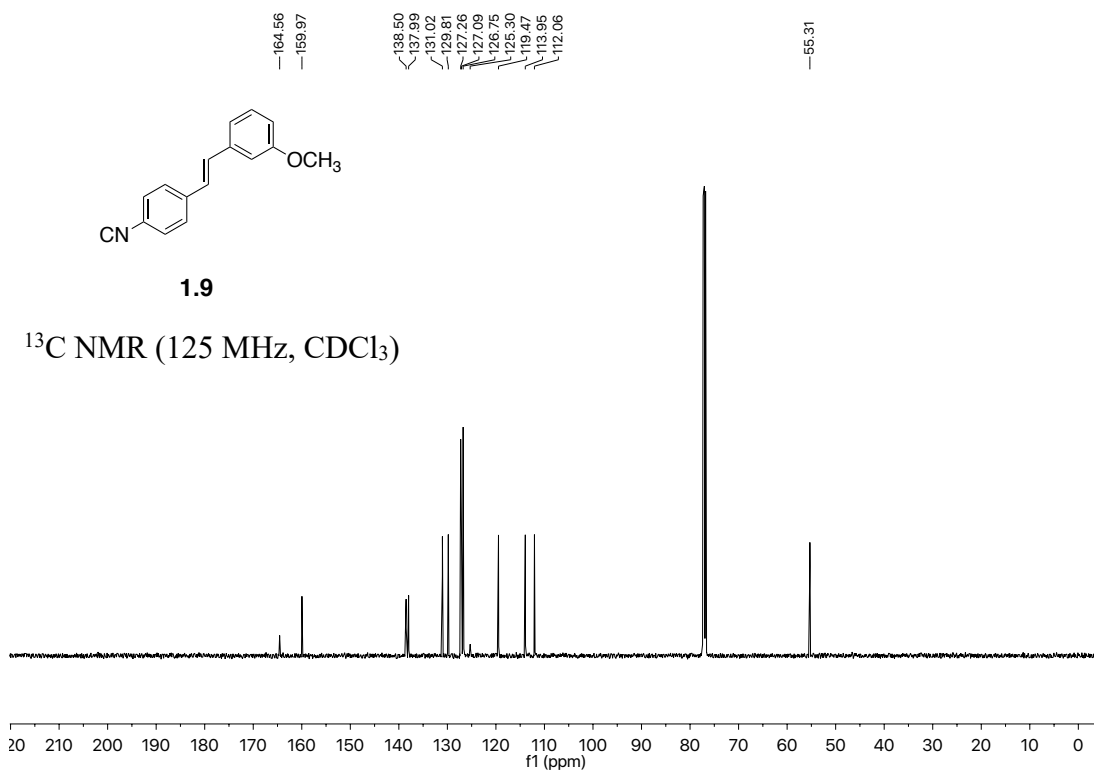
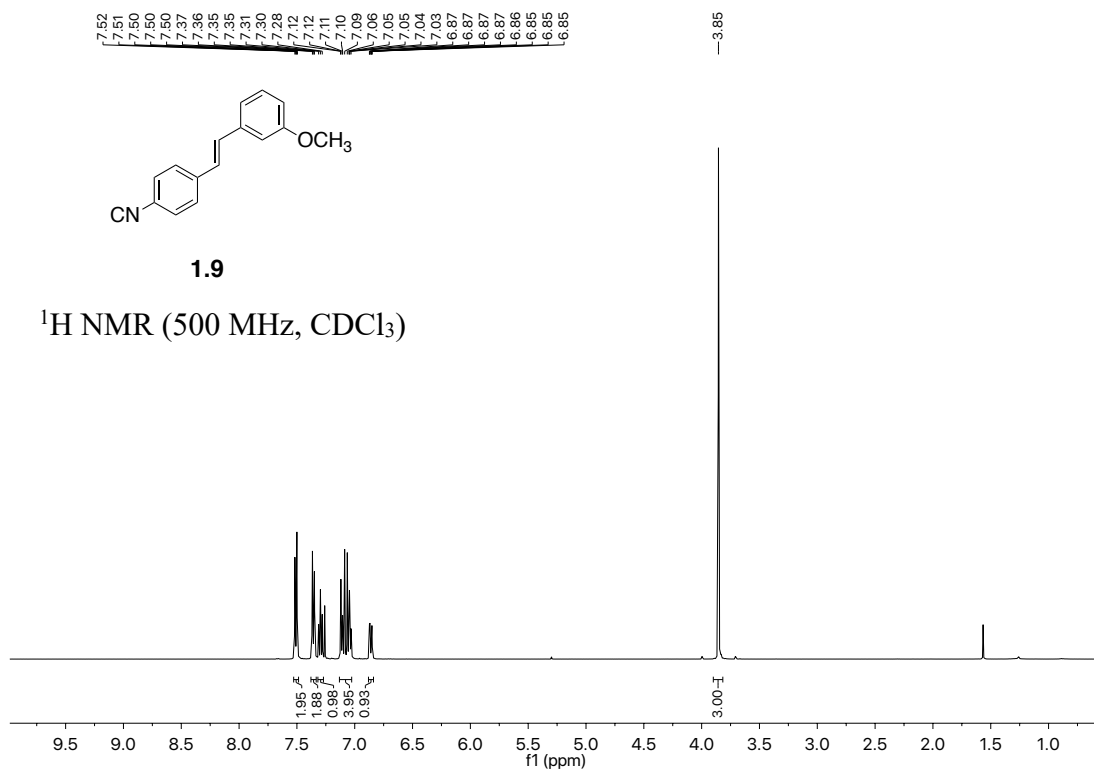
## 4.7 References

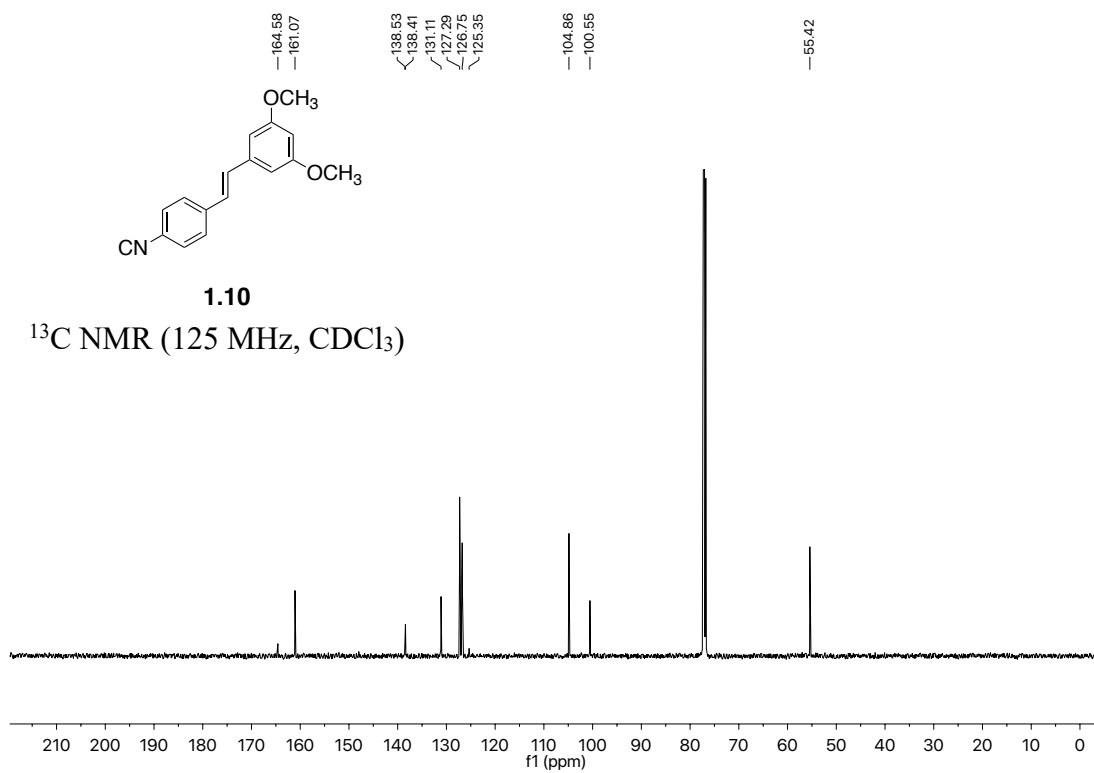
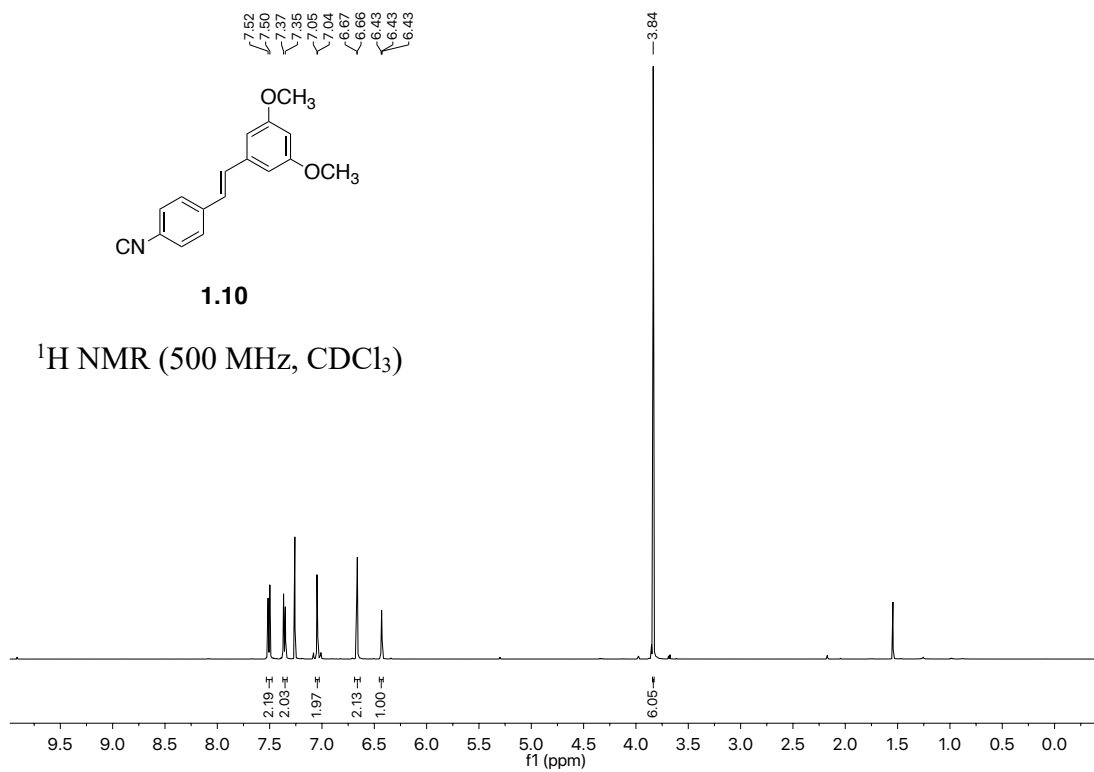
1. Rallapalli, S. K.; Namjoshi, O. A.; Tiruveedhula, V. V. N.; Deschamps, J. R.; Cook, J. M. Stereospecific Total Synthesis of the Indole Alkaloid Ervincidine. Establishment of the C-6 Hydroxyl Stereochemistry. *J. Org. Chem.* **2014**, *79*, 3776 – 3780.
2. Gao, P.; Liu, Y.; Zhang, L.; Xu, P-F.; Wang, S.; Lu, Y.; He, M.; Zhai, H. Total Synthesis of Indole Alkaloid ( $\pm$ )-Subincanadine F via SmI<sub>2</sub>-Mediated Ring Opening and Bridge-Forming Mannich Reaction *J. Org. Chem.* **2006**, *71*, 9495 – 9498.
3. Zhu, C.; Liu, Z.; Chen, G.; Zhang, K.; Ding, H. Total Synthesis of Indole Alkaloid Alsmaphorazine D. *Angew. Chem. Int. Ed.* **2015**, *54*, 879 – 882.
4. Zhang, L.; Zhang, C-J.; Zhang, D-B.; Wen, J.; Zhao, X-W.; Li, Ya.; Gao, Kun. An unusual indole alkaloid with anti-adenovirus and anti-HSV activities from *Alstonia scholaris*. *Tetrahedron letters.* **2014**, *55*, 1815 – 1817.
5. Baliga, M. S.; Jagetia, G. C.; Ulloor, J. N., et al *Toxicol. Lett.* **2004**, *151*, 317 – 326.
6. Compiling group of Yunman Traditional Chinese Medicine *Yunman Traditional Chinese Medicinal Plant*; Yunman People's Press: Kunming, **1977**.
7. Jarret, M.; Tap, A.; Kouklovsky, C.; Poupon, E.; Evanno, L.; Vincent, G. Bioinspired Oxidative Cyclization of the Geissoschizine Skeleton for the Total Synthesis of (–)-17-nor-Excelsinidine. *Angew. Chem. Int. Ed.* **2018**, *57*, 12294 – 12298.
8. Martin, S. F.; Chen, K. X.; Eary, T. An Enantioselective Total Synthesis of (+)-Geissoschizine. *Org. Lett.* **1999**, *1*, 79-82.
9. Herbert, R. B. *Chemistry of Heterocyclic Compounds* (Ed.: J. E. Saxton), Wiley, New York, **1983**, 1 – 46.
10. Yu, S.; Berner, O. M.; Cook, J. General Approach for the Synthesis of Indole Alkaloids via the Asymmetric Pictet-Spengler Reaction: First Enantiospecific Total Synthesis of (–)-Corynantheidine as well as the Enantiospecific Total Synthesis of (–)-Corynantheidol, (–)-Geissoschizol, and (+)-Geissoschizine. *J. Am. Chem. Soc.* **2000**, *122*, 7827 – 7828.
11. a) Schoenberg, A.; Bartoletti, I.; Heck, R. F. *J. Org. Chem.* **1974**, *39*, 3318. (b) Schoenberg, A.; Heck, R. F. *J. Org. Chem.* **1974**, *39*, 3327. (c) Schoenberg, A.; Heck, R. F. *J. Am. Chem. Soc.* **1974**, *96*, 7761.
12. Bai, Y.; Davis, D. C.; Dai, M. Synthesis of Tetrahydropyran/Tetrahydrofuran-Containing Macrolides by Palladium-Catalyzed Alkoxy-carbonylative Macrolactonizations. *Angew. Chem. Int. Ed.* **2014**, *53*, 6519 – 22.
13. Bai, Y.; Shen, X.; Li, Y.; Dai, M. Total synthesis of (–)-spinosyn A via carbonylative macrolactonization. *J Am Chem Soc.* **2016**, *138*, 10838 – 41.

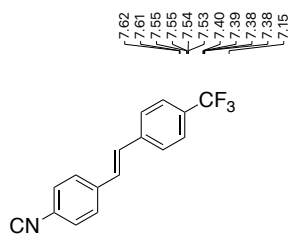
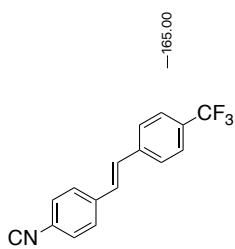
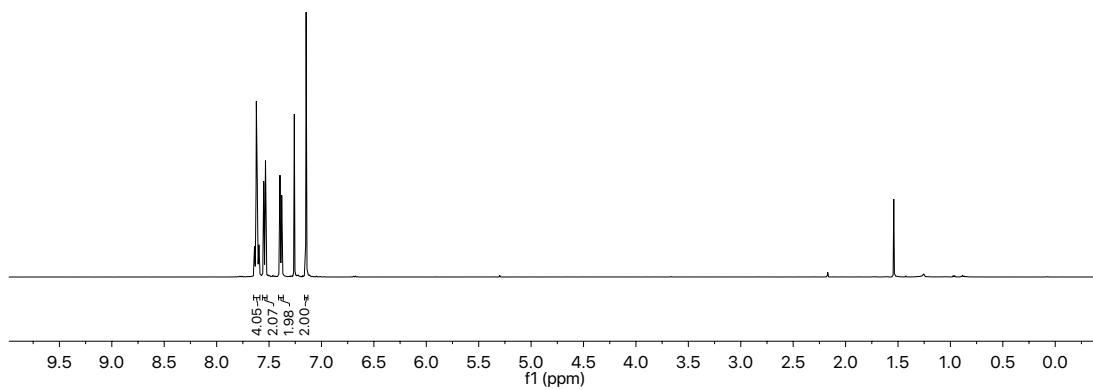
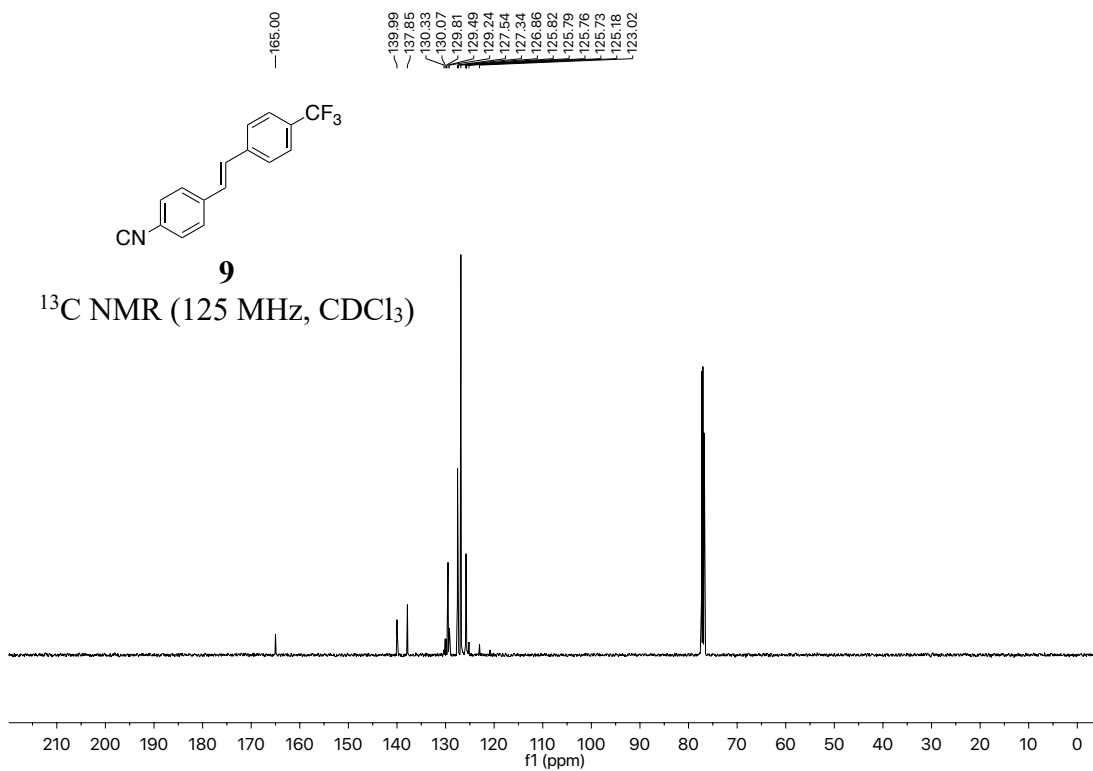
14. Davis, D. C.; Walker, K. L.; Hu, C.; Zare, R. N.; Waymouth, R. M.; Dai, M. Catalytic carbonylative spirolactonization of hydroxycyclopropanols. *J Am Chem Soc.* **2016**, *138*, 10693 – 9.
15. Ma, K.; Yin, X.; Dai, M. Total syntheses of bisdehydroneostemoninine and bisdehydrostemoninine by catalytic carbonylative spirolactonization. *Angew. Chem. Int. Ed.* **2018**, *57*, 15209 – 12.
16. Davis, D. C.; Hoch, D. G.; Wu, L.; Abegg, D.; Martin, B. S.; Zhang, Z.; Adibekian, A.; Dai, M. Total synthesis, biological evaluation, and target identification of rare abies sesquiterpenoids. *J Am Chem Soc.* **2018**, *140*, 17465–73.
17. Old, D. W.; Wolfe, J. P.; Buchwald, S. L. A Highly Active Catalyst for Palladium-Catalyzed Cross-Coupling Reactions: Room-Temperature Suzuki Couplings and Amination of Unactivated Aryl Chlorides. *J. Am. Chem. Soc.* **1998**, *120*, 9722-9723.
18. Fang, W.; Zhu, H.; Deng, Q.; Liu, S.; Liu, X.; Shen, Y.; Tu, T.; Design and Development of Ligands for Palladium-Catalyzed Carbonylation Reactions. *Synthesis.* **2014**, *46*, 1689 – 1708.
19. Jeffery, T. Highly stereospecific palladium-catalysed vinylation of vinylic halides under solid-liquid phase transfer conditions. *Tetrahedron Letters*, **1985**, *26*, 2667-2670.
20. Jeffery, T. Palladium-catalysed Vinylation of Organic Halides under Solid-Liquid Phase Transfer Conditions. *J. Chem. Soc., Chem. Commun.* **1984**, *19*, 1287-1289.
21. Jeffery, T. On the efficiency of tetraalkylammonium salts in Heck type reactions. *Tetrahedron Letters.* **1996**, *52*, 10113 – 10130
22. Smith, M. W.; Zhou, Z.; Gao, A. X.; Shimbayashi, T.; Snyder, S. A 7-Step Formal Asymmetric Total Synthesis of Strictamine via an Asymmetric Propargylation and Metal-Mediated Cyclization. *Org. Lett.* **2017**, *19*, 1004-1007.
23. Mirabal-Gallardo, Y.; Soriano, M. D. P. C.; Caballero, J.; Alzate-Morales, J.; Simirgiotis, M. J.; Santos, L. S. *Synthesis* **2012**, *44*, 144–150.
24. Deiters, A.; Pettersson, M.; Martin, S. F. General Strategy for the Syntheses of Corynanthe, Tacaman, and Oxindole Alkaloids *J. Org. Chem.* **2006**, *71*, 6547-6561.
25. Nakamura, M.; Hirai, A.; Nakamura, E. *J. Am. Chem. Soc.* **1996**, *118*, 8489.

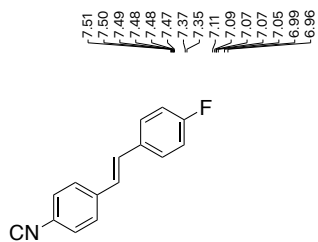
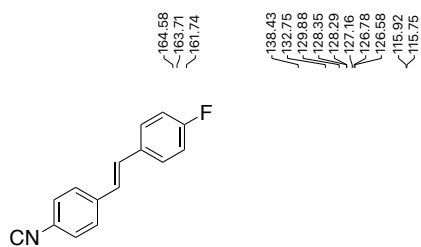
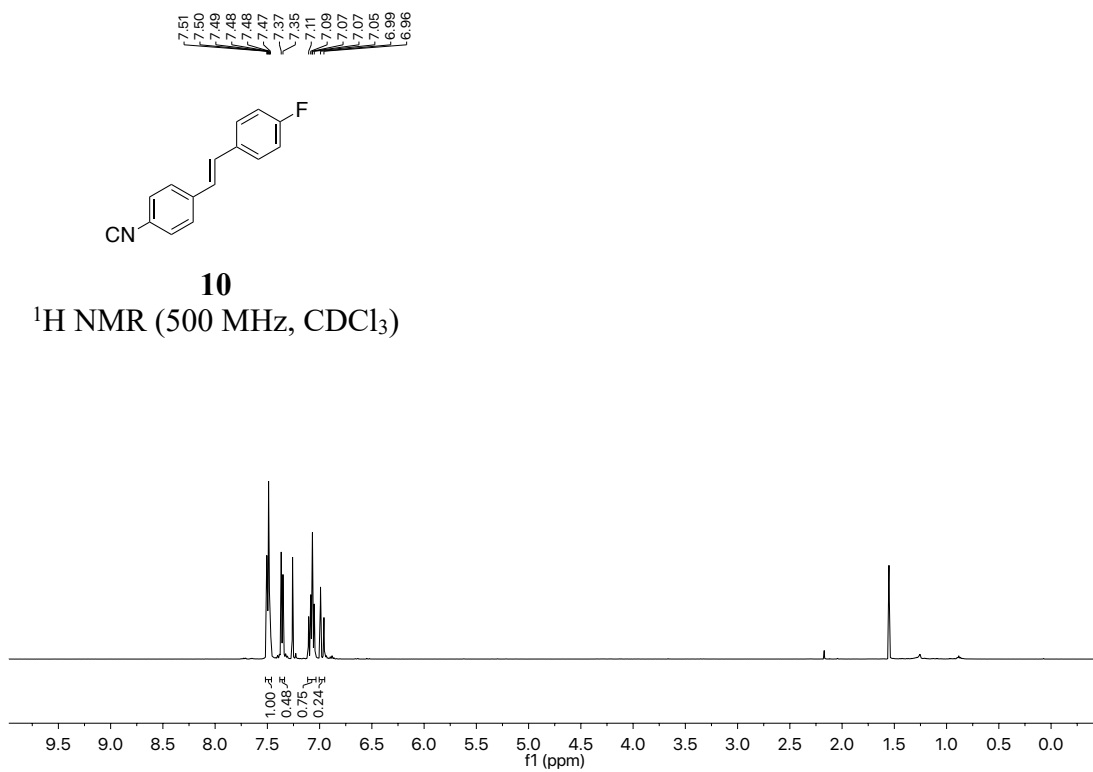
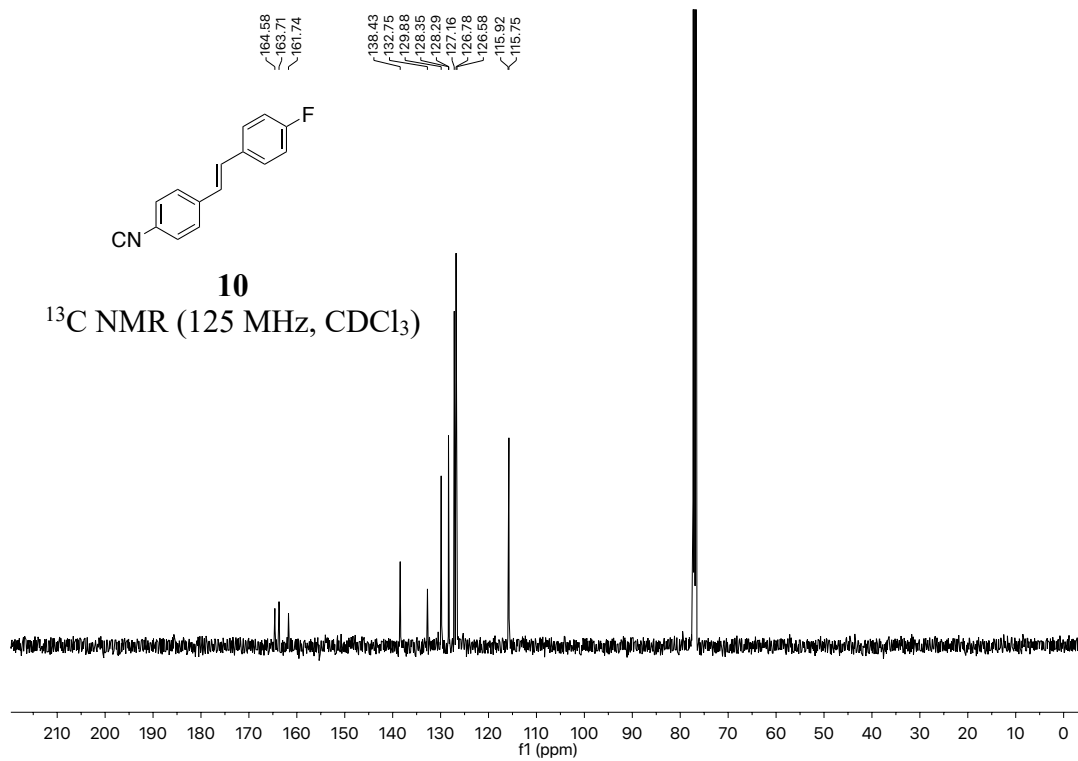
## SPECTRAL DATA I: DEVELOPMENT OF ARYL ISONITRILES AS ANTIMICROBIAL AGENTS

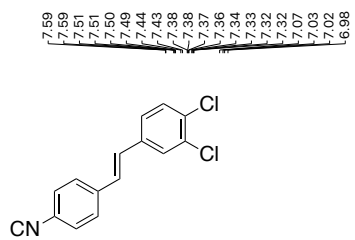
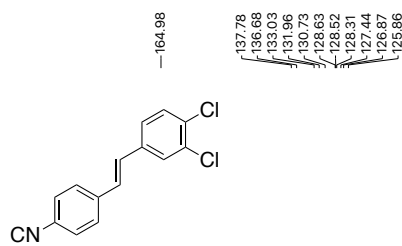
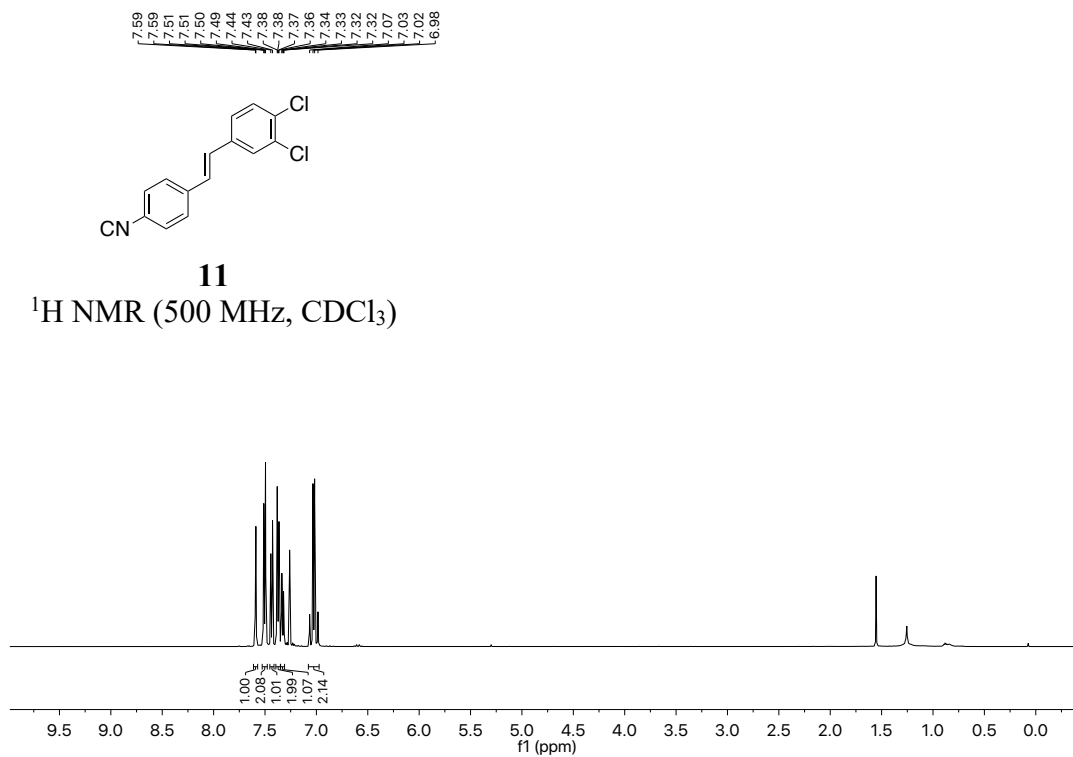
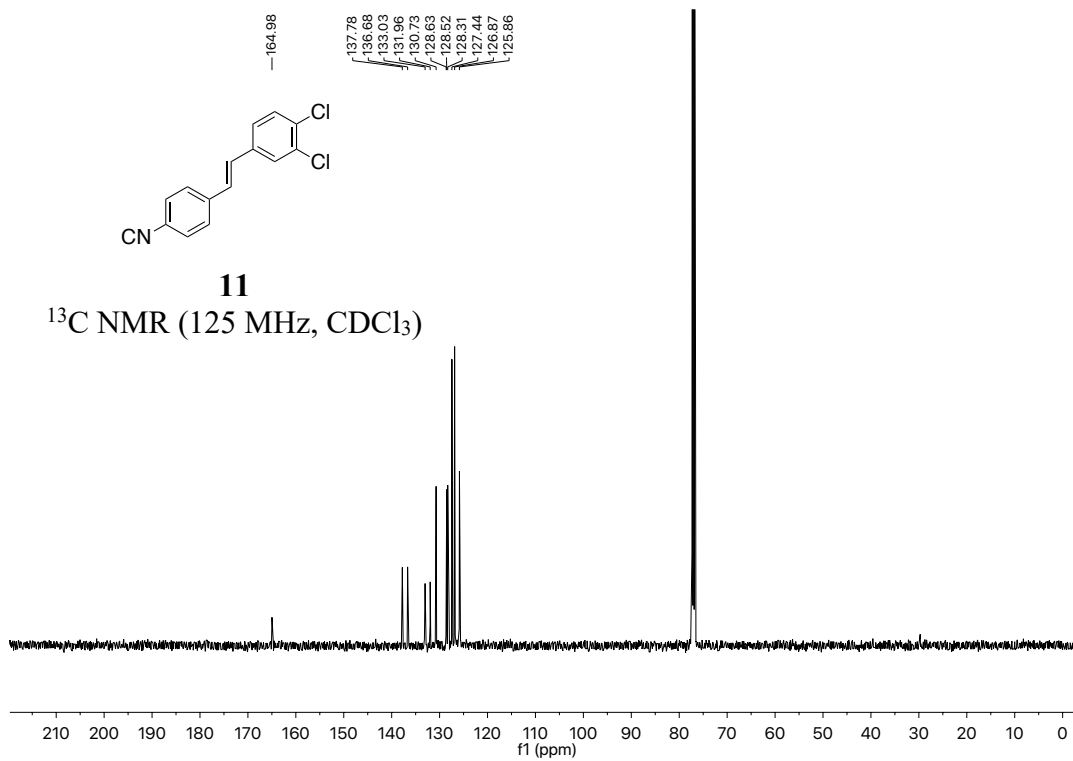


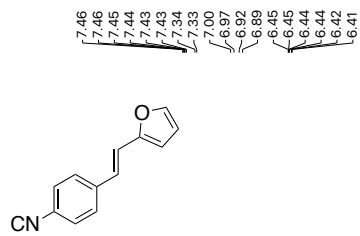
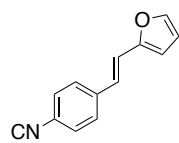
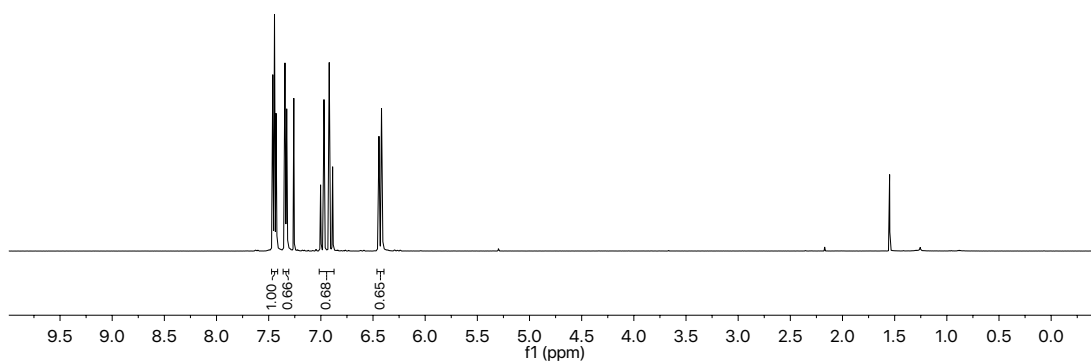
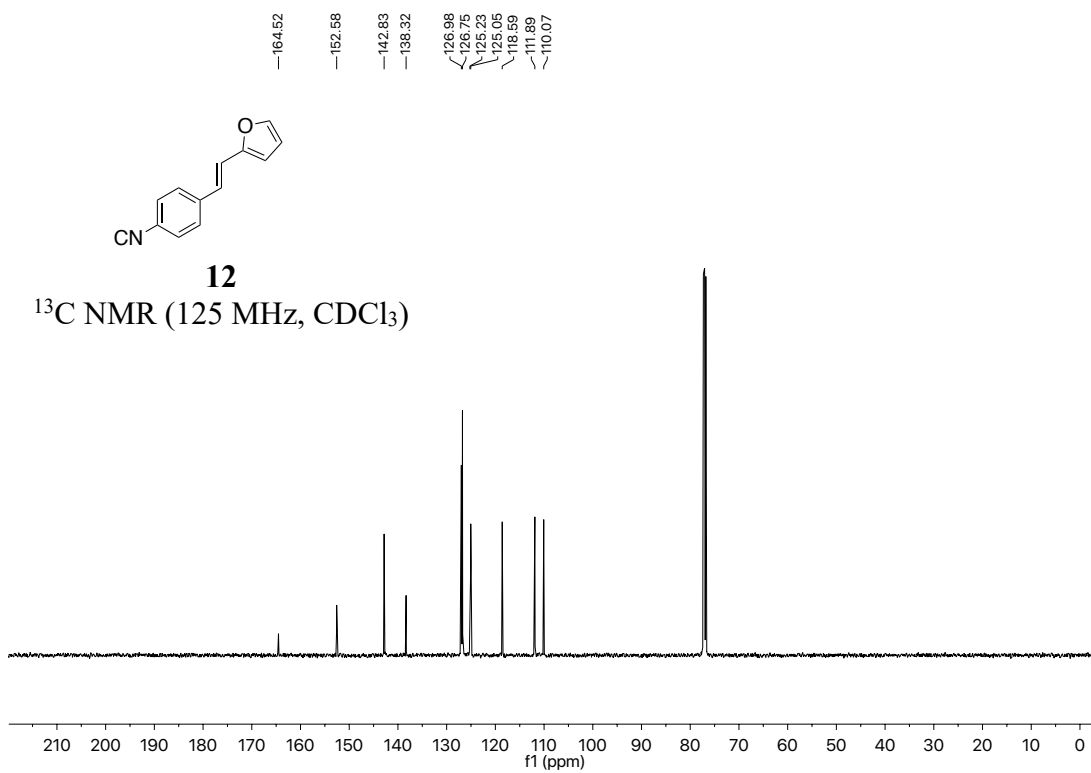




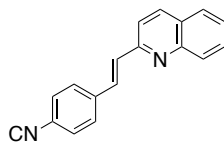
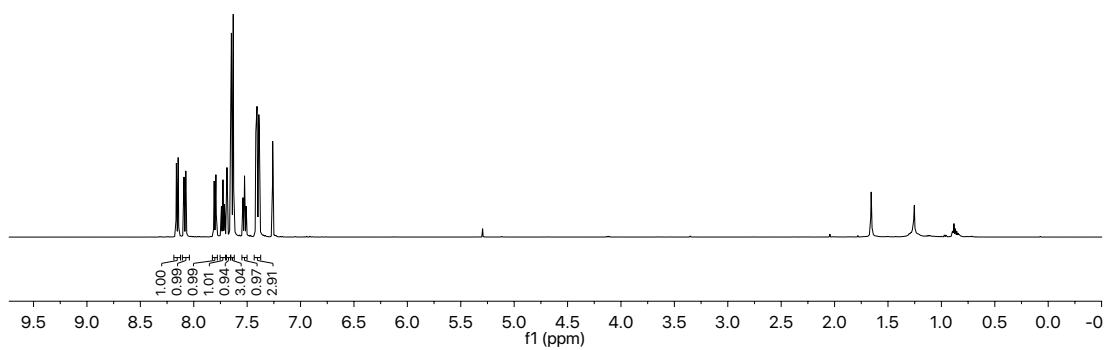
**9** $^1\text{H NMR}$  (500 MHz,  $\text{CDCl}_3$ )**9** $^{13}\text{C NMR}$  (125 MHz,  $\text{CDCl}_3$ )

**10** $^1\text{H}$  NMR (500 MHz,  $\text{CDCl}_3$ )**10** $^{13}\text{C}$  NMR (125 MHz,  $\text{CDCl}_3$ )

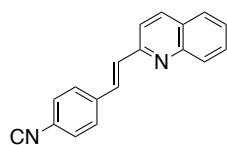
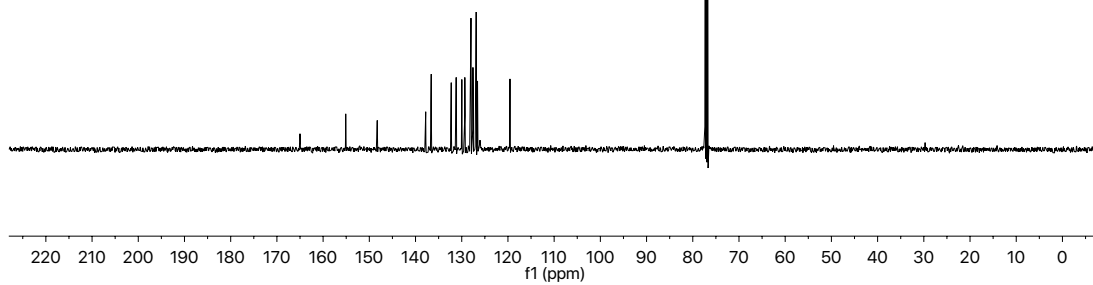
**11** $^1\text{H NMR}$  (500 MHz,  $\text{CDCl}_3$ )**11** $^{13}\text{C NMR}$  (125 MHz,  $\text{CDCl}_3$ )

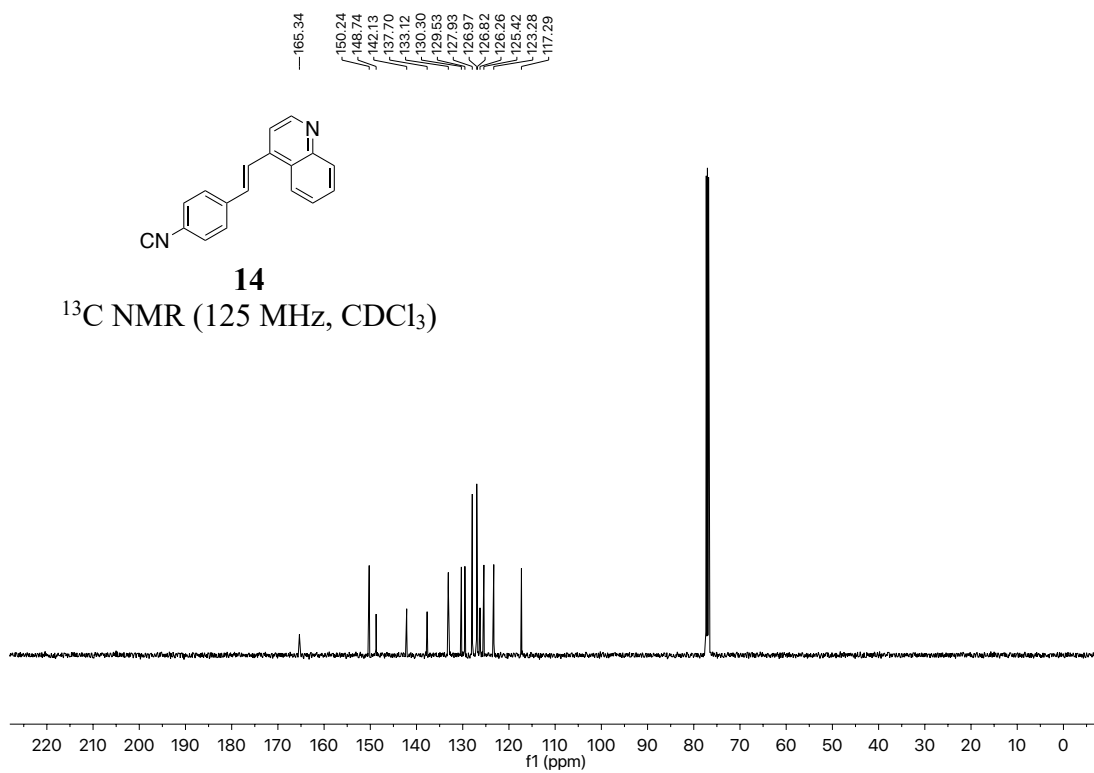
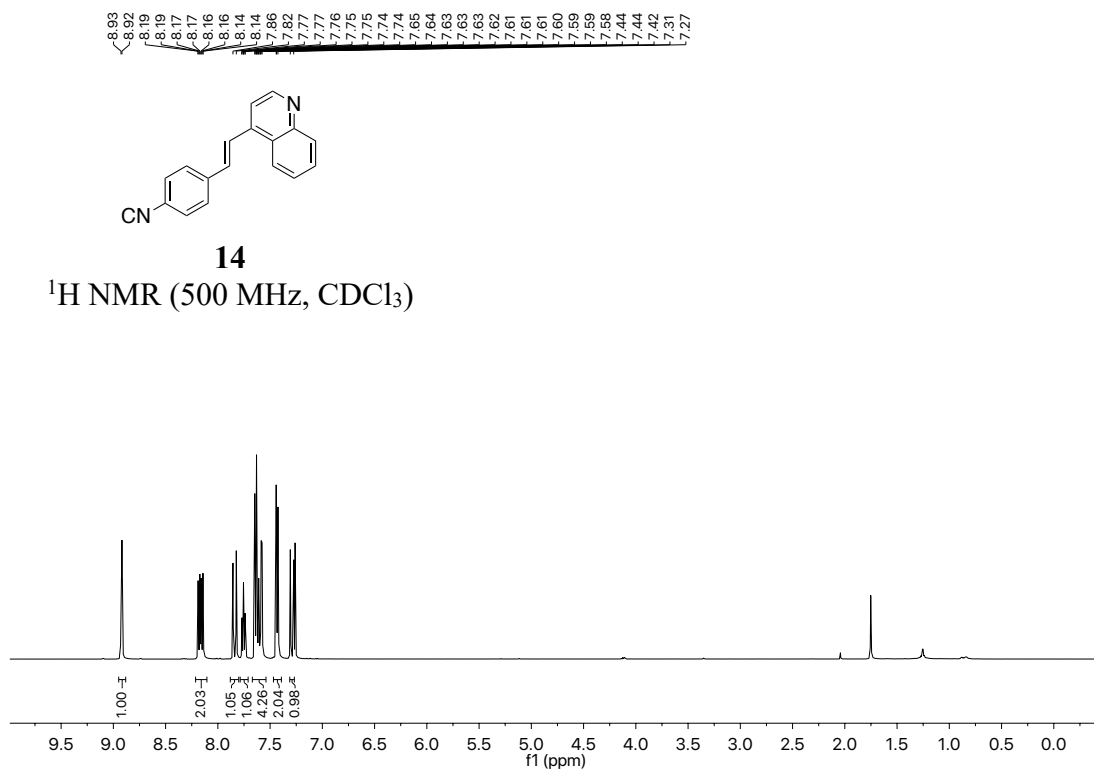
**12** $^1\text{H NMR}$  (500 MHz,  $\text{CDCl}_3$ )**12** $^{13}\text{C NMR}$  (125 MHz,  $\text{CDCl}_3$ )

8.16  
8.15  
8.09  
8.07  
7.81  
7.81  
7.79  
7.74  
7.74  
7.73  
7.73  
7.72  
7.71  
7.71  
7.69  
7.66  
7.65  
7.63  
7.54  
7.54  
7.53  
7.52  
7.51  
7.51  
7.42  
7.41  
7.40  
7.39  
7.39

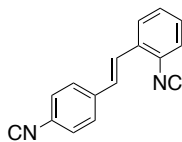
**13** $^1\text{H}$  NMR (500 MHz,  $\text{CDCl}_3$ )

165.00  
155.10  
148.28  
137.80  
136.60  
132.27  
131.20  
129.98  
129.33  
128.00  
127.93  
127.57  
127.55  
126.87  
126.58  
126.51  
119.56  
119.49

**13** $^{13}\text{C}$  NMR (125 MHz,  $\text{CDCl}_3$ )

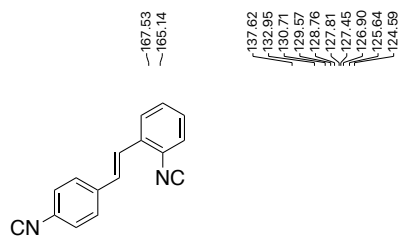
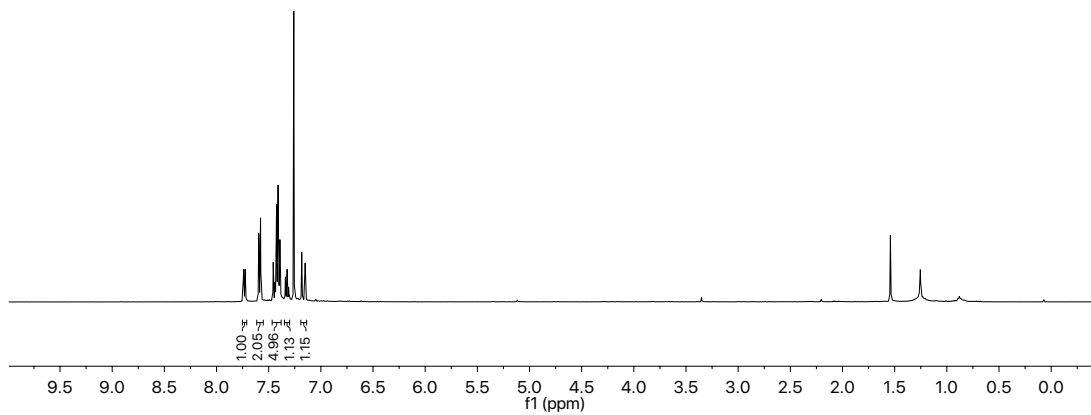


7.74  
7.73  
7.72  
7.60  
7.58  
7.46  
7.44  
7.44  
7.43  
7.42  
7.41  
7.41  
7.40  
7.39  
7.34  
7.34  
7.33  
7.32  
7.31  
7.31  
7.18  
7.15



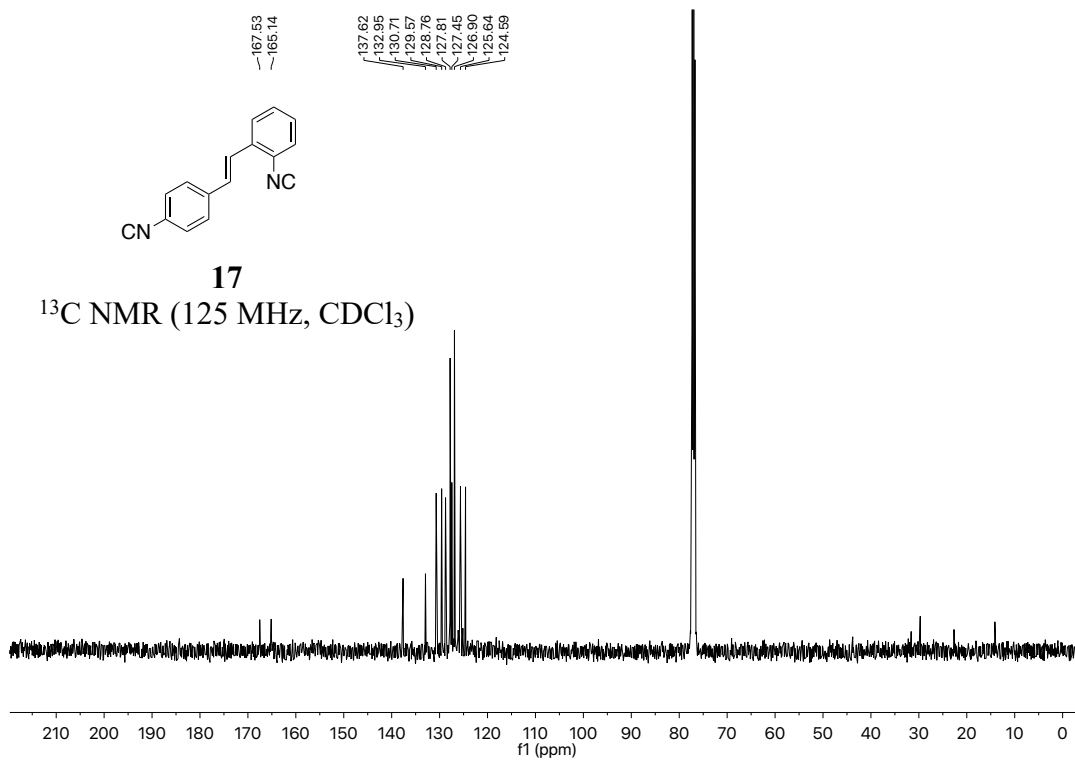
**17**

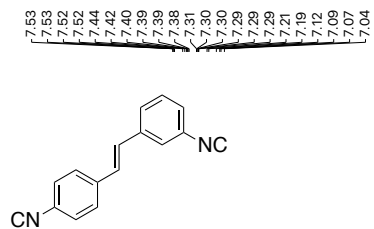
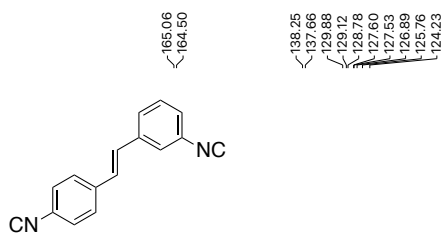
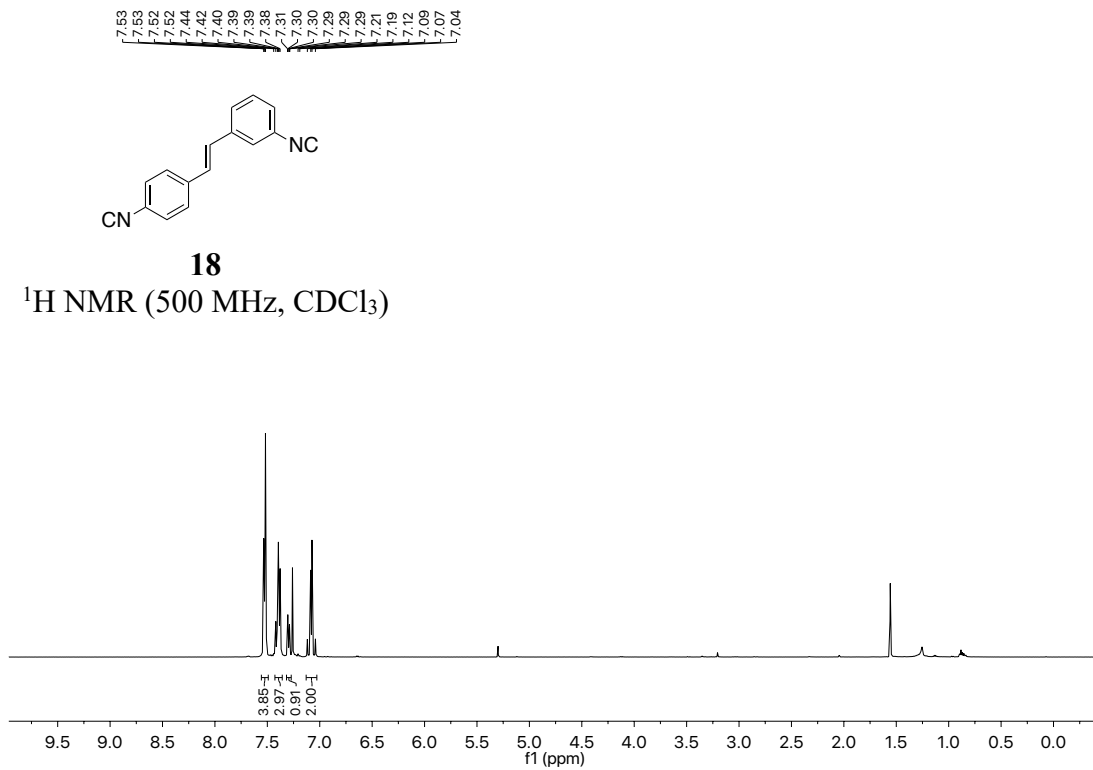
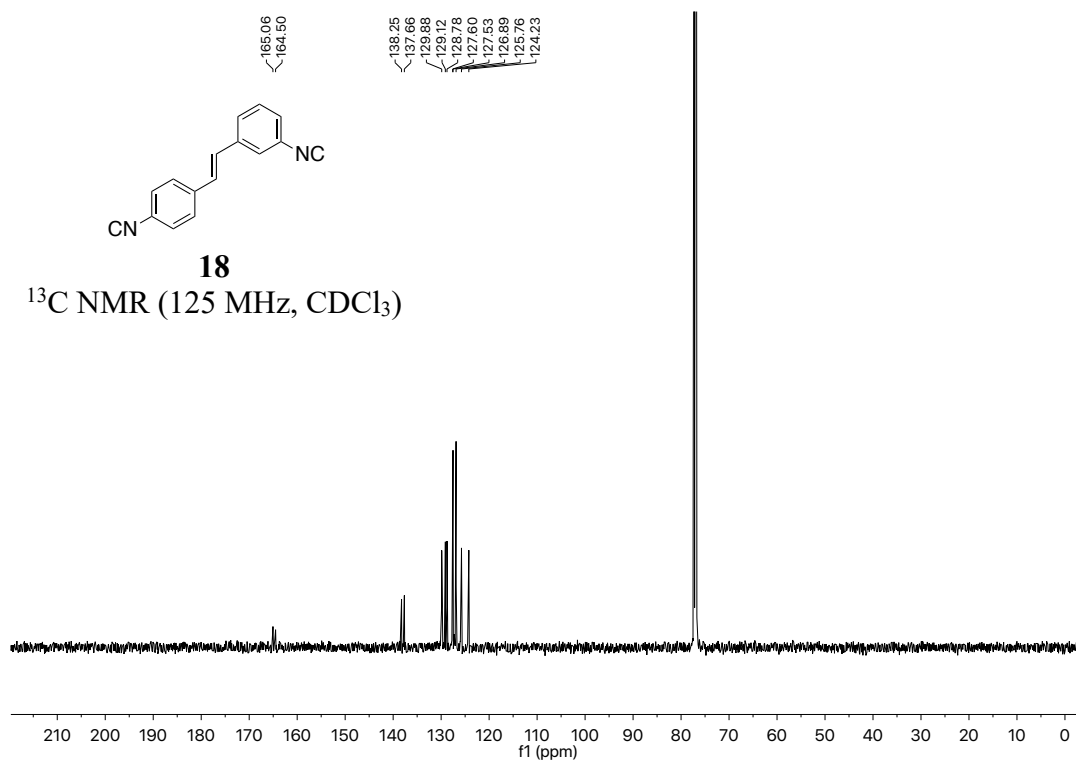
$^1\text{H NMR}$  (500 MHz,  $\text{CDCl}_3$ )

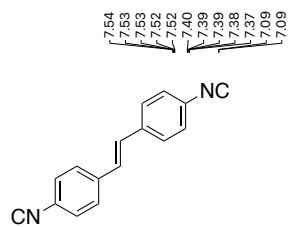
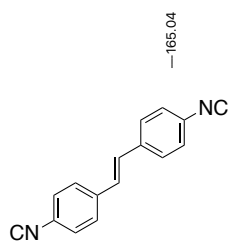
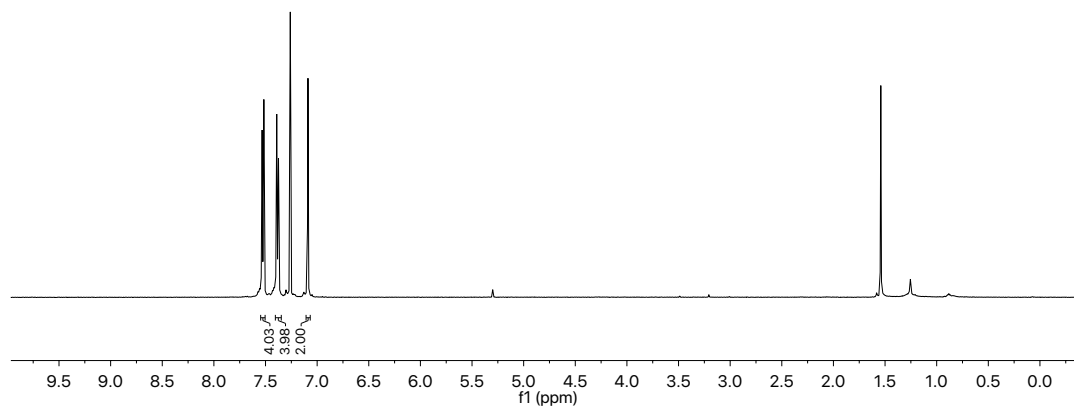
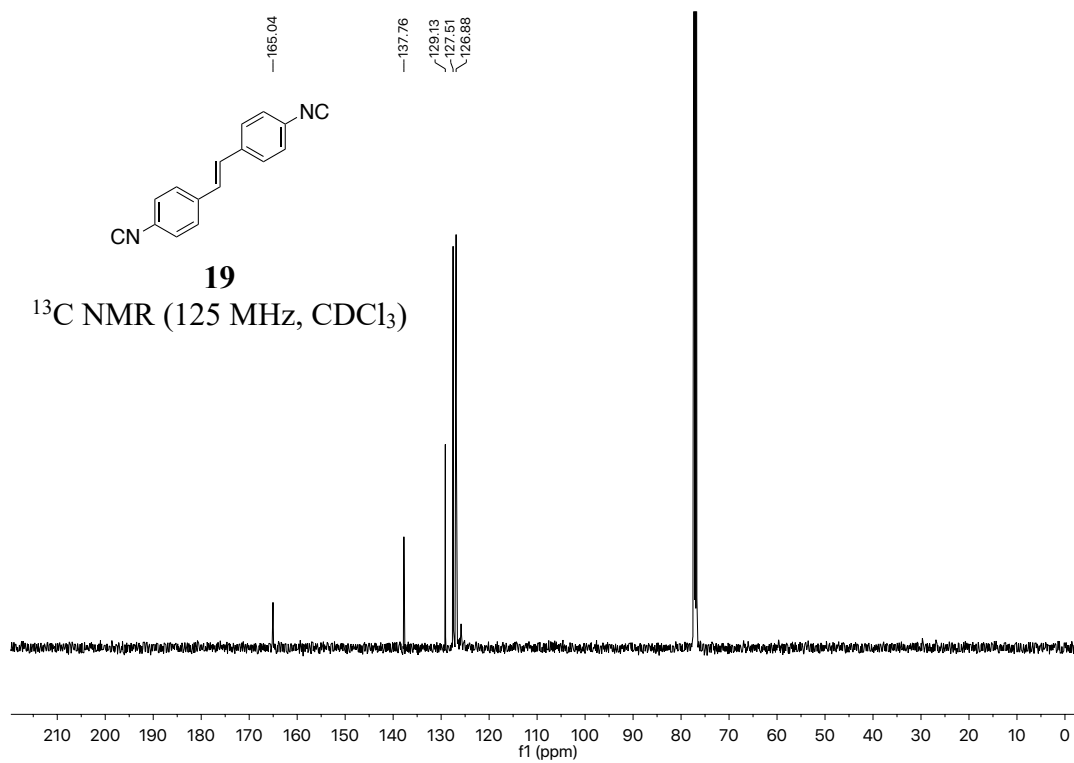


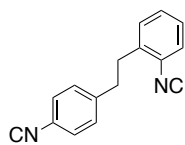
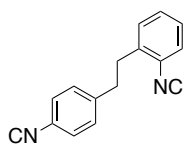
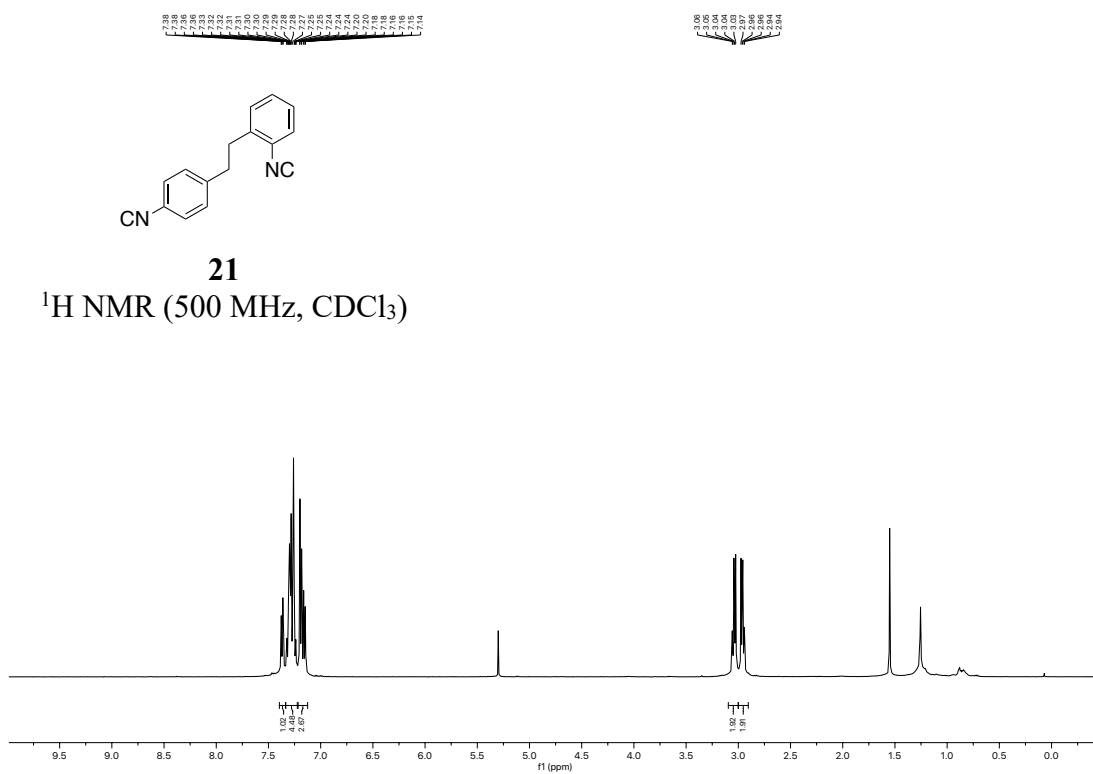
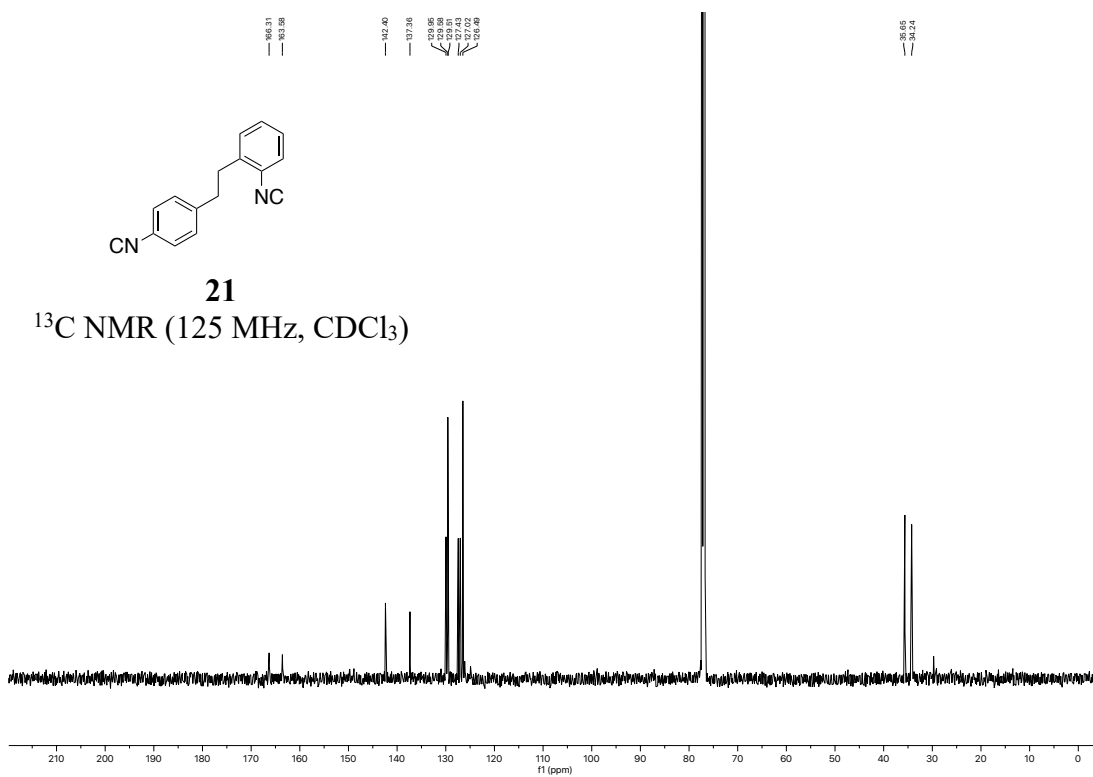
**17**

$^{13}\text{C NMR}$  (125 MHz,  $\text{CDCl}_3$ )

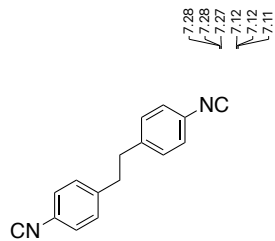
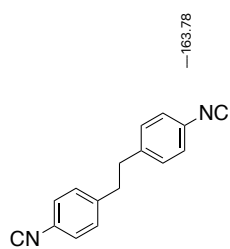
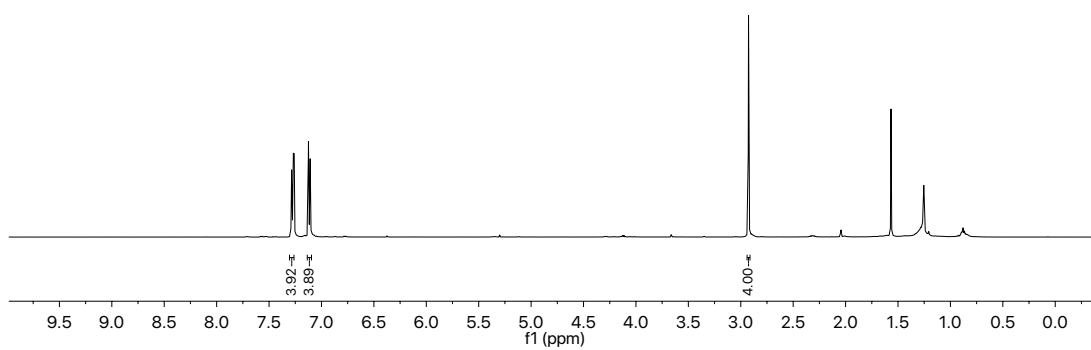
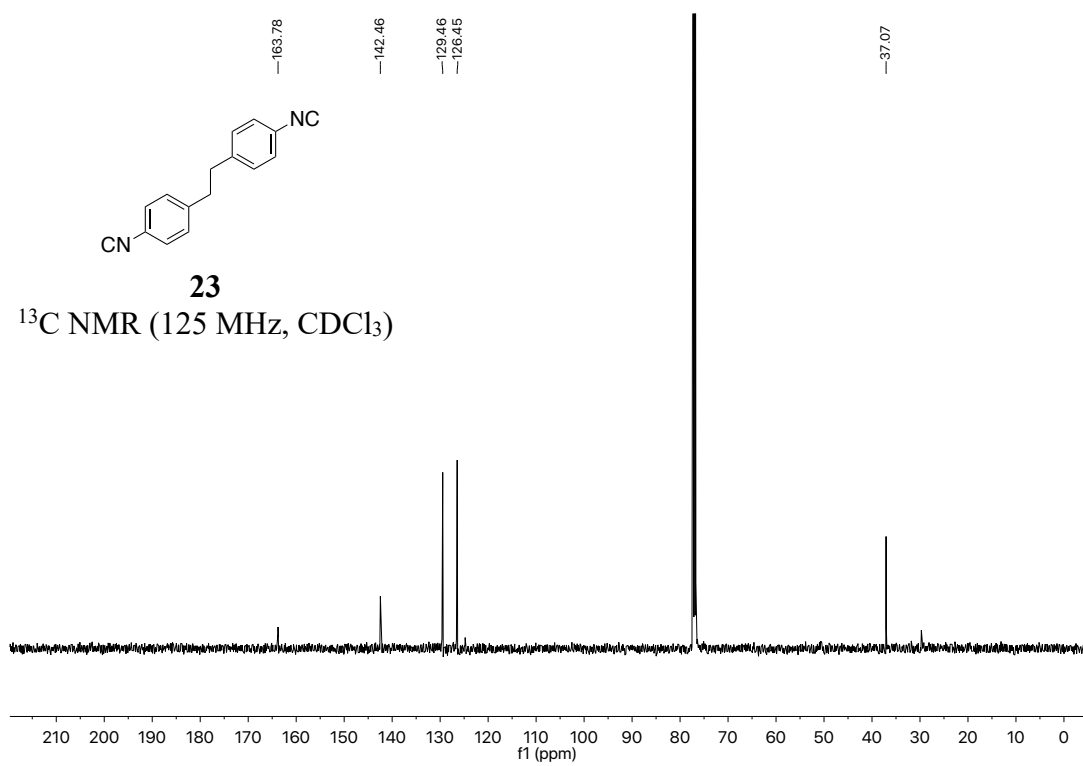


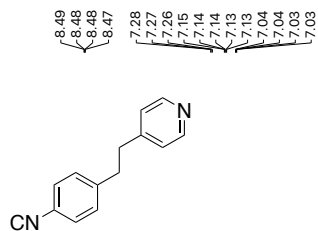
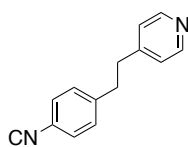
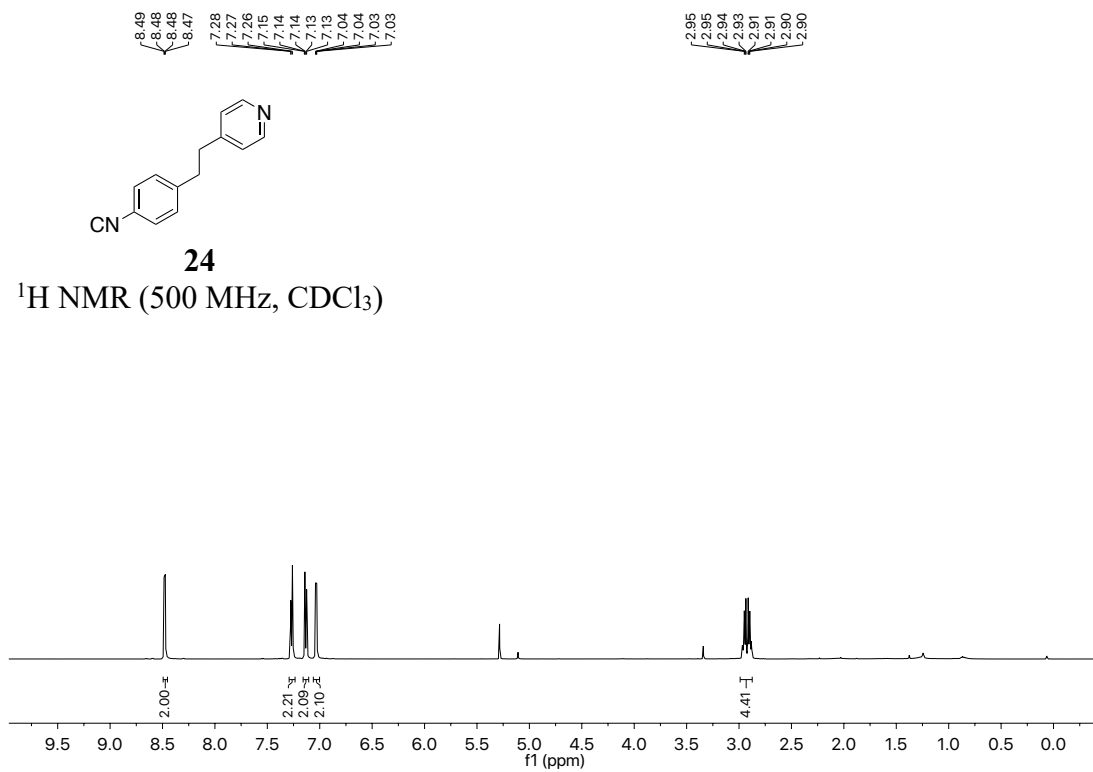
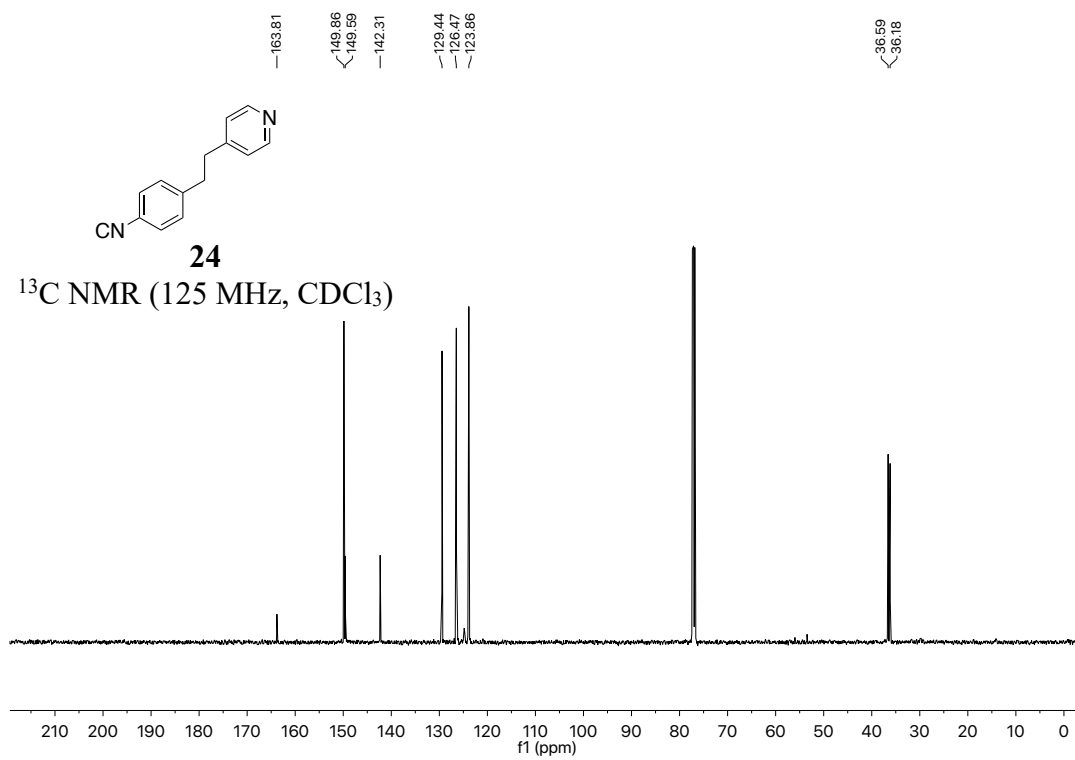
**18** $^1\text{H NMR}$  (500 MHz,  $\text{CDCl}_3$ )**18** $^{13}\text{C NMR}$  (125 MHz,  $\text{CDCl}_3$ )

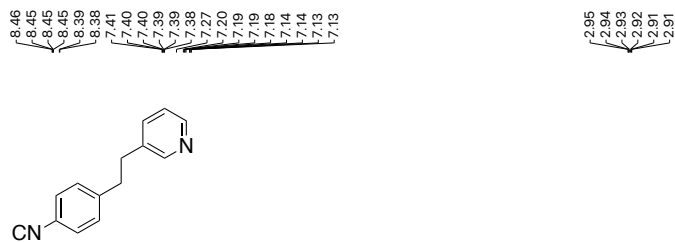
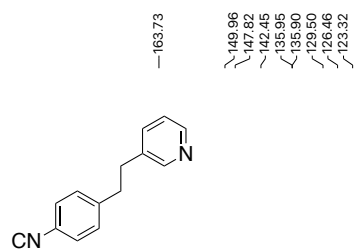
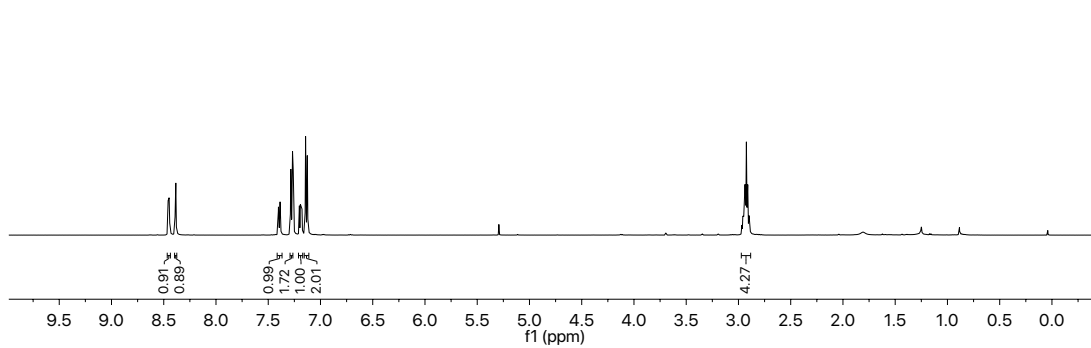
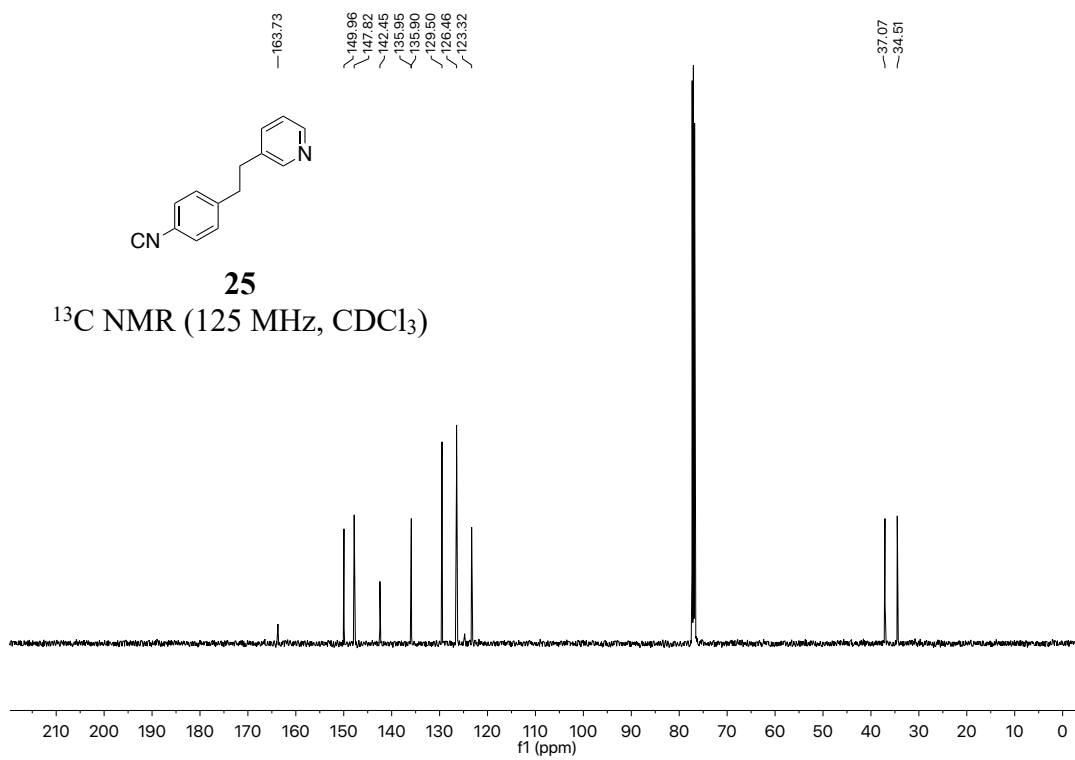
**19** $^1\text{H NMR}$  (500 MHz,  $\text{CDCl}_3$ )**19** $^{13}\text{C NMR}$  (125 MHz,  $\text{CDCl}_3$ )

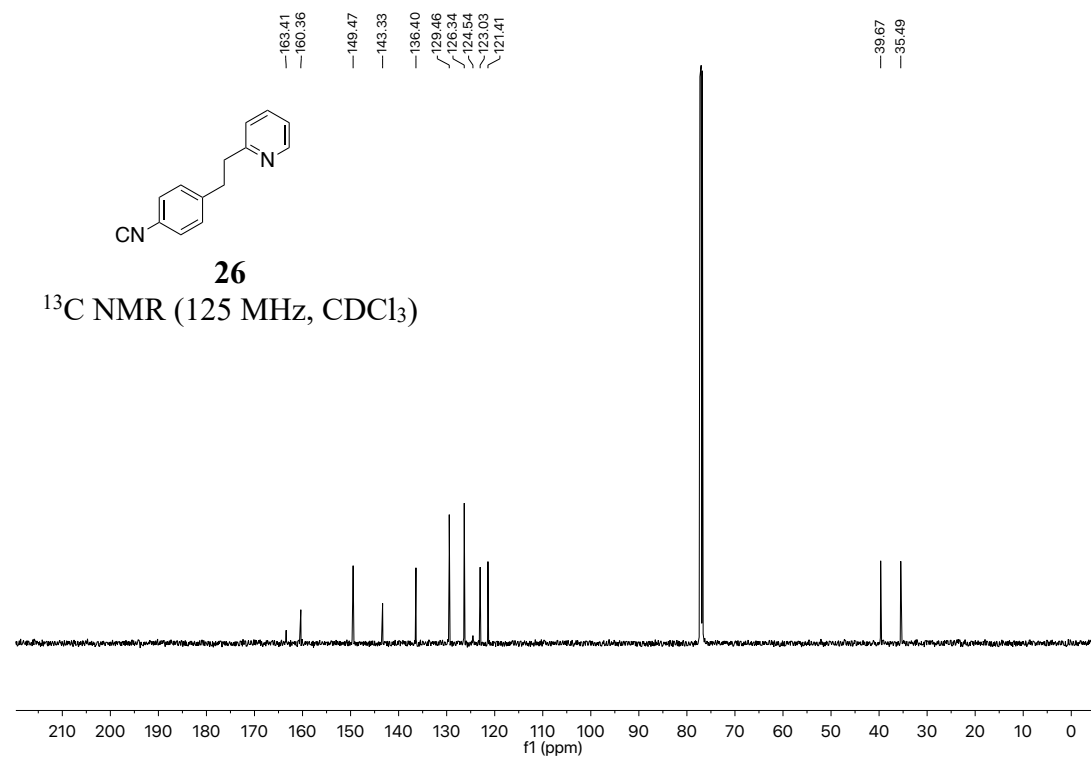
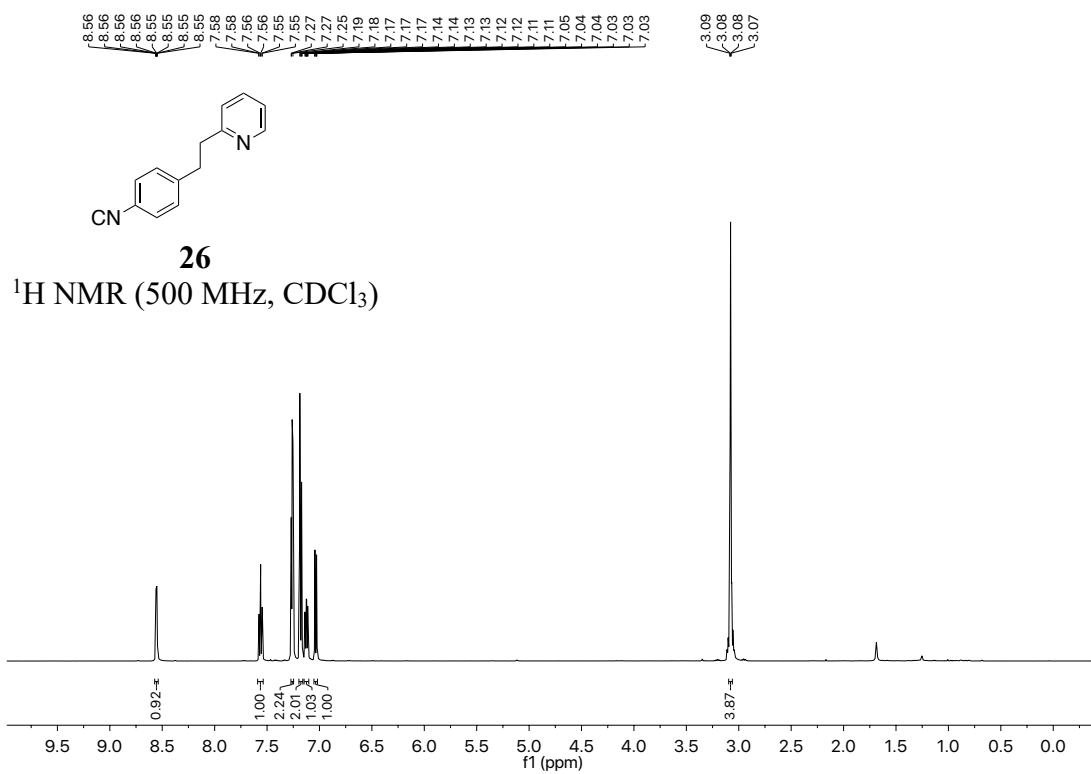
**21** $^1\text{H NMR}$  (500 MHz,  $\text{CDCl}_3$ )**21** $^{13}\text{C NMR}$  (125 MHz,  $\text{CDCl}_3$ )



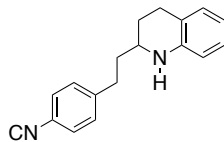
**23** $^1\text{H NMR}$  (500 MHz,  $\text{CDCl}_3$ )**23** $^{13}\text{C NMR}$  (125 MHz,  $\text{CDCl}_3$ )

**24** $^1\text{H}$  NMR (500 MHz,  $\text{CDCl}_3$ )**24** $^{13}\text{C}$  NMR (125 MHz,  $\text{CDCl}_3$ )

**25** $^1\text{H NMR}$  (500 MHz,  $\text{CDCl}_3$ )**25** $^{13}\text{C NMR}$  (125 MHz,  $\text{CDCl}_3$ )

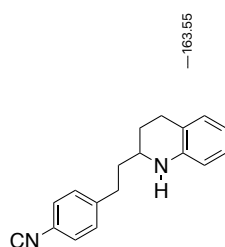
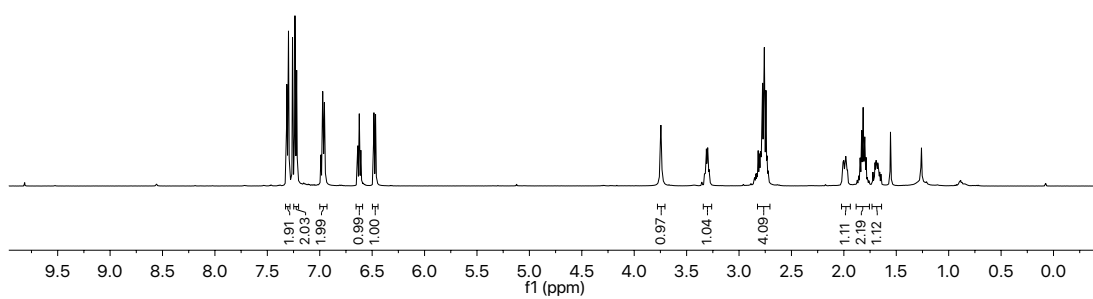


7.31  
7.31  
7.30  
7.24  
7.23  
7.22  
6.99  
6.98  
6.98  
6.97  
6.96  
6.95  
6.84  
6.84  
6.82  
6.82  
6.81  
6.81  
6.48  
6.47  
3.75  
3.32  
3.31  
3.30  
3.30  
3.29  
2.82  
2.81  
2.80  
2.79  
2.78  
2.77  
2.76  
2.74  
2.73  
2.01  
2.01  
2.00  
2.00  
1.99  
1.99  
1.98  
1.97  
1.96  
1.84  
1.83  
1.83  
1.82  
1.82  
1.80  
1.80  
1.79  
1.72  
1.71  
1.70  
1.70  
1.69  
1.69  
1.68  
1.68  
1.67  
1.66  
1.65



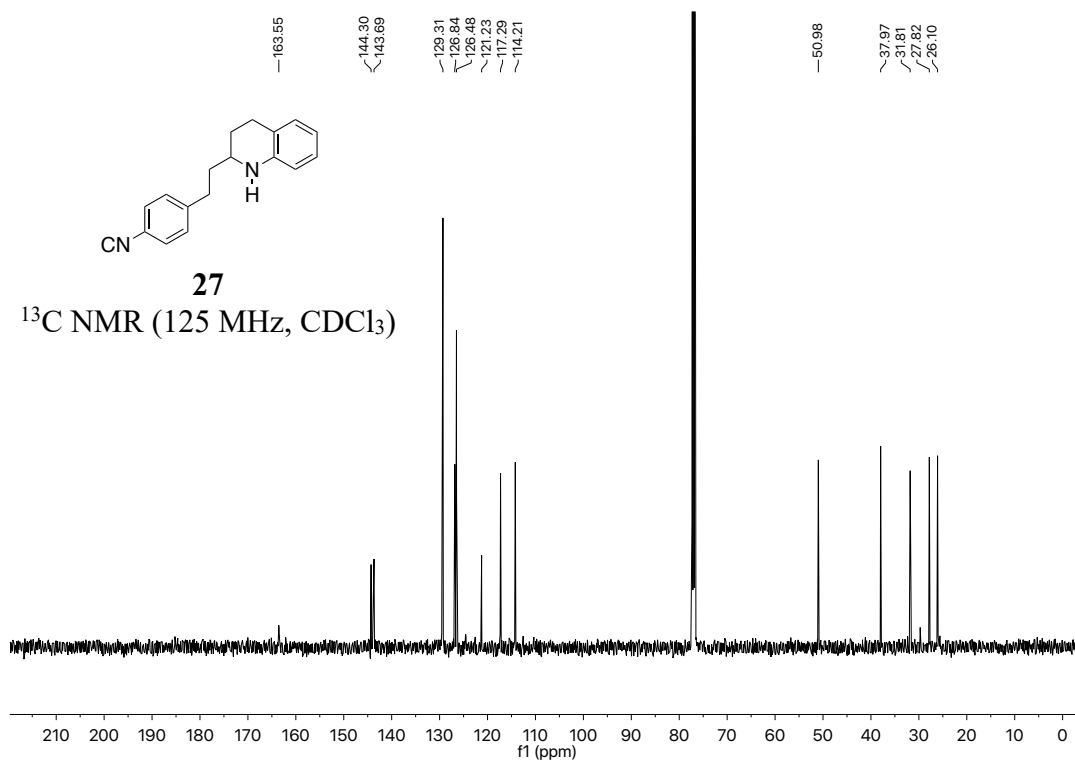
**27**

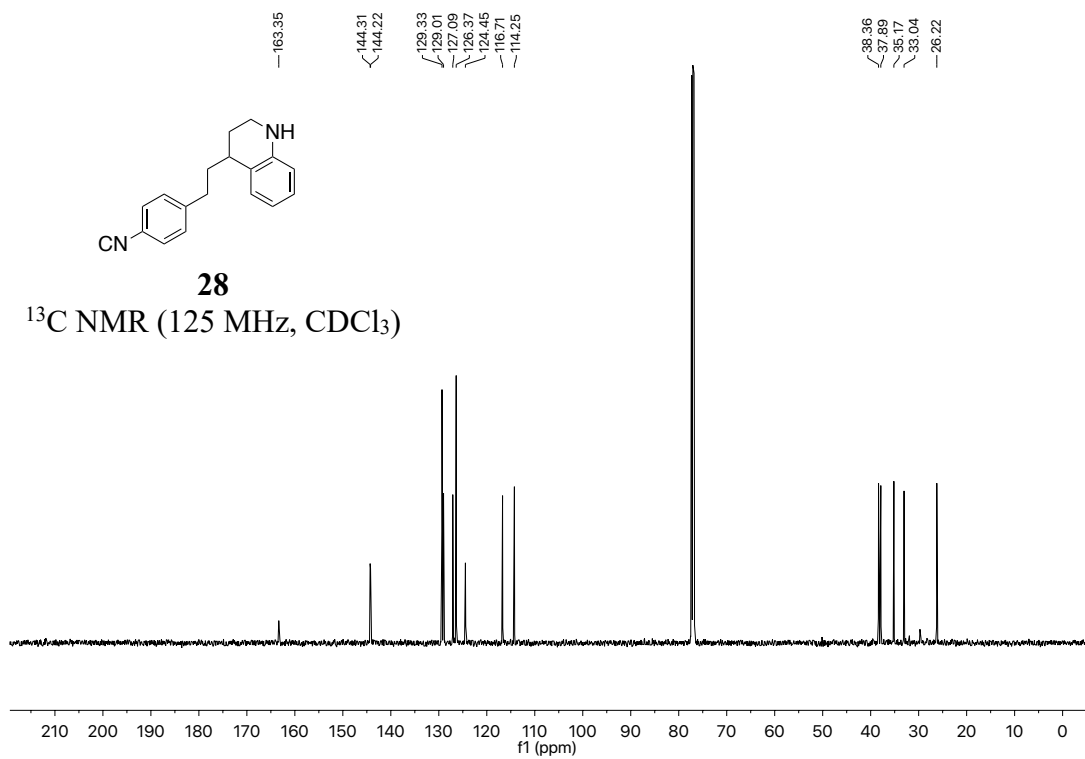
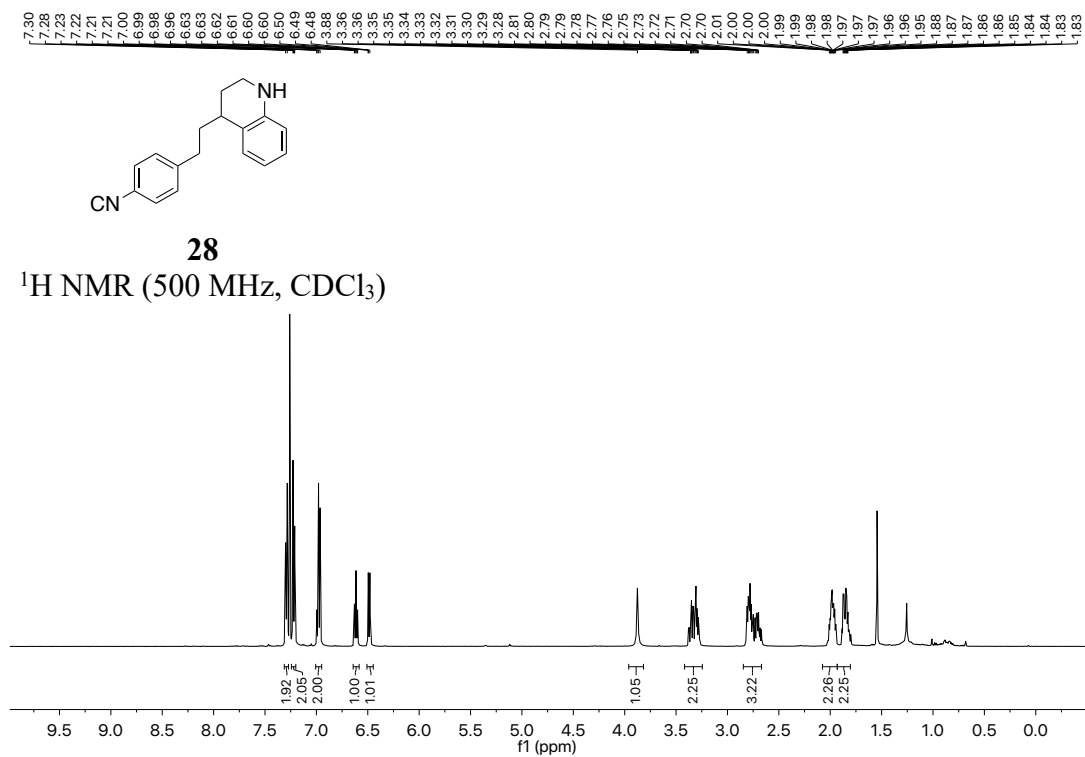
$^1\text{H}$  NMR (500 MHz,  $\text{CDCl}_3$ )



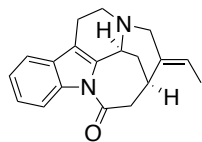
**27**

$^{13}\text{C}$  NMR (125 MHz,  $\text{CDCl}_3$ )

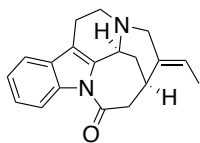
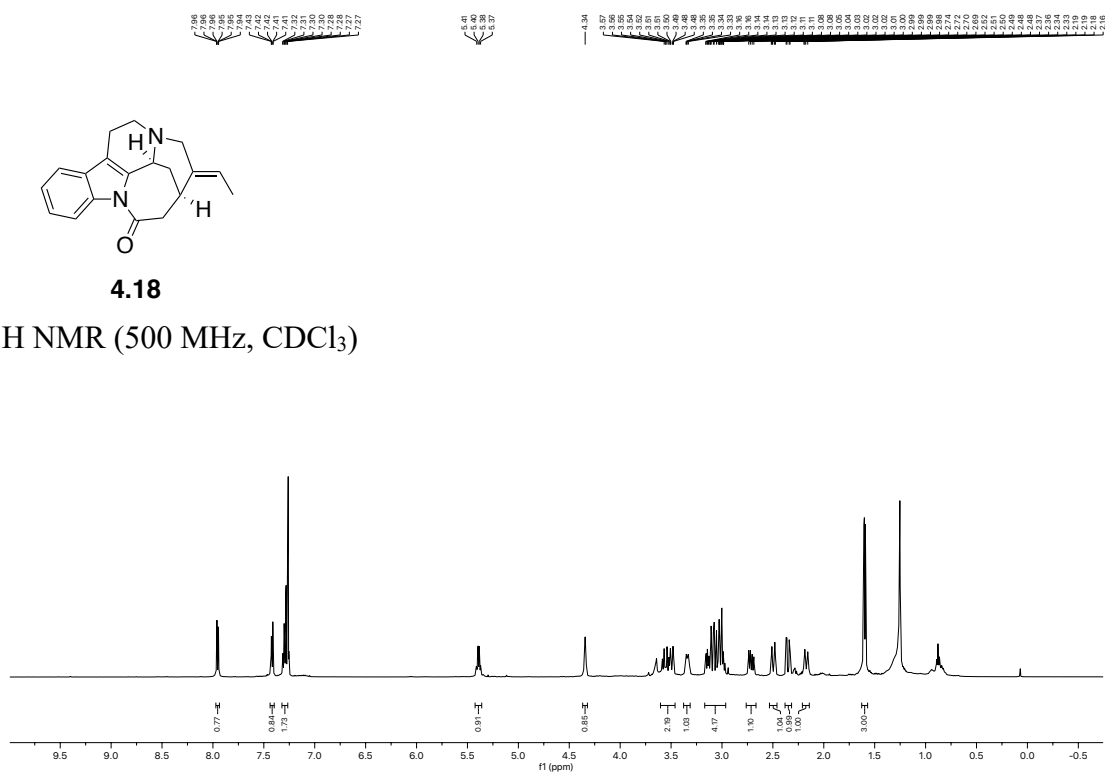




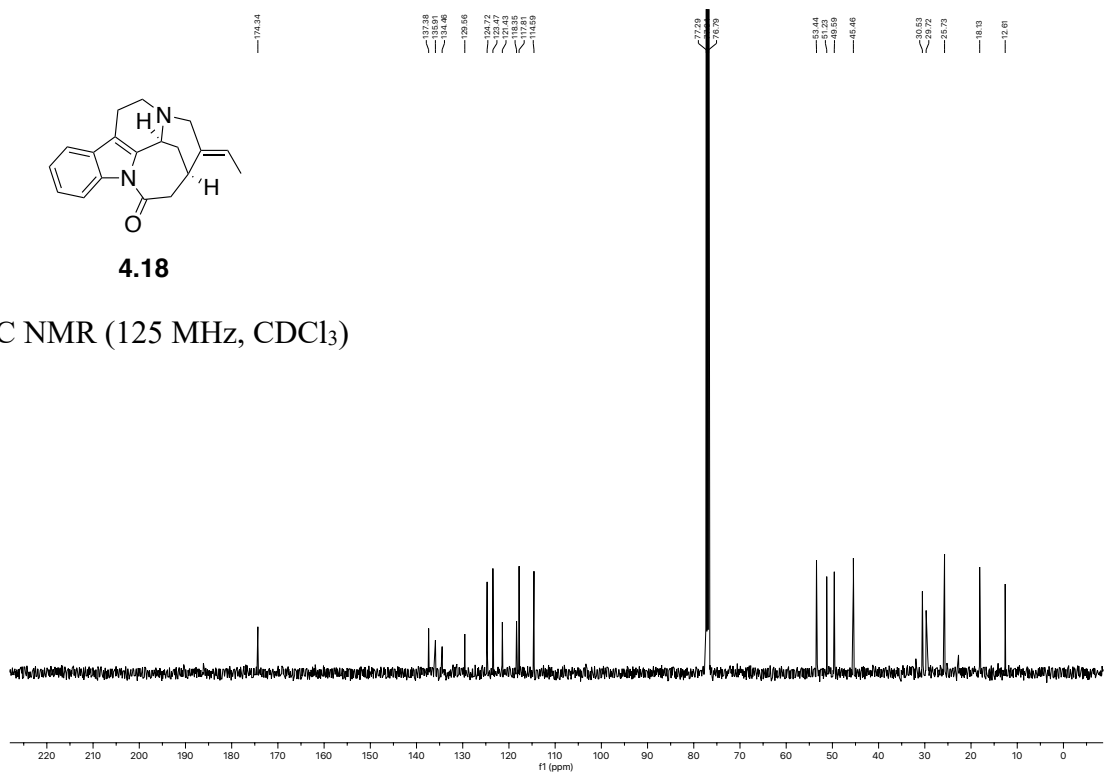




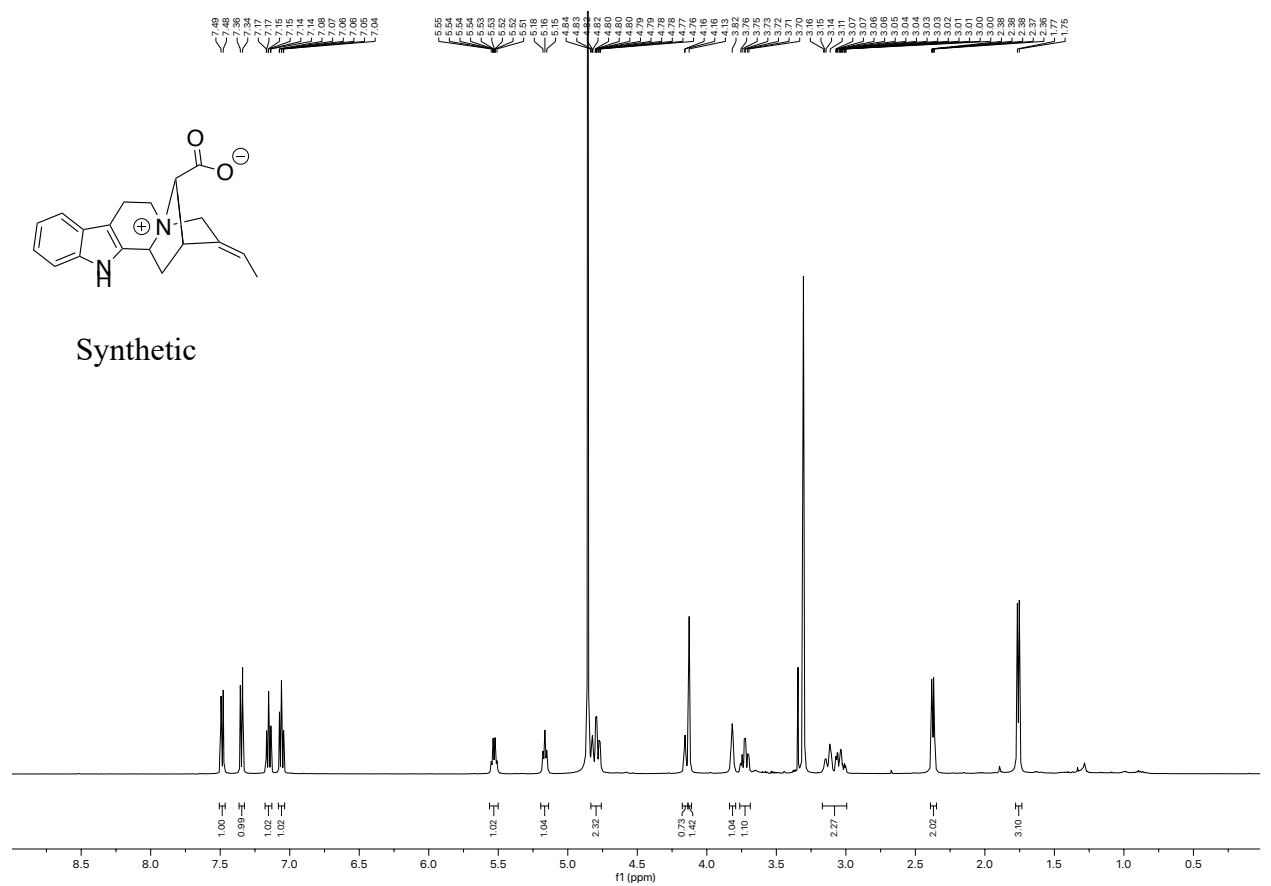
4.18

 $^1\text{H}$  NMR (500 MHz,  $\text{CDCl}_3$ )

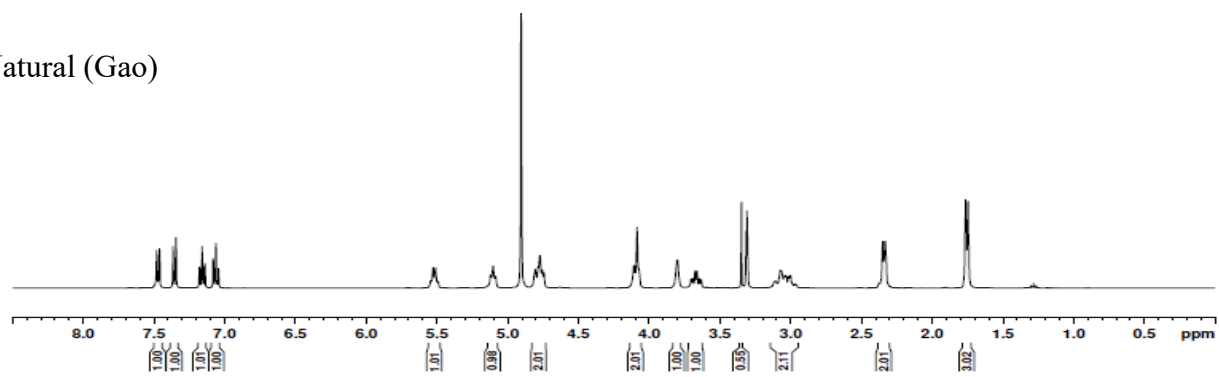
4.18

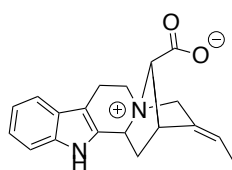
 $^{13}\text{C}$  NMR (125 MHz,  $\text{CDCl}_3$ )



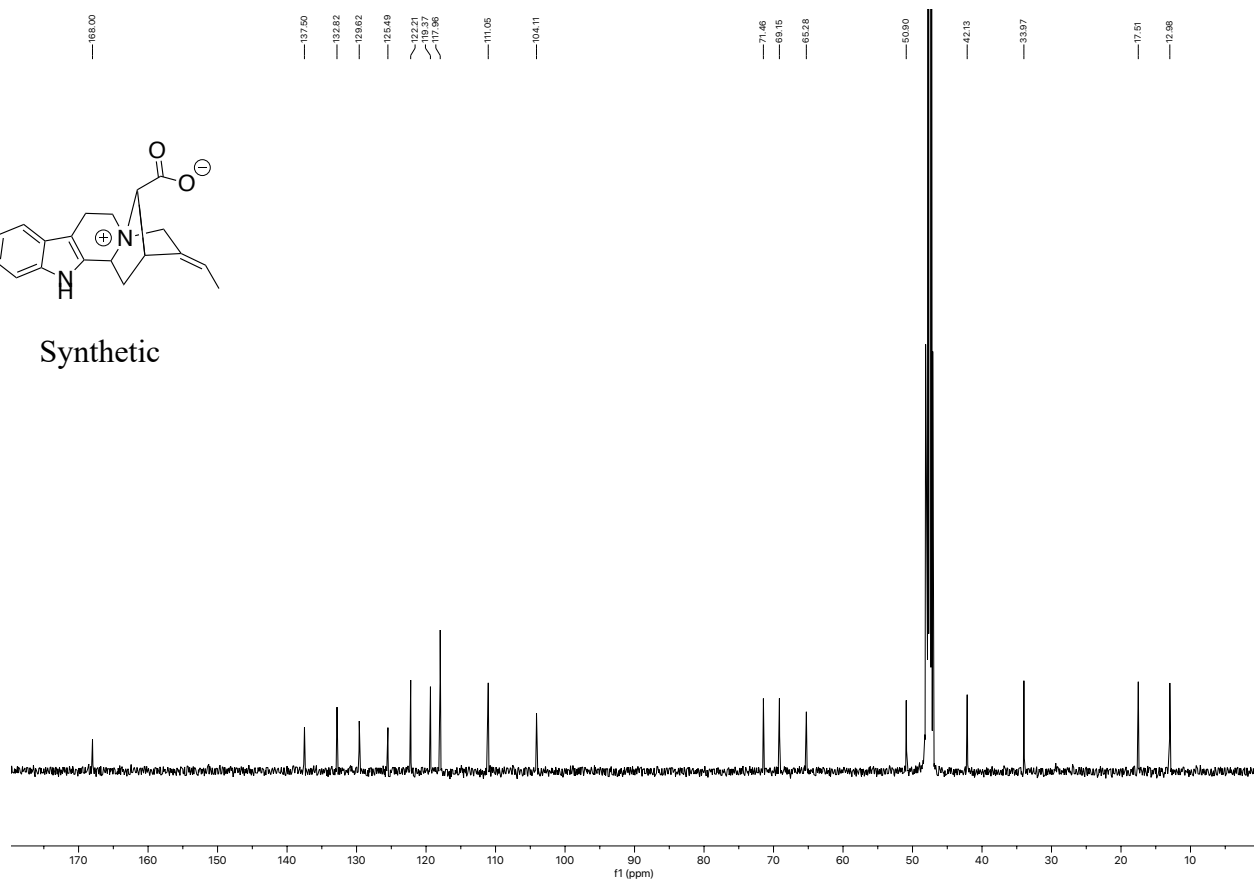


**Natural (Gao)**

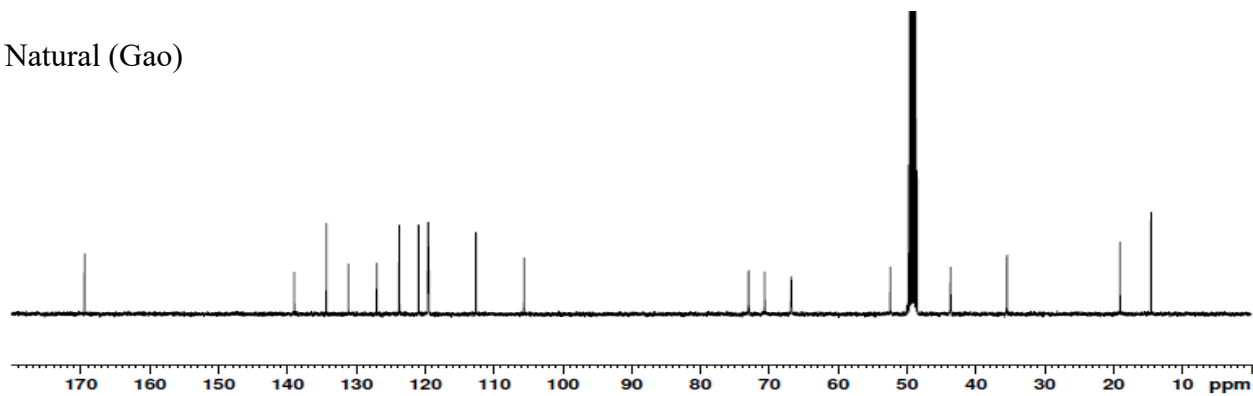




Synthetic



Natural (Gao)



## VITA

Kwaku Kyei-Baffour was born in Accra, Ghana in 1987. He obtained his Bachelor of Science degree in Chemistry with Honors from the University of Ghana. After obtaining a Master of Science degree in Chemistry at Youngstown State University in Ohio, Kwaku moved to Purdue University for his doctoral studies in 2014. At Purdue University, he worked in the group of Prof. Mingji Dai, where he performed research in the discovery of novel antimicrobial agents, and the total synthesis of 17-nor-Excelsinidine. He earned his Ph.D. from Purdue University in 2019. He is the recipient of the Bilsland Dissertation Fellowship, Herbert C. Brown Travel Grant, and the NOBCCChE Advancing Science Conference Grant.

## PUBLICATIONS

Bioorganic &amp; Medicinal Chemistry 27 (2019) 1845–1854



Contents lists available at ScienceDirect

Bioorganic &amp; Medicinal Chemistry

journal homepage: [www.elsevier.com/locate/bmc](http://www.elsevier.com/locate/bmc)

## Second-generation aryl isonitrile compounds targeting multidrug-resistant *Staphylococcus aureus*

Kwaku Kyei-Baffour<sup>a,d</sup>, Haroon Mohammad<sup>b,d</sup>, Mohamed N. Seleem<sup>b,c,\*</sup>, Mingji Dai<sup>a,c,\*</sup><sup>a</sup> Department of Chemistry, Center for Cancer Research and Institute for Drug Discovery, Purdue University, 720 Clinic Drive, West Lafayette, IN 47907, United States<sup>b</sup> Department of Comparative Pathobiology, College of Veterinary Medicine, Purdue University, 625 Harrison Street, West Lafayette, IN 47907, United States<sup>c</sup> Purdue Institute of Inflammation, Immunology and Infectious Disease, 610 Purdue Mall, West Lafayette, IN 47907, United States

### ABSTRACT

Antibiotic resistance remains a major global public health threat that requires sustained discovery of novel antibacterial agents with unexploited scaffolds. Structure-activity relationship of the first-generation aryl isonitrile compounds we synthesized led to an initial lead molecule that informed the synthesis of a second-generation of aryl isonitriles. From this new series of 20 compounds, three analogues inhibited growth of methicillin-resistant *Staphylococcus aureus* (MRSA) (from 1 to 4 μM) and were safe to human keratinocytes. Compound **19**, with an additional isonitrile group exhibited improved activity against MRSA compared to the first-generation lead compound. This compound emerged as a candidate worthy of further investigation and further reinforced the importance of the isonitrile functionality in the compounds' anti-MRSA activity. In a murine skin wound model, **19** significantly reduced the burden of MRSA, similar to the antibiotic fusidic acid. In summary, **19** was identified as a new lead aryl isonitrile compound effective against MRSA.

### 1. Introduction

Bacterial infections resistant to currently available antibiotics continue to pose a major global public health threat that requires the constant identification and development of new antibacterial agents. Though extensive research efforts and funding have recently been focused to identify new agents to treat Gram-negative bacterial infections, particularly those caused by carbapenem-resistant Enterobacteriaceae (CRE), the reality remains that Gram-positive bacteria (particularly methicillin-resistant *S. aureus* (MRSA)) are more prevalent sources of community-acquired and nosocomial infections, particularly in the United States of America.<sup>1–3</sup> In its landmark report in 2013, the US Centers for Disease Control and Prevention noted that serious infections caused by MRSA (> 80,000) alone outnumbered infections attributed to extended-spectrum β-lactamase producing Enterobacteriaceae (26,000), CRE (9000), multidrug-resistant *Acinetobacter* (7300), and multidrug-resistant *Pseudomonas aeruginosa* (6700) combined.<sup>4</sup> Furthermore, significantly more fatalities were attributed to MRSA infections (11,285 deaths) relative to infections caused by the aforementioned drug-resistant Gram-negative pathogens (3240 deaths).<sup>4</sup> Given MRSA infections continue to persist both in healthcare and community settings, and resistant isolates to key antibiotics (vancomycin and linezolid) used to treat MRSA infections have emerged,<sup>3,5–8</sup> new antibacterial agents are still needed.

Current antibacterial discovery programs often focus on optimizing existing antibiotic scaffolds (i.e. β-lactams, quinolones, glycopeptides, oxazolidinones) to develop new therapeutics. This approach has yielded regulatory approval for several new antibacterial agents to treat MRSA infections, including delafloxacin, dalbavancin, oritavancin, and tedizolid phosphate with improved potency relative to other antibiotics in the same drug class.<sup>9</sup> However, bacterial resistance to these newer agents is most probably inevitable, particularly given the similarity in structure to existing antibiotics, which will further hinder clinicians' ability to effectively treat drug-resistant bacterial infections. Identifying novel antibacterial agents with unique scaffolds or mechanisms of action is critical to circumvent the growing challenge of treating drug-resistant bacterial infections.

As part of efforts to identify compounds with unique functionalities and novel structural moieties capable of targeting multidrug-resistant bacterial infections, we recently identified aryl isonitriles as a unique class of compounds with anti-MRSA activity.<sup>10</sup> Though extensive efforts in isolating naturally occurring isonitriles from marine sponges and cyanobacteria have been fruitful, these and other naturally occurring isonitriles with antimicrobial activity have been precluded from extensive medicinal chemistry and structure-activity-relationship (SAR) studies.<sup>11–14</sup> This is primarily because their complex structural motifs make them very difficult to access and modify. Therefore, the isonitrile functionality and the aryl isonitrile scaffold remain one of the least

\* Corresponding authors at: Department of Comparative Pathobiology, Purdue University College of Veterinary Medicine, 625 Harrison St., West Lafayette, IN 47907, United States (M.N. Seleem). Department of Chemistry and Center for Cancer Research, 720 Clinic Drive, West Lafayette, IN 47907, United States (M. Dai).

E-mail addresses: [mselem@purdue.edu](mailto:mselem@purdue.edu) (M.N. Seleem), [mjdai@purdue.edu](mailto:mjdai@purdue.edu) (M. Dai).

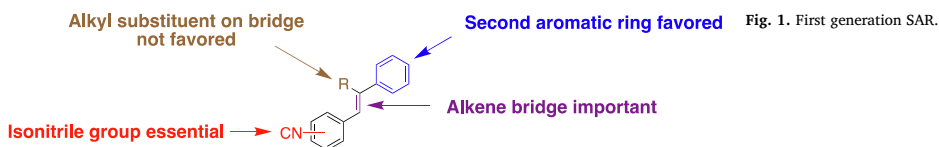
<sup>d</sup> These authors contributed equally.

<https://doi.org/10.1016/j.bmc.2019.03.034>

Received 16 February 2019; Received in revised form 9 March 2019; Accepted 19 March 2019

Available online 19 March 2019

0968-0896/© 2019 Elsevier Ltd. All rights reserved.



extensively studied scaffolds. Previous SAR studies on the first series of over 40 aryl isonitriles revealed the isonitrile functionality as the most essential structural component that contributed to the antibacterial activity of the compounds. The presence of a second non-isonitrile-bearing aromatic ring and an alkene bridge/linker were also shown to be important. However, substituents incorporated on this bridge did not result in improved antibacterial activity (Fig. 1).

With this in mind, the current work aims to further explore the structural-anti-MRSA activity of a second generation of aryl isonitriles, characterize their spectrum of antibacterial activity, and evaluate the most promising analogue's activity in a mouse model of MRSA infection. This exploration takes into consideration a novel group of stilbene bis-isonitriles. New stilbene aryl isonitriles with medicinally-relevant structural molecules and heterocyclic moieties, and those with a saturated linker have also been evaluated (Fig. 2). From this effort, compound **19** emerged as a new lead compound with antibacterial activity *in vitro* and *in vivo* against MRSA (Fig. 3).

## 2. Results

### 2.1. Synthesis of new aryl isonitrile analogues

Following the identification of **1** as the initial hit aryl isonitrile and subsequent synthetic exploration resulting in **2** as the lead molecule (Fig. 3), our initial synthetic efforts were focused on incorporating medicinally-relevant groups to the aryl isonitrile core. These groups included electron donating and electron withdrawing small molecules such as fluoro, chloro, trifluoromethyl, and methoxy groups.<sup>15–17</sup> To access these novel stilbene isonitriles, Michaelis-Arbuzov reaction involving the commercially available nitrobenzyl bromide starting material (**3**) was used to form nitrobenzyl phosphonate (**4**).<sup>18</sup> Subsequent reduction of the nitro group, followed by Hofmann isonitrile conversion of the resulting amine, led to the formation of the isonitrile phosphonate (**5**).<sup>19</sup> Serving as the divergent point, the isonitrile phosphonate was then subjected to Horner-Wadsworth-Emmons (HWE)<sup>20</sup> reaction to

produce isonitrile compounds **6**, **7**, **8**, **9**, **10**, and **11** from the corresponding aldehydes (Scheme 1). The aforementioned synthetic procedure was also used to synthesize aryl isonitriles to explore the importance of incorporating heterocyclic moieties as the second aromatic ring. These analogues included furan (**12**) and quinoline (**13** and **14**) groups.

As part of SAR studies on the first-generation molecules, the isonitrile functionality was identified as the integral component of the stilbene aryl isonitriles (Fig. 1). Bis-isonitriles **17**, **18**, and **19** were therefore synthesized to explore the influence of an additional isonitrile group on the antibacterial activity of the lead molecule **2**. Similarly, using **4** as the divergent point, the stilbene bis-isonitriles **17**, **18**, and **19** were synthesized (Scheme 2). HWE reaction involving **4** and the corresponding nitro substituted benzaldehydes was employed as the first step in the formation of dinitrostilbenes. The selective reduction of the nitro group followed by Hoffmann isonitrile synthesis led to compounds **17** and **18**. Bis-isonitrile **19** was prepared by a stepwise formylation and POCl<sub>3</sub>-promoted dehydration of the corresponding diamine.

Finally, after the synthesis of the stilbene isonitriles and the bis-isonitriles, the question of the impact of an alkane bridge on the biological activity arose. This led to the synthesis of compounds **21–28** (Scheme 3). In the synthesis of aryl isonitriles with an alkane linker, HWE reaction involving **4** and various aldehydes was first employed to form the stilbene compounds. A sequence of reduction and Hofmann isonitrile synthesis afforded the corresponding aryl isonitriles.

### 2.2. Initial screening and structure-activity relationship of new aryl isonitrile analogues against MRSA NRS123 (USA400)

In order to investigate the antibacterial activity of the newly synthesized isonitrile analogues, the minimum inhibitory concentration (MIC) against MRSA NRS123 was determined using the broth micro-dilution assay (Table 1). The newly synthesized stilbene bis-isonitriles **17** (MIC = 16 μM), **18** (MIC = 4 μM), and **19** (MIC = 8 μM) all exhibited moderate to good anti-MRSA activity. The most potent

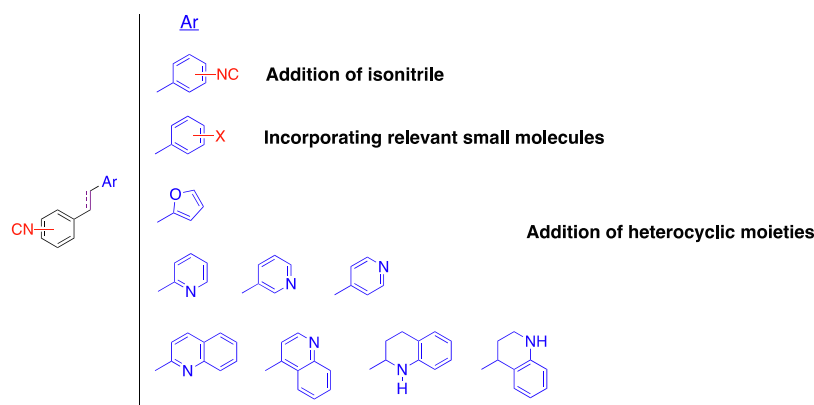


Fig. 2. Design strategy for the second-generation aryl isonitrile compounds.

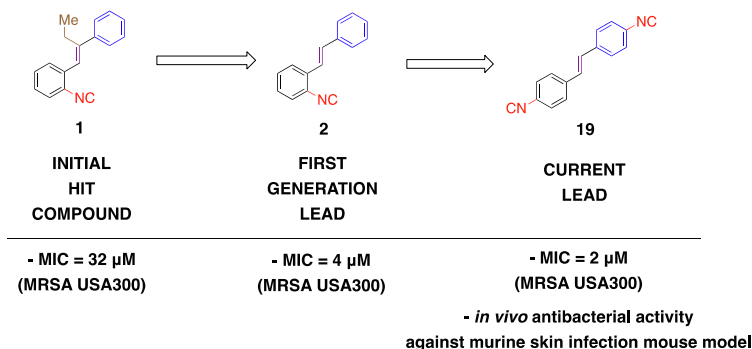
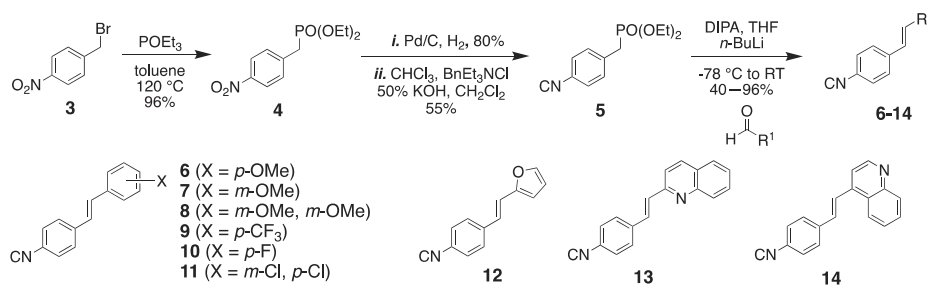
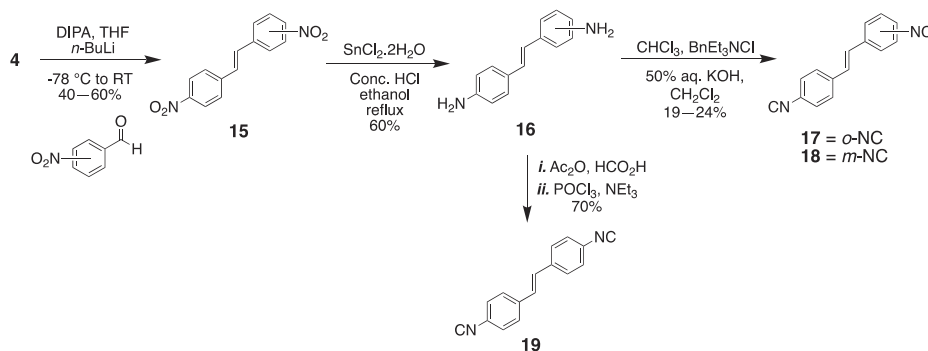


Fig. 3. Structural evolution leading to current lead aryl isonitrile compound and minimum inhibitory concentration (MIC) values against methicillin-resistant *S. aureus* (MRSA).



Scheme 1. Synthesis of stilbene aryl isonitrile compounds.



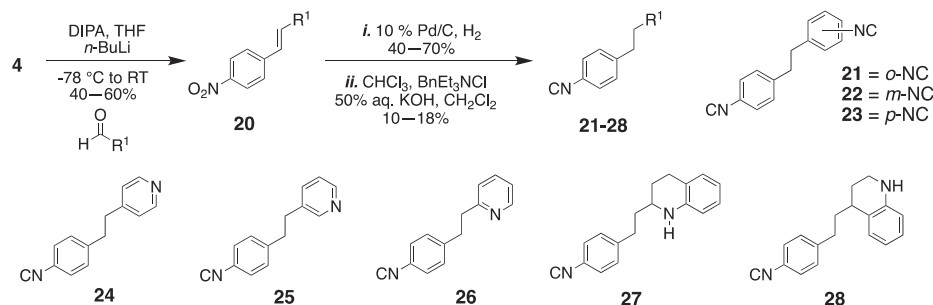
Scheme 2. Synthesis of stilbene bis-isonitriles.

analogues were compounds where the isonitrile moiety was located in the meta- (**18**) or para-position (**19**). The moderate to good activity exhibited by the stilbene bis-isonitriles further emphasized the importance of the isonitrile group for antibacterial activity against MRSA. An eight-fold reduction in activity was observed when the most potent stilbene bis-isonitrile **18** (MIC = 4 µM) was transformed to its saturated bis-isonitrile analogue **22** (MIC = 32 µM). The observation of a similar pattern for bis-isonitriles **17** (MIC = 16 µM) and **19** (MIC = 8 µM) with respect to the saturated bis-isonitrile analogues **21** and **23** (MIC > 64 µM) further emphasized the importance of the alkene linker.

Intrigued by the importance of the non-isonitrile-bearing aromatic ring resulting from the previous SAR studies, heterocyclic moieties with established therapeutic properties and widely known in medicinal

chemistry to improve the physicochemical and pharmacokinetic properties of lead molecules were investigated.<sup>21,22</sup> While none of these heterocyclic-containing aryl isonitriles positively improved the activity of the lead compound, the quinoline-containing compound **13** (MIC = 8 µM) was more potent than the quinoline analogue **14** (MIC > 64 µM) and furan analogue **12** (MIC = 32 µM).

With the knowledge of the medicinal importance of F, -OCH<sub>3</sub>, Cl and CF<sub>3</sub> and their value in the enhancement of the pharmacokinetic and physicochemical activity of several therapeutic small molecule candidates, installing these species on the aryl isonitrile compounds was investigated.<sup>15–17</sup> Of the methoxy substituted derivatives, the *meta*-substituted methoxy **7** (MIC = 2 µM) was the most potent analogue, but adding the second methoxy group (**8**) diminished the compound's anti-



Scheme 3. Synthesis of isonitriles with an alkane bridge.

Table 1

Minimum inhibitory concentration (MIC, in  $\mu\text{M}$ ) of second-generation aryl isonitrile analogues and control antibiotics against methicillin-resistant *Staphylococcus aureus* (MRSA) NRS123 (USA400).

Compound/Drug Name	MRSA NRS123 (USA400) MIC
6	32
7	2
8	64
9	32
10	64
11	> 64
12	32
13	8
14	> 64
17	16
18	4
19	8
21	> 64
22	32
23	> 64
24	64
25	> 64
26	> 64
27	16
28	32
Linezolid	1
Vancomycin	1

<sup>1</sup>N.D. = Not determined.

MRSA activity (MIC = 64  $\mu\text{M}$ ). Interestingly, none of the analogues with electron-withdrawing fluoro, chloro, and trifluoromethyl groups exhibited a major improvement in anti-MRSA activity. This reveals that having the right electronic environment around the second aromatic ring is important.

### 2.3. Evaluation of most potent analogues against additional strains of *S. aureus*

Based upon the initial screening results, the four most potent analogues from this series (**7**, **13**, **18**, and **19**) were further evaluated against additional multidrug-resistant *S. aureus* clinical isolates (Table 2). The *S. aureus* clinical isolates included strains resistant to linezolid (NRS119) and vancomycin (VRS10, VRS11a), two antibiotics frequently prescribed to treat MRSA infections. Against methicillin-sensitive *S. aureus*, the compounds inhibited growth from 2 to 16  $\mu\text{M}$ . When evaluated against MRSA NRS384 (USA300), all four aryl isonitrile compounds inhibited growth at concentrations ranging from 1 to 4  $\mu\text{M}$ . Methoxy analog **7** (MIC = 1  $\mu\text{M}$ ) and bis-isonitrile **19** (MIC = 2  $\mu\text{M}$ ) were more potent than first-generation lead **2** (MIC = 4  $\mu\text{M}$ ) against MRSA NRS384. However, quinoline isonitrile **13**

Table 2

Minimum inhibitory concentration (MIC, in  $\mu\text{M}$ ) of the four most potent aryl isonitrile compounds and control antibiotics against methicillin-sensitive (MSSA), methicillin-resistant (MRSA), linezolid-resistant (LRS), and vancomycin-resistant *S. aureus* (VRS).

Compound Name	<i>S. aureus</i> NRS107 (MSSA)	MRSA NRS119 (LRS)	MRSA NRS384 (USA300)	MRSA NRS385 (USA500)	VRS10 (VRS)	VRS11a (VRS)
7	2	1	1	4	2	4
13	N.D. <sup>1</sup>	4	4	N.D.	32	N.D.
18	16	4	4	16	8	16
19	4	1	2	8	8	8
Linezolid	2	32	2	4	2	2
Vancomycin	1	1	1	1	> 64	> 64

<sup>1</sup> N.D. = Not determined.

(MIC = 4  $\mu\text{M}$ ) and bis-isonitrile **18** (MIC = 4  $\mu\text{M}$ ) exhibited similar potency to **2**. Against MRSA NRS119, **7** and **19** were the most potent analogues (MIC = 1  $\mu\text{M}$ ), followed by **13** (MIC = 4  $\mu\text{M}$ ), and **18** (MIC = 4  $\mu\text{M}$ ). Once again, the second-generation analogues **7** and **19** were more potent than the first-generation lead **2** (MIC = 4  $\mu\text{M}$ ). All four compounds were more potent than linezolid (MIC = 32  $\mu\text{M}$ ) against MRSA NRS119. The MIC results obtained against MRSA NRS384 (USA300) and MRSA NRS119 (linezolid-resistant *S. aureus*) demonstrate that incorporating a second isonitrile functionality (as in compound **19**) improved the antibacterial activity of the first-generation lead molecule **2**.

Against two *S. aureus* strains (VRS10 and VRS11a) resistant to vancomycin (MIC > 64  $\mu\text{M}$ ), compounds **7** and **19** retained their antibacterial activity (MIC ranged from 2 to 8  $\mu\text{M}$ ). Interestingly, **13** (MIC = 32  $\mu\text{M}$ ) exhibited very poor antibacterial activity against VRS10. Thus, this compound was eliminated from further biological evaluation. Additionally, a time-kill assay was conducted with compounds **7**, **18**, and **19** against MRSA NRS123 and the results suggest that these aryl isonitrile compounds possess bacteriostatic activity (Fig. 4).

### 2.4. Investigation of the antibacterial spectrum of activity of the aryl isonitrile compounds

To examine their spectrum of antibacterial activity, compounds **7**, **18**, and **19** were examined against clinical isolates from the ESKAPE pathogens (*Enterococcus faecium* (E), *Klebsiella pneumoniae* (K), *Acinetobacter baumannii* (A), *Pseudomonas aeruginosa* (P), and *Enterobacter* species (E)) (Table 3). Collectively, these six pathogens are a significant source of hospital-acquired bacterial infections and exhibit resistance to most clinically available antibiotics.<sup>23,24</sup> All four compounds were significantly less potent or inactive (MIC  $\geq$  64  $\mu\text{M}$ ) against

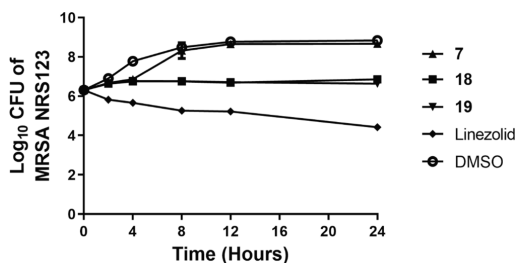


Fig. 4. Time-kill analysis of aryl isonitrile compounds 7, 18, 19, and linezolid (all at  $4 \times \text{MIC}$ ) against methicillin-resistant *Staphylococcus aureus* (MRSA NRS123) over a 24-h. incubation period at  $37^\circ\text{C}$ . DMSO served as a negative control. The error bars represent standard deviation values obtained from triplicate samples used for each compound/antibiotic studied.

vancomycin-resistant *E. faecium* (VRE), *K. pneumoniae*, *A. baumannii*, *P. aeruginosa*, and *E. cloacae*, similar to the antibiotics erythromycin, linezolid, and vancomycin. The compounds were also evaluated against two additional clinically-relevant Gram-positive bacterial pathogens, *Staphylococcus epidermidis* and *Streptococcus pneumoniae*. All three compounds exhibited potent activity against methicillin-resistant *S. epidermidis* ( $\text{MIC} = 1 \mu\text{M}$ ). Against, penicillin-resistant *S. pneumoniae*, 7 was the most potent compound ( $\text{MIC} = 4 \mu\text{M}$ ) followed by 19 ( $\text{MIC} = 8 \mu\text{M}$ ). Compound 18 was the least potent analogue against *S. pneumoniae* ( $\text{MIC} = 16 \mu\text{M}$ ).

#### 2.5. Effect of the outer membrane and efflux pump on antibacterial activity against Gram-negative bacterial pathogens

We hypothesized that the lack of antibacterial activity against Gram-negative bacteria observed for the aryl isonitrile compounds was either due to the presence of the outer membrane (OM) or expulsion via efflux pumps, two common resistance mechanisms utilized by Gram-negative bacterial pathogens.<sup>25</sup> The OM has been known to prevent

numerous antibiotics (including erythromycin) from gaining entry into the bacterial cell at sufficient concentrations to bind to/inhibit the molecular target. To examine if the OM was impeding the antibacterial activity of the aryl isonitrile compounds, compound 19 and control antibiotics were incubated with the same Gram-negative bacterial species presented in Table 2 in the presence of a subinhibitory concentration of the membrane-permeabilizing agent colistin. As presented in Table 4, a noticeable improvement in the antibacterial activity of compound 19 was observed against *A. baumannii* ( $\text{MIC} = 16 \mu\text{M}$ ) and *E. cloacae* ( $\text{MIC} = 4 \mu\text{M}$ ) indicating the OM was having a deleterious effect on the antibacterial activity of this compound. Interestingly, no improvement in antibacterial activity for 19, in the presence of colistin, was observed against *K. pneumoniae* and *P. aeruginosa*, (similar to linezolid) suggesting the presence of the outer membrane was not solely responsible for the lack of activity observed in these particular pathogens. The antibacterial activity of the antibiotic erythromycin, in the presence of colistin, improved against *A. baumannii* ( $\text{MIC} = 4 \mu\text{M}$ ), *E. cloacae* ( $\text{MIC} = 1 \mu\text{M}$ ), *K. pneumoniae* ( $\text{MIC} = 16 \mu\text{M}$ ), and *P. aeruginosa* ( $\text{MIC} = 4 \mu\text{M}$ ). Erythromycin is thought to be capable of diffusing across the OM but at a very slow rate.<sup>26</sup> Thus permeabilizing the OM is expected to enhance penetration of the antibiotic into bacterial cells.

We next examined if the presence of efflux pumps may be responsible for the lack of antibacterial activity observed for the aryl isonitrile compounds against Gram-negative bacteria (Table 4). These pathogens express different efflux pumps that confer resistance to numerous antibiotics including the AdeLJK efflux pump in *A. baumannii*, AcrAB-TolC efflux pump (present in *E. coli E. cloacae*, and *K. pneumoniae*) and its homologue MexAB-OprM (expressed by *P. aeruginosa*).<sup>26,27</sup> We evaluated the antibacterial activity of 19 against an *Escherichia coli* strain (JW25113) deficient in the AcrAB-TolC efflux pump responsible for excluding many xenobiotics from accumulating inside *E. coli* cells.<sup>25</sup> No discernible improvement in antibacterial activity of 19 was observed against the mutant *E. coli* strain relative to the wild-type strain (BW25113). In contrast, there was noticeable improvement in the antibacterial activity of erythromycin ( $\text{MIC} = 2 \mu\text{M}$ ) and linezolid ( $\text{MIC} = 16 \mu\text{M}$ ), two substrates of the AcrAB-TolC efflux pump.<sup>26,28</sup>

Table 3

Minimum inhibitory concentration (MIC, in  $\mu\text{M}$ ) of the three most potent aryl isonitrile compounds and control antibiotics against clinically-relevant Gram-positive and Gram-negative bacterial pathogens.

Test Agent	Bacterial Strain						
	<i>S. epidermidis</i> NRS101	<i>S. pneumoniae</i> ATCC 700677	<i>E. faecium</i> ATCC700221	<i>A. baumannii</i> BAA-1605	<i>E. cloacae</i> BAA-1134	<i>K. pneumoniae</i> ATCC BAA-1705	<i>Pseudomonas aeruginosa</i> ATCC 15442
7	1	4	> 64	> 64	> 64	> 64	> 64
18	1	16	> 64	> 64	> 64	> 64	> 64
19	1	8	> 64	> 64	> 64	> 64	> 64
Erythromycin	N.D. <sup>1</sup>	N.D.	N.D.	16	> 64	> 64	> 64
Linezolid	2	2	0.50	> 64	> 64	> 64	> 64
Vancomycin	4	1	> 64	32	> 64	> 64	> 64

<sup>1</sup> N.D. = Not determined.

Table 4

Minimum inhibitory concentration (MIC, in  $\mu\text{M}$ ) of 19 and control antibiotics against Gram-negative bacterial pathogens in the presence of a subinhibitory concentration of colistin (COL).

Test Agent	Bacterial Strain							
	<i>A. baumannii</i> BAA-1605	<i>E. cloacae</i> BAA-1134	<i>K. pneumoniae</i> ATCC BAA-1705	<i>P. aeruginosa</i> ATCC 15,442	<i>E. coli</i> BW25113		<i>E. coli</i> JW25113 ( $\Delta\text{tolC}$ )	
					(-COL) <sup>1</sup>	(+COL)	(-COL)	(+COL)
19	16	4	> 64	> 64	> 64	> 64	> 64	> 64
Erythromycin	4	1	16	4	64	1	2	0.50
Linezolid	> 64	16	> 64	> 64	> 64	> 64	16	16

<sup>1</sup> No colistin added to the media.

This suggests that the presence of efflux pumps alone on the surface of the OM on Gram-negative bacteria may not be responsible for conferring resistance to the aryl isonitrile compounds. We next investigated if the combination of the outer membrane and efflux pumps may impede the antibacterial activity of the aryl isonitrile compounds. The compound and control antibiotics were incubated with a subinhibitory concentration of colistin against *E. coli* BW25113 and *E. coli* JW25113. No improvement in the antibacterial activity of **19** (MIC > 64  $\mu$ M) was observed in the presence of colistin against *E. coli* JW25113. Similarly, no improvement in the MIC of linezolid was observed against *E. coli* JW25113 in the absence and presence of colistin, indicating the lack of antibacterial activity of linezolid observed against *E. coli* is due primarily to efflux. The MIC of erythromycin against *E. coli* JW25113, in contrast, improved one-fold in the presence of colistin indicating both the OM and efflux pumps interfere with the effect of this antibiotic against Gram-negative bacteria, in agreement with previous reports.<sup>26,29</sup> Due to the lack of antibacterial activity observed against VRE and Gram-negative bacterial pathogens, we moved to evaluate the aryl isonitrile compounds antibacterial activity *in vivo* against MRSA.

## 2.6. *In silico* pharmacokinetic evaluation of compound **19**

MRSA is a source of infection for both superficial skin lesions and complicated systemic infections. To determine a suitable animal model of MRSA infection to evaluate the aryl isonitrile compounds, the pharmacokinetic profile of compound **19** and linezolid were simulated utilizing a dose of 600 mg (as is commonly administered for linezolid in adult human patients). As shown in Table 5, the results indicate that compound **19** would not be suitable for oral administration for the treatment of systemic MRSA infections as it is not expected to attain a concentration in plasma/blood sufficient to inhibit bacterial growth. The maximum plasma concentration ( $C_{max}$ ) predicted for compound **19** is 0.17  $\mu$ g/mL (0.73  $\mu$ M), whereas the MIC against MRSA ranges from 1 to 8  $\mu$ M. Intravenous administration of compound **19** is predicted to result in a slow rate of clearance (12.58 mL/min/kg) correlating with a long half-life (22.90 h) which could alleviate the need for multiple daily dosing. The high values obtained for the volume of distribution at steady-state for **19** (24.94 L/kg compared to 1.11 L/kg for linezolid) indicate this compound is expected to distribute extensively into tissues. This may be due to the high degree of lipophilicity (cLogP = 3.88) present with the compound. These pharmacokinetic simulations suggest that though intravenous administration of **19** may be possible for

treatment of systemic MRSA infections, the extensive distribution of the compound into tissues would necessitate a higher dose be administered/continuous infusion of compound (to ensure the concentration remained above the MIC to inhibit MRSA growth). The values obtained for linezolid via the *in silico* pharmacokinetic simulation overall were in close proximity to experimental values obtained by Stalker, et al. from healthy human subjects administered a single 625 mg dose of linezolid either orally or intravenously.<sup>30</sup> However, the simulation underestimated the  $C_{max}$  for linezolid and overestimated the half-life and volume of distribution compared to the experimental values. Based upon the *in silico* pharmacokinetic simulation, **19** appears most suitable for evaluation topically to treat localized/uncomplicated MRSA skin infections.

## 2.7. The active aryl isonitrile compounds are safe to mammalian keratinocytes

*S. aureus* is a leading source of skin and soft tissue infections, both uncomplicated and invasive, globally.<sup>31–34</sup> As such, based upon the *in silico* pharmacokinetic data, we decided to investigate the antibacterial activity of the second-generation aryl isonitriles as topical antibacterial agents in a MRSA murine skin infection mouse model. Before exposing mice to the compounds, we evaluated the safety profile of **7**, **18**, and **19** against keratinocytes (HaCaT). All three compounds were safe up to the maximum tested concentration of 128  $\mu$ M (more than 90% of HaCaT cells remained viable after 24 h of exposure to the compounds) (Fig. 5).

## 2.8. Compound **19** significantly reduces the burden of MRSA in a skin infection mouse model

After confirming the aryl isonitrile compounds are safe to keratinocytes, we moved to investigate the antibacterial activity of the newly synthesized analogues in a mouse model of MRSA skin infection. Given the safety profile against keratinocytes was identical for all three aryl isonitrile compounds, **19** was selected for this experiment. Given **18** and **19** are structurally similar, the more potent compound *in vitro* against MRSA USA300 was selected for evaluation. After the formation of an abscess at the site of infection, mice were treated twice daily for five days. As the skin wounds were uncomplicated and localized, treatment was administered topically directly onto the surface of the abscesses. Mice were euthanized 12 h after the last dose was administered and the abscesses were harvested to enumerate MRSA CFU. As

**Table 5**  
*In silico* pharmacokinetic analysis for compound **19** and linezolid (simulated at 600 mg).

	Oral			Intravenous		
	<b>19</b> (Simulated)	Linezolid (Simulated)	Linezolid (Experimental) <sup>1</sup>	<b>19</b> (Simulated)	Linezolid (Simulated)	Linezolid (Experimental)
$C_{max}^2$ ( $\mu$ g/mL)	0.17	5.33	12.7	–	–	13.4
$t_{max}^3$ (hours)	3	2.75	1.33	–	–	0.5
Fraction absorbed (FA) <sub>last</sub>	0.80	0.92	1.03	–	–	–
CL <sup>4</sup> (mL/min/kg)	–	–	–	12.58	1.09	1.74 <sup>9</sup>
$t_{1/2}^5$ (hours)	–	–	–	22.90	12.31	4.40
MRT <sup>6</sup> (hours)	–	–	–	12.82	17.04	–
$V_d^7$ (L/kg)	–	–	–	24.94	1.11	0.58 <sup>10</sup>
$V_{ss}^8$ (L/kg)	–	–	–	9.68	1.12	–

<sup>1</sup> (adapted from Stalker DJ et al. J Antimicrob Chemother 2003, 51: 1239–46 (Table 2, 625 mg dose)).

<sup>2</sup>  $C_{max}$  = maximum concentration of drug in plasma/blood.

<sup>3</sup>  $t_{max}$  = time required to reach  $C_{max}$ .

<sup>4</sup> CL = rate of clearance.

<sup>5</sup>  $t_{1/2}$  = half-life.

<sup>6</sup> MRT = mean residence time.

<sup>7</sup>  $V_d$  = volume of distribution.

<sup>8</sup>  $V_{ss}$  = volume of distribution at steady-state.

<sup>9</sup> Clearance for linezolid (experimental) obtained by dividing the mean clearance value by the mean weight of patients.

<sup>10</sup> Volume of distribution for linezolid (experimental) obtained by dividing the mean  $V_d$  by the mean weight of patients.

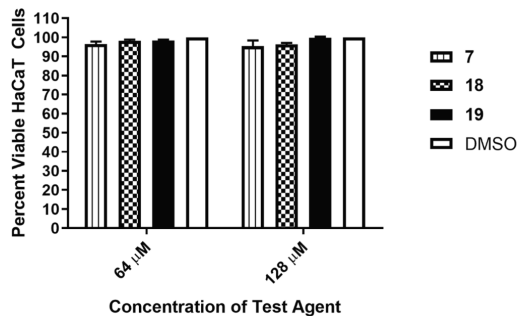


Fig. 5. Toxicity analysis of aryl isonitrile compounds against human keratinocytes (HaCaT). Percent viable mammalian cells (measured as average absorbance ratio (test agent relative to DMSO)) for cytotoxicity analysis of compounds 7, 18, and 19 (tested in triplicate) at 64 and 128  $\mu\text{M}$  against HaCaT cells over a 24 h period using the MTS 3-(4,5-dimethylthiazol-2-yl)-5-(3-carboxymethoxyphenyl)-2-(4-sulfophenyl)-2H-tetrazolium assay. Dimethyl sulfoxide (DMSO) was used as a negative control to determine a baseline measurement for the cytotoxic impact of each compound. The absorbance values represent an average of a minimum of three samples analyzed for each compound. Error bars represent standard deviation values. A one-way ANOVA, with post hoc Dunnett's multiple comparisons test, determined statistical difference between the values obtained for each compound and DMSO ( $P < 0.05$ ).

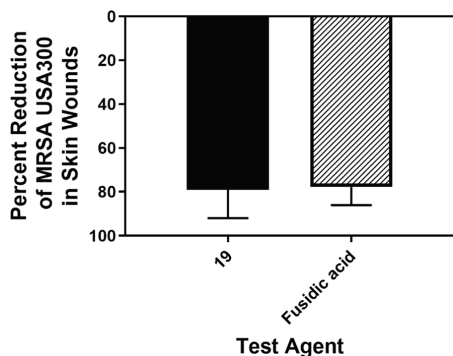


Fig. 6. Reduction of MRSA USA300 in infected lesions of mice. Average percent reduction of MRSA CFU/mL in murine skin lesions after treatment with 19 or fusidic acid. A one-way ANOVA with post-hoc Dunnett's multiple comparisons found no statistical difference between mice treated with fusidic acid and mice treated with compound 19.

presented in Fig. 6, 19 (79.02% reduction) was as effective as the control antibiotic fusidic acid (77.78% reduction) in reducing the burden of MRSA in the wounds of infected mice after five days of treatment. Importantly, no excess inflammation or toxicity was observed in wounds after exposure to the compounds or fusidic acid.

### 3. Discussion

Antibiotics have played a critical role in resolving bacterial infections throughout the world since their initial discovery. However, bacteria have proven to be shrewd microorganisms capable of acquiring resistance to multiple antibiotics utilizing an array of clever mechanisms (e.g. through modification of the drug target, degradation of the antibiotic, and efflux of the antibiotic). As such there is a continuous need to identify and develop novel antibacterial agents capable of treating drug-resistant bacterial infections. MRSA remains a significant

cause of superficial and invasive antibiotic-resistant infections globally. Though several antibacterial agents effective against MRSA are currently in clinical trials, the remarkable ability of this organism to develop resistance to different antibiotics necessitates new antibacterial agents, particularly from unexploited scaffolds, be identified and developed.

We previously synthesized and evaluated over 40 aryl isonitrile compounds for antibacterial activity against MRSA.<sup>10</sup> The first-generation compounds inhibited MRSA growth at concentrations ranging from 2 to 64  $\mu\text{M}$ <sup>10</sup> but none of the compounds possessed a suitable physicochemical profile to evaluate their effectiveness in an animal model of MRSA infection. The present study aimed to expand the library of aryl isonitrile compounds to better understand these limitations and further characterize the compounds' structure-antibacterial activity relationship. To this end, 20 second-generation aryl isonitrile compounds consisting of stilbene bis-isonitriles, stilbene aryl isonitriles with medically-relevant and heterocyclic moieties, and those with a saturated linker were synthesized and evaluated for antibacterial activity.

The newly synthesized analogues were initially evaluated against a clinical isolate of MRSA USA400. From the initial screening, inclusion of an additional isonitrile moiety, the stilbene core, and the non-isonitrile-bearing aromatic ring were all found to be key for anti-MRSA activity. Four compounds (7, 13, 18, and 19) inhibited growth of MRSA at a concentration ranging from 2 to 8  $\mu\text{M}$ , similar to the lead compound (2) from the first-generation aryl isonitriles. Bis-isonitrile 19 was more potent than the first-generation lead 2 against MRSA NRS384 (USA300) and MRSA NRS119 (LRSA) which further confirmed the importance of the isonitrile functionality.

Importantly, three compounds retained potent antibacterial activity against MRSA isolates exhibiting resistance to vancomycin and linezolid, antibiotics frequently used as agents of last resort for treatment of MRSA infections.<sup>35,36</sup> Though not prevalent clinically, the identification of *S. aureus* strains exhibiting resistance to vancomycin and linezolid, two key therapeutic options for treatment of MRSA infections, is a noteworthy problem. The lack of cross-resistance observed between the aryl isonitrile compounds and vancomycin and linezolid is important therapeutically as it provides a potential alternative source of treatment against linezolid-resistant and vancomycin-resistant *S. aureus* infections.

Previously, the first-generation aryl isonitrile analogues were only evaluated against clinical isolates of *S. aureus*. We were curious to investigate the spectrum of antibacterial activity of the second-generation aryl isonitrile compounds. Thus, three of the most potent analogues against MRSA (7, 18, and 19) were evaluated against a panel of clinically-relevant pathogens, including members of the ESKAPE group, *S. epidermidis*, and *S. pneumoniae*. The compounds exhibited potent antibacterial activity against the Gram-positive pathogens *S. epidermidis* and *S. pneumoniae*. Interestingly, the compounds were inactive against vancomycin-resistant *E. faecium*. The lack of antibacterial activity against VRE (a Gram-positive pathogen similar to MRSA) is not entirely surprising given certain antibiotics that are active against *S. aureus* (such as ampicillin and vancomycin) are inactive against vancomycin-resistant *E. faecium*.<sup>37</sup> The aryl isonitrile compounds also lacked antibacterial activity against five Gram-negative bacterial pathogens tested (*A. baumannii*, *K. pneumoniae*, *E. cloacae*, *E. coli*, and *P. aeruginosa*). The lack of antibacterial activity against Gram-negative pathogens is not surprising given most small molecules are unable to permeate the complex outer membrane (OM) present in Gram-negative bacteria. Those that are capable of diffusing across the OM may be susceptible to expulsion (decreasing the intracellular concentration of compound/drug) by a number of different efflux pumps expressed by Gram-negative bacteria, including the AcrAB-TolC pump present in *E. coli*.<sup>25</sup> Thus we evaluated the antibacterial activity of the aryl isonitrile compounds after permeabilizing the OM (using a subinhibitory concentration of colistin) and against an *E. coli* strain deficient in the AcrAB-TolC efflux

pump. Interestingly, there was improvement in the MIC for compound **19** observed in the presence of colistin against *A. baumannii* and *E. cloacae* but not against *E. coli*, *K. pneumoniae*, and *P. aeruginosa*. Against a mutant *E. coli* strain deficient in AcrAB-TolC, no improvement in the MIC of **19** was observed indicating that this compound may not be a substrate for efflux. This suggests that though the outer membrane may contribute to the lack of antibacterial activity for the aryl isonitrile compounds observed against specific Gram-negative bacterial pathogens, additional resistance mechanism(s) may play a role as well. Alternatively, the compounds may have a weaker affinity for the molecular target in Gram-negative bacteria as opposed to against MRSA, *S. epidermidis*, and *S. pneumoniae*. Though the molecular target of the aryl isonitrile compounds is currently unknown, this question is being intensely investigated using both genetic and phenotypic approaches. Identification of the molecular target may provide key insight into the difference in potency observed for the aryl isonitrile compounds against *S. aureus* relative to other bacterial pathogens.

The aryl isonitrile compounds possessed good *in vitro* activity against drug-resistant *S. aureus* isolates and were safe to mammalian cells (non-toxic to human keratinocytes at 128  $\mu$ M, more than 30-fold higher than the concentration where they inhibited MRSA growth *in vitro*). However, an *in silico* pharmacokinetic evaluation of **19** revealed this compound may not be effective in treatment of systemic MRSA infections (as the maximum predicted concentration of the compound in plasma was lower than the MIC of the compound against MRSA). As a means to address this problem while still retaining antibacterial activity, the alkene core of the current lead **19** is undergoing further structural diversification with molecular entities we hypothesize will help improve the physicochemical profile of the lead compound.

Based upon the *in vitro* antibacterial activity assay results and *in silico* pharmacokinetic simulation, we proceeded to evaluate the effectiveness of **19** as a topical antibacterial to treat MRSA skin infection. MRSA remains a major source of skin and soft tissue infections (SSTIs) throughout the world.<sup>31–34,38,39</sup> Treatment of SSTIs can be challenging given the emergence of resistance to several antibiotics frequently used in the clinic. One example is the antibiotic fusidic acid, which is prescribed for use topically in Europe for the treatment of SSTIs. Extensive use of fusidic acid has resulted in the emergence of resistant isolates<sup>40</sup> that necessitates new therapeutic agents to treat uncomplicated, localized *S. aureus* SSTIs. In the United States of America, MRSA USA300 is the predominant strain linked to community-acquired SSTIs.<sup>41</sup> As such, we moved to evaluate the efficacy of compound **19** administered topically in a MRSA USA300 skin wound mouse model. Compound **19** significantly reduced the burden of MRSA USA300 in infected abscesses by over 70% (after only five days of treatment) similar to fusidic acid.<sup>42</sup>

#### 4. Conclusions

In conclusion, the present study identified four new aryl isonitrile compounds bearing potent antibacterial activity against MRSA *in vitro*. The analogues were inactive against important Gram-negative bacterial pathogens, and their activity appeared to be negatively impacted by the presence of the outer membrane. The newly synthesized analogues were safe to keratinocytes at concentrations up to 128  $\mu$ M and significantly reduced the burden of MRSA in infected wounds in a mouse model of MRSA skin infection. However, *in silico* pharmacokinetic simulation revealed compound **19** would not effectively permeate across the GI tract and may extensively distribute into tissues thus precluding its evaluation in a systemic animal model of MRSA infection. Addressing these limitations and deducing the molecular target are necessary questions to resolve to further develop aryl isonitrile compounds as a novel class of antibacterial agents to treat drug-resistant *S. aureus* infections.

## 5. Experimental section

### 5.1. Biological methods

#### 5.1.1. Bacterial strains and reagents

Relevant information pertaining to all bacterial isolates used in this study are presented in Supplementary Table 1. Clinical isolates of *S. aureus* and *S. epidermidis* were obtained through the Network of Antimicrobial Resistance in *Staphylococcus aureus* (NARSA) program. Isolates of *S. pneumoniae*, *E. faecium*, *A. baumannii*, *K. pneumoniae*, *E. cloacae*, and *P. aeruginosa* were obtained from the American Type Culture Collection (ATCC). *E. coli* strains BW25113 and JW25113 were obtained from The Coli Genetic Stock Center (CGSC), Yale University. Antibiotics were purchased commercially and dissolved in DMSO (for linezolid), ethanol (for erythromycin), or sterile deionized water (for colistin and vancomycin). Stock 10 mM solutions were prepared for all antibiotics. Brain heart infusion broth (BHI), Tryptic soy broth (TSB), Tryptic soy agar (TSA), phosphate-buffered saline (PBS), Dulbecco's modified Eagle's medium (DMEM), fetal bovine serum (FBS), and 96-well plates were all purchased from commercial vendors.

#### 5.1.2. Evaluation of antibacterial activity of compounds and control antibiotics

The minimum inhibitory concentration of the aryl isonitrile analogues and control antibiotics was determined using the broth microdilution assay following the Clinical and Laboratory Standards Institute guidelines, with the following modifications.<sup>43</sup> Bacteria were cultured either in TSB or BHI (for *E. faecium*) and exposed to either compounds or control antibiotics, in triplicate, in 96-well plates. For permeabilization of the outer membrane, Gram-negative bacterial pathogens were exposed to a subinhibitory concentration of colistin equivalent to either  $\frac{1}{4} \times$  MIC (for *A. baumannii*, *E. cloacae*, *E. coli*, and *P. aeruginosa*) or  $\frac{1}{2} \times$  MIC (for *K. pneumoniae*). Plates were incubated aerobically at 37 °C for 18–24 h before the MIC values were recorded. *S. pneumoniae* was incubated with compounds at 37 °C + 5% CO<sub>2</sub>. The MICs reported represent the lowest concentration of each compound/drug necessary to inhibit visual bacterial growth.

#### 5.1.3. In silico pharmacokinetic evaluation of **19**

Compound **19**'s pharmacokinetic profile was examined *in silico*, using chemPK version 2.0 (Cyprotex, Inc.) simulating a dose of 600 mg administered both orally and intravenously.

#### 5.1.4. Toxicity assessment of aryl isonitrile analogues against human keratinocytes

Compounds **7**, **18**, and **19** were assayed (at concentrations of 16, 32, 64, and 128  $\mu$ M) against a human keratinocyte (HaCaT) cell line (AddexBio, San Diego, CA, USA) to determine the potential toxic effect to mammalian skin cells *in vitro*, as previously described.<sup>44–48</sup> In brief, cells were cultured in DMEM supplemented with 10% FBS at 37 °C with CO<sub>2</sub> (5%). Control cells received DMSO alone at a concentration equal to that in drug-treated cell samples. The cells were incubated with the compounds (in triplicate) in a 96-well plate at 37 °C with CO<sub>2</sub> (5%) for 24 h. The assay reagent MTS 3-(4,5-dimethylthiazol-2-yl)-5-(3-carboxymethoxyphenyl)-2-(4-sulfophenyl)-2H-tetrazolium (Promega, Madison, WI, USA) was subsequently added and the plate was incubated for four hours. Absorbance readings (at OD<sub>490</sub>) were taken using a kinetic microplate reader (Molecular Devices, Sunnyvale, CA, USA). The quantity of viable cells after treatment with each compound was expressed as a percentage of the viability of DMSO-treated control cells (average of triplicate wells  $\pm$  standard deviation). The toxicity data was analyzed via a one-way ANOVA, with post hoc Dunnett's multiple comparisons test ( $P < 0.05$ ), utilizing GraphPad Prism 6.0 (GraphPad Software, La Jolla, CA).

### 5.1.5. Evaluation of 19 in a murine model of MRSA skin infection

The mice study was conducted under the guidelines of the Purdue University Animal Care and Use Committee (PACUC) and carried out in strict accordance with the recommendations in the Guide for the Care and Use of Laboratory Animals of the National Institutes of Health. The method used for this study was similar to one described in previous reports, with slight modifications.<sup>44,49-53</sup> Three groups (n = 5) of eight-week old female Balb/c mice (obtained from Envigo, Indianapolis, IN, USA) received an intradermal injection (40 µL) containing  $1.32 \times 10^9$  CFU/mL MRSA USA300. Following formation of an abscess at the injection site (~48 h post-infection), topical treatment was initiated subsequently with each group of mice receiving a 2% suspension (formulated in petroleum jelly) of fusidic acid or 19. One group of mice received the vehicle alone (negative control). Each group of mice was housed separately in a ventilated cage with appropriate bedding, food, and water. Mice were checked at least four times daily during infection and treatment to ensure no adverse reactions were observed. Mice were treated twice daily for five days, before they were humanely euthanized via CO<sub>2</sub> asphyxiation 12 h after the last dose was administered. Wounds were aseptically extracted and subsequently homogenized in PBS (2 mL). The homogenized tissue was then serially diluted in PBS before plating onto mannitol salt agar plates. Plates were incubated for at least 16 h at 37 °C before viable CFU were counted and MRSA reduction in the skin wound (relative to the negative control) post-treatment was determined for each group.

### Acknowledgements

The authors would like to thank the Network of Antimicrobial Resistance in *Staphylococcus aureus* (NARSA) program supported under NIAID/NIH Contract # HHSN272200700055C for providing the MRSA and VRSA strains used in this study. MD thanks financial support from NIH (R35 GM128570) and unrestricted grants from Eli Lilly and Amgen. The NIH P30 CA023168 is acknowledged for supporting shared NMR resources to Purdue Center for Cancer Research. The authors would like to thank Dr. Waleed Younis (South Valley University, Qena, Egypt) and Nader S. Abutaleb (Purdue University) for assistance with biological experiments.

### Appendix A. Supplementary data

Supplementary data to this article can be found online at <https://doi.org/10.1016/j.bmc.2019.03.034>.

### References

- Blaskovich MAT, Hansford KA, Butler MS, Jia Z, Mark AE, Cooper MA. Developments in glycopeptide antibiotics. *ACS Infect Dis*. 2018;4:715–735.
- Sievert DM, Ricks P, Edwards JR, et al. Antimicrobial-resistant pathogens associated with healthcare-associated infections: summary of data reported to the National Healthcare Safety Network at the Centers for Disease Control and Prevention, 2009–2010. *Infect Control Hosp Epidemiol*. 2013;34:1–14.
- Mohammad H, Thangamani S, Seleem MN. Antimicrobial peptides and peptidomimetics – potent therapeutic allies for staphylococcal infections. *Curr Pharm Des*. 2015;21:2073–2088.
- Centers for Disease Control and Prevention (CDC). Antibiotic Resistance Threats in the United States, 2013; 2013; pp 1–114.
- De Dios Caballero J, Pastor MD, Vindel A, et al. Emergence of cfr-mediated linezolid resistance in a methicillin-resistant *Staphylococcus aureus* epidemic clone isolated from patients with cystic fibrosis. *Antimicrob Agents Chemother*. 2015;60:1878–1882.
- Gu B, Kelesidis T, Tsiodras S, Hindler J, Humphries RM. The emerging problem of linezolid-resistant *Staphylococcus*. *J Antimicrob Chemother*. 2013;68:4–11.
- Smith TL, Pearson ML, Wilcox KR, et al. Emergence of vancomycin resistance in *Staphylococcus aureus*. Glycopeptide-Intermediate *Staphylococcus aureus* Working Group. *N Engl J Med*. 1999;340:493–501.
- Srinivasan A, Dick JD, Perl TM. Vancomycin resistance in staphylococci. *Clin Microbiol Rev*. 2002;15:430–438.
- Khan A, Wilson B, Gould IM. Current and future treatment options for community-associated MRSA infection. *Expert Opin Pharmacother*. 2018;19:457–470.
- Davis DC, Mohammad H, Kyei-Baffour K, et al. Discovery and characterization of aryl isonitriles as a new class of compounds versus methicillin- and vancomycin-resistant *Staphylococcus aureus*. *Eur J Med Chem*. 2015;101:384–390.
- Brown DG, Lister T, May-Dracka TL. New natural products as new leads for antibacterial drug discovery. *Bioorg Med Chem Lett*. 2014;24:413–418.
- Mo S, Kronic A, Chlipala G, Orjala J. Antimicrobial ambiguine isonitriles from the cyanobacterium *Fischerella ambigua*. *J Nat Prod*. 2009;72:894–899.
- Schwarz O, Brun R, Bats JW, Schmalz H. Synthesis and biological evaluation of new antimalarial isonitriles related to marine diterpenoids. *Tetrahedron Lett*. 2002;1009–1013.
- Wright AD, Wang H, Gurrath M, et al. Inhibition of heme detoxification processes underlies the antimalarial activity of terpene isonitrile compounds from marine sponges. *J Med Chem*. 2001;44:873–885.
- Kirk KL. Fluorine in medicinal chemistry: recent therapeutic applications of fluorinated small molecules. *J Fluorine Chem*. 2006;127:1013–1029.
- Wilcken R, Zimmermann MO, Lange A, Joerges AC, Boeckler FM. Principles and applications of halogen bonding in medicinal chemistry and chemical biology. *J Med Chem*. 2013;56:1363–1388.
- Yale HL. The trifluoromethyl group in medicinal chemistry. *J Med Pharm Chem*. 1959;1:121–133.
- Arbusow BA. Michaelis-Arbusow- und Perkow-Reaktionen. *Pure Appl Chem*. 1964;9:307.
- Weber WP, Gokel GW. An improved procedure for the Hofmann carbylamine synthesis of isonitriles. *Tetrahedron Lett*. 1972;13:1637–1640.
- Zhang B, Studer A. 2-Trifluoromethylated indoles via radical trifluoromethylation of isonitriles. *Org Lett*. 2014;16:1216–1219.
- Banerjee R, Hks K, Banerjee M. Medicinal significance of furan derivatives: A review. 2018.
- Kaur K, Jain M, Reddy RP, Jain R. Quinolines and structurally related heterocycles as antimalarials. *Eur J Med Chem*. 2010;45:3245–3264.
- Pendleton JN, Gorman SP, Gilmore BF. Clinical relevance of the ESKAPE pathogens. *Expert Rev Anti Infect Ther*. 2013;11:297–308.
- Santajit S, Indrawattana N. Mechanisms of antimicrobial resistance in ESKAPE pathogens. *Biomed Res Int*. 2016;2016:2475067.
- Munita JM, Arias CA. Mechanisms of antibiotic resistance. *Microbiol Spectr*. 2016;4.
- Zgurskaya HI, Lopez CA, Gnanakaran S. Permeability barrier of Gram-negative cell envelopes and approaches to bypass it. *ACS Infect Dis*. 2015;1:512–522.
- Padilla E, Llobet E, Domenech-Sanchez A, Martinez-Martinez L, Bengochea JA, Alberti S. Klebsiella pneumoniae AcrAB efflux pump contributes to antimicrobial resistance and virulence. *Antimicrob Agents Chemother*. 2010;54:177–183.
- Schumacher A, Tritler R, Bohnert JA, Kummerer K, Pages JM, Kern WV. Intracellular accumulation of linezolid in *Escherichia coli*, *Citrobacter freundii* and *Enterobacter aerogenes*: role of enhanced efflux pump activity and inactivation. *J Antimicrob Chemother*. 2007;59:1261–1264.
- Krishnamoorthy G, Wolloscheck D, Weeks JW, Croft C, Rybenkov VV, Zgurskaya HI. Breaking the permeability barrier of *Escherichia coli* by controlled hyperosmotic of the outer membrane. *Antimicrob Agents Chemother*. 2016;60:7372–7381.
- Stalker DJ, Jungbluth GL, Hopkins NK, Batts DH. Pharmacokinetics and tolerance of single- and multiple-dose oral or intravenous linezolid, an oxazolidinone antibiotic, in healthy volunteers. *J Antimicrob Chemother*. 2003;51:1239–1246.
- European Centre for Disease Prevention and Control (ECDC). Surveillance of antimicrobial resistance in Europe 2016. *Annual Report of the European Antimicrobial Resistance Surveillance Network (EARS-Net)*. Stockholm. 2017; 2017:1–88.
- Edelsberg J, Weycker D, Barron R, et al. Prevalence of antibiotic resistance in US hospitals. *Diagn Microbiol Infect Dis*. 2014;78:255–262.
- Moet GJ, Jones RN, Biedenbach DJ, Stilwell MG, Fritsche TR. Contemporary causes of skin and soft tissue infections in North America, Latin America, and Europe: report from the SENTRY Antimicrobial Surveillance Program (1998–2004). *Diagn Microbiol Infect Dis*. 2007;57:7–13.
- Russo A, Concia E, Cristini F, et al. Current and future trends in antibiotic therapy of acute bacterial skin and skin-structure infections. *Clin Microbiol Infect*. 2016;22(Suppl 2):S27–S36.
- Gardete S, Tomasz A. Mechanisms of vancomycin resistance in *Staphylococcus aureus*. *J Clin Invest*. 2014;124:2836–2840.
- Rodvold KA, McConeghy KW. Methicillin-resistant *Staphylococcus aureus* therapy: past, present, and future. *Clin Infect Dis*. 2014;58(Suppl 1):S20–S27.
- Kristich CJ, Rice LB, Arias CA. Enterococcal infection-treatment and antibiotic resistance. Boston In: Gilmore MS, Clewell DB, Ike Y, Shankar N, eds. *Enterococci: From Commensals to Leading Causes of Drug Resistant Infection*. 2014; 2014 Boston.
- Grundmann H, Schouls LM, Aanensen DM, et al. The dynamic changes of dominant clones of *Staphylococcus aureus* causing bloodstream infections in the European region: results of a second structured survey. *Euro Surveill*. 2014;19.
- Tian L, Sun Z, Zhang Z. Antimicrobial resistance of pathogens causing nosocomial bloodstream infection in Hubei Province, China, from 2014 to 2016: a multicenter retrospective study. *BMC Public Health*. 2018;18:1121.
- Castanheira M, Watters AA, Mendes RE, Farrell DJ, Jones RN. Occurrence and molecular characterization of fusidic acid resistance mechanisms among *Staphylococcus* spp. from European countries (2008). *J Antimicrob Chemother*. 2010;65:1353–1358.
- Johnson JK, Khoie T, Shurland S, Kreisel K, Stine OC, Roghmann MC. Skin and soft tissue infections caused by methicillin-resistant *Staphylococcus aureus* USA300 clone. *Emerg Infect Dis*. 2007;13:1195–1200.
- Vingsbo Lundberg C, Frimodt-Moller N. Efficacy of topical and systemic antibiotic treatment of methicillin-resistant *Staphylococcus aureus* in a murine superficial skin wound infection model. *Int J Antimicrob Agents*. 2013;42:272–275.
- Clinical and Laboratory Standards Institute (CLSI). Methods for Dilution Antimicrobial Susceptibility Tests for Bacteria That Grow Aerobically—Ninth Edition: Approved Standard M07-A9. In Wayne, PA, 2012.
- Mohammad H, Cushman M, Seleem MN. Antibacterial evaluation of synthetic

- thiazole compounds in vitro and in vivo in a methicillin-resistant *Staphylococcus aureus* (MRSA) skin infection mouse model. *PLoS ONE*. 2015;10:e0142321.
45. Kotb A, Abutaleb NS, Seleem MA, et al. Phenylthiazoles with tert-Butyl side chain: metabolically stable with anti-biofilm activity. *Eur J Med Chem*. 2018;151:110–120.
  46. Hagra M, Abutaleb NS, Ali AO, et al. Targeting multidrug-resistant and intracellular *Staphylococcus aureus* with biofilm disruption activity. *ACS Infect Dis*. 2018.
  47. Elsebaei MM, Mohammad H, Abouf M, et al. Alkynyl-containing phenylthiazoles: systemically active antibacterial agents effective against methicillin-resistant *Staphylococcus aureus* (MRSA). *Eur J Med Chem*. 2018;148:195–209.
  48. ElAwamy M, Mohammad H, Hussien A, et al. Alkoxyphenylthiazoles with broad-spectrum activity against multidrug-resistant gram-positive bacterial pathogens. *Eur J Med Chem*. 2018;152:318–328.
  49. Thangamani S, Mohammad H, Abushahba MF, Sobreira TJ, Seleem MN. Repurposing aurano-fin for the treatment of cutaneous staphylococcal infections. *Int J Antimicrob Agents*. 2016;47:195–201.
  50. Thangamani S, Younis W, Seleem MN. Repurposing celecoxib as a topical antimicrobial agent. *Front Microbiol*. 2015;6:750.
  51. Thangamani S, Younis W, Seleem MN. Repurposing ebselen for treatment of multi-drug-resistant staphylococcal infections. *Sci Rep*. 2015;5:11596.
  52. Thangamani S, Mohammad H, Abushahba MF, et al. Exploring simvastatin, an antihyperlipidemic drug, as a potential topical antibacterial agent. *Sci Rep*. 2015;5:16407.
  53. Mohamed MF, Seleem MN. Efficacy of short novel antimicrobial and anti-inflammatory peptides in a mouse model of methicillin-resistant *Staphylococcus aureus* (MRSA) skin infection. *Drug Des Devel Ther*. 2014;8:1979–1983.



Contents lists available at ScienceDirect

## Bioorganic &amp; Medicinal Chemistry

journal homepage: [www.elsevier.com/locate/bmc](http://www.elsevier.com/locate/bmc)

## Investigation of aryl isonitrile compounds with potent, broad-spectrum antifungal activity

Haroon Mohammad<sup>a,d</sup>, Kwaku Kyei-Baffour<sup>b,d</sup>, Waleed Younis<sup>a,e</sup>, Dexter C. Davis<sup>b</sup>, Hassan Eldesouky<sup>a</sup>, Mohamed N. Seleem<sup>a,c,\*</sup>, Mingji Dai<sup>b,c,\*</sup><sup>a</sup> Department of Comparative Pathobiology, Purdue University College of Veterinary Medicine, West Lafayette, IN 47907, USA<sup>b</sup> Department of Chemistry and Center for Cancer Research, Purdue University, West Lafayette, IN 47907, USA<sup>c</sup> Purdue Institute for Drug Discovery and Institute for Inflammation, Immunology, and Infectious Diseases, West Lafayette, IN 47907, USA

## ARTICLE INFO

## Article history:

Received 19 February 2017

Revised 10 March 2017

Accepted 17 March 2017

Available online 27 March 2017

## Keywords:

Antifungal

*Candida**Cryptococcus**Aspergillus*

Isonitrile

## ABSTRACT

Invasive fungal infections present a formidable global public health challenge due to the limited number of approved antifungal agents and the emergence of resistance to the frontline treatment options, such as fluconazole. Three fungal pathogens of significant concern are *Candida*, *Cryptococcus*, and *Aspergillus* given their propensity to cause opportunistic infections in immunocompromised individuals. New antifungal agents composed of unique chemical scaffolds are needed to address this public health challenge. The present study examines the structure–activity relationship of a set of aryl isonitrile compounds that possess broad-spectrum antifungal activity primarily against species of *Candida* and *Cryptococcus*. The most potent derivatives are capable of inhibiting growth of these key pathogens at concentrations as low as 0.5  $\mu\text{M}$ . Remarkably, the most active compounds exhibit an excellent safety profile and are non-toxic to mammalian cells even at concentrations up to 256  $\mu\text{M}$ . The present study lays the foundation for further investigation of aryl isonitrile compounds as a new class of antifungal agents.

© 2017 Elsevier Ltd. All rights reserved.

## 1. Introduction

Invasive fungal infections caused by species of *Candida*, *Cryptococcus*, and *Aspergillus* afflict more than 1.5 million humans globally each year with a staggering mortality rate that often exceeds 50%.<sup>1</sup> *Candida* is the most frequent source of fungal infections worldwide; notably, *Candida albicans* is the fourth-leading cause of bloodstream infections, and is particularly problematic in immunocompromised patients.<sup>2</sup> There has been a global increase in the prevalence of invasive *Candida* infections in part due to the emergence of non-*albicans* *Candida* species including *Candida glabrata*, *Candida tropicalis*, *Candida parapsilosis*, and *Candida krusei*.<sup>3,4</sup> In addition to *Candida*, species of *Cryptococcus* (including *C. neoformans* and *C. gattii*) are responsible for more than one million new invasive fungal infections each year that result in

an astounding 625,000 deaths.<sup>5</sup> Patients co-infected with HIV are susceptible to severe cryptococcal infections that manifest primarily as pneumonia or meningoencephalitis.<sup>6</sup> The third fungal pathogen of concern involves species of *Aspergillus* (namely *A. fumigatus*) which are responsible for more than 300,000 fungal infections each year.<sup>7</sup> Invasive disease (particularly pulmonary infections) caused by *Aspergillus* primarily occur in patients with underlying conditions such as AIDS, cancer, cystic fibrosis, asthma, or individuals undergoing solid organ transplants. The severity of such infections can be seen by the low rate of survival (59%) reported for solid organ transplant recipients afflicted with invasive aspergillosis.<sup>8</sup>

The difficulty in treating invasive fungal infections has been exacerbated by the limited number of approved antifungal drugs. Currently, only three structurally-distinct classes of antifungal drugs are primarily used for treatment of invasive fungal infections – azoles (such as fluconazole), polyenes (such as amphotericin B), and echinocandins (such as caspofungin).<sup>9</sup> All three classes exert their antifungal activity by interfering with synthesis of a key component of the fungal cell membrane (ergosterol synthesis by both azoles and polyenes) or cell wall ( $\beta(1,3)$ -d-glucan synthesis by echinocandins).<sup>9</sup> Azole antifungals, including fluconazole, are considered the drugs of choice given their high oral bioavailability and reduced toxicity to host tissues. However, the clinical utility of fluconazole and other antifungal drugs has become increasingly

\* Corresponding authors at: Department of Comparative Pathobiology, Purdue University College of Veterinary Medicine, 625 Harrison St., West Lafayette, IN, 47907, USA (M.N. Seleem). Department of Chemistry and Center for Cancer Research, 720 Clinic Drive, West Lafayette, IN 47907, USA (M. Dai).

E-mail addresses: [mseleem@purdue.edu](mailto:mseleem@purdue.edu) (M.N. Seleem), [mjdai@purdue.edu](mailto:mjdai@purdue.edu) (M. Dai).

<sup>d</sup> Contributed equally.

<sup>e</sup> Current address: Department of Microbiology, Faculty of Veterinary Medicine, South Valley University, Qena, Egypt.

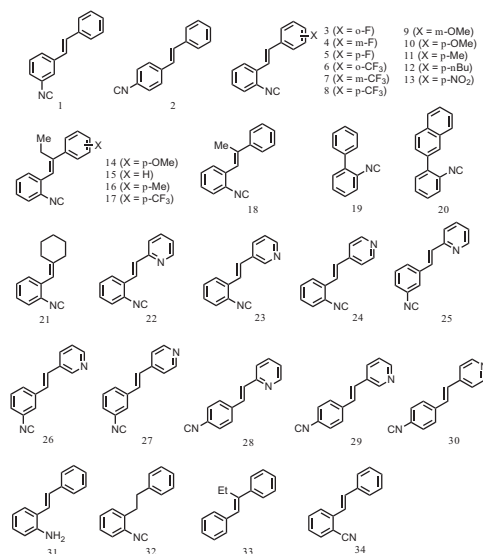


Fig. 1. Chemical structures of compounds presented in this study.

limited due to the emergence of clinical isolates exhibiting resistance to these agents.<sup>10,11</sup> This necessitates the development of new therapeutic agents. However, only one new antifungal drug class has been successfully developed in the past 30 years.<sup>12</sup> The development of new antifungal agents is very challenging given fungi and mammals are both eukaryotes; thus many proteins that are potential targets for antifungal therapy are also found in human cells, opening the door for potential toxicity concerns.<sup>12,13</sup>

Ideally, a novel therapeutic agent for invasive fungal infections should possess broad-spectrum antifungal activity with limited toxicity to host (human) tissues. In the search for new antimicrobial drug scaffolds, we recently discovered synthetic aryl isonitrile compounds that exhibit notable antibacterial activity against drug-resistant *Staphylococcus aureus*.<sup>14</sup> It has been shown that natural product compounds containing the isonitrile functional group can possess dual antibacterial and antifungal activity, particularly against *C. albicans*.<sup>15,16</sup> Per this observation, the present study investigates the structure-activity relationship of our synthetic aryl isonitrile compounds (Fig. 1) as antifungal agents, examines their spectrum of activity against pertinent species of *Candida*, *Cryptococcus*, and *Aspergillus*, and evaluates the most promising compounds' toxicity against mammalian cells. The stilbene-backbone isonitriles and their analogues (1–18, 21–34) were synthesized by using the Horner-Wadsworth-Emmons reaction to build the double bond with the corresponding isonitrile, nitrile, or nitro group-substituted benzyl phosphonates and aldehydes/ketones. The biaryl isonitriles (19, 20) were synthesized from a sequence of Suzuki cross coupling, formamide formation, and dehydration.<sup>14</sup>

## 2. Results and discussion

### 2.1. Structure-activity relationship of compounds against *Candida albicans*

As noted by Beck-Sague et al., *Candida albicans* has been identified as the most common fungal pathogen isolated from health-

Table 1

The minimum inhibitory concentration (MIC in  $\mu\text{M}$ ) and minimum fungicidal concentration (MFC in  $\mu\text{M}$ ) of synthesized compounds and fluconazole screened against *C. albicans* NR-29448.

Compound/Drug Name	<i>Candida albicans</i>	
	MIC	MFC
1	4	32
2	2	>64
3	2	>64
4	8	64
5	64	N.D. <sup>1</sup>
6	>64	>64
7	2	>64
8	32	N.D.
9	16	N.D.
10	1	>64
11	2	>64
12	8	64
13	8	64
14	>64	>64
15	16	N.D.
16	4	>64
17	>64	>64
18	8	>64
19	0.5	>64
20	2	16
21	4	>64
22	1	16
23	1	32
24	4	4
25	0.5	64
26	2	2
27	4	4
28	2	16
29	2	16
30	1	1
31	64	N.D.
32	0.5	64
33	>64	>64
34	>64	>64
Fluconazole	0.5	>64

<sup>1</sup> N.D. = Not determined.

care-associated infections in humans.<sup>17</sup> Thus we initially evaluated our collection of compounds for antifungal activity against a clinical isolate of *C. albicans* (Table 1). Using the broth microdilution assay, the minimum inhibitory concentration (MIC) was determined. The initial screening provided key insight into the structure-antifungal activity relationship of the compounds. Most notably, the presence of the isonitrile group appears to be critical for the compounds to possess antifungal activity. Compounds lacking the isonitrile group (as in 33) or where the isonitrile was substituted with alternative groups including an isosteric nitrile group (34) or an amine (31) were inactive (MIC  $\geq$  64  $\mu\text{M}$ ).

For the stilbene-backbone isonitriles, most of them showed promising antifungal activity against *C. albicans* (MIC = or <8  $\mu\text{M}$ ) with a few exceptions (cf. 5, 6, 8, 9, 14, 15, 17, MIC = or >16  $\mu\text{M}$ ). The effect of different substituents on the aromatic ring without the isonitrile group varies. Both electron-donating (cf. OMe, Me, nBu) and electron-withdrawing (F, CF<sub>3</sub>, NO<sub>2</sub>) groups can be tolerated to a certain extent based on the positions of the substituents. In general, adding alkyl substituents (Me or Et) on the *trans* double bond decreased the antifungal activity. For example, compound 10 (MIC = 1  $\mu\text{M}$ ) is much more potent than compound 14 with an extra ethyl group on the double bond (MIC = 64  $\mu\text{M}$ ); compound 11 (MIC = 2  $\mu\text{M}$ ) and compound 8 (MIC = 32  $\mu\text{M}$ ) are twofold more potent than compound 16 (MIC = 4  $\mu\text{M}$ ) and compound 17 (MIC > 64  $\mu\text{M}$ ), respectively. The *para*-CF<sub>3</sub> group of compounds 8 and 17 has a dramatic effect on their antifungal activity and both compounds 8 and 17 are significantly less potent (16-fold higher

in MIC value) than the corresponding *para*-CH<sub>3</sub> substituted analogues. The possession of the stilbene backbone is not necessary for the aryl isonitriles' antifungal activity against *C. albicans* though it does enhance potency in several cases. For example, replacing the second aromatic group with a cyclohexane (**21**) resulted in a compound with good antifungal activity against *C. albicans* (MIC = 4  $\mu$ M). The biaryl isonitriles **19** and **20** are potent antifungal compounds against *C. albicans* with 0.5  $\mu$ M and 2  $\mu$ M MIC values respectively and the naphthyl group decreased the potency about 4-fold. Interestingly, in our previous studies,<sup>14</sup> both **19** and **20** only showed weak or even no antimicrobial activity against methicillin-resistant *Staphylococcus aureus* (MRSA) strains. Compound **32** with a saturated two-carbon linker between the two aryl groups showed potent anti *C. albicans* activity as well (MIC = 0.5  $\mu$ M). Again, compound **32** was not a good candidate against several MRSA strains in our previous studies. These observations suggest that the antifungal and antibacterial modes of actions for these isonitrile compounds are very likely to be different.

Replacing the non-isonitrile-bearing aromatic ring with pyridine showed beneficial effect on the antifungal activity against *C. albicans*. For example, the MIC values of isomeric compounds **22** to **30** range from 0.5  $\mu$ M to 4  $\mu$ M, with compound **25** emerging as the most potent analogue. The effect of the positions of the isonitrile group on the aromatic ring as well as the nitrogen atom of the pyridine ring ranges from two- to eightfold, which are quite significant. When the isonitrile group is *ortho* to the double bond (**22**, **23**, **24**), the 2 and 3-pyridyl substituted compounds **22** and **23** (MIC = 1  $\mu$ M) are four times more potent than the 4-pyridyl substituted compound **24** (MIC = 4  $\mu$ M). When the isonitrile group is *meta* to the double bond (**25**, **26**, **27**), the 2-pyridyl substituted compound **25** (MIC = 0.5  $\mu$ M) is four- or eightfold more active than the 3 or 4-pyridyl substituted **26** (MIC = 2  $\mu$ M) or **27** (MIC = 4  $\mu$ M), respectively. When the isonitrile group is *para* to the double bond (**28**, **29**, **30**), the effect of the position of the pyridine nitrogen is quite small and 4-pyridyl substituted **30** (MIC = 1  $\mu$ M) is twofold more active than the 2 and 3-pyridyl substituted ones.

Overall, the structure-activity analysis revealed three key findings: the presence of the aryl isonitrile functional group is essential for the observed antifungal activity, the addition of a second aromatic functional group enhances the antifungal activity of the compounds, and the positioning of the isonitrile group on the aromatic ring also impacts the biological activity of the compounds. Interestingly, analogues exhibiting the most potent antifungal activity (including **7**, **11**, **19**, **20**, and **32**) possessed only modest or weak antibacterial activity against drug-resistant *S. aureus*.<sup>14</sup> This information is critical to help guide the synthesis of future aryl isonitrile analogues to improve their specificity as antifungal agents.

## 2.2. Aryl isonitrile compounds exhibit fungistatic behavior against *C. albicans*

After discovering the aryl isonitrile compounds are potent inhibitors of *C. albicans* growth, we were curious to evaluate whether the compounds simply inhibit fungal growth (are fungistatic) or are capable of killing the microorganism (are fungicidal). Previously, we determined that the aryl isonitrile compounds are bacteriostatic, thus we postulated that the compounds would be fungistatic. To investigate this point, the minimum fungicidal concentration (MFC) required to reduce the number of colony-forming units (CFU) by 99.9%,<sup>18</sup> was determined for the active compounds against *C. albicans* NR-29351. The MFC values for the active compounds were found to be noticeably higher (more than 8-fold) compared to their MIC results (Table 1), supporting the notion that the compounds are fungistatic. These results aligned with the

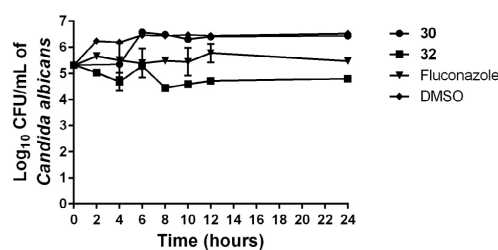


Fig. 2. Time-kill analysis of aryl isonitrile compounds **30**, **32**, and fluconazole against *Candida albicans* NR-29351 over a 24 h incubation period at 37 °C. DMSO served as a negative control. The error bars represent standard deviation values obtained from triplicate samples used for each compound/antifungal drug studied.

results obtained with fluconazole, an antifungal drug known to exhibit fungistatic activity against *C. albicans*.<sup>18</sup>

In order to verify this observation, two of the most potent antifungal compounds were subjected to a traditional time-kill assay. Even at a high concentration (4 × MIC), the aryl isonitrile compounds exhibited fungistatic behavior against *C. albicans* (Fig. 2). Neither **30** nor **32** produced a 3-log<sub>10</sub> reduction in fungal CFU within 24 h, which would be characteristic of fungicidal activity. The compounds' behavior matches that observed with fluconazole. Thus preliminary inspection indicates the aryl isonitrile compounds are fungistatic agents (particularly against *C. albicans*).

## 2.3. Aryl isonitrile compounds exhibit broad-spectrum antifungal activity

Given the potent antifungal activity observed with several aryl isonitrile compounds against *C. albicans*, we next moved to assess their spectrum of activity against key pathogenic fungi. Interestingly, several current antifungal drugs suffer from their inability to inhibit growth of multiple species of fungi. For example, azole antifungals such as fluconazole are generally very effective at inhibiting growth of yeasts such *Candida albicans* and species of *Cryptococcus*; however, fluconazole is ineffective at inhibiting growth of molds such as *Aspergillus* species.<sup>12</sup> Even more discouraging, non-*albicans* *Candida* species including *Candida glabrata* and *Candida krusei* are intrinsically resistant or less susceptible to fluconazole.<sup>12</sup> In contrast, echinocandins are effective against *Candida* and *Aspergillus* but are ineffective as treatment options for infections caused by *Cryptococcus*.<sup>12</sup> Thus finding antifungal compounds capable of inhibiting growth of species of *Candida*, *Cryptococcus*, and *Aspergillus* is highly desirable.

Based upon their potent inhibitory effect against *C. albicans*, six aryl isonitrile compounds (**2**, **22**, **23**, **25**, **26**, and **32**) were screened against 21 additional clinical isolates including non-*albicans* *Candida* species such as *Candida glabrata*, *Candida tropicalis*, *Candida parapsilosis*, *Candida krusei* (Table 2) in addition to species of *Cryptococcus* and *Aspergillus* (Table 3). Interestingly, all six compounds were able to inhibit growth of all species of the yeasts *Candida* and *Cryptococcus*. In general, compound **32** proved to be the most potent compound as it inhibited growth of all clinical isolates, with the exception of *C. krusei*, with a MIC ranging from 0.5 to 1  $\mu$ M (Table 2). This proved to be more potent than fluconazole (MIC = 2  $\mu$ M) against strains of *C. albicans* and *Cryptococcus gattii* that are sensitive to this drug. Against fluconazole-resistant strains of *Candida albicans*, compounds where the second aromatic substituent was replaced with a pyridine were generally more active than **32**. For example, compounds **22**, **23**, **25**, and **26** had MIC values that were lower than compound **32** against

**Table 2**

The minimum inhibitory concentration (MIC in  $\mu\text{M}$ ) of synthesized compounds and fluconazole screened against clinical isolates of *Candida albicans* and non-*albicans Candida* species.

Strain Name	Compound/Drug Name						Fluconazole
	2	22	23	25	26	32	
<i>Candida albicans</i> ATCC 29351	1	1	2	1	$\leq 0.5$	$\leq 0.5$	$\leq 0.5$
<i>Candida albicans</i> ATCC 27365	1	1	2	2	1	$\leq 0.5$	1
<i>Candida albicans</i> NR-29368	2	$\leq 0.5$	4	2	2	8	>64
<i>Candida albicans</i> NR-29446	1	$\leq 0.5$	1	2	2	8	>64
<i>Candida albicans</i> ATCC MYA 573	1	$\leq 0.5$	1	2	2	16	>64
<i>Candida albicans</i> ATCC 64124	2	$\leq 0.5$	2	2	2	64	>64
<i>Candida krusei</i> ATCC 14243	32	4	32	64	32	>64	64
<i>Candida krusei</i> ATCC 34135	16	2	16	32	8	>64	64
<i>Candida parapsilosis</i> ATCC 22019	2	4	8	4	1	$\leq 0.5$	1
<i>Candida glabrata</i> ATCC MYA-2950	8	16	8	8	$\leq 0.5$	$\leq 0.5$	>64
<i>Candida glabrata</i> ATCC 66032	8	16	8	4	1	1	>64
<i>Candida tropicalis</i> ATCC 1369	16	16	8	2	2	1	>64
<i>Candida tropicalis</i> ATCC 13803	4	4	8	4	1	$\leq 0.5$	>64

**Table 3**

The minimum inhibitory concentration (MIC in  $\mu\text{M}$ ) of synthesized compounds and fluconazole screened against clinical isolates of *Cryptococcus* and *Aspergillus*.

Strain Name	Compound/Drug Name						Fluconazole
	2	22	23	25	26	32	
<i>Cryptococcus gattii</i> NR-43208	$\leq 0.5$	$\leq 0.5$	$\leq 0.5$	$\leq 0.5$	$\leq 0.5$	$\leq 0.5$	8
<i>Cryptococcus gattii</i> NR-43209	$\leq 0.5$	$\leq 0.5$	1	$\leq 0.5$	$\leq 0.5$	$\leq 0.5$	8
<i>Cryptococcus neoformans</i> NR-41292	$\leq 0.5$	$\leq 0.5$	1	$\leq 0.5$	$\leq 0.5$	$\leq 0.5$	8
<i>Aspergillus brasiliensis</i> ATCC 16404	>64	4	32	64	32	>64	>64
<i>Aspergillus niger</i> ATCC 6275	>64	8	16	>64	32	>64	>64
<i>Aspergillus niger</i> ATCC 16888	>64	8	8	>64	16	>64	>64
<i>Aspergillus fumigatus</i> NR-35302	32	32	>64	64	16	>64	>64
<i>Aspergillus fumigatus</i> NR-35301	64	32	>64	64	16	>64	>64

fluconazole-resistant *C. albicans*. However, against non-*albicans Candida* species, compounds containing the pyridine functional group, with the exception of **26**, had MIC values that were two to 32-fold higher than the analogue containing a second aromatic group (**32**).

Though the six aryl isonitrile compounds exhibited potent antifungal activity against yeasts (*Candida* and *Cryptococcus*), they were less active against molds. Against *Aspergillus fumigatus*, the MIC values were equal to or higher than 16  $\mu\text{M}$  for all six compounds (Table 3). Compound **22** exhibited the most potent activity against both *A. niger* and *A. brasiliensis* with MIC values ranging from 4 to 8  $\mu\text{M}$ . This was a marked improvement over fluconazole, which proved ineffective at inhibiting growth of both *A. niger* and *A. brasiliensis* (MIC > 64  $\mu\text{M}$ ).

#### 2.4. Compounds are not toxic to mammalian cells at high concentrations

Toxicity is a fundamental parameter to evaluate in early-stage drug discovery to ensure compounds with promising biological activity do not also possess harmful effects to host (human) tissues. A significant challenge with several currently approved antifungal drugs is toxicity. Amphotericin B is a broad-spectrum, fungicidal agent effective against *Candida*, *Cryptococcus*, and *Aspergillus*. However, one of amphotericin B's (and polyenes in general) most significant limitations is its severe toxicity to host tissues.<sup>12</sup> Though a lipid formulation of amphotericin B has been developed that exhibits less toxicity, the formulation is too expensive to be administered in resource-limited regions where invasive fungal infections are endemic.<sup>12</sup> Thus identifying antifungal agents with broad-spectrum activity and limited toxicity to host tissues is highly desirable.

Previously, we evaluated the toxicity of the aryl isonitrile compounds against murine macrophage cells and found the most

potent analogues were not toxic up to a concentration of 64  $\mu\text{M}$ .<sup>14</sup> To further examine the toxicity profile of the aryl isonitrile compounds, the MTS assay was utilized to evaluate the compounds' toxicity against a human epithelial colorectal (HRT-18) cell line at very high concentrations (up to 256  $\mu\text{M}$ ). As presented in Fig. 3, no compound was toxic to HRT-18 cells at a concentration of 128  $\mu\text{M}$ . Astonishingly, even at a concentration of 256  $\mu\text{M}$ , all compounds were non-toxic with the exception of **11** and **20**. This represents a nearly 512-fold difference between the MIC of the most potent compounds against fungi (such as **26** and **32**) and the highest concentration where no toxicity was observed to mammalian cells. This result supports our previous findings that the aryl isonitrile compounds have an excellent safety profile against mammalian cells that warrants further evaluation. The lack of toxicity observed against mammalian cells suggests the aryl isonitrile compounds may exert their antifungal effect via a unique mechanism. Though the antifungal mechanism of action of the aryl isonitrile compounds is currently unknown, it is being intensely investigated.

### 3. Conclusions

Given the dearth of antifungal drug classes and the emergence of resistance to key antifungal drugs (such as fluconazole), there is a need for new chemical scaffolds and compounds exhibiting potent, broad-spectrum antifungal activity and low toxicity to host (mammalian) tissues. The present study examines the promise of aryl isonitrile compounds as a new scaffold for the development of antifungal agents. Structure-activity relationship studies reveal the presence of the isonitrile group and the inclusion of a second aromatic functional group are important for the compounds to possess potent antifungal activity. Compounds bearing the aryl isonitrile functional group exhibited broad-spectrum activity in inhibiting growth of notable species of *Candida* and *Cryptococcus*

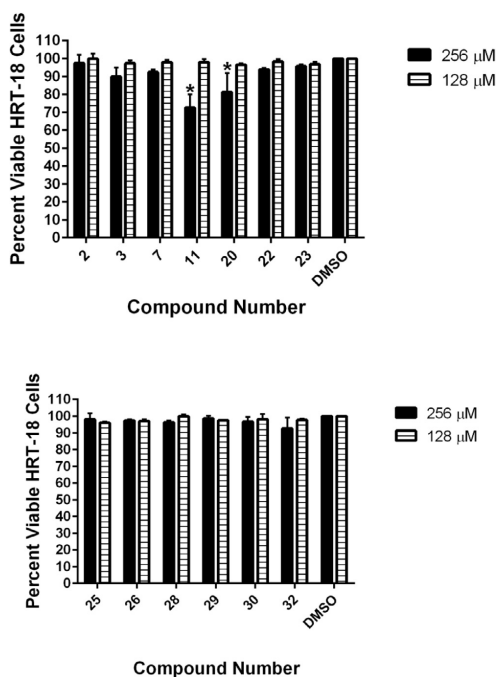


**Fig. 3.** Toxicity analysis of aryl isonitrile compounds against human epithelial colorectal cells (HRT-18). Percent viable mammalian cells (measured as average absorbance ratio (test agent relative to DMSO)) for cytotoxicity analysis of compounds (tested in triplicate) at 128 and 256  $\mu\text{M}$  against HRT-18 cells using the MTS assay. Dimethyl sulfoxide (DMSO) served as a negative control to determine a baseline measurement for the cytotoxic impact of each compound. The absorbance values represent an average of a minimum of three samples analyzed for each compound. Error bars represent standard deviation values for the absorbance values. A two-way ANOVA, with post hoc Dunnet's multiple comparisons test, determined no statistical difference between the values obtained for each compound and DMSO ( $P < 0.05$ ).

at a concentration as low as 0.5  $\mu\text{M}$ . The compounds appear to be fungistatic against *C. albicans*. The most active compounds exhibit an excellent safety profile, as they are non-toxic to mammalian cells, even at concentrations up to 256  $\mu\text{M}$ . The SAR information presented in this report will prove critical for the medicinal chemistry community to develop new aryl isonitrile analogues to advance them to the next step in the antifungal drug discovery process.

#### 4. Materials and methods

##### 4.1. Synthesis of compounds

Synthetic schemes, and spectral data of all compounds, in addition to all intermediates, have been previously reported.<sup>14</sup>

##### 4.2. Fungal strains and reagents used in this study

Clinical isolates of *Candida*, *Cryptococcus*, and *Aspergillus* were obtained from the American Type Cell Culture (ATCC, Manassas, VA, USA) and BEI Resources (Manassas, VA, USA). HRT-18 cells were purchased from the American Type Culture Collection. Flu-

conazole was purchased commercially and dissolved in dimethyl sulfoxide (DMSO) to prepare a stock solution (10 mM). Yeast extract peptone dextrose (YPD), RPMI-1640 for MIC determination, 3-(*N*-Morpholino)propanesulfonic acid, 4-Morpholinepropanesulfonic acid (MOPS), phosphate-buffered saline (PBS), RPMI-1640 medium for cell culture assay, fetal horse serum, and 96-well plates were all purchased from commercial vendors.

##### 4.3. Determination of minimum inhibitory concentration (MIC) and minimum fungicidal concentration (MFC)

The broth dilution assay, following the guidelines of the Clinical and Laboratory Standards Institute for yeasts (M27-A3)<sup>19</sup> and molds (M38-A2)<sup>20</sup>, was utilized to determine the MIC of compounds and fluconazole against species of *Candida*, *Cryptococcus*, and *Aspergillus* using 96-well plates. Plates containing fungi and test agents were incubated at 37 °C for at least 44 h for *Candida* spp. and *Aspergillus* spp. or 68 h for *Cryptococcus* spp. before the MIC was determined by visual inspection. For determination of the minimum fungicidal concentration (MFC) against *C. albicans* NR-29448, aliquots (5  $\mu\text{L}$ ) were transferred from wells with no growth onto yeast extract peptone dextrose (YPD) agar plates. Plates were incubated at 37 °C for 18 h before MFC (> 99.9% decrease in colony-forming units) was recorded.

##### 4.4. Time-kill assay against *C. albicans*

*C. albicans* NR-29351 cells ( $\text{OD}_{600} = 0.524$ ) were diluted to  $2.08 \times 10^5$  colony-forming units (CFU/mL) and exposed to concentrations equivalent to  $4 \times \text{MIC}$  (in triplicate) of compounds **30**, **32**, and fluconazole in YPD medium. Aliquots (100  $\mu\text{L}$ ) were collected from each treatment after 0, 2, 4, 6, 8, 10, 12, and 24 h of incubation at 37 °C and subsequently serially diluted in PBS. Fungi were then spotted onto YPD agar plates and incubated at 37 °C for at least 20 h before viable CFU/mL was determined.

##### 4.5. Cytotoxicity analysis of aryl isonitrile compounds

Compounds were assayed (at concentrations of 32, 64, 128, and 256  $\mu\text{M}$ ) against a human colorectal (HRT-18) cell line to determine the potential toxic effect to mammalian cells *in vitro*. Briefly, cells were cultured in RPMI-1640 medium supplemented with 10% fetal horse serum at 37 °C with  $\text{CO}_2$  (5%). Control cells received DMSO alone at a concentration equal to that in drug-treated cell samples. The cells were incubated with the compounds (in triplicate) in a 96-well plate at 37 °C with  $\text{CO}_2$  (5%) for two hours. The assay reagent MTS 3-(4,5-dimethylthiazol-2-yl)-5-(3-carboxymethoxyphenyl)-2-(4-sulfophenyl)-2H-tetrazolium (Promega, Madison, WI, USA) was subsequently added and the plate was incubated for four hours. Absorbance readings (at  $\text{OD}_{490}$ ) were taken using a kinetic microplate reader (Molecular Devices, Sunnyvale, CA, USA). The quantity of viable cells after treatment with each compound was expressed as a percentage of the viability of DMSO-treated control cells (average of triplicate wells  $\pm$  standard deviation). The toxicity data was analyzed via a two-way ANOVA, with post hoc Dunnet's multiple comparisons test ( $P < 0.05$ ), utilizing GraphPad Prism 6.0 (GraphPad Software, La Jolla, CA).

#### Acknowledgements

**Funding:** We thank the NIH P30CA023168 for supporting shared NMR resources to Purdue Center for Cancer Research. M.D. thanks Purdue University for startup support. H. M. is supported with a fellowship from the Purdue University Institute for Drug Discovery. The authors would like to thank BEI Resources, NIAID, and NIH for support.

## References

1. Brown GD, Denning DW, Gow NAR, et al. Hidden killers: human fungal infections. *Sci Transl Med*. 2012;4.
2. Wisplinghoff H, Bischoff T, Tallent SM, et al. Nosocomial bloodstream infections in US hospitals: analysis of 24,179 cases from a prospective nationwide surveillance study. *Clin Infect Dis*. 2004;39:309–317.
3. Pfaller MA. Antifungal drug resistance: mechanisms, epidemiology, and consequences for treatment. *Am J Med*. 2012;125:S3–13.
4. Sardi JC, Scorzoni L, Bernardi T, et al. *Candida* species: current epidemiology, pathogenicity, biofilm formation, natural antifungal products and new therapeutic options. *J Med Microbiol*. 2013;62:10–24.
5. Park BJ, Wannemuehler KA, Marston BJ, et al. Estimation of the current global burden of cryptococcal meningitis among persons living with HIV/AIDS. *AIDS*. 2009;23:525–530.
6. Butts A, Koselny K, Chabrier-Rosello Y, et al. Estrogen receptor antagonists are anti-cryptococcal agents that directly bind EF hand proteins and synergize with fluconazole *in vivo*. *Mbio*. 2014;5:1–11.
7. The Fungal Infection Trust. How common are fungal diseases? Updated September 2016. URL: <http://www.fungalinfectiontrust.org/wp-content/uploads/2015/12/How-Common-are-Fungal-Diseases5.pdf>.
8. Pappas PG, Alexander BD, Andes DR, et al. Invasive fungal infections among organ transplant recipients: results of the transplant-associated infection surveillance network (TRANSNET). *Clin Infect Dis*. 2010;50:1101–1111.
9. Koselny K, Green J, DiDone L, et al. The celecoxib derivative AR-12 has broad-spectrum antifungal activity *in vitro* and improves the activity of fluconazole in a murine model of cryptococcosis. *Antimicrob Agents Chemother*. 2016;60:7115–7127.
10. Kanafani ZA, Perfect JR. Antimicrobial resistance: resistance to antifungal agents: mechanisms and clinical impact. *Clin Infect Dis*. 2008;46:120–128.
11. Ben-Ami R, Garcia-Effron C, Lewis RE, et al. Fitness and virulence costs of *Candida albicans* FKS1 hot spot mutations associated with echinocandin resistance. *J Infect Dis*. 2011;204:626–635.
12. Roemer T, Krysan DJ. Antifungal drug development: challenges, unmet clinical needs, and new approaches. *Cold Spring Harbor Perspectives in Medicine*. 2014;4.
13. Denning DW, Bromley MJ. How to bolster the antifungal pipeline. *Science*. 2015;347:1414–1416.
14. Davis DC, Mohammad H, Kyei-Baffour K, et al. Discovery and characterization of aryl isonitriles as a new class of compounds versus methicillin- and vancomycin-resistant *Staphylococcus aureus*. *Eur J Med Chem*. 2015;101:384–390.
15. Raveh A, Carmeli S. Antimicrobial ambiguines from the cyanobacterium *Fischerella* sp. collected in Israel. *J Nat Prod*. 2007;70:196–201.
16. Mo SY, Kronic A, Chilpala G, Orjala J. Antimicrobial Ambiguine Isonitriles from the Cyanobacterium *Fischerella ambigua*. *J Nat Prod*. 2009;72:894–899.
17. Beck-Sague C, Jarvis VR. Secular trends in the epidemiology of nosocomial fungal infections in the United States, 1980–1990. National Nosocomial Infections Surveillance System. *J Infect Dis*. 1993;167:1247–1251.
18. Graybill JR, Burgess DS, Hardin TC. Key issues concerning fungistatic versus fungicidal drugs. *Eur J Clin Microbiol*. 1997;16:42–50.
19. Clinical and Laboratory Standards Institute. M27-A3, Reference Method for Broth Dilution Antifungal Susceptibility Testing of Yeasts; Approved Standard – Third Edition. Wayne, PA; 2008.
20. Clinical and Laboratory Standards Institute. M38-A2; Reference Method for Broth Dilution Antifungal Susceptibility Testing of Filamentous Fungi; Approved Standard Wayne, PA; 2008.



Contents lists available at ScienceDirect

European Journal of Medicinal Chemistry

journal homepage: <http://www.elsevier.com/locate/ejmec>

Research paper

## Discovery and characterization of aryl isonitriles as a new class of compounds versus methicillin- and vancomycin-resistant *Staphylococcus aureus*



Dexter C. Davis<sup>a,1</sup>, Haroon Mohammad<sup>b,1</sup>, Kwaku Kyei-Baffour<sup>a</sup>, Waleed Younis<sup>b</sup>, Cassidy Noel Creemer<sup>a</sup>, Mohamed N. Seleem<sup>b,\*\*</sup>, Mingji Dai<sup>a,\*</sup>

<sup>a</sup> Department of Chemistry and Center for Cancer Research, Purdue University, West Lafayette, IN 47907, United States

<sup>b</sup> Department of Comparative Pathobiology, Purdue University College of Veterinary Medicine, West Lafayette, IN 47907, United States

### ARTICLE INFO

#### Article history:

Received 27 March 2015

Received in revised form

9 June 2015

Accepted 13 June 2015

Available online 16 June 2015

#### Keywords:

Antibiotic

Drug resistance

MRSA

VRSA

Isonitrile

### ABSTRACT

Methicillin- and vancomycin-resistant *Staphylococcus aureus* (MRSA and VRSA) have emerged as a global health concern. A new class of compounds featuring an aryl isonitrile moiety has been discovered that exhibits potent inhibitory activity against several clinically-relevant MRSA and VRSA isolates. Structure–activity relationship studies have been conducted to identify the aryl isonitrile group as the key functional group responsible for the observed antibacterial activity. The most potent antibacterial aryl isonitrile analogs (MIC 2  $\mu\text{M}$ ) did not show any toxicity against mammalian cells up to a concentration of 64  $\mu\text{M}$ .

© 2015 Elsevier Masson SAS. All rights reserved.

### 1. Introduction

Multidrug-resistant bacterial infections pose a significant global health challenge afflicting more than 2 million people each year in the United States alone, resulting in over 23,000 fatalities [1]. Nearly half of these casualties are due to infections caused by a single pathogen, methicillin-resistant *Staphylococcus aureus* (MRSA). Currently prevalent in the community setting, MRSA is responsible for a wide spectrum of illnesses from superficial skin infections to invasive diseases including pneumonia, osteomyelitis, and bloodstream infections [2–5]. While a robust arsenal of antibiotics was once capable of treating MRSA infections, strains of this pathogen have emerged that exhibit resistance to nearly every class of antibiotics, including agents of last resort such as vancomycin and linezolid [6–11]. This underscores the urgent need for the identification and development of novel therapeutic options

capable of treating infections due to MRSA [12].

Recently, we have conducted a whole-cell screening of a small number of in-house generated small molecules (about 250 molecules) against MRSA USA300 with the aim to identify compounds with novel skeletons to target antibiotic drug resistance. To our delight, among several hit molecules revealed by this screening effort, compound **1** with an isonitrile group attached to a stilbene system was shown to be capable of inhibiting bacterial growth at a concentration of 32  $\mu\text{M}$  (Fig. 1). Further analysis revealed this compound is bacteriostatic (the minimum bactericidal concentration exceeded 128  $\mu\text{M}$ ). The presence of an isonitrile moiety in this compound is quite unique given that few antimicrobial compounds possessing the isonitrile moiety in their core structure have been described in literature and all of them are complex natural products and are difficult to access [13–19]. Natural terpene isonitrile-containing molecules and simplified analogs have been reported to show antimalarial activity as well [20–22]. The novel structural skeleton of compound **1** as an antibacterial compound against drug resistant strains prompted us to further study of this type of isonitrile compounds. Herein, we report our chemical synthesis, structure–activity relationship study, and evaluation of the antibacterial performance of compound **1** and closely related analogs

\* Corresponding author.

\*\* Corresponding author.

E-mail addresses: [mseleem@purdue.edu](mailto:mseleem@purdue.edu) (M.N. Seleem), [mjdai@purdue.edu](mailto:mjdai@purdue.edu) (M. Dai).

<sup>1</sup> These two authors contributed equally.

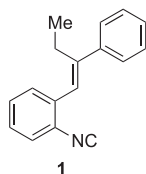


Fig. 1. Structure of hit compound 1.

against several clinically-relevant MRSA and VRSA strains. These efforts have led to the identification of more potent compounds with MIC as low as 2  $\mu\text{M}$  but do not show any cytotoxicity against mammalian cells up to a concentration of 64  $\mu\text{M}$ . Physicochemical analysis of this potent lead compound has been described to guide the next stage of developing these promising compounds into the antibiotic drug pipeline.

## 2. Chemical synthesis

In general, the stilbene isonitrile analogs were prepared from benzylic bromide **2** (Scheme 1), which was converted to phosphonate **3** by Michaelis–Arbuzov reaction [23]. The nitro group of **3** was then converted to an isonitrile group upon a sequence of hydrogenation and Hofmann isonitrile synthesis using dichlorocarbene [24]. Compound **4** then served as a divergent point to synthesize a collection of analogs with a Horner–Wadsworth–Emmons reaction [25]. By treating various ketones and aldehydes with stabilized phosphonate carbanions derived from phosphonates **4**, we obtained thirty-three stilbene isonitrile analogs (**1**, **5–25**, and **27–37**) and one styrene isonitrile analog (**26**). This collection also includes compounds with the isonitrile group at different positions on the aromatic ring as well as pyridine containing analogs. In order to investigate the importance of the isonitrile group for the observed biological activity, compounds containing a hydrogen atom (**42**) or a nitrile group (**43**) at the isonitrile-substitution position were prepared as well using the Horner–Wadsworth–Emmons reaction. Additionally, four biaryl isonitrile analogs (**46** and **49–51**) were prepared [26]. Compound **46** was prepared from commercially available amine **44** via formamide formation followed by dehydration. Compounds **49–51** were synthesized from 2-bromoaniline derivatives (**47**) and aryl-boronic acids. Suzuki cross-coupling converted **47** to biaryl amines **48** smoothly. The latter was then converted to **49–51** via the aforementioned formamide formation and dehydration sequence. Lastly, we prepared compound **53** with a saturated two-carbon chain to investigate the importance of the double bond linker between the two aromatic moieties. All the newly synthesized compounds were purified using flash chromatography before entering biological evaluations.

## 3. Biological results and discussion

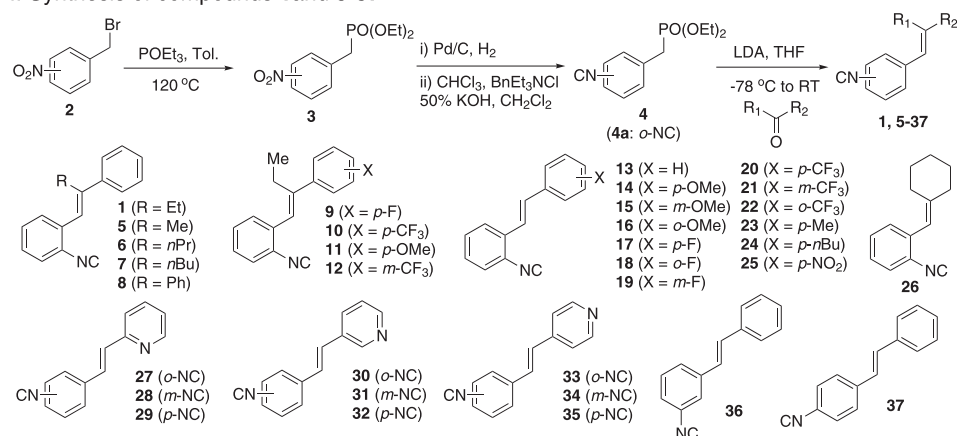
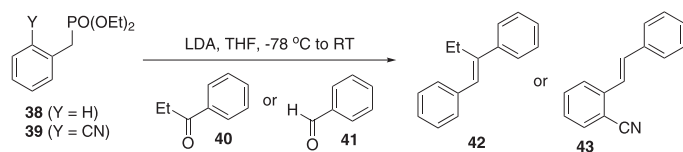
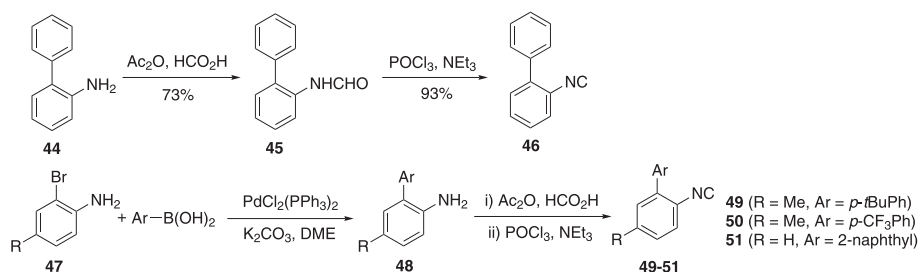
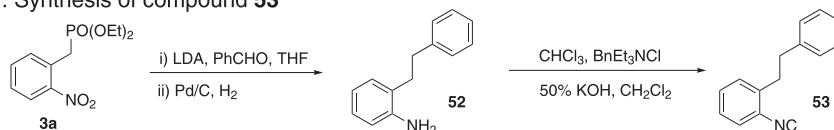
*Antimicrobial susceptibility analysis of the isonitrile compounds against clinically-relevant isolates of MRSA and VRSA.* The bacterial growth inhibiting activity of these synthetic analogs of hit compound **1** were subsequently evaluated (Table 2). When these derivatives were screened against MRSA via the broth microdilution assay, the results revealed several interesting structural elements that appear to play an important role in the antimicrobial activity of these compounds. Initial inspection of the structural moieties of **1** revealed that the presence of an isonitrile group is essential for its

antimicrobial activity. When the isonitrile group of **1** (MIC against MRSA ranging from 8 to 64  $\mu\text{M}$ ) was removed (as in compound **42**), a complete loss in the anti-MRSA activity of **42** is observed (MIC > 128  $\mu\text{M}$ ). A similar pattern is observed when reviewing the MIC results for compounds **13** and **43**. Compound **13**, one of the most potent derivatives constructed (with MIC values against MRSA as low as 2  $\mu\text{M}$ ), contains the isonitrile group; when the isonitrile group of **13** is replaced with an isosteric nitrile group (resulting in compound **43**), complete loss of antimicrobial activity was observed. Similarly, compound **53** with an isonitrile group is active against several strains evaluated particularly MRSA USA100, MRSA USA300, MRSA NRS119, and VISA NRS1, while compound **52** without the isonitrile group lacks antimicrobial activity. These results confirm that the isonitrile group appears necessary for these compounds to possess activity against MRSA and may play an important role in binding to the compound's molecular target.

The presence of a second aromatic substituent (connected to the isonitrile-phenyl group) also appears critical to the biological activity observed; replacement of this moiety in **1** with a diethyl phosphonate (as in analog **4a** with an *ortho*-isonitrile group) results in complete loss of activity against MRSA (MIC > 128  $\mu\text{M}$ ). Likewise, substitution of this second aromatic substituent with a cycloalkane (cf. **26**) renders this compound inactive against several MRSA isolates (including MRSA USA300, MRSA USA500, and MRSA NRS119). The presence of an alkene bridge between the two aromatic substituents in **1** also appears to be important. When the alkene bridge between the two aromatic substituents is removed, as in compound **46**, this compound lacks activity against three strains of MRSA (USA300, USA500, and NRS119). A similar loss in antimicrobial activity is observed with compounds **49** and **50** indicating that the stilbene isonitrile core of **1** plays an important role in its antimicrobial activity. This notion was further supported by a direct comparison of compounds **13** and **53**. Compound **53** is a saturated analog of compound **13** and contains a flexible two-carbon linker between the two aromatic moieties. In general, compound **53** is less potent than compound **13** against all the strains tested except for VISA NRS1.

We then evaluated how substituents on the double bond would affect the antimicrobial activity. Interestingly, removal of the ethyl group of **1** (cf. **13**) resulted in a dramatic improvement in antimicrobial activity (a two-to-eight fold reduction in the MIC against MRSA was observed). When the ethyl group was replaced by methyl (**5**), *n*-propyl (**6**), *n*-butyl (**7**) and phenyl (**8**) groups, a noticeable change in the MIC value for these compounds is observed.

We next assessed how substituents on the non-isonitrile-containing aromatic ring would affect the potency against MRSA. Analogs constructed include substitution of methoxy group (**14–16**), fluoride (**17–19**), trifluoromethyl group (**20–22**), methyl group (**23**), *n*-butyl group (**24**), and nitro group (**25**). Interestingly most of these modifications do not produce a major improvement in the MIC observed against MRSA, when compared to the activity of **13**. Additionally the positioning of these groups around the benzene ring do not appear to have an impact on the antimicrobial activity of the compound. While most of these modifications have little effect on improving the antimicrobial activity of these compounds, one substitution had an observed deleterious effect. Compound **24**, containing a *n*-butyl group, lacked activity against most MRSA strains tested (MIC > 128  $\mu\text{M}$ ); interestingly, **23**, with a methyl group is active against all MRSA strains tested albeit at a higher concentration than **13** (MIC of **23** ranges from 4 to 64  $\mu\text{M}$  against MRSA). This would appear to indicate that the presence of an alkyl group (in particular one of increased length) is undesirable and can have a negative effect on the activity of these compounds against MRSA. Analogs containing a pyridine ring were synthesized

I. Synthesis of compounds **1** and **5–37**II. Synthesis of compounds **42** and **43**III. Synthesis of compounds **46** and **49–51**IV. Synthesis of compound **53**Scheme 1. Synthesis of analogs of lead compound **1**.

and tested as well (**27**, **30**, and **33**) and reduced antimicrobial activities were observed.

All the analogs discussed above contain an *ortho*-substituted isonitrile group. We wondered how the relative position of the isonitrile group would affect the antimicrobial activity and prepared eight analogs with the isonitrile group in *para*- and *meta*-relationship to the double bond (cf. **28**, **29**, **31**, **32**, **34–37**). Different

antimicrobial activity patterns are observed. For the group of **13**, **36**, and **37**, the *ortho*-substituted compound **13** is still the most potent one against most of the strains tested and slight improvement was observed for the *para*-substituted compound **37** against MSSA (NRS72) and MRSA USA500. Interestingly, for the group of **33**, **34**, and **35**, the *para*-substituted compound **35** is much more active against all the strains tested than the *ortho*- and *meta*-substituted

**Table 1**  
Strains of *Staphylococcus aureus* utilized in this study.

Strain name		Isolation		Molecular typing		Antimicrobial resistance phenotype
NARSA ID <sup>a</sup>	Alternate designation	Origin	Source	SCCmec type	spa type	
NRS1	ATCC700699	Japan	—	II	TJMBMDMGMK	Resistant to aminoglycosides and tetracycline (minocycline)
NRS72 <sup>b</sup>	MSSA 476	—	—	—	UKJFKBPE	Glycopeptide-intermediate <i>S. aureus</i>
NRS119	SA LinR#12	United States (Massachusetts)	Dialysis-associated peritonitis	IV	YHGCMBQBLO	Resistant to linezolid
NRS382	USA100	United States (Ohio)	Bloodstream	II	TJMBMDMGMK	Resistant to erythromycin, clindamycin and levofloxacin
NRS383	USA200	United States (North Carolina)	Bloodstream	II	WGKAKAOMQQQ	Resistant to erythromycin, clindamycin and gentamicin
NRS384	USA300-0114	United States (Mississippi)	Wound	IV	YHGFMBQBLO	Resistant to erythromycin, methicillin, and tetracycline
NRS385	USA500	United States (Connecticut)	Bloodstream	IV	YHGCMBQBLO	Resistant to erythromycin, clindamycin, trimethoprim/sulfamethoxazole, levofloxacin, gentamicin and tetracycline
NRS386	USA700	United States (Louisiana)	Bloodstream	IV	UJGFMGGM	Resistant to erythromycin and methicillin
VR52	VRSA	United States (Pennsylvania)	Plantar ulcer	II	TJMBMDMGMK	Resistant to vancomycin

<sup>a</sup> NARSA = Network on Antimicrobial Resistance in *Staphylococcus aureus*.

<sup>b</sup> NRS72 = Methicillin-sensitive *Staphylococcus aureus* (MSSA).

ones. The groups of **27–29** and **30–32** are less potent than the aforementioned two groups, which indicate that the position of the nitrogen atom in the pyridine ring is important for the observed antimicrobial activity as well.

After completing a preliminary examination of the structure–activity relationship of these compounds, we next moved to assess whether these compounds would retain their activity against several of the most challenging strains of MRSA (Tables 1 and 2). When tested against an array of clinically-relevant MRSA isolates, the most potent compounds (**6**, **8–18**, **20–21**, **25**, and **37**) did retain their antimicrobial activity. Indeed, these compounds possess potent activity against MRSA isolates prevalent in the healthcare-setting such as MRSA USA100 (responsible for invasive diseases in infected hospitalized patients) [27], and MRSA USA200 (associated with more severe morbidity in affected patients due to the production of toxins that can lead to toxic shock syndrome) [28]. In addition to this, these compounds exhibit potent activity against MRSA USA300, a strain that has been linked to the majority of MRSA skin and soft tissue infections present in the community setting [10,29]. Furthermore, these compounds demonstrate strong antimicrobial activity against MRSA strains exhibiting resistance to numerous antibiotic classes including penicillins, aminoglycosides (NRS1, USA200, and USA500), macrolides (USA100, USA200, USA300, USA500, and USA700), lincosamides (USA100, USA200, USA500), tetracyclines (NRS1, USA300, and USA500), and fluoroquinolones (USA100 and USA500). Additionally, compounds **10**, **11**, **12**, **21**, **25**, **32**, and **35** exhibit potent antimicrobial activity (MIC between 4 and 16  $\mu$ M) against clinical isolates of *S. aureus* exhibiting resistance to antibiotics deemed agents of last resort, namely vancomycin (VR52). These results indicate cross-resistance between these antibiotics and the aryl isonitrile compounds is unlikely; this lends further credence to the notion that the aryl isonitrile compounds have potential to be developed as future alternatives to these antibiotics.

*Toxicity analysis of most potent aryl isonitrile compounds against mammalian cells.* Identification of compounds exhibiting potent antimicrobial activity is the first step in a lengthy process for drug development. Many compounds with promising antimicrobial activity fail to advance further in this process due to concerns about toxicity to mammalian tissues. Selective toxicity is a critical feature novel antimicrobial compounds must possess. The ability for antimicrobial agents to exhibit their activity on the target microorganism while not causing harm to host (mammalian) tissues is important to ascertain early in the drug discovery process. To determine if compound **1** and its most potent derivatives against MRSA exhibited toxicity to mammalian tissues, these compounds

were screened against a murine macrophage (J774) cell line utilizing the MTS assay (Fig. 2). Initial inspection of the structure–activity relationship revealed that the isonitrile moiety appeared to be a vital component in the antimicrobial activity of these compounds. This was a point of concern given the isonitrile group has been associated with a high degree of toxicity in certain compounds present in nature [30]. However, when the most potent compound, **13** (containing the isonitrile moiety), and its analog **42** (lacking the isonitrile moiety) were tested against J774 cells, they produced identical results (neither compound was toxic up to a concentration of 64  $\mu$ M). This would indicate that the isonitrile group in these compounds does not contribute to undesirable toxicity to mammalian cells. This result is similar to a study conducted at Bayer AG that found compounds in their discovery pipeline, containing the isonitrile moiety were not toxic to mice when administered orally or subcutaneously (even at concentrations in excess of 500 mg/kg) [31]. In addition to this, at a concentration of 32  $\mu$ M, all of the compounds tested, with the exception of **25** with a nitro group, were not toxic. When the compounds were tested at a concentration of 64  $\mu$ M, nineteen out of twenty-three compounds were found to not be toxic to J774 cells (Fig. 2). Compounds **11**, **12**, **19**, and **25** were found to be toxic at 64  $\mu$ M. When the compounds were tested at 128  $\mu$ M, all compounds were found to be toxic with the exception of compounds **15**, **30**, and **37** (data not presented). For the most active compounds (such as **13**), a 16-to-32 fold difference exists between the concentration at which the compounds exhibit anti-MRSA activity (MIC) compared to the concentration where toxicity is observed.

*Preliminary study of physicochemical properties of the isonitrile compounds using kinetic solubility analysis and Caco-2 permeability assay.* After confirming that most of the isonitrile compounds exhibited strong antimicrobial activity against MRSA were not toxic to mammalian cells up to a concentration of 64  $\mu$ M, we next moved to analyze the physicochemical properties of the most promising compound **13**. These properties play an important role in determining the appropriate route of administration (i.e. systemic vs. local) by which compounds with biological activity can be delivered to the host [32]. Additionally, the physicochemical properties of a compound will have a direct impact on its pharmacokinetic profile (in particular absorption and metabolism), and ability to be translated into a viable drug candidate. Indeed, one study found that 40% of new drug candidates were withdrawn due to issues pertaining to significant pharmacokinetic problems [33]. Compounds possessing a limited physicochemical profile can have issues pertaining to solubility and permeability which can hinder a compound's ability to cross biological membranes, reach the bloodstream, and arrive at the

**Table 2**  
Minimum inhibitory concentration (MIC, in  $\mu\text{M}$ ) of isonitrile compounds, linezolid, and vancomycin against methicillin-sensitive (MSSA) and methicillin-resistant *Staphylococcus aureus* (MRSA) strains.

Compound name	MSSA <sup>a</sup> (NRS72)	MRSA USA100	MRSA USA200	MRSA USA300	MRSA USA500	MRSA USA700	MRSA NRS119	VISA <sup>b</sup> NRS1	VRSA <sup>c</sup> VRS2
<b>1</b>	8	8	16	32	32	8	64	8	32
<b>4a</b>	>128	>128	128	>128	>128	>128	>128	128	>128
<b>5</b>	8	8	64	>128	>128	16	>128	4	>128
<b>6</b>	16	16	16	32	16	16	32	8	32
<b>7</b>	32	32	32	>128	32	16	>128	16	64
<b>8</b>	8	8	8	16	8	4	16	4	16
<b>9</b>	8	16	16	32	16	8	64	8	32
<b>10</b>	8	16	16	32	16	16	64	8	16
<b>11</b>	8	8	8	16	8	4	>128	4	8
<b>12</b>	4	4	8	>128	8	2	8	2	8
<b>13</b>	16	2	4	4	32	4	4	2	32
<b>14</b>	4	8	2	16	>128	8	32	4	32
<b>15</b>	8	8	4	16	32	16	32	4	32
<b>16</b>	8	8	8	8	8	8	16	4	16
<b>17</b>	4	8	2	8	16	8	16	4	32
<b>18</b>	4	8	2	16	16	8	32	4	32
<b>19</b>	8	16	16	32	128	16	128	8	128
<b>20</b>	4	4	2	8	16	2	16	2	16
<b>21</b>	2	4	4	8	8	4	8	2	8
<b>22</b>	8	16	16	32	16	16	>128	8	32
<b>23</b>	16	4	4	16	32	8	64	4	32
<b>24</b>	>128	–	>128	>128	>128	–	>128	–	>128
<b>25</b>	2	4	4	8	8	8	16	4	8
<b>26</b>	8	16	64	>128	>128	16	>128	4	>128
<b>27</b>	64	64	64	16	64	32	128	64	32
<b>28</b>	64	32	64	32	64	64	128	128	128
<b>29</b>	64	128	128	32	64	128	128	64	64
<b>30</b>	64	32	32	16	32	32	64	64	32
<b>31</b>	64	32	64	32	64	64	64	64	64
<b>32</b>	16	16	32	8	32	16	64	32	8
<b>33</b>	64	32	32	32	32	32	64	64	64
<b>34</b>	64	32	64	32	64	64	32	32	64
<b>35</b>	2	8	8	4	4	8	4	8	4
<b>36</b>	16	32	32	16	>128	16	64	32	32
<b>37</b>	4	4	32	4	16	64	>128	>128	>128
<b>42</b>	>128	>128	>128	>128	>128	>128	>128	>128	>128
<b>43</b>	>128	>128	>128	>128	>128	>128	>128	>128	>128
<b>46</b>	>128	16	16	>128	>128	16	>128	8	>128
<b>49</b>	>128	16	16	>128	>128	16	64	4	>128
<b>50</b>	>128	>128	>128	>128	>128	>128	>128	>128	>128
<b>51</b>	16	16	64	64	32	16	32	4	64
<b>52</b>	>128	>128	32	>128	>64	>64	>128	8	>64
<b>53</b>	64	4	16	4	128	32	2	2	64
Linezolid	2	<1	2	2	<1	2	64	<1	<1
Vancomycin	<1	2	–	–	4	–	–	8	128

<sup>a</sup> MSSA = Methicillin-sensitive *Staphylococcus aureus*.

<sup>b</sup> VISA = Vancomycin-intermediate *Staphylococcus aureus*.

<sup>c</sup> VRSA = Vancomycin-resistant *Staphylococcus aureus*.

target site of an infection (thus limiting their use systemically) [34].

A kinetic solubility screen (using phosphate-buffered saline) and Caco-2 permeability analysis was performed with compound **13**. The solubility screen determined the highest concentration **13** and three control drugs were capable of being fully dissolved in an aqueous solvent (PBS). As presented in Table 3, this experiment revealed that compound **13** possessed partial aqueous solubility (soluble up to 15.6  $\mu\text{M}$ ), identical to the control drugs reserpine and tamoxifen.

The Caco-2 permeability assay revealed that compound **13** was not able to permeate across the Caco-2 bilayer. As presented in Table 4, this compound was unable to cross from the apical (A) to basolateral (B) surface of the membrane (apparent permeability,  $P_{app} = 0.0 \text{ cm/s}$ ). A similar pattern is observed in the basolateral to apical direction with  $P_{app} = 0.0 \text{ cm/s}$  (indicating this compound is unlikely a substrate for an efflux transporter, like talinolol, which would be one plausible explanation for the inability of this compound to traverse the membrane). This is in stark contrast to the control drug warfarin, which is able to effectively permeate across

the membrane from the basolateral to apical surface ( $P_{app} = 27.0 \times 10^{-6} \text{ cm/s}$ ). This result is a bit surprising given the size, structure, and calculated partition coefficient ( $\text{clog } P = 4.107$ ) for **13**. Thus, in addition to possessing only partial aqueous solubility, **13** also possesses a poor permeability profile, indicating that, in its present state, this compound would not be suitable for use systemically.

The result from the Caco-2 permeability analysis is in agreement with the overall result obtained from the kinetic solubility screen indicating that **13**, though a promising antimicrobial candidate, needs to undergo further structural modifications to enhance its physicochemical profile (in order for it to be used systemically). In addition to modifying the structure of this compound, formulation technology can be utilized to overcome this compound's current limitations. This technology has been used to improve the drug-like properties of promising compounds with similar kinetic profiles to **13** in order to propel these compounds into further stages of drug development. By using a spray drying dispersion technique [35], the antisolvent crystallization method [36], or combining the active

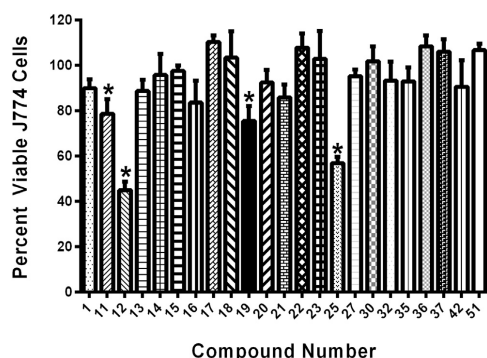


**Fig. 2.** Percent viable mammalian cells (measured as average absorbance ratio (test agent relative to DMSO)) for cytotoxicity analysis of compounds **1**, **11**–**23**, **25**, **27**, **30**, **32**, **35**, **36**, **37**, **42**, and **51** at 64  $\mu\text{M}$ . Compounds were tested against J774 cells using the MTS (3-(4,5-dimethylthiazol-2-yl)-5-(3-carboxymethoxyphenyl)-2-(4-sulfophenyl)-2H-tetrazolium) assay. DMSO was used as a negative control to determine a baseline measurement for the toxic impact of each compound. The values represent an average of three samples analyzed for each compound. Error bars represent standard deviation values for the absorbance values. Asterisks (\*) indicate a statistical difference between the values obtained for the compound relative to the cells treated with DMSO ( $P < 0.05$ ).

**Table 3**

Kinetic solubility assessment of compound **13**, reserpine, tamoxifen, and verapamil in phosphate-buffered saline (PBS).

Compound tested	Solubility limit ( $\mu\text{M}$ ) <sup>a</sup>	Solubility analysis
<b>13</b>	15.6	Low solubility
Reserpine	15.6	Low solubility
Tamoxifen	15.6	Low solubility
Verapamil	>500	High solubility

<sup>a</sup> Solubility limit corresponds to the highest concentration of test compound where no precipitate was detected.

compound with an excipient (to create an amorphous solid dispersion) [37], the aqueous solubility, permeability and bioavailability profile of this compound can be significantly improved. Identifying that **13** has a problematic physicochemical profile early in the drug discovery process will permit medicinal chemists and formulation scientists to invest time and effort to enhancing both the physicochemical and pharmacokinetic profiles of this promising new antimicrobial compound.

**Metabolic stability analysis of 13 via microsomal stability analysis.** In addition to studying the solubility and permeability profile of compound **13**, the stability of this compound to metabolic processes present in the liver was investigated using human liver

microsomes (Table 5). Drugs administered systemically often are subject to various metabolic processes that can convert the active compound to inactive metabolites. Pharmaceutical compounds that are slow to be metabolized have multiple advantages including an improved pharmacokinetic profile, reduced frequency of doses that need to be given to patients (leading to better patient compliance), while also ensuring the active drug circulates within the patient's system to assist with treating and clearing an infection. As the liver is the primary organ for metabolism of drugs administered systemically in the body, incubating compounds with liver microsomes can shed valuable insight into the stability of these compounds to metabolic processes [32].

When **13** was incubated with human liver microsomes, it was found to be rapidly metabolized (only 24% of the parent compound remained after one hour) similar to the highly metabolized control drug, verapamil (13% remained after one hour incubation with liver microsomes) (Table 5). While verapamil appeared to be metabolized via a NADPH-mediated process (as 94% of the drug remained after one hour when the co-factor NADPH was removed from the reaction mixture), **13** does not appear to mimic this result as only 51% of the parent compound remained after one hour when NADPH was not present. This would appear to suggest that **13** is metabolized by more than one enzyme system/reaction (one dependent on the co-factor NADPH (most likely the cytochrome P450 system), and one independent of NADPH). The metabolic stability analysis performed lends further credence to the argument that in its present state **13** would not be suitable for use in systemic applications to treat MRSA infections.

#### 4. Conclusion

In summary, we have discovered a novel class of aryl isonitrile compounds as promising and potent antimicrobial compounds without apparent toxicity against mammalian cells up to a concentration of 64  $\mu\text{M}$ . Physicochemical profiling, including solubility, membrane permeability, and metabolic stability of one of the most potent compounds, **13**, has been conducted as well. These results indicate that modification of the physical structure of compound **13** is needed to enhance its physicochemical and pharmacokinetic profile so that it can be developed for systemic use against MRSA infections. In addition, identifying other routes of administration (such as topical/local administration) is another avenue to pursue to further develop this promising compound as a novel antimicrobial candidate. Given that *S. aureus* and its resistant strains (including MRSA) are a leading cause of uncomplicated skin infections (such as abscesses, impetigo, and cellulitis) [2,10], it is logical to assess if compound **13** and its analogs, can be used as topical antimicrobial agents for treatment of MRSA skin infections. Topical agents avoid many concerns relating to solubility, permeability, and systemic toxicity associated with drugs administered orally or intravenously. Future work with these compounds will

**Table 4**

Permeability analysis of compound **13**, ranitidine, warfarin, and talinolol via the Caco-2 permeability assay.

Compound/drug tested	Mean A $\rightarrow$ B <sup>a</sup> $P_{app}$ ( $10^{-6}$ cm/s)	Mean B $\rightarrow$ A <sup>b</sup> $P_{app}$ ( $10^{-6}$ cm/s)	Efflux ratio <sup>c</sup>	Permeability analysis
<b>13</b>	0.0 <sup>d</sup>	0.0	N/A <sup>e</sup>	Not permeable
Ranitidine	0.23	3.1	13.5	Low permeability
Warfarin	27.0	7.2	0.3	High permeability
Talinolol	0.05	8.9	178	P-gp <sup>f</sup> efflux control

<sup>a</sup> Mean A  $\rightarrow$  B  $P_{app}$  = mean apparent permeability of test compound from apical to basolateral surface.

<sup>b</sup> Mean B  $\rightarrow$  A  $P_{app}$  = mean apparent permeability of test compound from basolateral to apical surface.

<sup>c</sup> Efflux ratio =  $P_{app}(B \rightarrow A) / P_{app}(A \rightarrow B)$ .

<sup>d</sup> Compound not detected in receiver compartment.

<sup>e</sup> N/A, not applicable.

<sup>f</sup> P-gp, P-glycoprotein.